JSCSEN 89(12) 1525-1704 (2024)

ISSN 1820-7421(Online)

Journal of the Serbian Chemical Society

Electronic version

VOLUME 89

NO 12

BELGRADE 2024

Available on line at

www.shd.org.rs/JSCS/

The full search of JSCS is available through

DOAJ DIRECTORY OF OPEN ACCESS JOURNALS

www.doaj.org

The **Journal of the Serbian Chemical Society** (formerly Glasnik Hemijskog društva Beograd), one volume (12 issues) per year, publishes articles from the fields of chemistry. The **Journal** is financially supported by the **Ministry of Education, Science and Technological Development of the Republic of Serbia.**

Articles published in the **Journal** are indexed in **Clarivate Analytics products: Science Citation Index-Expanded™** – accessed *via* **Web of Science®** and **Journal Citation Reports®**.

Impact Factor announced on 28 June, 2023: **1.000; 5-year Impact Factor**: **1.100**.

Articles appearing in the **Journal** are also abstracted by: **Scopus, Chemical Abstracts Plus (CAplus℠), Directory of Open Access Journals, Referativnii Zhurnal (VINITI), RSC Analytical Abstracts, EuroPub, Pro Quest** and **Asian Digital Library.**

Publisher:	**Serbian Chemical Society**, Karnegijeva 4/III, P. O. Box 36, 1120 Belgrade 35, Serbia tel./fax: +381–11–3370–467, E-mails: **Society** – shd@shd.org.rs; **Journal** – jscs@shd.org.rs Home Pages: **Society** – http://www.shd.org.rs/, **Journal** – http://www.shd.org.rs/JSCS/
Internet Service:	Contents, Abstracts and full papers (from Vol 64, No. 1, 1999) are available in the electronic form at the Web Site of the **Journal** (http://www.shd.org.rs/JSCS/).
Former Editors:	**Nikola A. Pušin** (1930–1947), **Aleksandar M. Leko** (1948–1954), **Panta S. Tutundžić** (1955–1961), **Miloš K. Mladenović** (1962–1964), **Đorđe M. Dimitrijević** (1965–1969), **Aleksandar R. Despić** (1969–1975), **Slobodan V. Ribnikar** (1975–1985), **Dragutin M. Dražić** (1986–2006).
Editor-in-Chief:	BRANISLAV Ž. **NIKOLIĆ**, Serbian Chemical Society (E-mail: jscs-ed@shd.org.rs)
Deputy Editor:	DUŠAN **SLADIĆ**, Faculty of Chemistry, University of Belgrade
Sub editors:	
Organic Chemistry	DEJAN **OPSENICA**, Institute of Chemistry, Technology and Metallurgy, University of Belgrade JÁNOS **CSANÁDI**, Faculty of Science, University of Novi Sad
Biochemistry and Biotechnology	OLGICA **NEDIĆ**, INEP – Institute for the Application of Nuclear Energy, University of Belgrade
Inorganic Chemistry	BILJANA **GLIŠIĆ**, Faculty of Science, University of Kragujevac
Theoretical Chemistry	IVAN **JURANIĆ**, Serbian Chemical Society
Physical Chemistry	LJILJANA **DAMJANOVIĆ-VASILIĆ**, Faculty of Physical Chemistry, University of Belgrade
Electrochemistry	SNEŽANA **GOJKOVIĆ**, Faculty of Technology and Metallurgy, University of Belgrade
Analytical Chemistry	RADA **BAOŠIĆ**, Faculty of Chemistry, University of Belgrade
Polymers	BRANKO **DUNJIĆ**, Faculty of Technology and Metallurgy, University of Belgrade
Thermodynamics	MIRJANA **KIJEVČANIN**, Faculty of Technology and Metallurgy, University of Belgrade
Chemical Engineering	TATJANA **KALUĐEROVIĆ RADOIČIĆ**, Faculty of Technology and Metallurgy, University of Belgrade
Materials	RADA **PETROVIĆ**, Faculty of Technology and Metallurgy, University of Belgrade
Metallic Materials and Metallurgy	ANA **KOSTOV**, Mining and Metallurgy Institute Bor, University of Belgrade
Environmental and Geochemistry	VESNA **ANTIĆ**, Faculty of Agriculture, University of Belgrade
History of and Education in Chemistry	DRAGICA **TRIVIĆ**, Faculty of Chemistry, University of Belgrade
English Language Editors:	LYNNE **KATSIKAS**, Serbian Chemical Society VLATKA **VAJS**, Serbian Chemical Society JASMINA **NIKOLIĆ**, Faculty of Technology and Metallurgy, University of Belgrade
Technical Editors:	VLADIMIR **PANIĆ**, Institute of Chemistry, Technology and Metallurgy, University of Belgrade, MARIO **ZLATOVIĆ**, Faculty of Chemistry, University of Belgrade
Journal Manager & Web Master:	MARIO **ZLATOVIĆ**, Faculty of Chemistry, University of Belgrade
Office:	VERA **ĆUŠIĆ**, Serbian Chemical Society

Editorial Board

From abroad: **R. Adžić**, Brookhaven National Laboratory (USA); **A. Casini**, University of Groningen (The Netherlands); **G. Cobb**, Baylor University (USA); **D. Douglas**, University of British Columbia (Canada); **G. Inzelt**, Etvos Lorand University (Hungary); **J. Kenny**, University of Perugia (Italy); **Ya. I. Korenman**, Voronezh Academy of Technology (Russian Federation); **M. D. Lechner**, University of Osnabrueck (Germany); **S. Macura**, Mayo Clinic (USA); **M. Spiteller**, INFU, Technical University Dortmund (Germany); **M. Stratakis**, University of Crete (Grecce); **M. Swart**, University de Girona (Cataluna, Spain); **G. Vunjak-Novaković**, Columbia University (USA); **P. Worsfold**, University of Plymouth (UK); **J. Zagal**, Universidad de Santiago de Chile (Chile).

From Serbia: **B. Abramović**, **V. Antić**, **R. Baošić**, **V. Beškoski**, **J. Csanadi**, **Lj. Damjanović-Vasilić**, **A. Dekanski**, **V. Dondur**, **B. Dunjić**, **M. Đuran**, **B. Glišić**, **S. Gojković**, **I. Gutman**, **B. Jovančićević**, **I. Juranić**, **T. Kaluđerović Radoičić**, **L. Katsikas**, **M. Kijevčanin**, **A. Kostov**, **V. Leovac**, **S. Milonjić**, **V.B. Mišković-Stanković**, **O. Nedić**, **B. Nikolić**, **J. Nikolić**, **D. Opsenica**, **V. Panić**, **M. Petkovska**, **R. Petrović**, **I. Popović**, **B. Radak**, **S. Ražić**, **D. Sladić**, **S. Sovilj**, **S. Šerbanović**, **B. Šolaja**, **Ž. Tešić**, **D. Trivić**, **V. Vajs, M. Zlatović**.

Subscription: The annual subscription rate is **150.00 €** including postage (surface mail) and handling. For Society members from abroad rate is **50.00 €**. For the proforma invoice with the instruction for bank payment contact the Society Office (E-mail: shd@shd.org.rs) or see JSCS Web Site: http://www.shd.org.rs/JSCS/, option Subscription.

Godišnja pretplata: Za članove SHD: **2.500,00 RSD**, za penzionere i studente: **1000,00 RSD**, a za ostale: **3.500,00 RSD**:za organizacije i ustanove: **16.000,00 RSD**. Uplate se vrše na tekući račun Društva: **205-13815-62**, poziv na broj **320**, sa naznakom "pretplata za JSCS".

Nota: Radovi čiji su svi autori članovi SHD prioritetno se publikuju.

Odlukom Odbora za hemiju Republičkog fonda za nauku Srbije, br. 66788/1 od 22.11.1990. godine, koja je kasnije potvrđena odlukom Saveta Fonda, časopis je uvršten u kategoriju međunarodnih časopisa (**M-23**). Takođe, aktom Ministarstva za nauku i tehnologiju Republike Srbije, 413-00-247/2000-01 od 15.06.2000. godine, ovaj časopis je proglašen za publikaciju od posebnog interesa za nauku. **Impact Factor** časopisa objavljen 28. juna 2023. godine je **1,000**, a petogodišnji **Impact Factor 1,100**.

This issue is an In Memoriam issue dedicated to late Professor Dragan Veselinović

Publication of this issue is financially co-supported by

University of Belgrade
Faculty of Physical Chemistry

Универзитет у Београду
Факултет за физичку хемију

University of Belgrade
Faculty of Chemistry

UNIVERSITY OF BELGRADE
FACULTY OF CHEMISTRY

Anahem laboratorija
Belgrade

Anahem Laboratorija

Institut Mol d.o.o.
Stara Pazova

INSTITUT MOL d.o.o.

Journal of the Serbian Chemical Society
JSCS-info@shd.org.rs • www.shd.org.rs/JSCS

J. Serb. Chem. Soc. Vol. 89, No. 12 (2024)

CONTENTS*

Published by the Serbian Chemical Society
Karnegijeva 4/III, P.O. Box 36, 11120 Belgrade, Serbia
Printed by the Faculty of Technology and Metallurgy
Karnegijeva 4, P.O. Box 35-03, 11120 Belgrade, Serbia

* For colored figures in this issue please see electronic version at the Journal Home Page: http://www.shd.org.rs/JSCS/

Journal of the Serbian Chemical Society
JSCS-info@shd.org.rs • www.shd.org.rs/JSCS

EDITORIAL

Our respected and dear colleague Professor Veselinović passed away on May 8 of this year, at the age of 94.

Professor Dragan Veselinović was born on November 12, 1930, and that, as he used to say – due to circumstances, in Niš, where his parents, Angelina and Stevan, natives of Užice, were on duty. His father, a judge, died when Dragan was 9 months old, so he didn't even remember him. Together with their mother, who was a jurist, they moved to Belgrade in 1933. where they mostly spent the pre-war, war and post-war years.

He began his studies at the Faculty of Science and Mathematics, first in mathematics department, in 1949 and soon, thanks to the name of Pavle Savić, he continued his studies in the department of physical chemistry, where he graduated in 1954. He was employed at the Department of Physical Chemistry at the PMF in 1955 and spent his entire working life in physical chemistry, later under different organizational names, and remained scientifically active for more than 20 years after his retirement.

He defended his doctoral dissertation named „Complex compounds of ascorbic acid and metal ions" in 1965, and for its scientific contribution, he and his mentor, academician Milenko Šušić, were awarded in 1966. by the October Award of the City of Belgrade. It is just one of the awards and recognitions that prof. Veselinović got.

During his teaching and scientific work, he went through all associate and teaching positions - from assistant to full professor. Apart from the home Faculty of Physical Chemistry and the University of Belgrade, prof. Veselinović made a great teaching and scientific contribution to other faculties and universities: Faculties of Chemistry, Physics and Pharmacy in Belgrade, Faculty of Science (earlier Philosophy) in Niš, Faculty of Philosophy in Priština, Faculty of Science and Mathematics in Kragujevac.

Prof. Veselinović dealt with numerous scientific fields, but we would like to single out: physical chemistry of complex compounds, electroanalytical chemistry, and especially environmental physical chemistry in which he was one of the pioneers in our region. He published more than 150 papers in domestic and foreign scientific journals, presented more than 400 papers at scientific meetings

in the country and abroad, managed 12 projects for the needs of the Ministry of Science, as well as for the needs of the production companies and the military.

Pedagogical work of prof. Veselinović was also rich: he supervised the researche within 82 diploma works, 10 specialist works, 16 master's theses and 15 doctoral dissertations. A large number of successful experts, teachers in primary and secondary schools and university professors are proud to consider themselves as his students. He was the co-author of 6 high school textbooks in the field of environmental protection, as well as 3 university textbooks that are still used in teaching today.

In addition to the October Award of the City of Belgrade, he was awarded by the Order of Labor with a Golden Wreath in 1986. He was also the recipient of awards and recognitions from the faculties of several universities as well as professional associations, factories, state bodies, as well as the Serbian Chemical Society for his lasting and outstanding contribution to science. He was very proud of the Gramat of Patriarch Irinej of Serbia for his selfless love and zeal for the Serbian Orthodox Church and the Gramat of the Patriarchate of Jerusalem issued by Patriarch Theophilus of Jerusalem for the dedication to the holy places of the city of Jerusalem.

During his life, Dragan Veselinović was a sincere believer and was distinguished by all Christian virtues: he lived modestly, virtuously, morally, he was philanthropic, patient, loyal, zealous. He donated his family house, one of the oldest in Užice, which was originally built in 1862, and was later extended and renovated, to the Užice Church Municipality for church purposes. Church and town ceremonies, lectures and exhibitions are held in the donated restored house, which partly serves as a parish house.

Guest Editors,
Ljubiša Ignjatović
Branimir Jovančićević

Journal of the Serbian Chemical Society
JSCS@tmf.bg.ac.rs • www.shd.org.rs/JSCS
J. Serb. Chem. Soc. *89* (12) 1527–1541 (2024)
JSCS–5804
Original scientific paper
Published 26 December, 2024

Effects of persistent organic pollutants and mercury in protected area „Obrenovački zabran"

SNEŽANA ŠTRBAC[1], MILICA KAŠANIN-GRUBIN[1]*, JELENA STAJIĆ[2], NATAŠA STOJIĆ[3], SANJA STOJADINOVIĆ[1#], NEVENA ANTIĆ[1] and MIRA PUCAREVIĆ[3]

[1]*Institute of Chemistry, Technology and Metallurgy, University of Belgrade, Belgrade, Serbia,* [2]*Institute for Information Technologies, University of Kragujevac, Kragujevac, Serbia and* [3]*Faculty of Environmental, Educons University, Sremska Kamenica, Serbia*

(Received 4 September, revised 18 November, accepted 2 December 2024)

Abstract: This study aims to assess and monitor the health of an urban protected area by analysing the levels of persistent organic pollutants (POPs) and mercury (Hg) in soil and sediments. Based on the results, the detected concentrations of organochlorine pesticides (OCPs), polychlorinated biphenyls (PCBs), polycyclic aromatic hydrocarbons (PAHs) and Hg are above the threshold maximum values for soils and the prescribed target values for sediments. In the investigated protected area PCBs pose a very high ecological risk. The presence of 16 priority PAHs in analysed soils and sediments poses a moderate to high cancer risk and Hg poses a considerable health risk to children. The research suggests that preserving urban protected areas is crucial for environmental and urban sustainability. In urban environments these areas should be evaluated in terms of their environmental, eco-geochemical, economic and socio-cultural dimensions. The value of the existence of this natural oasis lies in its aesthetic and psycho-hydrological impact, local climate regulation, residential isolation and significant art-architectural and horticultural shaping. The interconnection between eco-geochemical and management practices, planning, and urban green spaces policy should become an adopted innovation in the cities in the future.

Keywords: mercury; organochlorine pesticides; polybrominated diphenyl ethers; polychlorinated biphenyls; polycyclic aromatic hydrocarbons.

INTRODUCTION

Today half of humanity lives in urban areas. According to the prediction, the urban population will increase to 68 % by 2050.[1] Protected areas with distinct environmental qualities in urban areas require special protection measures. They

* Corresponding author. E-mail: milica.kasanin@ihtm.bg.ac.rs
# Serbian Chemical Society member.
https://doi.org/10.2298/JSC240904101S

provide ecosystem services such as nutrient cycling, climate regulation, infiltration and stabilization of groundwater levels, retention of flood waters and recreational activities.[2]

When pollutants reach the environment, the effects on the ecosystems and their services will depend on a range of factors, such as persistence, mobility, and their bioavailability. The monitoring of polluting substances can contribute to the prevention and elimination of the consequences of degradation processes. The presence of persistent organic pollutants (POPs) and mercury (Hg) in the environment is of great concern, due to their toxicity and ability to accumulate in organisms.[3] The POPs and Hg can biomagnify in the food chain, leading to the increased concentrations and potential adverse effects in organisms at the top of the food chain.[3]

Among the most important synthetic POPs, organochlorine pesticides (OCPs) and polychlorinated biphenyls (PCBs) are universal environmental pollutants.[4] As agricultural chemicals, especially disease control chemicals, OCPs are widely used worldwide. Due to high toxicity and long-term environmental accumulation, OCPs are prohibited from use.[5,6] Since the 1930s, PCBs, due to their properties have found wide application as ideal additives for insulators in electrical equipment.[7] Although PCBs production was banned from the 1970s to the 1980s in most countries, their environmental concentrations are still high in many areas worldwide.[8] In the environment PCBs lead to a public health concern and a decline in wildlife since they are highly persistent, bioaccumulative and toxic.[9–11] The polybrominated diphenyl ethers (PBDEs) are industrial chemicals (flame retardants) that have been used for over 40 years. There are 209 congeneric PBDEs.[12] PBDEs can cause environmental pollution and human health problems.[13,14] The polycyclic aromatic hydrocarbons (PAHs) are of particular concern among pollutants, especially in urban areas. The PAHs have been intensively studied in various parts of the environment as a group of organic pollutants that are carcinogenic, mutagenic, and teratogenic.[15,16]

Hg is released into the environment from natural and anthropogenic sources.[17] Hg undergoes chemical transformations (primarily by microbiological processes) in the environment and can be changed from inorganic into methylmercury, which can accumulate in living organisms (bioaccumulation) and concentrate up the food chain (biomagnification), especially in the aquatic one.

This study aims to assess and monitor the health of an urban protected area by analysing the levels of POPs and Hg in soil and sediments. The research hypothesis is that preserving urban protected areas is crucial for environmental and urban sustainability. This research chose a protected area „Obrenovački zabran" (OZ, Fig. S-1 of Supplementary material to this paper), Serbia, as a case study.

EXPERIMENTAL

Following a combination of a sieve and sedimentation test determination of particle size distribution was done.[18] Soil organic matter (OM) weight percent was determined using the loss on ignition (*LOI*) method.[19] Sharing OM content with the conventional "Van Bemmelen factor" of 1.724 total organic carbon (*TOC*) content was calculated.[20]

For the simultaneous analysis of multiple compounds (OCPs, PCBs, PBDEs and PAHs) QuEChERS analysis was used. Into 50 ml polypropylene centrifugal tubes were weighed 5 g of sample, 10 ml of water, and 10 ml of acetonitrile. CHROMABOND QuEChERS Mix I, Extraction, EN 15662, 6.5 g were added to the suspension. The tube was centrifuged and the aliquot was placed in the freezer. The cold extract was purified by CHROMABOND QuEChERS Mix VI, Clean-up, EN 15662, 1.2 g. The aliquot was evaporated to almost dry and reconstituted with acetone for gas chromatography (GC) analysis and acetonitrile for liquid chromatography (HPLC) analysis. The OCPs and PBDEs were analysed by GS with an electron capture detector (GC–ECD). The analysis of PCBs was performed by GC with a mass spectrometry detector (GC–MS). The PAHs were analysed by HPLC with a diode array detector (HPLC–DAD). The methodology of the sample preparation, quantification of POPs, and quality control assurance was described in detail in a previous publication.[20]

For total Hg content, the samples were analysed using direct mercury analyzer DMA 80 Milestone. The Mercury Atomic Absorption Standard (ref. N: AA34N-1) from AccuStandard manufacturer was used as certified reference material.

To test the differences between studied sites in the content of POPs, TOC values, as well as the particle size distribution principal component analysis (PCA) was performed. A more profound comprehension, of the perspective trend of the POPs content feature profile, was realized by embracing the grouped samples' PCA plot. The unrooted cluster tree was performed to visually investigate the likenesses among various samples. Origin 2021 software (OriginLab Corporation, Northampton, MA, USA) was used for the statistical study of the data.

RESULTS AND DISCUSSION

Soil and sediment properties

The *TOC* content ranged from 8.69 to 13.58 % with a mean value of 11.59 % and a median value of 12.16 % in soil samples, and from 4.92 to 5.76 % with a mean value of 5.37 % and a median value of 5.41 % in sediment samples. Particle size data for the 12 sites showed that the majority of samples comprise fine sands (≈ 70 %), silt (≈ 20 %) and clay (≈ 10 %).

Organochlorine pesticides (OCPs) in soil and sediments

The total concentrations of $\sum_{20}$OCP in soil samples in the study area range from not detected (n.d.) to 740 μg kg^{-1}, and in sediment samples from 120 to 330 μg kg^{-1}. The coefficient of variation (*CV*) of $\sum_{20}$OCP in soil and sediment samples was 58.82 %, which indicates that there is no considerable variation in the content of OCPs in the OZ region.

Among the total concentrations of $\sum_{20}$OCP, endrin aldehyde, and endrin ketone accounted for the largest share. The Endrin aldehyde and the endrin ketone were found in concentrations of n.d. to 190 μg kg^{-1} and n.d. to 120 μg kg^{-1} in

soil, and of 40 to 180 μg kg^{-1} and n.d. to 70 μg kg^{-1} in sediment samples. The endrin aldehyde and the endrin ketone were never commercial products but occurred as impurities of endrin or as degradation products.[22] In 1951, endrin was first used as a rodenticide, insecticide, and avicide to control voles, cutworms, grasshoppers and other pests on tobacco, cotton, sugarcane, grain and apple orchards.[23] However, endrin has never been used for termite proofing or other applications in urban areas, unlike aldrin/dieldrin.[23] The main reason for discontinuing its use is endrin's toxicity to non-target populations of raptors (birds of prey) and migratory birds. The detected concentrations of endrin in the samples may indicate their earlier application.[22] Aldrin was determined on sites M3 and S5, endrin at site M7, and dieldrin was determined only in soil samples (average concentration 70 μg kg^{-1}). Aldrin is very easily metabolized into dieldrin, as the concentrations of dieldrin in soil samples are higher, the detected concentrations of aldrin in the samples may indicate their earlier application.

The OCPs such as HCHs and DDTs were extensively used in agriculture and forestry.[24,25] The concentrations of $\sum_4$HCH in soil and sediment samples are presented in Fig. 1.

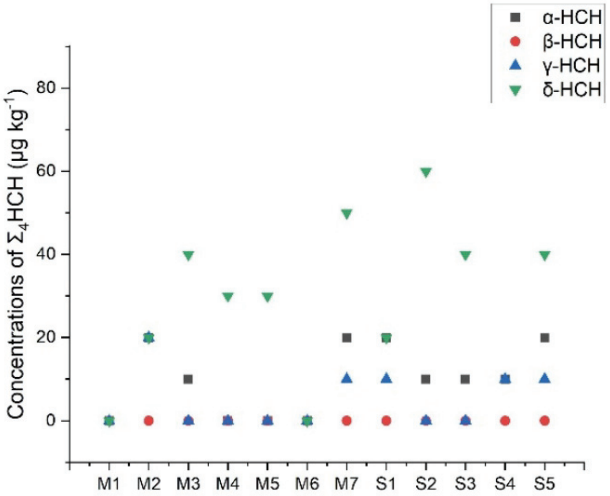

Fig. 1. The concentrations of $\sum_4$HCH (μg kg^{-1}) in sediment samples from the Sava River (S1–S5) and soil samples that are flooded at high Kolubara River groundwater levels (M1–M7).

In the soil samples, the concentration of $\sum_4$HCH ranged from n.d. to the highest levels found at the sites M6 100 μg kg^{-1}. The sediment samples showed lower $\sum_4$HCH concentrations (n.d. – 60 μg kg^{-1}). Among the HCH isomers, *δ*-HCH makes up the largest share, while *β*-HCH was n.d. in the samples (Fig. 2). The residues of *δ*-HCH could be used as indicators of the historical usage of HCHs.[26] The absence of *β*-HCH in the samples could potentially be explained by

the fact that the isomerization of γ- to α- and then α- to β-HCH didn't happen.[27,28] Lindane and technical HCH are two formulations of the pesticide HCHs that are commercially available. The α-/γ-HCH isomer ratio can be used to distinguish the source of HCHs. The α-/γ-HCH isomer ratio < 3 indicates that HCHs mainly originate from the input of lindane. The α-/γ-HCH isomer ratio > 7 indicates that HCHs probably originated from industrial HCH and the contaminants have been degraded over a long period. In this study, the isomeric HCH composition indicates that the main source of HCHs is lindane (α-/γ-HCH ratio < 3).

In the soil samples concentration of $\sum_3$DDT ranges between n.d. to 70 μg kg^{-1} (highest level at site M3), and sediment samples between 10 to 50 μg kg^{-1} (highest level at site S1). The 4,4′-DDT was the predominant compound in soil samples, followed by 4,4′-DDE, while 4,4′-DDD was n.d. In sediment samples, 4,4′-DDE and 4,4′-DDD were n.d. not in any sample. Lower concentrations of DDE and DDD and the high concentration of DDT in the samples indicate recent use of this pesticide.[29–31]The ratio $\sum$DDE + $\sum$DDD)/$\sum$DDTs > 0.5 suggests that accumulated DDT has undergone long-term degradation; whereas a lower ratio indicates recent DDT input. In this study, the ratio between the transformation products ($\sum$DDE +$\sum$DDD) and $\sum$DDTs also indicate recent DDT input. This most likely happened due to the illegal use of DDT for agricultural purposes and for controlling vector-borne diseases in the region. In the OZ region, DDT was not approved for further use in agriculture in the period 1971–1973, and in 1989 DDT was banned in forestry, until 1994 it was still used in public health.

Industrial endosulfan contains two main components α- and β-endosulfan in a ratio of 7:3. Since α-endosulfan was determined only in soil samples at site M7, β-endosulfan was detected in soil samples at sites M4, M6, and M7, and endosulfan sulphate was detected in soil with an average concentration of 32 μg kg^{-1} it is suggested that there is no new input of endosulfan in the region, and that the detected concentrations mainly originates from the historical use of endosulfan that may have been degraded to endosulfan sulphate. The main source of trans and cis chlordane in the environment is industrial chlordane. Its main components include 11 % cis chlordane, 13 % trans chlordane, 5 % heptachlor and 5 % heptachlor-epoxide. In this study, there is no recent or historical use of chlordane since chlordane and metabolites were n.d. In the soil samples, the methoxychlor concentrations ranged between n.d. to 140 μg kg^{-1}, and in the sediment samples concentrations ranged between n.d. to 10 μg kg^{-1}. Methoxychlor is an OCP that has been used as a replacement for DDT.

To assess ecotoxicological risks associated with OCP contamination, determined concentrations were compared with national soil and sediment quality guidelines.[32,33] The detected concentrations of OCPs are above the threshold the maximum values for soil, and the prescribed target values for sediments. Due to the existence of larger areas under crops near the OZ, it is to be expected that the

increased use and the spreading of herbicides, pesticides, and other protective chemical agents would occur. Beetles and bats of OZ, as carnivores of the first order consumers, are particularly sensitive to chemical measures in agriculture and the use of insecticides. The accumulation of chemicals in the body of consumers can have a lethal effect, which is transmitted through trophic chains to higher-order consumers.

Polychlorinated biphenyls in soil and sediments

The CV of PCBs in soil and sediment samples was 141.42 %, which indicates that there is considerable variation in the content of PCBs in the OZ region and a high degree of their local enrichment in soil samples (sites M4 and M7). The $\sum_6$PCB in soil samples was in the range between n.d. and 340 μg kg^{-1}, peaking at site M4. The results demonstrated the presence of lower PCB congeners (PCB-28 and PCB-52). Higher concentrations of lower PCB congeners are probably the result of the atmospheric deposition rates.[34–36] Since they are more volatile, PCB congeners with lower chlorine content can be transported through the atmosphere and deposited at long distances from the emission source.[37]

Although earlier research has shown that river sediment acts as a sink for PCBs[38] in this study, PCBs were n.d. in the sediment samples. The reason for not determining PCBs in sediments from the Sava River can be caused by changes in river flow rate (small movement), depth, direction, breadth and other morphodynamical factors in the investigated area.[39,40]

Considering that PCBs were n.d. in the sediment samples the national soil quality guideline[33] was used to estimate the contaminants in the OZ region. The $\sum_6$PCB in soil samples are above the threshold maximum values for soil (20 μg kg^{-1}).

To estimate the ecological risk posed by PCBs Hakanson's potential ecological risk index (Er^i) was used.[41,42] The Er^i was calculated normalized concentration using PCB background concentration (10 μg kg^{-1}) and using a toxicity factor of 40.[42] Samples with $Er^i < 40$ have low potential ecological risk, $40 \leq Er^i < 80$ moderate potential ecological risk, $80 \leq Er^i < 160$ considerable potential ecological risk; $160 \leq Er^i < 320$ high potential ecological risk, and with $Er^i \geq 320$ have very high ecological risk. In the OZ region, PCBs pose a very high ecological risk.

Polybrominated diphenyl ethers in soil and sediments

The CV of PBDEs in soil and sediment samples was 94.28 %, which indicates that there is considerable variation in the content of PBDEs in the OZ region and a high degree of their local enrichment in soil samples (sites M4 and M7).

The concentrations of the $\sum_8$PBDE in soil samples ranged from 60 to 170 μg kg^{-1}, and in sediment samples from 10 to 20 μg kg^{-1}. The PBDE-209 was the predominant congener in the soil and sediment samples. This congener is normally detected in high concentrations in soil in e-waste sites.[3] Environmentally unsound management of e-waste results in soil contamination and could lead to the diffusion of PBDEs from the point pollution source to contaminate the surrounding environment about 5 km from the dumpsites.[43] The possibility of PBDEs from the e-waste recycling area diffusing into the ambient regions could result in a halo pattern of PBDEs contamination to at least 74 km radius.[44] The influence of point pollution sources on the surrounding environment has been termed the "halo effect".[44] The presence of PBDEs in soils from the territory of OZ is probably the consequence of the uncontrolled disposal of e-waste.

National soil and sediment quality guidelines[32,33] do not prescribe threshold maximum values for soils and the prescribed target values for sediments.

Polycyclic aromatic hydrocarbons in soil and sediments

Sixteen target PAHs were detected in all the samples, suggesting the wide distribution of PAHs in the urban stream. The CV of PAHs in soil and sediment samples was 55.19 %, which indicates that there is no considerable variation in the content of PAHs in the OZ region. The $\sum_{16}$PAH in soil samples ranged from 850 to 8880 μg kg^{-1} (mean = 44740 μg kg^{-1}, median = 3910 μg kg^{-1}), and in sediment samples from 7860 to 14620 μg kg^{-1} (mean = 10202 μg kg^{-1}, median = 8780 μg kg^{-1}). The sum of 7 probable human carcinogenic PAHs ($\sum_7$CPAH: BaA, CHR, BbF, BkF, BaP, IND and dBahA)[45] varied from 100 to 570 μg kg^{-1} (mean = 418 μg kg^{-1}, median = 445 μg kg^{-1}) indicating moderate contamination ($\sum_7$CPAH ranging from 100 to 1000 μg kg^{-1}).[46]

PAHs are primarily released into the environment from petrogenic, pyrogenic and biogenic sources.[47] To investigate the potential sources of PAHs diagnostic ratios methods have been widely used.[48] Commonly used diagnostic ratios include ANT/(ANT+PHE), IND/(IND+BghiP), BaA/(BaA+CHR) and FLT/ /(FLT+PYR).[49] In this study, the ratios of IND/(IND+BghiP) were in the range of 0.5–1 (combustion), the ratios of ANT/(ANT+PHE) were above 0.5 (combustion), the ratios of BaA/(BaA+CHR) were above 0.6 (combustion), and the ratios of FLT/(FLT+PYR) were above 0.6 (biomass/coal combustion) (Fig. 2).

In the OZ region according to the results, PAHs in soil and sediments mainly come from pyrogenic sources. In the wider surroundings of the observed area, there is a high number of pollution sources. Here, above all, we mean the thermal power plant, which is located about 500 m southeast of OZ and the centre of the urban area. Since most sources of PAHs are located in, or near urban centres, PAHs are usually found in high concentrations in aquatic sediments[50,51], which is also the case in this research.

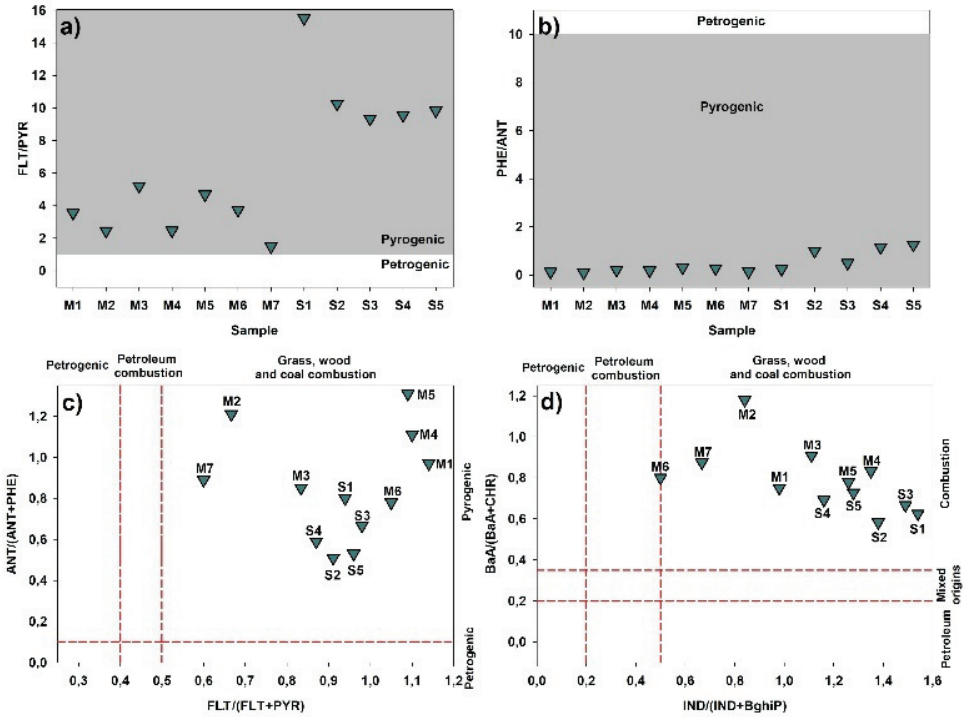

Fig. 2. Molecular relations used for identifying sources of PAH emissions in sediment samples from the Sava River (S1–S5) and soil samples that are flooded at high Kolubara River groundwater levels (M1–M7).

To assess ecotoxicological risks associated with PAHs contamination, the determined concentrations were compared with the national soil and sediment quality guidelines.[32,33] The detected concentrations of PAHs are above the threshold maximum values for soils, and the prescribed target values for sediments (1000 μg kg^{-1}).

Health risk induced by the presence of PAH congeners in the soils can be estimated by calculation of incremental lifetime cancer risk (*ILCR*) associated with three pathways of exposure: oral ingestion – *ILCR*ing, dermal contact – *ILCR*derm and inhalation – *ILCR*inh.[52–54] All the parameters used for *ILCR*s calculation are given in Table S-I.

Table S-II presents *ILCR*s and total cancer risks (TCR_{PAH}) for children and adults. TCR_{PAH} in soils ranged from 6.1×10^{-4} to 2.9×10^{-3} for adults and from 6.9×10^{-4} to 3.3×10^{-3} for children. The *ILCR* values can be interpreted as follows: *ILCR*s $\leq 10^{-6}$ indicate negligible risk, *ILCR*s in the range of 10^{-6}–10^{-4} are treated as low risk, *ILCR*s from 10^{-4} to 10^{-3} are considered moderate, and the values between 10^{-3} and 10^{-1} indicate a high health risk to the population.[54] The

presence of 16 priority PAHs in analysed soils and sediments poses moderate to high cancer risk to the population (Table S-II).

Total Hg in soil and sediments

Total Hg concentrations ranged from 0.29 to 3.20 mg kg^{-1} (mean 2.20 mg kg^{-1}, median 2.26 mg kg^{-1}) in soil samples, and from 2.78 to 3.24 mg kg^{-1} (mean 3.05 mg kg^{-1}, median 3.12 mg kg^{-1}) in sediment samples. The results demonstrated a relatively high Hg concentration in the study area. However, the distribution of Hg in sediments of the Sava River was studied in more detail. The elevated Hg concentration is partly the consequence of a geological anomaly, that is, a natural Hg enrichment of the upstream Slovenian drainage basins of the Sava River.[60] Earlier research found a 100-fold Hg enrichment in deep overbank sediments, as compared to the surface sediment, and attributed this to an even higher Hg input from the Slovenian catchment area in the past. As the number of samples taken during this screening is limited, definite conclusions on Hg contamination levels will have to wait for more detailed research.

Health risks induced by Hg in soils were estimated by applying the model proposed by the United States Environmental Protection Agency (US EPA).[61] Three possible mechanisms of exposure were considered (ingestion, inhalation and dermal contact) to assess carcinogenic and non-carcinogenic risks from Hg. The methodology of risk determination was described in detail in a previous publication.[62]

Non-carcinogenic risk was estimated through hazard quotients (*HQ*) for ingestion (*HQ*ing), inhalation (*HQ*inh) and dermal exposure (*HQ*der). The descriptive statistics of these quotients are shown in Table S-III for both children and adults.

The effect of soil Hg pollution intake through inhalation is negligible compared to ingestion and dermal exposure. Summing up *HQ*s from all three exposure pathways' hazard indexes *HI* were obtained. A hazard index higher than 1 implies an increased possibility of incidence of non-carcinogenic harmful health effects.[61] Hg in the analysed soil poses a considerable health risk to children who are generally more sensitive to environmental pollution than adults.

To assess ecotoxicological risks associated with Hg contamination, determined concentrations were compared with national soil and sediment quality guidelines.[31,33] The detected Hg concentrations are above the threshold maximum values for soils, and the prescribed target values for sediments (0.3 mg kg^{-1}).

Differences between studied sites

The cluster analysis engaged the complete linkage algorithm and the City block (Manhattan) distances to estimate the proximity of the samples (Fig. S-2 of the Supplementary material). The linkage distance, between the main clusters

was substantial, approximately 8500. Samples M4 and M5 were the most similar, as the samples M6 and M7. Furthermore, the height of the dendrogram indicates the order in which the clusters were joined. The dendrogram shows the big difference between the cluster of soil (M1–M7) and sediment (S1–S5) samples, indicating that the two groups of samples differ in chemical properties, particularly different POP concentrations.

The parting within samples can be seen from the PCA analysis (Fig. 3A–D). Samples M4 and M7 are separated according to the highest concentrations of OCPs. Predominant congener PCB-52 and PBDE-209 were in soil sample M4. The sediment samples were differentiated by PAH concentrations.

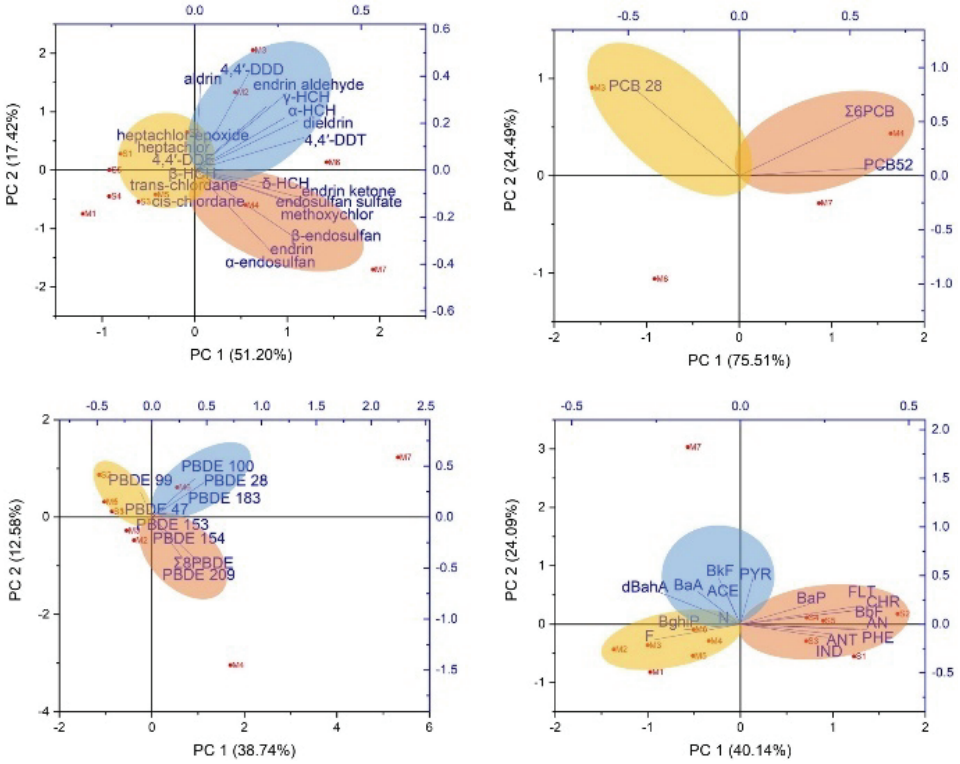

Fig. 3. The PCA biplot diagram describes the relations between the contents of POPs, Hg, soil and sediment properties in sediment samples from the Sava River (S1–S5) and soil samples that are flooded at high Kolubara River groundwater levels (M1–M7).

CONCLUSION

Based on the results, the detected concentrations of OCPs, PCBs, PAHs and Hg are above the threshold maximum values and the prescribed target values for sediments for the soils analysed in this reseach. In the OZ region, PCBs pose a very high ecological risk. The presence of 16 priority PAHs in analysed soils and

sediments poses a moderate to high cancer risk to the population, and Hg poses a considerable health risk to children who are generally more sensitive to environmental pollution than adults. Based on the results, the protected areas in urban environments should receive special attention and should be evaluated regarding their environmental, eco-geochemical, economic and socio-cultural dimension. One of the reasons for this is that the protected area is particularly affected by human action most often due to inferior decision making. The management strategies that incorporate socio-economic activities and the protection of urban protected areas are required for future demands. This should primarily include the valuation of ecosystem services that protected areas provide and the assessment of the pollution status. Urbanization and pollution in general can influence the ability of ecosystems to support the human population. The interconnection between management, planning, policy and overall urban green spaces policy represents a new future innovation in the cities.

SUPPLEMENTARY MATERIAL

Additional data and information are available electronically at the pages of journal website: https://www.shd-pub.org.rs/index.php/JSCS/article/view/13034, or from the corresponding author on request.

Acknowledgements. This research was supported by the Science Fund of the Republic of Serbia, No. 7043, Urban Forest Soil Indicators as a tool for Climate-Smart Forestry – UrbanFoS and has been financially supported by the Ministry of Science, Technological Development and Innovation of Republic of Serbia (Contracts No: 451-03-66/2024-03/ /200026, 451-03-66/2024-03/200378).

ИЗВОД

УТИЦАЈ ДУГОТРАЈНИХ ОРГАНСКИХ ЗАГАЂУЈУЋИХ СУПСТАНЦИ И ЖИВЕ НА ЗАШТИЋЕНО ПОДРУЧЈЕ „ОБРЕНОВАЧКИ ЗАБРАН”

СНЕЖАНА ШТРБАЦ[1], МИЛИЦА КАШАНИН-ГРУБИН[1], ЈЕЛЕНА СТАЈИЋ[2], НАТАША СТОЈИЋ[3], САЊА СТОЈАДИНОВИЋ[1], ГОРИЦА ВЕСЕЛИНОВИЋ[1] и МИРА ПУЦАРЕВИЋ[3]

[1]Институт за хемију технологију и металургију, Универзитет у Београду, Београд, [2]Институт за информационе технологије, Универзитет у Крагујевцу, Крагујевац и [3]Факултет заштите животне средине, Универзитет Едуконс, Сремска Каменица

Ова студија има за циљ да процени и прати стање урбаног заштићеног подручја анализом нивоа дуготрајних органских загађујућих супстанци (POPs) и живе (Hg) у земљишту и седиментима. На основу резултата, детектоване концентрације органохлорних пестицида (OCP), полихлорованих бифенила (PCB), полицикличних ароматичних угљоводоника (PAH) и Hg су изнад граничних максималних вредности за земљиште и прописаних циљних вредности за седименте. У истраживаном подручју концентрације PCB представљају веома висок еколошки ризик. Укупна концентрација 16 приоритетних PAH у анализираном земљишту и седиментима представља умерен до висок ризик од рака, а концентрације Hg представљају значајан здравствени ризик за децу. Истраживање је показало да је очување урбаних заштићених подручја кључно за одрживост животне средине. У урбаним срединама ове области треба вредновати у смислу њихових еколошких, еко-геохемијских, економских и социо-културних димензија. Вредност

постојања ове природне оазе је у њеном естетском и хидролошком утицају, локалној регулацији климе, стамбеној изолованости и значајном уметничко-архитектонском и хортикултурном обликовању. Повезаност између еко-геохемијских и управљачких пракси, планирања и политике урбаних зелених површина требало би да постане усвојена иновација у градовима у будућности.

(Примљено 4. септембра, ревидирано 18. новембра, прихваћено 2. децембра 2024)

REFERENCES

1. Food and Agriculture Organization of the United Nations, *Forests and Sustainable Cities*: *Inspiring stories from around the world*, FAO, 2018 (ISBN 978-92-5-130417-4) (https://openknowledge.fao.org/handle/20.500.14283/i8838en)
2. M. Kašanin-Grubin, S. Štrbac, S. Antonijević, S. Djogo Mračević, D. Randjelović, J. Orlić, A. Šajnović, *J. Environ. Manage.* **251** (2019) 109574 (https://doi.org/10.1016/j.jenvman.2019.109574)
3. R. A. Lavoie, T. D. Jardine, M. M. Chumchal, K. A. Kidd, L. M. Campbell, *Environ. Sci. Technol.* **47** (2013) 13385 (https://doi.org/10.1021/es403103t)
4. T. A. M. Tran, G. Malarvannan, T. L. Hoang, V. H. Nguyen, A. Covaci, M. Elskens, *Mar. Pollut. Bull.* **141** (2019) 521 (https://doi.org/10.1016/j.marpolbul.2019.03.006)
5. A. Mishra, J. Kumar, J. S. Melo, B. P. Sandaka, *J. Environ. Chem. Eng.* **9** (2021) 105067 (https://doi.org/10.1016/j.jece.2021.105067)
6. I. A. Saleh, N. Zouari, M. A. Al-Ghouti, *Environ. Technol. Innov.* **19** (2020) 101026 (https://doi.org/10.1016/j.eti.2020.101026)
7. Y. Shao, S. Han, J. Ouyang, G. Yang, W. Liu, L. Ma, M. Luo, D. Xu, *Environ. Sci. Pollut. Res.* **23** (2016) 24824 (https://doi.org/10.1007/s11356-016-7663-4)
8. C. A. Weitekamp, L. J. Phillips, L. M. Carlson, N. M. DeLuca, E. A. Cohen Hubal, G. M. Lehmann, *Sci. Total Environ.* **776** (2021) 145912 (https://doi.org/10.1016/j.scitotenv.2021.145912)
9. A. Remili, R. J. Letcher, F. I. Samarra, R. Dietz, C. Sonne, J. Desforges, G. Víkingsson, D. Blair, M. A. McKinney, *Environ. Sci. Technol.* **55** (2021) 4923 (https://doi.org/10.1021/acs.est.0c08563)
10. H. Shi, J. Jan, J. E. Hardesty, K. C. Falkner, R. A. Prough, A. N. Balamurugan, S. P. Mokshagundam, S. T. Chari, M. C. Cave, *Toxicol. Appl. Pharmacol.* **363** (2019) 22 (https://doi.org/10.1016/j.taap.2018.10.011)
11. J. Al-Alam, Z. Fajloun, A. Chbani, M. Millet, *Chemosphere* **168** (2017) 1411 (https://doi.org/10.1016/j.chemosphere.2016.11.103)
12. P. I. Johnson, H. M. Stapleton, B. Mukherjee, R. Hauser, J. D. Meeker, *Sci. Total Environ.* **445–446** (2013) 177 (https://doi.org/10.1016/j.scitotenv.2012.12.017)
13. M. F. Reis, in *Encyclopedia of Environmental Health*, J. O. Nriagu, Ed., Elsvier Science, Amsterdam, 2011 (ISBN 978-0-444-52272-6)
14. S. D. Shaw, A. Blum, R. Weber, K. Kannan, D. Rich, D. Lucas, C. P. Koshland, D. Dobraca, S. Hanson, L. S Birnbaum, *Rev. Environ. Health* **25** (2010) 261 (https://doi.org/10.1515/reveh.2010.25.4.261)
15. Y. Zhang, C. Peng, Z. Guo, X. Xiao, R. Xiao, *Environ. Pollut.* **254** (2019) 112930 (https://doi.org/10.1016/j.envpol.2019.07.098)
16. S. P. Maletić, J. M. Beljin, S. D. Rončević, M. G. Grgić, B. D. Dalmacija, *J. Hazard. Mater.* **365** (2019) 467 (https://doi.org/10.1016/j.jhazmat.2018.11.020)
17. N. Mikac, V. Roje, N. Cukrov, D. Foucher, *Arh. Hig. Rada Toksikol.* **57** (2006) 325 (PMID PMID: 17121005)

18. S. I. Dolgov, A. I. Michmanova, in *Agrophysical methods of soil examination*, S. I. Dolgov, Ed., Nauka, Moscow, 1966, p. 35
19. O. Heiri, A. F. Lotter, G. Lemcke, *J. Paleolimnol.* **25** (2001) 101 (https://doi.org/10.1023/A:1008119611481)
20. E. Shamrikova, B. Kondratenok, E. Tumanova, E. Vanchikova, E. Lapteva, T. Zonova, E. I. Lu-Lyan-Min, A. P. Davydova, Z. Libohova, N. Suvannang, *Geoderma.* **412** (2022) 115547 (https://doi.org/10.1016/j.geoderma.2021.115547)
21. S. Štrbac, M. Kašanin-Grubin, N. Stojić, L. Pezo, B. Lončar, R. Tognetti, M. Pucarević, *Plant Soil* **495** (2024) 313 (https://doi.org/10.1007/s11104-023-06329-4)
22. L. Joseph, S. V. Paulose, N. Cyril, S. K. Santhosh, A. Varghese, A. B. Nelson, S. V. Kunjankutty, S. Kasu, *Environ. Chem. Ecotoxicol.* **2** (2020) 1 (https://doi.org/10.1016/j.enceco.2020.01.001)
23. Hexadrin, https://pubchem.ncbi.nlm.nih.gov/compound/12358480
24. Y. Li, A. Zhulidov, R. Robarts, L. Korotova, D. Zhulidov, T. Gurtovaya, L. P. Ge, *Sci. Total Environ.* **357** (2006) 138 (https://doi.org/10.1016/j.scitotenv.2005.06.009)
25. F. Wong, H. Hung, H. Dryfhout-Clark, W. Aas, P. Bohlin-Nizzetto, K. Breivik, M. Nerentorp Mastromonaco, E. Brorström Lundén, K. Ólafsdóttir, Á. Sigurðsson, K. Vorkamp, R. Bossi, H. Skov, H. Hakola, E. Barresi, E. Sverko, P. Fellin, H. Li, A. Vlasenko, M. Zapevalov, D. Samsonov, S. Wilson, *Sci. Total Environ.* **775** (2021) 145109 (https://doi.org/10.1016/j.scitotenv.2021.145109)
26. A. Ivanova, K. Wiberg, L. Ahrens, E. Zubcov, A. Dahlberg. *Chemosphere* **279** (2021) 130923 (https://doi.org/10.1016/j.chemosphere.2021.130923)
27. V. Kumar, P. Sahu, P. K. Singh, T. Markandeya, *Int. J. Environ. Res.* **14** (2020) 653 (https://doi.org/10.1007/s41742-020-00290-1)
28. Z. Zhang, H. Hong, J. Zhou, J. Huang, G. Yu, *Chemosphere* **52** (2003) 1423 (https://doi.org/10.1016/S0045-6535(03)00478-8)
29. A. B. Kassegne, J. O. Okonkwo, T. Berhanu, A. P. Daso, O. I. Olukunle, S. L. Asfaw, *Emerg. Contam.* **6** (2020) 396 (https://doi.org/10.1016/j.emcon.2020.11.004)
30. I. N. Pérez-Maldonado, A. Trejo, C. Ruepert, Rd. C. Jovel, M. P. Méndez, M. Ferrari, E. Saballos-Sobalvarro, C. Alexander, L. Yáñez-Estrada, D. Lopez, S. Henao, E. R. Pinto, F. Díaz-Barriga, *Chemosphere* **78** (2010) 1244 (https://doi.org/10.1016/j.chemosphere.2009.12.040)
31. J. M. Aislabie, N. K. Richards, H. L. Boul, *N. Z. J. Agric. Res.* **40** (1997) 269 (https://doi.org/10.1080/00288233.1997.9513247)
32. Regulation on limit values of polluting, harmful and dangerous substances in the soil, *Sl. glasnik RS*, 30/2018 and 64/2019 (https://pravno-informacioni-sistem.rs/eli/rep/sgrs/vlada/uredba/2018/30/2/reg) (in Serbian)
33. M. Pandelova, B. Henkelmann, B. M. Bussian, K. Schramm, *Sci. Total Environ.* **610–611** (2018) 1 (https://doi.org/10.1016/j.scitotenv.2017.07.246)
34. B. Naso, D. Perrone, M. C. Ferrante, M. Bilancione, A. Lucisano, *Sci. Total Environ.* **343** (2005) 83 (https://doi.org/10.1016/j.scitotenv.2004.10.007)
35. S. A. Eqani, R. N. Malik, A. Cincinelli, G. Zhang, A. Mohammad, A. Qadir, A. Rashid, H. Bokhari, K. C. Jones, A. Katsoyiannis, *Sci. Total Environ.* **450–451** (2013) 83 (https://doi.org/10.1016/j.scitotenv.2013.01.052)
36. P. Schmid, E. Gujer, M. Zennegg, T. D. Bucheli, A. Desaules, *Chemosphere* **58** (2005) 227 (https://doi.org/10.1016/j.chemosphere.2004.08.045)

37. Q. Lu, Y. Liang, W. Fang, K. Guan, C. Huang, X. Qi, Z. Liang, Y. Zeng, X. Luo, Z. He, B. Mai, S. Wang, *Environ. Sci. Technol.* **55** (2021) 9579 (https://doi.org/10.1021/acs.est.1c01095)
38. A. Herrero, J. Vila, E. Eljarrat, A. Ginebreda, S. Sabater, R. J. Batalla, D. Barceló, *Sci. Total Environ.* **633** (2018) 1392 (https://doi.org/10.1016/j.scitotenv.2018.03.205)
39. Y. Li, J. Li, Z. Shao, Z. Duan, Y. Xie, Z. Cui, J. Li, H. Zhou, M. Chen, S. Li, C. Chen, *Water Supply* **20** (2020) 2400 (https://doi.org/10.2166/ws.2020.130)
40. L. Hakanson, *Water Res.* **14** (1980) 975 (https://doi.org/10.1016/0043-1354(80)90143-8)
41. M. Baqar, Y. Sadef, S. R. Ahmad, A. Mahmood, A. Qadir, I. Aslam, J. Li, G. Zhang, *Environ. Sci. Pollut. Res.* **24** (2017) 27913 (https://doi.org/10.1007/s11356-017-0182-0)
42. K. Oloruntoba, O. Sindiku, O. Osibanjo, C. Herold, R. Weber, *Environ. Pollut.* **277** (2021) 116794 (https://doi.org/10.1016/j.envpol.2021.116794)
43. Y. Zhao, X. Qin, Y. Li, P. Liu, M. Tian, S. Yan, Z-F. Qin, X-B. Xu, Y-J. Yang, *Chemosphere* **76** (2009) 1470 (https://doi.org/10.1016/j.chemosphere.2009.07.023)
44. P. Gao, E. da Silva, L. Hou, N. D. Denslow, P. Xiang, L. Q. Ma, *Environ. Int.* **119** (2018) 466 (https://doi.org/10.1016/j.envint.2018.07.017)
45. P. Baumard, H. Budzinski, P. Garrigues, *Mar. Pollution. Bull.* **36** (1998) 577 (https://doi.org/10.1016/S0025-326X(98)00014-9)
46. M. P. Zakaria, H. Takada, S. Tsutsumi, K. Ohno, J. Yamada, E. Kouno, H. Kumata, *Environ. Sci. Technol.* **36** (2002) 1907 (https://doi.org/10.1021/es011278+)
47. X. Wu, H. Liu, Z. Yuan, S. Wang, A. Chen, B. He, *Atmos. Pollut. Res.* **10** (2019) 1276 (https://doi.org/10.1016/j.apr.2019.02.011)
48. M. B. Yunker, R. W. Macdonald, R. Vingarzan, R. H. Mitchell, D. Goyette, S. Sylvestre, *Org. Geochem.* **33** (2002) 489 (https://doi.org/10.1016/S0146-6380(02)00002-5)
49. H. I. Abdel-Shafy, M. S.Mansour, *Egyp. J. Pet.* **25** (2016) 107 (https://doi.org/10.1016/j.ejpe.2015.03.011)
50. B. Barhoumi, M. S. Beldean-Galea, A. M. Al-Rawabdeh, C. Roba, I. M. Martonos, R. Bălc, M. Kahlaoui, S. Touil, M. Tedetti, M. Ridha Driss, C. Baciu, *Sci. Total Environ.* **660** (2019) 660 (https://doi.org/10.1016/j.scitotenv.2018.12.428)
51. N. Soltani, B. Keshavarzi, F. Moore, T. Tavakol, A. R. Lahijanzadeh, N. Jaafarzadeh, M. Kermani, *Sci. Total Environ.* **505** (2015) 712 (https://doi.org/10.1016/j.scitotenv.2014.09.097)
52. B. Škrbić, N. Đurišić-Mladenović, J. Živančev, Đ. Tadić, *Sci. Total Environ.* **647** (2019) 191 (https://doi.org/10.1016/j.scitotenv.2018.07.442)
53. S. U. A. Bhutto, X. Xing, M. Shi, Y. Mao, T. Hu, Q. Tian, C. Cheng, W. Liu, Z. Chen, S. Qi, *J. Geochem. Explor.* **226** (2021) 106769 (https://doi.org/10.1016/j.gexplo.2021.106769)
54. J. Cristale, F. S. Silva, G. J. Zocolo, M. R. R. Marchi, *Environ. Pollut.* **169** (2012) 210 (https://doi.org/10.1016/j.envpol.2012.03.045)
55. T. Mihankhah, M. Saeedi, A. Karbassi, *Ecotoxicol. Environ. Saf.* **187** (2020) 109838 (https://doi.org/10.1016/j.ecoenv.2019.109838)
56. U.S. EPA, *Exposure Factors Handbook*, 2011 ed., Final Report, U.S. Environmental Protection Agency, Washington, DC, EPA/600/R-09/052F, 2011 (https://ordspub.epa.gov/ords/eims/eimscomm.getfile?p_download_id=522996)
57. W. Wang, M. Huang, Y. Kang, H. Wang, A. O. Leung, K. C. Cheung, M. H. Wong, *Sci. Total Environ.* **409** (2011) 4519 (https://doi.org/10.1016/j.scitotenv.2011.07.030)
58. EPA, *Risk Assessment Guidance for Superfund (RAGS): Part B* (https://www.epa.gov/risk/risk-assessment-guidance-superfund-rags-part-b)

59. G. Pavlovic, D. Barisic, I. Lovrencic, V. Orescanin, E. Prohic, *Environ. Geol.* **47** (2005) 475 (https://doi.org/10.1007/s00254-004-1167-0)
60. EPA, *Superfund Soil Screening Guidance* (https://www.epa.gov/superfund/superfund-soil-screening-guidance)
61. B. Milenkovic, J. M. Stajic, T. Zeremski, S. Strbac, N. Stojic, D. Nikezic, *Chemosphere* **245** (2020) 125610 (https://doi.org/10.1016/j.chemosphere.2019.125610).

Journal of the Serbian Chemical Society
JSCS@tmf.bg.ac.rs • www.shd.org.rs/JSCS
J. Serb. Chem. Soc. *89* (12) S508–S511 (2024) *Supplementary material*

SUPPLEMENTARY MATERIAL TO

Effects of persistent organic pollutants and mercury in protected area „Obrenovački zabran"

SNEŽANA ŠTRBAC[1], MILICA KAŠANIN-GRUBIN[1]*, JELENA STAJIĆ[2], NATAŠA STOJIĆ[3], SANJA STOJADINOVIĆ[1], NEVENA ANTIĆ[1] and MIRA PUCAREVIĆ[3]

[1]*Institute of Chemistry, Technology and Metallurgy, University of Belgrade, Belgrade, Serbia,* [2]*Institute for Information Technologies, University of Kragujevac, Kragujevac, Serbia and* [3]*Faculty of Environmental, Educons University, Sremska Kamenica, Serbia*

J. Serb. Chem. Soc. *89* (12) (2024) 1527–1541

STUDY AREA

The protected area „Obrenovački zabran" (OZ) is located between the Sava and Kolubara Rivers in northwest Serbia (Fig. S-1). More precisely, with its extreme north-eastern border, OZ reaches the right bank of the Sava River, and in the south and east, it almost abuts the left bank of the Kolubara River. The OZ is located 1.5 km east of the city of Obrenovac and 12 km southwest of the suburbs of the city of Belgrade (the capital of Serbia). The total protected area is 47,77.18 ha. The whole location is specific by its hydrological, morphological, and geological characteristics. The protected area belongs to the plain terrain, i.e., the alluvial plains of the Sava and Kolubara Rivers above, which is a river terrace Lower Pliocene age, marly clay are dark gray to gray, and underlying river terrace sediments. Due to the meandering of the Sava and Kolubara Rivers during the Holocene, the formated terrace represents a common terrace for both Rivers. Five sediment samples (S1 – S5) and 7 soil samples (M1 – M7) were taken from the protected area OZ. The surface sediments and the soil were taken at a depth of 0 – 10 cm. The sediment samples were taken from the Sava River and soil samples were taken from the area that is flooded at high Kolubara River groundwater levels. The collected samples were immediately transferred into dark glass bottles and transported to the laboratory.

* Corresponding author. E-mail: milica.kasanin@ihtm.bg.ac.rs

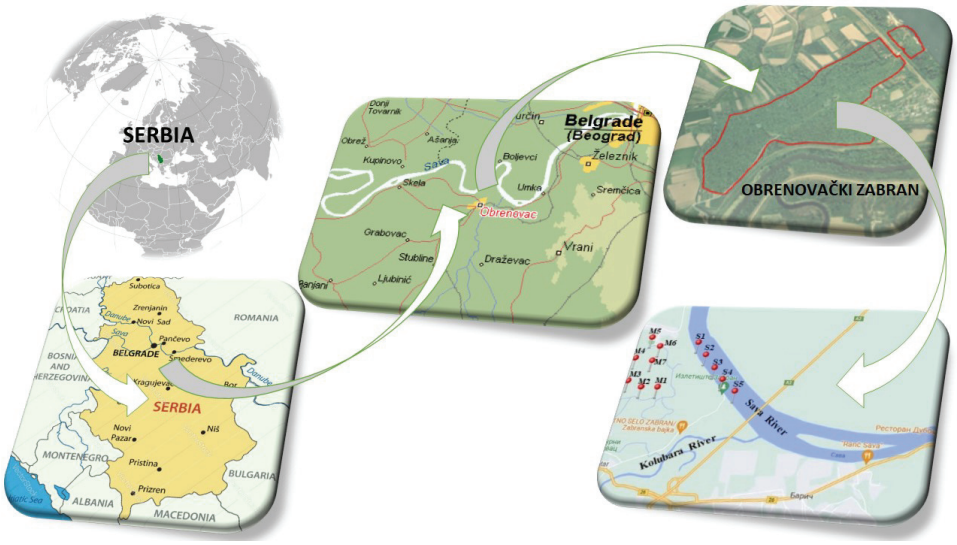

Fig. S-1. Study area of „Obrenovački zabran" with sampling locations (S1 – S5 are sediment samples, M1 – M7 soil samples).

TABLE S-I. Parameters used for incremental lifetime cancer risk (ILCR) calculation

Parameter	Description	Unit	Adults	Children	Reference
CSF_{ing}	Ingestion carcinogenic slope factor	kg d mg^{-1}	7.3	7.3	56
IR_{ing}	Ingestion rate	mg d^{-1}	100	200	57
EF	Exposure frequency	d y^{-1}	350	350	57
ED	Exposure duration	y	24	6	58
BW	Body weight	kg	70	15	59
AT	Average life span	d	25550	25550	58
CSF_{derm}	Dermal carcinogenic slope factor	kg d mg^{-1}	25	25	56
SA	Dermal surface exposure	cm^2 d^{-1}	5700	2800	57
AF	Dermal adherence factor	mg cm^{-2}	0.07	0.2	57
ABS	Dermal adsorption fraction	Unitless	0.13	0.13	57
CSF_{inh}	Inhalation carcinogenic slope factor	kg d mg^{-1}	3.85	3.85	56
IR_{inh}	Inhalation rate	m^3 d^{-1}	20	10	56
PEF	Particle emission factor	m^3 kg^{-1}	1.36×10^9	1.36×10^9	57

TABLE S-II. Incremental lifetime cancer risk (ILCR) and total cancer risk (TCR_{PAH}) from PAHs

		ADULTS				CHILDREN			
Samples		ILCRing	ILCRder	ILCRinh	TCR_{PAH}	ILCRing	ILCRder	ILCRinh	TCR_{PAH}
	M1	2.2E-04	3.9E-04	1.7E-08	6.1E-04	3.1E-04	3.8E-04	5.9E-09	6.9E-04
	M2	4.7E-04	8.3E-04	3.6E-08	1.3E-03	6.6E-04	8.2E-04	1.3E-08	1.5E-03
	M3	5.9E-04	1.0E-03	4.6E-08	1.6E-03	8.2E-04	1.0E-03	1.6E-08	1.8E-03
	M4	3.5E-04	6.3E-04	2.8E-08	9.9E-04	5.0E-04	6.2E-04	9.6E-09	1.1E-03
	M5	5.1E-04	9.0E-04	3.9E-08	1.4E-03	7.1E-04	8.8E-04	1.4E-08	1.6E-03
	M6	2.2E-04	3.9E-04	1.7E-08	6.1E-04	3.0E-04	3.8E-04	5.9E-09	6.9E-04
	M7	1.0E-03	1.9E-03	8.1E-08	2.9E-03	1.5E-03	1.8E-03	2.8E-08	3.3E-03
	S1	3.1E-04	5.5E-04	2.4E-08	8.6E-04	4.3E-04	5.4E-04	8.4E-09	9.7E-04
	S2	4.1E-04	7.2E-04	3.2E-08	1.1E-03	5.7E-04	7.1E-04	1.1E-08	1.3E-03
	S3	3.3E-04	5.8E-04	2.5E-08	9.0E-04	4.5E-04	5.7E-04	8.8E-09	1.0E-03
	S4	5.7E-04	1.0E-03	4.4E-08	1.6E-03	8.0E-04	1.0E-03	1.5E-08	1.8E-03
	S5	6.4E-04	1.1E-03	5.0E-08	1.8E-03	9.0E-04	1.1E-03	1.7E-08	2.0E-03
Soil	Min	2.2E-04	3.9E-04	1.7E-08	6.1E-04	3.0E-04	3.8E-04	5.9E-09	6.9E-04
	MAX	1.0E-03	1.9E-03	8.1E-08	2.9E-03	1.5E-03	1.8E-03	2.8E-08	3.3E-03
	Average	4.9E-04	8.6E-04	3.8E-08	1.3E-03	6.8E-04	8.5E-04	1.3E-08	1.5E-03
	SD	2.8E-04	5.0E-04	2.2E-08	7.9E-04	4.0E-04	4.9E-04	7.7E-09	8.9E-04
	Median	4.7E-04	8.3E-04	3.6E-08	1.3E-03	6.6E-04	8.2E-04	1.3E-08	1.5E-03
Sediment	Min	3.1E-04	5.5E-04	2.4E-08	8.6E-04	4.3E-04	5.4E-04	8.4E-09	9.7E-04
	MAX	6.4E-04	1.1E-03	5.0E-08	1.8E-03	9.0E-04	1.1E-03	1.7E-08	2.0E-03
	Average	4.5E-04	8.0E-04	3.5E-08	1.3E-03	6.3E-04	7.9E-04	1.2E-08	1.4E-03
	SD	1.5E-04	2.7E-04	1.2E-08	4.2E-04	2.1E-04	2.6E-04	4.0E-09	4.7E-04
	Median	4.1E-04	7.2E-04	3.2E-08	1.1E-03	5.7E-04	7.1E-04	1.1E-08	1.3E-03

TABLE S-III. Non-cancer and cancer health risks from Hg in soil (samples M1 – M7)

		NON-CANCER RISK							
		HQing		HQinh		HQder		HI	
		Child	Adult	Child	Adult	Child	Adult	Child	Adult
Hg	Mean	9.4E-02	1.0E-02	9.2E-06	2.7E-05	5.8E-02	7.7E-03	1.5E-01	1.8E-02
	Min	1.2E-02	1.3E-03	1.2E-06	2.3E-05	7.6E-03	1.0E-03	2.0E-02	2.4E-03
	Max	1.4E-01	1.5E-02	1.3E-05	3.3E-05	8.4E-02	1.1E-02	2.2E-01	2.6E-02

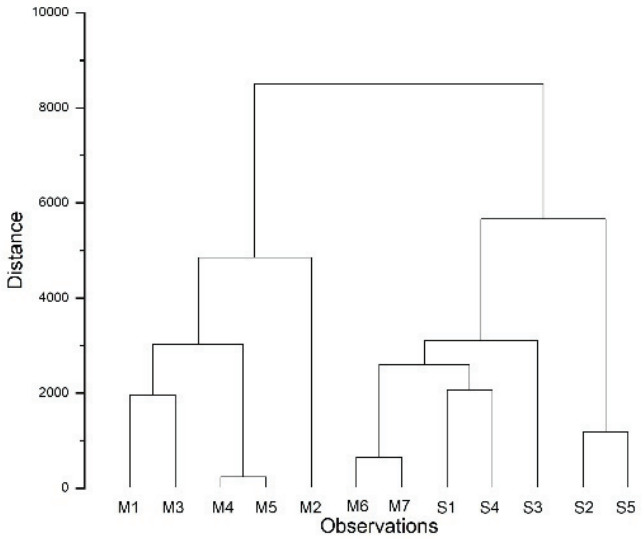

Fig. S-2. Cluster analysis of observed sediment samples from the Sava River (S1 – S5) and soil samples (M1 – M7) that are flooded at high Kolubara River groundwater levels.

Journal of the Serbian Chemical Society
JSCS@tmf.bg.ac.rs • www.shd.org.rs/JSCS
J. Serb. Chem. Soc. *89* (12) 1543–1557 (2024)
JSCS–5805
Original scientific paper
Published 26 December, 2024

Atmospheric deposition of potentially toxic elements over the territory of Serbia assessed by moss biomonitoring in five-year time: 2015 *vs.* 2020

MIRA P. ANIČIĆ UROŠEVIĆ[1]*, DRAGAN V. RADNOVIĆ[2], MILOŠ M. ILIĆ[2], MIODRAG D. KRMAR[2], IGOR D. KODRANOV[3], DUBRAVKA J. RELIĆ[3] and ALEKSANDAR R. POPOVIĆ[3#]

[1]*Institute of Physics Belgrade, University of Belgrade, Pregrevica 118, Belgrade, Serbia,* [2]*Faculty of Science, University of Novi Sad, Trg Dositeja Obradovića 4, Novi Sad, Serbia and* [3]*Faculty of Chemistry, University of Belgrade, Studentski trg 12–16, Belgrade, Serbia*

(Received 10 January, revised 20 January, accepted 6 April 2024)

Abstract: The presented research, performed under the framework of the ICP Vegetation program in Serbia, had a goal to provide field-based evidence of spatial patterns and temporal trends of some potentially toxic element deposition, using naturally growing moss (*Hypnum cupressiforme*), as a biomonitor in surveys conducted in 2015 and 2020. The results showed a decline of the element concentrations in the moss with time for Cr (42 %), Cu (39 %), Fe (22 %), Pb (10 %) and Zn (54 %), a decrease for Cd (18 %), while staying at the same level for As and V. The concentrations of examined elements in the moss samples were comparable to those found in the neighbouring countries, with the median country values often being five or more times larger than in the pollution background countries like Switzerland and Norway. Calculation of ecological implication indices generally suggested the presence of low to moderate pollution all over the study area, with severe contamination with As, Cr, Cu and Pb at some studied locations in the eastern and northern parts of the country.

Keywords: air pollution; PTEs; moss survey; ICP vegetation; *H. cupressiforme*.

INTRODUCTION

Air pollution is perceived as the second biggest environmental concern for Europeans after climate change.[1] The presence of potentially toxic elements (PTEs) in the air is highly variable in time and space, thus, the challenge is to establish an extensive network of measurement sites identifying the pollution level. Despite the evident progress in the development of devices for air quality measurements, both stationary and mobile, still technical maintenance, energy

* Corresponding author. E-mail: mira.anicic@ipb.ac.rs
# Serbian Chemical Society member.
https://doi.org/10.2298/JSC240906100U

supply and potential vandalism represent disadvantages of instrumental monitoring systems. The alternative lays in the use of natural systems (organisms) as indicators/monitors of pollution changes in the environment.[2] The use of mosses for the assessment of PTEs in atmospheric deposition has been studied due to their morpho-physiological features orienting mosses to air as nutritional media,[3] thus, hypothetically, reflecting the content of the surrounding air within the moss tissue. This premise has been investigated in numerous studies, which has led to systematic application of mosses in PTE (bio)monitoring across Europe and beyond, within the framework of the UNECE ICP Vegetation surveys on Effects of Air Pollution on Natural Vegetation and Crops.[4] This monitoring program has been performed every five years aiming to detect the spatio-temporal distribution of agreed PTEs (Al, As, Cd, Cr, Cu, Fe, Hg, Ni, Pb, Sb, V and Zn) in atmospheric deposits leading to pollution source detection.

Serbia has participated in the ICP Vegetation since 2000. Due to consistency in the sample pretreatment and analytical techniques, used the aim of this study was an evaluation of the PTE spatio-temporal distribution, in the moss samples collected over Serbia during the two last surveys, performed in 2015 and 2020. In addition, the assessment of factors affecting the PTE content in the moss and their ecological implications indices was performed.

EXPERIMENTAL

Study area

Details related to the study area, sampling and sample preparation[5-9] are given in the Supplementary material to this paper.

Chemical analysis

In the laboratory, after removal of soil and plant debris, the moss subsamples per sampling site were homogenized in the unique one, which was analyzed in triplicate. The mineralization of the 0.5 g of the samples was performed by the solution of 7 mL HNO_3 (65 %, Sigma–Aldrich, puriss. p.a.) and 1 mL H_2O_2 (30 %, Sigma–Aldrich, puriss. p.a.) in a microwave (Ethos 1, advanced microwave digestion system, Milestone, Italy) for 45 min at 200 °C. The digested samples were diluted with distilled water up to a volume of 50 mL.

The concentrations of Al, As, Cd, Cr, Cu, Fe, Ni, Pb, V and Zn were determined from the solution, using inductively coupled plasma-optical emission spectrometry (ICP-OES, Thermo Scientific iCAP 6500 Duo, Thermo Scientific, UK) and inductively coupled plasma--mass spectrometry (ICP-MS, Thermo Scientific iCAP Q, Thermo Scientific, UK). For the calibration of ICP-OES and ICP-MS a multi-element plasma standard solution 4, Specpure (Alfa Aesar GmbH & Co KG, Germany) was used to prepare intermediate solutions. The measurements were corrected to analytical blanks, and the quality control was performed by analysing certified reference materials M2 and M3 (moss *P. schreberi* (Brid.) Mitt., Finnish Forest Research Institute).[10] The recovery of the elements was in the range of 86–109 % and 87–107 % for M2 and M3, respectively, except for Cr (≈70 %), which was below the lower ranges for surveys in 2015 and 2020, and Ni (≈140 %) above the higher values of the range in 2020. Hence, in the following discussion, Cr and Ni will be considered with caution.

Data analysis

The obtained results were analysed using software Statistica 8.0 (StatSoft Inc., Tulsa, OK, USA) and ArcGIS 10.4 (ESRI). All the statistical analyses were performed at a confidence level of $p < 0.05$. The normality of the data distribution was tested by the Kolmogorov–Smirnov test. Background values of element concentrations, in the moss samples for the study area, were estimated as 10 percentiles of element concentrations found in all the samples. In addition, the moss PTE concentrations, from this study, were compared with "fingerprint moss" (FM) values of elemental concentrations in two moss species: *Hylocomium splendens* and *Pleurozium schreberi*, which is assumed as a typical moss PTE value in remote areas.[11]

Enrichment factor (*EF*) is a widely used metric for determining how much the presence of an element in a sampling medium has increased, relative to average natural abundance in the Earth's crust or topsoil, due to anthropogenic influence. The element EFs in the moss samples was calculated, with respect to their average crustal content,[12] according to the following equation:[13]

$$EF = \frac{(C_x / C_{ref})_{Moss}}{(C_x / C_{ref})_{E.\ crust}} \quad (1)$$

where C_x represents the moss element concentration and C_{ref} is the concentration of the reference element (Al) in the relevant background (*e.g.*, the Earth's crust). According to some theoretical assumptions, if *EF* is close to unity, then crustal material is likely to be the predominant source of the element, while the more *EF* exceeds unity the higher are contributions from non-crustal sources.[14,15] A finer scaling of EFs is given in Aničić Urošević *et al.* (2018).[16]

Geo-accumulation index (I_{geo}) is defined by the following equation:[17]

$$I_{geo} = \log (2 \times 1.5 C_i C_{ri}) \quad (2)$$

where C_i represents the sample element concentration and C_{ri} is the background or reference value for element *i*. In this study, background values of C_{ri} in the moss samples were estimated as 10 percentiles of element concentrations found in all the samples over the study area. The constant 1.5 in Eq. (2) is the background matrix correction factor due to variability. The classification for I_{geo}[17,18] is given in Aničić Urošević et al. (2018).[16]

Contamination factors (*CF*s) were calculated to assess the contamination level of the study area, *i.e.*, the increment levels of an element along sampling sites due to human activity according to equation:[19]

$$CF = C_{element}/C_{background} \quad (3)$$

Pollution load index (*PLI*), as a measure of cumulative pollution of the measured pollutants,[20] was calculated for the moss samples as the n^{th} root of *n CF*s:

$$PLI = (CF_1 \times CF_2 \times CF_3 \times \ldots \times CF_n)^{1/n} \quad (4)$$

where *n* represents the total number of measured PTEs. The values of *PLI* are indicative of the overall level of pollution caused by the measured pollutant and scaled.[21]

RESULTS AND DISCUSSION

Spatio-temporal trend of PTE concentration in moss samples over the investigated area

In this study, due to the relevance of comparison, the data related to the overlapping sampling sites (177 in all) at the territory of Serbia outside of Kosovo and Metohija province in two consecutive surveys, 2015 *vs*. 2020, were compared.

Descriptive statistics of concentrations of ten elements, determined in moss *H. cupressiforme* samples are presented in Table I. Analysed elements are defined as important for monitoring due to their harmful effects on crops and (semi-)natural vegetation.[4] The PTEs in moss samples collected across the investigated area were normally or log-normally distributed depending on the element. The data characterized moderate to high values of coefficient of variation (429 % > *CV* > 53 %), skewness (2–13) and kurtosis (6–173), thus indicating high variability of the element concentrations in the moss samples across the study area.

TABLE I. Descriptive statistics for element concentrations (mg kg^{-1}) in the moss samples of *H. cupressiforme* collected in the surveys performed in 2015 (grey rows) and 2020; number of overlapping sites, (*N*) =177; fingerprint mosses: FM1 – *H. splendens* and FM2 – *P. schreberi*[11]

Year	Element	Mean	Median	Min	Max	10 %	*SD*	*CV*	Skew	Kurt	FM1	FM2
2015	Al	1247	990	358	11000	573	1027	82	5	44	322	–
2020	Al	1833	1148	162	12356	432	1970	107	2	7		
2015	As	1.186	0.695	0.164	71	0.376	5.07	428	14	190	–	0.2
2020	As	0.952	0.808	0.0112	5	0.155	0.71	75	2	6		
2015	Cd	0.207	0.180	0.050	0.93	0.120	0.11	55	3	13	0.3	0.2
2020	Cd	0.302	0.224	0.0082	1.51	0.139	0.24	81	3	9		
2015	Cr	3.739	2.908	0.006	25	0.006	3.90	104	2	7	1.07	0.9
2020	Cr	3.006	2.128	0.0014	23	0.718	3.28	109	3	13		
2015	Cu	12.101	8.275	3.247	213	5.107	18	151	8	78	4.9	4.5
2020	Cu	9.947	5.393	0.002	121	0.815	14	141	4	26		
2015	Fe	1275	995	275	10119	564	1024	80	4	31	210	150
2020	Fe	1033	814	0.0021	9913	201	1056	102	4	29		
2015	Ni	4.189	2.868	0.621	49	1.532	5.39	129	6	46	1.4	0.6
2020	Ni	1.999	0.039	0.0075	24	0.013	4.14	207	3	11		
2015	Pb	5.141	3.969	0.363	30	1.620	4.38	85	3	11	9.1	5.9
2020	Pb	4.183	3.900	0.0023	18	1.823	2.44	58	2	8		
2015	V	3.083	2.649	0.907	21	1.454	2.13	69	5	32	1.75	1.4
2020	V	3.622	2.584	0.0085	22	1.238	3.12	86	2	8		
2015	Zn	24	21	8	115	13	15	60	4	18	26.5	25
2020	Zn	12	10	4	87	6	9	76	5	35		

High positive values of skewness and kurtosis indicate the data are skewed positively with a tendency to maximum values, which characterized the lognormal distribution model and environmental data in general.[22] Although the

samples were collected in remote areas, high spatial variability of data is likely linked to the impacts of anthropogenic sources as well as geogenic and meteorological conditions on the sampling sites. In both surveys 2015 and 2020, the median PTE concentrations kept the similar order of abundance (Fe > Al > Zn > Cu > Pb > Cr > Ni > V > As > Cd, 2015; Al > Fe > Zn > Cu > Pb > V > Cr > As > Cd > Ni, 2020) in the moss tissue (Table I).

Comparing the results of 2020 and 2015 moss sampling campaigns, the median concentrations of the elements follow a decreasing pattern for Cr (41.6 %), Cu (39.4 %), Fe (21.7 %), Pb (9.5 %) and Zn (53.6 %), increasing for Cd (18.4 %), while staying about the same level for As and V. In general, these results follow the findings relevant for most EU countries participating in the program about the clear decreasing trend of the element concentrations with time.[23] The only element that did not follow the European time-trend of the PTE concentrations was Cd, which kept the stable or slightly increased concentrations in the investigated part of Serbia throughout the surveys performed.

Since descriptive statistics hide details about the distribution of the PTEs across the investigated terrain, the maps of the spatio-temporal element distribution in 2015 and 2020 surveys are presented in Figs. 1 and 2.

Arsenic is an element whose concentration in the moss samples increased with time at some studied sites situated in Vojvodina, the northern province of the country, and at the particular sites within the central and southeast parts of the country as well, while the decrease in concentration was observed at the particular sites within the southwest and central part of the country (Fig. 1). Contrary, at the European level, the concentration of As in the mosses have declined by 13 % since year 1995, when the biomonitoring program started.[23,24] It should be noted that high background values of As characterize the central Balkan peninsula and come from specific geological formations and ore deposits.[25] This peculiarity may cause an important contribution of this element in any environmental samples, *e.g.*, sediments and groundwater within the Pannonian Basin[26] or even drinking water,[27] birch and linden samples.[28] Other sources of As include anthropogenic activities, such as the application of pesticides and mineral fertilizers, fossil fuel combustions, mining activities, and disposal of industrial wastes.[29] In the investigated area, anthropogenically emitted As probably comes from pyrometallurgical processes of copper recovery from the sulfide mineral arsenopyrite (FeAsS) in Bor's region,[30] and from coal combustion in coal-fuelled power plants (the sites along such plants, located in Obrenovac, Kostolac, Lazarevac and Svilajnac).

Cadmium is an element whose spatial distribution is rather uniform throughout the study area, with an increase of concentrations across Vojvodina province in the 2020 moss survey and with some hot spots distributed evenly throughout the country, especially in the later survey (Fig. 1). A possible source of Cd are

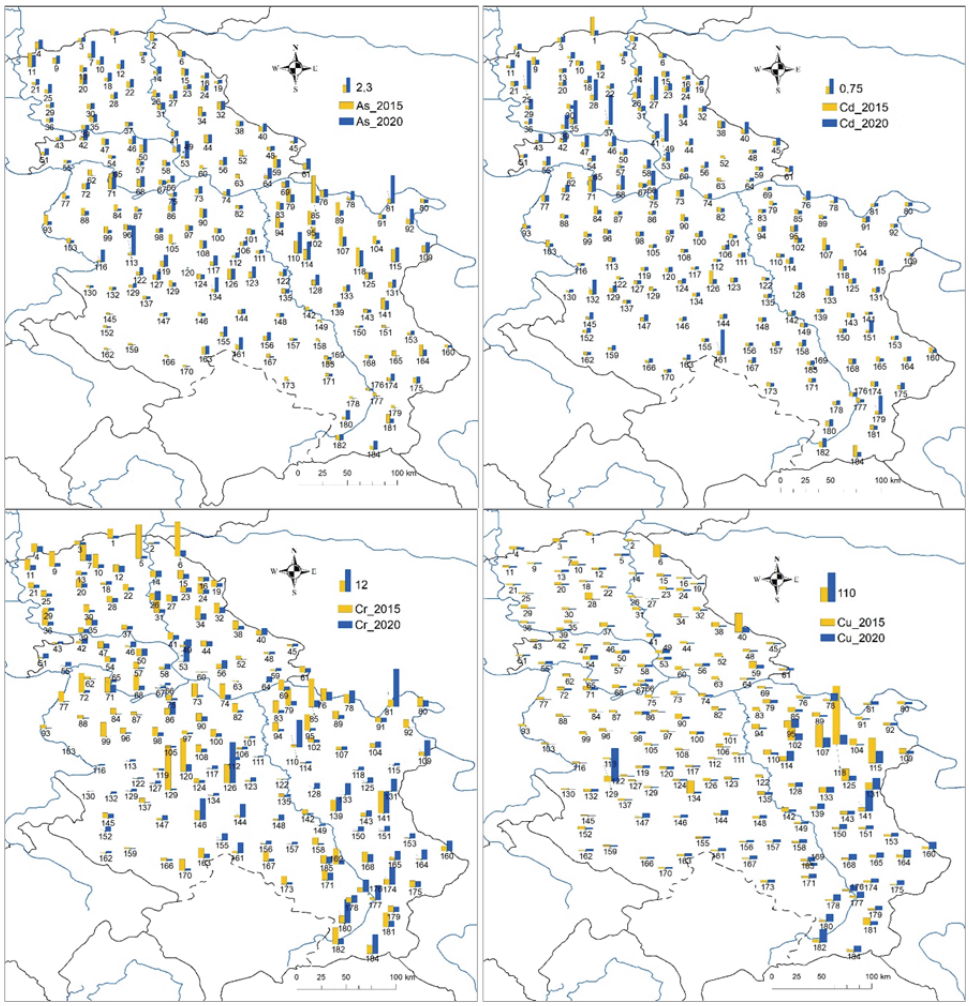

Fig. 1. Concentrations (mg kg^{-1}) of As, Cd, Cr and Cu in the samples of moss *H. cupressiforme* in two moss surveys, 2015 and 2020.

phosphate fertilizers[31] with characteristic applications in the agricultural province in the north of the country. Naturally, Cd is a crustal element found in igneous and sedimentary rocks, with an average content of 0.41 mg kg^{-1} in soil worldwide and a substantially higher coal content (0.5–170 mg kg^{-1}).[32] Although at the European level, this element records a strong drop in concentration over time (63 %),[23] in the investigated part of Serbia, the median Cd recorded an increase over the years of investigations.

Chromium is an element with uneven spatial distribution in moss samples across the investigated part of Serbia. Having natural origin in parent (basaltic) rocks, Cr is released to the air primarily by coal mining and combustion pro-

cesses,[33,34] but also by cement factories and the metal processing industry.[35] The concentration of chromium decreased (24 %) in the moss samples of other European countries,[23,24] and the same trend was also recorded in this study.

Copper is an element with a prominent concentration in the moss samples collected across the eastern part of the country with the active copper mining and processing industry,[30] and particular sites in the west Serbia close to Copper Rolling Mill "Sevojno". In the areas with intensive agricultural production, there are several sites with an increased level of Cu (*e.g.*, Vršac vineyards), fully in accordance with the history of long-term application of mineral fertilizers and fungicides.[36] Still, the concentrations of Cu in the mosses decrease through the years to the median level of 5.4 mg kg^{-1} in the last survey (2020), having the same pattern as the geometric mean of the same element in European countries,[24] which since 1990 has declined by 30 %.

Nickel is evenly distributed (Fig. 2) in the moss samples collected over investigated part of Serbia, probably due to numerous anthropogenic usages of this widely used ferromagnetic metal, such as production of stainless steel and alloys and corrosion-resistant plating. It is also being extensively emitted in oil combustion processes.[37] This element also showed a declining trend of concentrations in the moss samples with time.

Lead is an element evenly distributed (Fig. 2) in moss samples across investigated part of Serbia. Possible historical pollution of soil by deposition of lead gasoline combustion products and their resuspension processes can contribute to the relatively high presence of Pb in the environment. Still, Pb showed a decline in the concentration levels in two last moss surveys for about 10 %. This element showed the highest decline of the moss concentration since 1990, for 82 % over the Europe.[23]

Vanadium is an element with the highest presence in the moss samples collected across the eastern part of the country (Fig. 2), somewhat less in the moss of the northern province of Vojvodina, while the content in moss samples across the western and central parts of the country was the lowest.

Despite the V concentrations substantially decreasing with time (for 57 %) at the European level,[23] in the Serbian moss samples, the median element concentrations remain at the same level in the two last surveys. Releases of V to the environment are mainly associated with industrial sources, especially oil refineries and power plants using fuel oil and coal.[38]

Zinc is an element evenly distributed in the moss samples over the investigated part of Serbia (Fig. 2), with markedly increase concentrations at some sites in western Serbia (close to Copper Rolling Mill "Sevojno") which is also found in the stream and river water in this regia.[39] The element concentrations showed a substantial decrease in the two consecutive surveys over the inves-

tigated area, which is in accordance with the decrease of its content at the European level (for 23 %).[23]

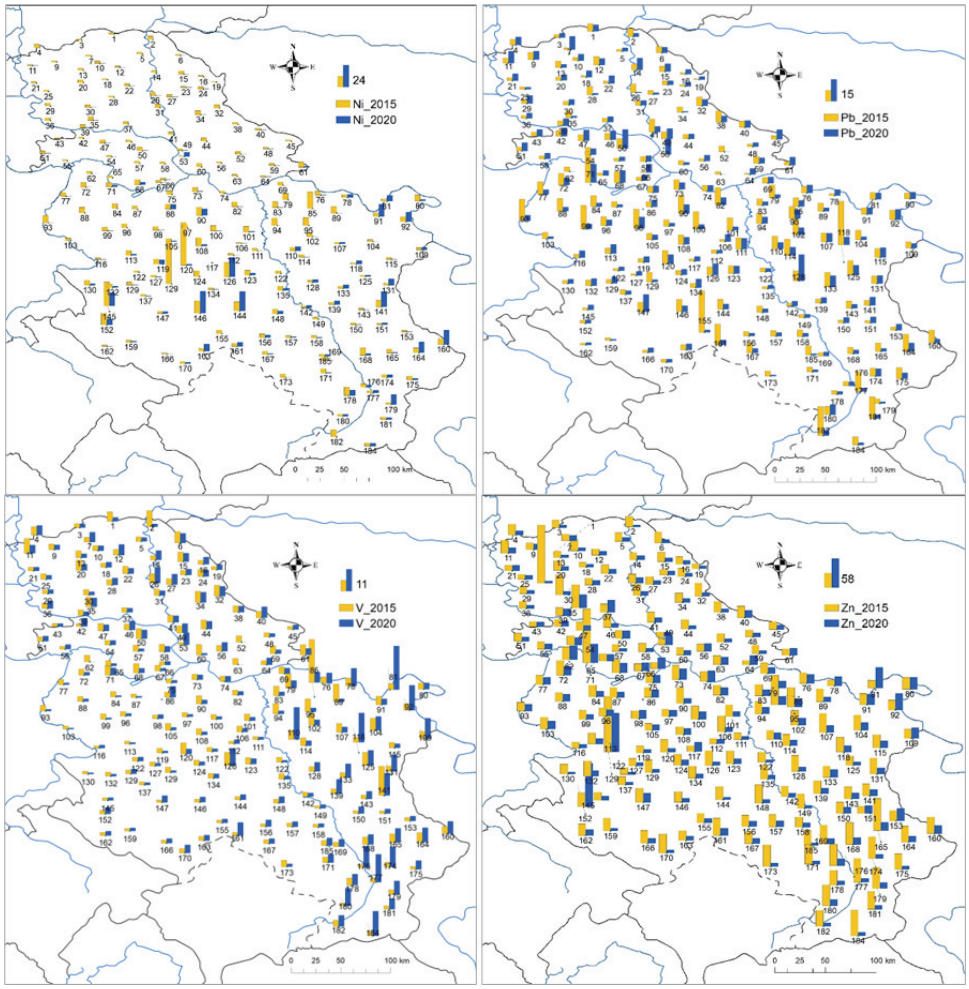

Fig. 2. Concentrations (mg kg^{-1}) of Ni, Pb, V and Zn in the samples of moss *H. cupressiforme* in two moss surveys, 2015 and 2020.

Ecological implications indices

Calculating various ecological indices helps to put the absolute values of the PTEs determined in the studied samples into the context of environmental pollution, while scaling the contamination level of the studied moss samples allows the comparison of data from different regions.

*Enrichment factor (*EF*).* In the 2015 moss survey, the median $EF_{E.crust}$ is indication of elemental contamination levels that range from extremely severe for

Cd (73), over very severe for As (29), and severe for Zn (23), Pb (22) and Cu (12), to moderate for Ni (3), and minor for Cr (1.8), Fe (1.7), and V (1.5), Fig. 3. Five years later, in the 2020 moss survey, the PTEs kept the same range of enrichment for Cd (83), As (33), Pb (23), Zn (12), V (1.4), and Cr (1.3), while Cu (8.7), Fe (0.6) and Ni (0.5) moved to the lower category of enrichment.

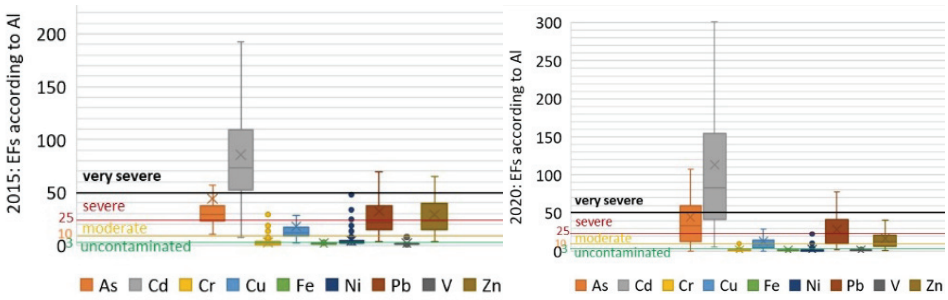

Fig. 3. Enrichment factors (*EF*s) calculated for the element concentrations in the moss samples collected over the investigated part of Serbia in 2015 and 2020 with classification of contamination levels.

Searching for contamination levels of elements originating from non-natural sources, the PTE concentrations in the studied moss samples were compared with FM values assumed as the background elemental concentrations for mosses.[11] Median concentrations of Al, As, Cr, Cu, Fe and V in this study were elevated compared to the FM values, while Zn in both surveys, and Cd in 2015 and Ni in 2020, were below the FM values; Pb was the only element that was below the FM values in both surveys (Table I).

However, minimal PTE values in *H. cupressiforme* obtained for the study area were far below the FM values, especially for Pb. It should be emphasized that FM values are related to different moss species (*H. splendens* and *P. schreberi*) recommended for use within the ICP Vegetation program as well as *H. cupressiforme* used in this study. Some studies pointed out that comparative use of different species within the same survey could lead to wrong conclusions.[40,41] Thus, in further estimations of environmental indices through different pollution indexes (I_{geo}, *PLI*), the PTE background values were specifically estimated for the investigated part of Serbia as 10 percentiles of the concentrations found in all the samples.

Geo-accumulation index (I_{geo}). In the 2015 moss survey, the median values of I_{geo} in the moss samples suggested the contaminantion by the PTEs over the investigated area in the range from uncontaminated to moderately contaminated ($0< I_{geo}<1$), Fig. 4.

However, there are particular sites that are characterized as extremely contaminated by As and Cr (6.9 and 5.07 at sites 120 and 129, respectively); strongly

to extremely by Cu and Ni (4.8 and 4.3 at sites 118 and 120, respectively); strongly by Pb, Fe and V (3.6, 3.6, and 3.3 at sites 118, 85, and 85, respectively); and moderately to strongly by Zn and Cd (2.5 and 2.3 for site 1, Fig. 3. In the 2020 moss survey, median I_{geo} also implied slight contamination for most PTEs over the study area except for Cu (2.1) and Fe (1.4), which testified about moderate contamination. Again, for some sites, values of I_{geo} showed up to extreme contamination for Ni (up to 10 at dozen sites) and Cu (up to 6.6 at sites 133, 67, 116, 117, 184); strong to extreme for Fe (5.0 at site 81), Cr (up to 4.4 at sites 81 and 126), As (up to 4.3 at sites 113 and 81); strong for V (up to 3.5 at site 81 and 110) and Zn (up to 3.2 at sites 153 and 130); and moderate to strong for Cd (up to 2.9 at sites 37, 25, 27, 28) and Pb (up to 2.7 at sites 128, 148 and 71).

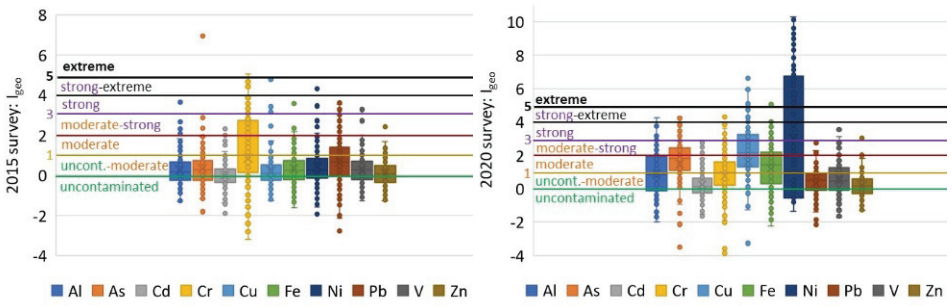

Fig. 4. Geo-accumulation index (I_{geo}) calculated for the element concentrations in the moss samples collected over the investigated part of Serbia in 2015 and 2020 with classification of contamination levels.

*Pollution load index (*PLI*).* In 2015, the median *PLI* (1.23) for the PTEs in the moss samples over the investigated part of Serbia suggested that the area is mostly uncontaminated to moderately contaminated (Fig. 5). However, several sites reached the range of moderately contaminated ($2 < PLI < 3$). Regarding the 2020 survey, the median *PLI* stayed in the same range as in the previous survey, but with an increasing number of sites reaching the range of moderately contaminated.

Regional distribution of moss PTE content

The PTE content in the moss samples collected over the investigated part of Serbia in 2015 and 2020 was compared with the moss PTE content in the corresponding studies of the neighboring countries (Romania, Bulgaria, North Macedonia and Albania), and the countries with low levels of environmental pollution such as Switzerland and Norway (Table II). Substantially higher PTE concentrations were found in the moss collected over Balkan countries compared to the corresponding background countries, especially of As, Cr and Pb (5–10, 3–15, 2–6 fold higher, respectively); and with somewhat less extent of Cd, V and Cu

(1.5–3, 2–3.5, about 2 times higher, respectively). Regarding Serbia, the difference in the moss element content compared to Norway was always close to the lower border of the abovementioned ranges. The peculiarity represented the As concentrations in the investigated part of Serbia, which were twice as high as in the neighboring countries, except for Romania, which is probably linked to the geological presence of this element combined with strong anthropogenic sources such as pyrometallurgical processes of copper recovery from the mineral arsenopyrite in the Bor region[30] and combustion in coal-fired power plants ("Nikola Tesla", "Kolubara" and "Kostolac").[34] Based on moss biomonitoring observations at the European level, the evaluated region is a factor ten, or higher, than in other parts of Europe.[23,24]

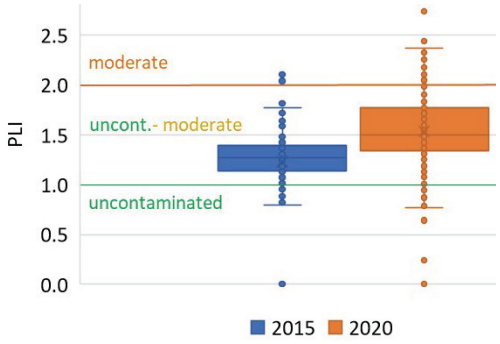

Fig. 5. Cumulative pollution (pollution load index, *PLI*) by ten PTEs in the moss samples collected over the investigated part of Serbia in 2015 and 2020.

TABLE II. Median concentrations of the PTEs in moss *H. cupressiforme* collected over the investigated part of Serbia (SRB), Albania (ALB), North Macedonia (MKD), Bulgaria (BGR), Romania (ROU), Switzerland (CHE) and Norway (NOR) in 2015 and 2020 surveys

Element	2015							2020		
	SRB	ALB[23]	MKD[23]	BGR[23]	ROU[23]	CHE[23]	NOR[23]	SRB	ALB[42]	MKD[43]
	$n = 177$	$n = 55$	$n = 72$	$n = 115$	$n = 214$	$n = 73$	$n = 464$	$n = 177$	$n = 55$	$n = 72$
Al	990	1521	2100	2310	2895	318	461	1148	1240	500
As	0.70	0.42	0.54	0.45	1.08	0.14	0.13	0.81	0.36	–
Cd	0.18	0.12	0.23	0.10	0.27	0.12	0.08	0.22	0.10	0.15
Cr	2.9	9.3	5.7	2.73	4.72	0.85	0.66	2.1	6.2	3.5
Cu	8.3	10	4.6	7.4	5.8	4.8	4.2	5.4	4.7	6.3
Fe	995	1735	1700	1190	1533	314	310	814	1444	620
Ni	2.9	7.6	3.5	2.1	3.11	1.12	1.2	0.04	8.6	2.3
Pb	4.0	2.4	4.9	10.7	4.2	2.13	1.6	3.9	3.5	2
V	2.6	3.3	3.3	3.9	4.32	1.05	1.2	2.6	3.2	–
Zn	21	18	30	28	40	27	31	10	16	21

It should be noted that the same moss species (*H. cupressiforme*) were sampled in the countries of the region while different moss species were collected in Switzerland (*H. cupressiforme* and *P. schreberi*) and Norway (*H. spleendens* and *P. schreberi*) thus possibly influencing the comparison of the

results. In addition, in most countries, destructive analytical techniques were used for element determination (ICP-OES, ICP-MS), except in Bulgaria and Romania, where nondestructive INNA was used. These analytical techniques require different sample pre-treatment, non-destructive and destructive, respectively, which can influence the total element content measured.[44]

CONCLUSION

Moss *H. cupressiforme* was used for the biomonitoring of PTEs, at about 200 sites across remote areas in the investigated part of Serbia, following the international Moss survey protocol. Comparison of results in the last two surveys (2015 and 2020), showed a decline in the median deposition of Cr (42 %), Cu (39 %), Fe (22 %), Pb (10 %) and Zn (54 %), an increase of Cd (18 %), and similar deposition of As and V. Concerning the average element content in the Earth's crust (*EF*), severe anthropogenic pollution input was found for As, Cd, Pb and V. However, compared to the background values of the elements in the moss (I_{geo}), the highest indices (strong) were assessed for Cr (in 2015), and As, Cu and Ni (in 2020). Still, the cumulative measure of pollution (*PLI*) indicates that the study area suffers from moderate pollution by the measured elements. The critical points of a moss survey are strictly following the manual, using one moss species, and properly assessing the background concentration of the pollutant in the moss.

Acknowledgements. We are grateful to the Ministry of Science, Technological Development and Innovation and the Science Fund (Green program) of the Republic of Serbia for the financial support provided to the Institute of Physics Belgrade (documents: 0801116/1 and 5661, respectively); University of Novi Sad (grants No. 451-03-66/2024-03/ 200125 & 451--03-65/2024-03/200125); Faculty of Chemistry, University of Belgrade (451-03-47/2023-01/ /200168), and to the bilateral cooperation of the Institute of Physics Belgrade with the Joint Institute for Nuclear Research, Dubna, Russia (ref: JINR-Serbia_P05), which enabled the realization of this study.

ИЗВОД

БИОМОНИТОРИНГ АТМОСФЕРСКЕ ДЕПОЗИЦИЈЕ ПОТЕНЦИЈАЛНО ТОКСИЧНИХ ЕЛЕМЕНАТА НА ТЕРИТОРИЈИ СРБИЈЕ КОРИШЋЕЊЕМ МАХОВИНЕ: 2015. *vs.* 2020. ГОДИНА

МИРА П. АНИЧИЋ УРОШЕВИЋ[1], ДРАГАН В. РАДНОВИЋ[2], МИЛОШ М. ИЛИЋ[2], МИОДРАГ Д. КРМАР[2], ИГОР Д. КОДРАНОВ[3], ДУБРАВКА Ј. РЕЛИЋ[3] и АЛЕКСАНДАР Р. ПОПОВИЋ[3]

[1]Институт за физику у Београду, Универзитет у Београду, Прегревица 118, Београд, [2]Природно–-математички факултет, Универзитет у Новом Саду, Трг Доситеја Обрадовића 4, Нови Сад и [3]Хемијски факултет, Универзитет у Београду, Студентски трг 12–14, Београд

У оквиру *ICP Vegetation* програма, почевши од 2000. год., сваких 5 година се спроводи биомониторинг потенцијално токсичних елемената у неурбаним подручјима на територији Србије, коришћењем маховина (врста *Hypnum cupressiforme*). Због конзистентне методологије и анализе, у овој студији су приказани резултати два последња истраживања: 2015. *vs.* 2020. год. Резултати истраживања су указали на опадање концентрације Cr (42 %), Cu (39 %), Fe (22 %), Pb (10 %) и

Zn (54 %); As и V остали на истом нивоу, док је дошло до повећања концентрације Cd (18 %). Концентације елемената у маховини су биле упоредиве са оним измереним у суседним земљама, док су медијана вредности биле пет и више пута веће од вредности измерених у маховини тзв. чистих земаља – Швајцарске и Норвешке. Израчунавањем различитих индекса еколошких утицаја закључује се да постоји ниско до умерено загађење на подручју Србије. Ипак, за поједине локалитете у источној Србији, као и Војводини, озбиљан ниво загађења је процењен за As, Cr, Cu и Pb.

(Примљено 6. септембра, ревидирано 24. октобра, прихваћено 1. децембра 2024)

REFERENCES

1. European Environment Agency, *Europe's air quality status 2024*, https://www.eea.europa.eu/publications/europes-air-quality-status-2024 (date accessed: 08/2024)
2. B. A. Markert, A. M. Breure, H. G. Zechmeister, in *Bioindicators and Biomonitors*, B.A. Markert, A. M. Breure, H. G. Zechmeister, Eds., Elsevier Science Ltd., Amstrdam, 2003, p. 3 (https://doi.org/10.1016/S0927-5215(03)80131-5)
3. H. G. Zechmeister, K. Grodzińska, G. Szarek-Łukaszewska, in *Bioindicators and Biomonitors*, B. A. Markert, A. M. Breure, H. G. Zechmeister, Eds., Elsevier Science, Amsterdam, 2003, p. 329 (https://doi.org/10.1016/S0927-5215(03)80140-6)
4. *International Cooperative Programme on Effects of Air Pollution on Natural Vegetation and Crops (ICP Vegetation*), https://icpvegetation.ceh.ac.uk/, (date accessed: 08/2024)
5. *Climate Data. Climate Serbia*, https://en.climate-data.org/europe/serbia-37/ (date accessed: 08/2024)
6. J. Smailagić, A. Savović, D. Marković, D. Nesić, *Climate characteristics of Serbia*, Republic Hydrometeorological Service of Serbia, Belgrade, 2013 (https://www.hidmet.gov.rs/data/klimatologija_static/eng/Klimatske_karakteristike_Srbije_prosirena_verzija.pdf)
7. B. Papp, J. Pantović, M. S. Sabovljević, *Herzogia* **32** (2019) 154 (https://doi.org/10.13158/heia.32.1.2019.154)
8. M. Sabovljević, R. Natcheva, G. Dihoru, E. Tsakiri, S. Dragićević, A. Erdağ, B. Papp, *Phytol. Balcan.* **14** (2008) 207 (http://www.bio.bas.bg/~phytolbalcan/PDF/14_2/14_2_05_Sabovljevic_&_al.pdf)
9. Moss Survey Protocol, *Heavy metals, nitrogen and POPs in European mosses*, *2020 survey*, https://icpvegetation.ceh.ac.uk/sites/default/files/ICP%20Vegetation%20moss%20monitoring%20manual%202020.pdf (date accessed: 08/2024)
10. E. Steinnes, Å. Rühling, H. Lippo, A. Mäkinen, *Accred. Qual. Assur.* **2** (1997) 243 (https://doi.org/10.1007/s007690050141)
11. R. Djingova, I. Kuleff, B. Markert, *Ecol. Res.* **19** (2004) 31.
12. B. Mason, *Principles of Geochemistry*, Wiley, New York, 1966 (https://www.scribd.com/document/335488342/GEOCHEMISTRY-docx)
13. R. Bargagli, D. H. Brown, L. Nelli, *Environ. Pollut.* **89** (1995) 169 (https://doi.org/10.1016/0269-7491(94)00055-I)
14. T. Berg, O. Røyset, E. Steinnes, *Atmos. Environ.* **28** (1994) 3519 (https://doi.org/10.1016/1352-2310(94)90009-4)
15. X. Wang, S. Sato, B. Xing, S. Tamamura, S. Tao, *J. Aerosol Sci.* **36** (2005) 197 (https://doi.org/10.1016/j.jaerosci.2004.08.005)

16. M. Aničić Urošević, G. Vuković, P. Vasić, T. Jakšić, D. Nikolić, S. Škrivanj, A. Popović, *Ecol. Ind.* **90** (2018) 528 (https://doi.org/10.1016/j.ecolind.2018.03.048)
17. G. Müller, *GeoJournal* **2** (1969) 108 (Corpus ID: 128079163)
18. H. H. O. Huu, R. Swennen, A. V. Damme, *Geol. Belg.* **13** (2010) **37** (https://popups.uliege.be/1374-8505/index.php?id=2852&file=1)
19. J. A. Fernández, A. Carballeira, *Arch. Environ. Contam. Toxicol.* **40** (2001) 461 (https://doi.org/10.1007/s002440010198)
20. D. L.Tomlinson, J. G.Wilson, C. R. Harris, D. W. Jeffrey, *Helgoländer Meeresuters* **33** (1980) 566 (https://link.springer.com/content/pdf/10.1007/BF02414780.pdf)
21. C. Zhang, Q. Qiao, J. D. A. Piper, B. Huang, *Environ. Pollut.* **159** (2011) 3057 (https://doi.org/10.1016/j.envpol.2011.04.006)
22. A. Andersson, *Sci. Rep.* **11** (2021) 16418 (https://doi.org/10.1038/s41598-021-96010-6)
23. M. Frontasyeva, H. Harmens, A. Uzhinskiy, O. Chaligava and participants of the moss survey Mosses as biomonitors of air pollution, *2015/2016 survey on heavy metals, nitrogen and POPs in Europe and beyond. Report of the ICP Vegetation Moss Survey Coordination Centre*, Joint Institute for Nuclear Research, Dubna, 2020, p. 136 (https://icpvegetation.ceh.ac.uk/mosses-biomonitors-air-pollution-20152016-survey-heavy-metals-nitrogen-and-pops-europe-and-beyond)
24. H. Harmens, D. A. Norris, K. Sharps, G. Mills, R. Alber, Y. Aleksiayenak, O. Blum, S-M. Cucu-Man, M. Dam, L. De Temmerman, A. Ene, J. A. Fernández, J. Martinez-Abaigar, M. Frontasyeva, B. Godzik, Z. Jeran, P. Lazo, S. Leblond, S. Liiv, S. H. Magnússon, B. Maňkovská, G. Pihl Karlsson, J. Piispanen, J. Poikolainen, J. M. Santamaria, M. Skudnik, Z. Spiric, T. Stafilov, E. Steinnes, C. Stihi, I. Suchara, L. Thöni, R. Todoran, L. Yurukova, H. G. Zechmeister, *Environ. Pollut.* **200** (2015) 93 (https://doi.org/10.1016/j.envpol.2015.01.036)
25. A. Dangić, J. Dangić, in *Arsenic in Soil and Groundwater Environment; Trace Metals and other Contaminants in the Environments*, P. Bhattacharya, B .B. A. Mukherjee, J. Bundschuh, R. Zevenhoven, H. R. Loeppert, Eds., Elsevier, Amterdam, 2007, p. 207 (https://doi.org/10.1016/S1875-1121(06)09007-9)
26. I. Varsányi, L.Ó. Kovács, *Appl. Geochem.* **21** (2006) 949 (https://doi.org/10.1016/j.apgeochem.2006.03.006)
27. D. Jovanović, B. Jakovljević, Z. Rašić-Milutinović, K. Paunović, G. Peković, T. Knežević, *Environ. Res.* **111** (2011) 315 (https://doi.org/10.1016/j.envres.2010.11.014)
28. S.Č. Alagić, S.S. Šerbula, S.B. Tošić, A.N. Pavlović, J.V. Petrović, *Arch. Environ. Contam. Toxicol.* **65** (2013) 671 (https://doi.org/10.1007/s00244-013-9948-7)
29. B. Mandal, K. Suzuki, *Talanta* **58** (2002) 201 (http://dx.doi.org/10.1016/S0039-9140(02)00268-0)
30. S. Urošević M. Vuković, B. Pejčić, N. Štrbac, *Rev. Int. Contam. Ambi.* **34** (2018) 103 (https://doi.org/10.20937/rica.2018.34.01.09)
31. N.A. Suciu, R. De Vivo, N. Rizzati, E. Capri, *Curr. Opin. Env. Sci. Hl.* **30** (2022) 100392 (https://doi.org/10.1016/j.coesh.2022.100392)
32. A. Kabata-Pendias, B. Szetke, *Trace Elements in Abiotic and Biotic Environment*, CRC Press, Boca Raton, FL, 2019 (https://doi.org/10.1201/b18198)
33. S. Dragović, M. Ćujić, L. Slavković-Beškoski, B. Gajić, B. Bajat, M. Kilibarda, A. Onjia, *Catena* **104** (2013) 288 (https://doi.org/10.1016/j.catena.2012.12.004)
34. J.Z. Buha Marković, A. D. Marinković, J. Z. Savić, M. R. Mladenović, M. D. Erić, Z. J. Marković, M. Đ. Ristić, *Toxics* **11** (2023) 396 (https://doi.org/10.3390/toxics11040396)

35. M. M. Poznanović Spahić, S. M. Sakan, B. M. Glavaš-Trbić, P. I. Tančić, S. B. Škrivanj, J. R. Kovačević, D. D. Manojlović, *J. Environ. Sci. Health A*. **54** (2018) 219 (https://doi.org/10.1080/10934529.2018.1544802)
36. E. Y. Thomas, J. A. I. Omueti, O. Ogundayomi, *Agric. Biol. J. N. Am.* **3** (2012) 145 (https://www.scihub.org/ABJNA/PDF/2012/4/ABJNA-3-4-145-149.pdf)
37. A. Kabata-Pendias, H. Pendias, *Trace Elements in Soils and Plants*, 3rd ed., CRC Press, Boca Raton, FL, 2001 (https://doi.org/10.1201/b10158)
38. B. Xiaoxuan, L. Lining, T. Hezhong, L. Shuhan, H. Yan, Z. Shuang, L. Shumin, Z. Chuanyong, G. Zhihui, L. Yunqian, *Environ. Sci. Technol.* **55** (2021) 11568 (https://doi.org/10.1021/acs.est.1c04766)
39. M. Vučnić Vasić, J. Kiurski, S. Aksentijević, U. Kozmidis-Luburić, *Int. J. Environ. Sci. Technol.* **10** (2013) 923 (https://doi.org/10.1007/s13762-013-0203-6)
40. J. A. Fernández, M. T. Boquete, A. Carballeira, J. R. Aboal, *Sci. Tot. Environ.* **517** (2015) 132 (https://doi.org/10.1016/j.scitotenv.2015.02.050)
41. M. Aničić Urošević, M. Ilić, D. Radnović, K. Vergel, N. Yushin, O. Chaligava, I. Zinicovscaia, *Environ. Sci. Pollut. Res.* **31** (2024) 48296 (https://doi.org/10.1007/s11356-024-34353-z)
42. P. Lazo, S. Shehu Kane, F. Qarri, S. Allajbeu, L. Bekteshi, *Aerosol Air Qual. Res.* **24** (2024) 240011 (https://doi.org/10.4209/aaqr.240011)
43. R. Šajn, K. Bačeva Andonovska, T. Stafilov, L. Barandovski, *Atmosphere* **15** (2024) 297 (https://doi.org/10.3390/atmos15030297)
44. J. Orlić, M. Aničić Urošević, K. Vergel, I. Zinicovscaia, S. Stojadinović, I. Gržetić, K. Ilijević, *J. Serb. Chem. Soc.* **87** (2022) 69 (https://doi.org/10.2298/JSC210921101O).

Journal of the Serbian Chemical Society
JSCS@tmf.bg.ac.rs • www.shd.org.rs/JSCS
J. Serb. Chem. Soc. 89 (12) S512–S513 (2024) *Supplementary material*

SUPPLEMENTARY MATERIAL TO

Atmospheric deposition of potentially toxic elements over the territory of Serbia assessed by moss biomonitoring in five-year time: 2015 *vs.* 2020

MIRA P. ANIČIĆ UROŠEVIĆ[1]*, DRAGAN V. RADNOVIĆ[2], MILOŠ M. ILIĆ[2], MIODRAG D. KRMAR[2], IGOR D. KODRANOV[3], DUBRAVKA J. RELIĆ[3] and ALEKSANDAR R. POPOVIĆ[3]

[1]*Institute of Physics Belgrade, University of Belgrade, Pregrevica 118, Belgrade, Serbia,* [2]*Faculty of Science, University of Novi Sad, Trg Dositeja Obradovića 4, Novi Sad, Serbia and* [3]*Faculty of Chemistry, University of Belgrade, Studentski trg 12–16, Belgrade, Serbia*

J. Serb. Chem. Soc. 89 (12) (2024) 1543–1557

STUDY AREA

Serbia is a country that covers a total of 88 499 km^2, situated between 41–47° N latitude and of 18–23° E longitude. Serbia's terrain ranges from agriculture plains of the northern Vojvodina region, limestone ranges and basins in the east, ancient mountains in the southeast, while in the central part it dominates chiefly of hills and low and medium-high mountains, interspersed with numerous rivers and creeks. The climate of Serbia is classified mainly as a warm-humid continental and humid subtropical.[1] Major part of Serbia has a continental precipitation regime with higher quantities in the warmer part of the year.[2] The predominantly warm-humid climate favors bryophyte richness and diversity. According to present knowledge, the bryophyte flora of Serbia includes 833 species.[3] The moss *Hypnum cupressiforme* Hedw. is a common and widespread species in all the countries of Southeast Europe.[4] It is epigeic, pleurocarpous, and fairly pollution tolerant. Due to these reasons, *H. cupressiforme* is recommended as one of four species to be used for biomonitoring of PTEs on an international scale within the ICP Vegetation Program.[5]

Sampling, sample preparation and chemical analysis

The samples of *H. cupressiforme* were collected on 212 and 185 sites in autumn of 2015 and 2020, respectively (overlapping for 177 sites), following the regular network established across the country, with the exception of the south–western Serbian province of Kosovo and Metohija that was not included in the 2020 sampling (Fig. S-1). The data regarding Kosovo and Metohija in the 2015 moss survey, were evaluated and described in a separate paper.[6]

* Corresponding author. E-mail: mira.anicic@ipb.ac.rs

Fig. S-1. Sampling sites over Serbia in 2015 and 2020 (left); moss *Hypnum cupressiforme* Hedw. (right).

The sampling was performed according to the Moss Survey Protocol, taking care of the distance from local pollution sources, roads, and tree crowns, and wearing polyethylene gloves during manipulation with samples.[5]

REFERENCES

1. Climate Data. Climate Serbia. https://en.climate-data.org/europe/serbia-37/, (date accessed: 08/2024)
2. J. Smailagić, A. Savović, D. Marković, D. Nesić, Climate characteristics of Serbia, Republic Hydrometeorological Service of Serbia, 2013 (https://www.hidmet.gov.rs/data/klimatologija_static/eng/Klimatske_karakteristike_Srbije_prosirena_verzija.pdf)
3. B. Papp, J. Pantović, M.S. Sabovljević, *Herzogia* **32** (2019) 154 (https://doi.org/10.13158/heia.32.1.2019.154)
4. M. Sabovljević, R. Natcheva, G. Dihoru, E. Tsakiri, S. Dragićević, A. Erdağ, B. Papp, *Phytol. Balcan.* **14** (2008) 207 (http://www.bio.bas.bg/~phytolbalcan/PDF/14_2/14_2_05_Sabovljevic_&_al.pdf)
5. Moss Survey Protocol, Heavy metals, nitrogen and POPs in European mosses: 2020 survey, https://icpvegetation.ceh.ac.uk/sites/default/files/ICP%20Vegetation%20moss%20monitoring%20manual%202020.pdf (date accessed: 08/2024)
6. M. Aničić Urošević, G. Vuković, P. Vasić, T. Jakšić, D. Nikolić, S. Škrivanj, A. Popović, *Ecol. Ind.* **90** (2018) 528 (https://doi.org/10.1016/j.ecolind.2018.03.048).

Journal of the Serbian Chemical Society
JSCS-info@shd.org.rs • www.shd.org.rs/JSCS
J. Serb. Chem. Soc. *89* (12) 1559–1570 (2024)
JSCS–5806
Original scientific paper
Published 26 December, 2024

Maturation changes of hydrocarbons in solid parts of peloids from Serbian spas – Catalytic influence of clay minerals

ZLATKO NIKOLOVSKI[1], ALEKSANDRA ŠAJNOVIĆ[2]*, GORDANA GAJICA[2], NIKOLA BURAZER[2], ILIJA BRČESKI[1#], PREDRAG DABIĆ[3] and BRANIMIR JOVANČIĆEVIĆ[1#]

[1]*University of Belgrade, Faculty of Chemistry, Studentski trg 12–16, 11001 Belgrade, Serbia,* [2]*University of Belgrade, Institute of Chemistry, Technology and Metallurgy, National Institute of the Republic of Serbia, Njegoševa 12, 11001 Belgrade, Serbia and* [3]*University of Belgrade, Faculty of Mining and Geology, Đušina 7, 11120 Belgrade, Serbia*

(Received 12 September, revised 12 November, accepted 1 December 2024)

Abstract: The study focused on inspecting the composition of *n*-alkane, sterane and terpane biomarkers in healing mud (peloid) organic matter in the Rusanda, Bujanovac and Vranje spas. It was assumed that the catalytic influence of minerals on changes in biomarkers could be effectively evaluated based on the distribution of their biolipid and thermodynamically more stable geolipid structural and stereochemical isomers. Quartz, illite, kaolinite, plagioclase, smectite and chlorite were identified in the samples by powder X-ray diffraction. *n*-Alkanes, terpanes and steranes were analyzed in the solid parts of the peloids using the gas chromatography–mass spectrometric, GC–MS, technique. In Rusanda and Bujanovac samples, *n*-alkanes were identified with distributions characteristic of immature sediments. In contrast, distributions of terpanes and steranes are typical for the mature organic matter of old sedimentary formations. It was concluded that the identified clay minerals do not have an obvious catalytic effect on the maturation of *n*-alkanes. At the same time, the presence of illite, chlorite, and smectite compensated for all other missing factors (heat, pressure and geological time) by catalytic action and, as a result, gave terpanes and steranes with distributions that are characteristic for petroleum, as the most mature form of organic matter in the geosphere.

Keywords: biomarkers; GC–MS analysis; maturity; smectite.

INTRODUCTION

The organic matter of sedimentary rocks changes through diagenetic and catagenetic processes. Under the influence of heat, pressure and mineral catalysts,

* Corresponding author. E-mail: aleksandra.sajnovic@ihtm.bg.ac.rs
# Serbian Chemical Society member.
https://doi.org/10.2298/JSC240912099N

changes occur towards forming more thermodynamically stable isomers of organic compounds. Most of these alterations are slow and take a long geological time, measured in millions of years. That is why geological time is justifiably considered the fourth necessary factor in these processes.[1–5]

Crude oil (petroleum) is considered to be the most mature form of organic matter in the geosphere. It is formed from an organic matter from the biosphere that undergoes intense transformations through geological time. Everything takes place in sedimentary formations, from recent to oldest, that is, to source and reservoir rocks for oil. At the end of those transformations that have passed through fulvic and humic acids, humin, kerogen and bitumen, the most mature form, crude oil, will be created. It is natural and expected that the hydrocarbons in it will have structural and stereochemical forms at the highest degree of thermodynamic stability. In organic geochemistry, the most attention is paid to the examination of changes in hydrocarbon biomarkers of the *n*-alkane type, as well as polycyclic alkanes of the sterane and terpane type.[1–5]

Heat and pressure are considered the most critical organic geochemical factors influencing the transformation of biomarkers. In catagenesis, the temperature ranges from 70 to a maximum of 150 °C, and the pressures are between 700 and 1300 bar. In such cases, minerals may act as catalysts, influencing the intensity and speed of biomarker transformations. Some changes cannot even occur if the organic matter is not in contact with certain minerals. For example, it is known that the transformations of steroids into the most thermodynamically stable sterane isomers, diasteranes, cannot take place without the catalytic action of silicate-type minerals, even when they are under the influence of heat at high temperatures and the influence of high pressure. The same applies to the transformation of the hopane isomer C_{27}-17α(H)-trisnorhopane (Tm) into the thermodynamic isomer C_{27}-18α(H)-trisnorneohopane (Ts).[3,6,7] Our earlier works also proved that these changes, and many others, are significantly influenced by the clay minerals, e.g., montmorillonite, illite, kaolinite and chlorite.[6–8]

This research studied the composition of *n*-alkane, sterane and terpane biomarkers in the organic matter of sediments used as healing mud (peloids) in the Serbian spas of Rusanda, Bujanovac and Vranje. These sediments contain a significant portion of clays and do not belong to formations located at greater geological depths and, therefore, were not exposed to high temperatures and pressures. Therefore, it was assumed that the catalytic influence of minerals on changes in biomarkers could be effectively evaluated based on the distribution of their biolipid and thermodynamically more stable geolipid structural and stereochemical isomers.

EXPERIMENTAL

Samples

The present study examined samples of the solid part of peloids, which are used as "healing mud" in the Serbian spas of Rusanda, Bujanovac and Vranje. Peloids are two-phase systems consisting of a solid and a liquid part.[9] The solid part mostly comprises of clay minerals, and the liquid part is thermomineral water. It can contain various inorganic and organic components formed during geological, geochemical and biological processes. Peloid characteristics depend on the composition of the solid and liquid phases and the duration of the mixing process between these phases. This process is called maturation or aging.[8-11] Due to various biological and biochemical processes, depending on the habitat in which the clay is left to mature, during peloid formation, the amount of microorganisms (including microalgae) increases. Microalgae, together with the cyanobacteria that grow on them, improve the dermocosmetic properties of the peloid. It is described in the literature that they have soothing, regenerating, antioxidant, anti-inflammatory and antimicrobial effects. All of this together contributes to the strong positive cosmetic and healing properties of peloid.[9,11-16]

Earlier studies also proved that the presence of long-chain normal alkanes and some of their substituted derivatives contributes to the thermotherapeutic and anti-inflammatory effects of peloids.[17,18] On the other hand, the presence of steroid and terpenoid compounds contribute to analgesic, antioxidant and antitumor properties.[19-22] Other classes of organic compounds contribute to the healing effect. For example, polyunsaturated fatty acids protect against free radicals and have an anti-inflammatory effect,[17,18] and methyl esters of fatty acids contribute to antibacterial and antifungal activity.[21-23]

Methods

The solid parts of the peloid samples from the Serbian spas of Rusanda (Rus), Bujanovac (Bu) and Vranje (Vr) were dried under ambiental conditions. The organic matter was isolated using the Soxhlet method from the samples freed of hygroscopic moisture. An azeotropic mixture of methylene chloride and methanol (88:12 volume ratio) was used as a solvent. The saturated hydrocarbon fraction was isolated by column chromatography. Silica gel and aluminum oxide (2:1) were used as adsorbent and *n*-hexane was used as eluent.

Total aliphatic fractions were analyzed by gass chromatograpy–mass spectrometry (GC––MS, TIC mode), using an Agilent 7890A gas chromatograph (HP-5MS column, 30 m×0.25 mm, 0.25 μm film thickness, He carrier gas 1.5 cm^3 min^{-1}), coupled to an Agilent 5975C mass selective detector. For a more detailed analysis of *n*-alkanes, steranes and terpanes in aliphatic fractions, typical mass fragmentograms (*m*/*z* 71, 217 and 191, respectively) were extracted.

The mineral composition in the samples was determined using the powder X-ray diffraction method (PXRD). The data were collected at room temperature on a Rigaku SmartLab X-ray diffractometer using Bragg–Brentano geometry and CuKα radiation. The presence and type of clay minerals were determined from the oriented aggregates.

RESULTS AND DISCUSSION

The mineralogical composition of the samples was defined using powder X-ray diffraction (PXRD) method. Fig. 1 shows the X-ray diffractograms of Rus, Bu and Vr samples.

The Rusanda sample contained quartz, illite, plagioclase, calcite, chlorite and smectite, with possible presence of kaolinite, K-feldspar, dolomite and para-

gonite, Bujanovac – quartz, plagioclase, illite, kaolinite, chlorite and smectite, with possible presence of K-feldspar and dolomite and Vranje – quartz, analcime, illite, plagioclase, chlorite and smectite, with possible presence of calcite and clinoptilolite.

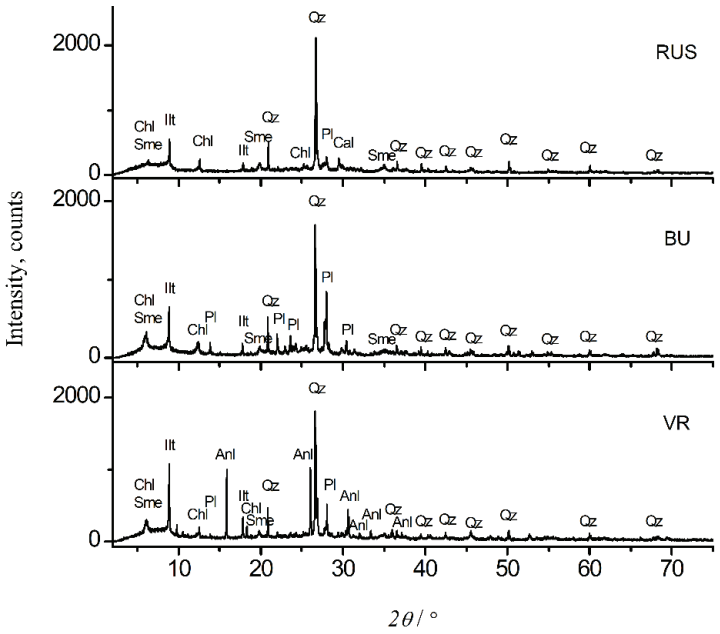

Fig. 1. X-Ray diffractograms of the investigated samples Rusanda, Bujanovac and Vranje. Ilt – illite, Chl – chlorite, Sme – smectite, Qz – quartz, Pl – plagioclase, Anl – analcime.

Previous studies of the effect of minerals on thermal changes in sedimentary organic matter have shown that smectite, illite, chlorite and kaolinite can have catalytic properties.[5–8] Smectite, chlorite and illite were identified in the investigated samples (Fig. 1).

Fig. 2 shows fragmentograms of *n*-alkanes obtained by GC–MS analysis of isolated fractions of saturated hydrocarbons (*m*/*z* 71). Table I demonstrates commonly used organic geochemical parameters calculated based on their distributions.

The distribution of *n*-alkanes of the Rusanda sample shows a bimodal character. The most abundant member in the homologous series is *n*-C_{29}. However, within the short-chain *n*-alkane series, a maximum at *n*-C_{17} is observed. In contrast, within the long-chain *n*-alkane group, a strong dominance of odd homologs is noticed ($CPI_{\text{full range}}$ = 2.77; Table I) and unambiguously originate from the organic matter of higher terrestrial plants with a low degree of thermal maturity.[5] The short-chain *n*-alkanes mainly originate from algal precursor biomass.[5] Given

the proximity of the Rusanda oil field, these *n*-alkanes may be part of an allochthonous organic matter originating from migrated crude oil.

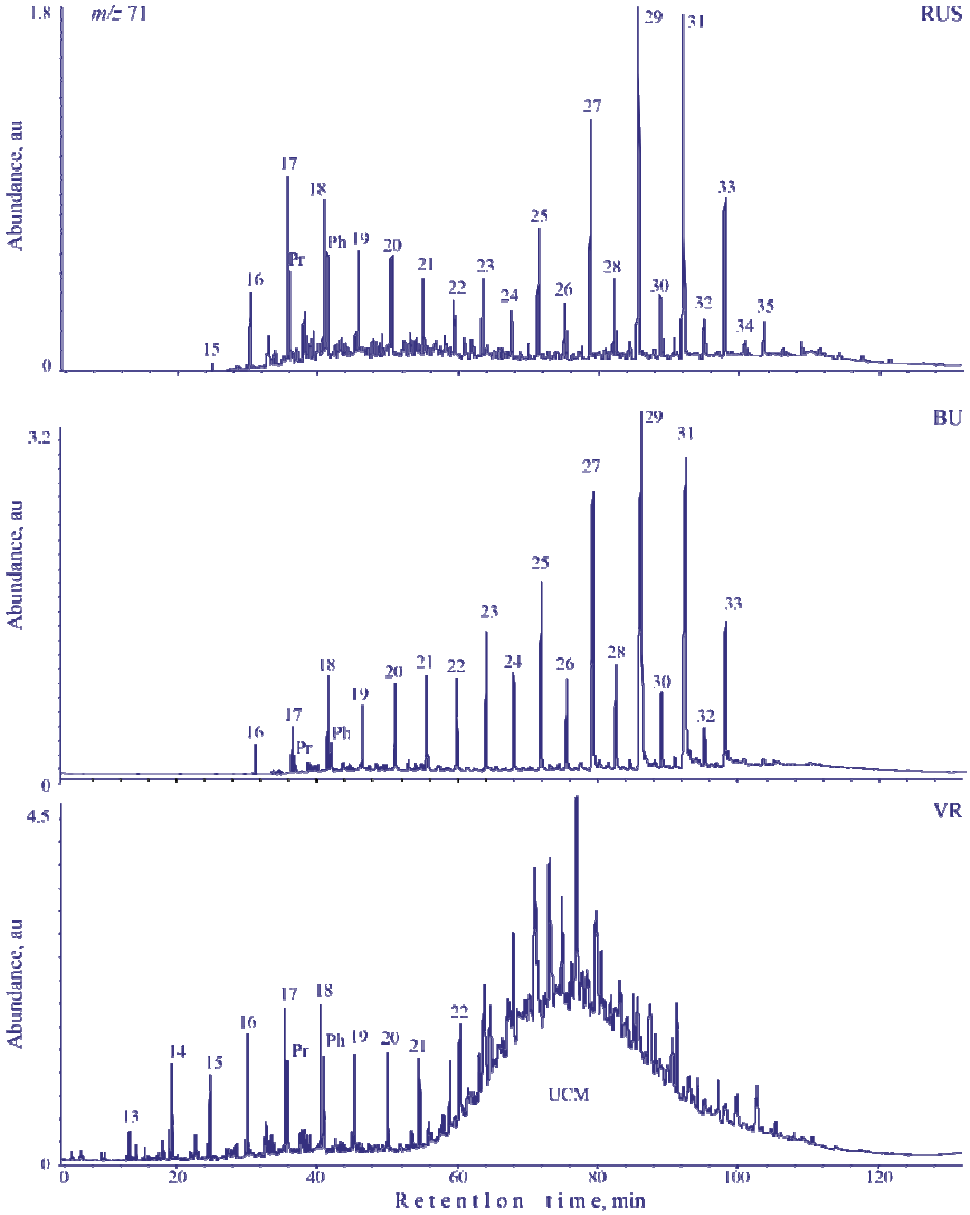

Fig. 2. Fragmentograms of *n*-alkanes obtained by GC-MS analysis of isolated saturated hydrocarbon fractions (*m*/*z* 71). *n*-Alkanes are labelled according to their carbon number; Pr – pristane; Ph – phytane; UCM – unresolved complex mixture.

TABLE I. Parameters calculated from *n*-alkane distributions; *CPI* – carbon preference index

Sample	The range of *n*-alkanes	The most abundant *n*-alkane	*CPI*
Rus	C_{16}–C_{37}	C_{17}, C_{29}	2.77
Bu	C_{16}–C_{33}	C_{29}	3.78
Vr	C_{13}–C_{22}	C_{18}	0.91

n-Alkanes of the Bujanovac extract are characterized by the dominance of odd homologs in the C_{16}–C_{33} range with the most abundant *n*-C_{29} (*CPI* = 3.78; Fig. 2, Table I). This distribution is characteristic of organic matter of terrestrial origin and a low degree of maturation. In the Vranje sample, only lower *n*-alkanes in the C_{13}–C_{22} range and with a slight dominance of even homologs were identified (*CPI* = 0.91; Table I). The second part belongs to the "unresolved complex mixture" (UCM).[24] Considering that there are no oil deposits near this location, it can be assumed that these *n*-alkanes are autochthonous. In that case, it can be concluded that they have an algal origin.

Fig. 3a and b show fragmentograms of steranes (*m*/*z* 217) and terpanes (*m*/*z* 191) of investigated samples. The peak identification is given in Tables II and III, and the values of some maturation parameters calculated from the distributions of steranes and tepanes are given in Table IV.

The distribution and abundance of terpanes in the *m*/*z* 191 fragmentogram for the Rusanda sample (Fig. 3a) are typical for the mature organic matter of sedimentary rocks, usually found in bitumens of source rocks for oil or in oils themselves.[1–5] Numerous parameter values from Table IV confirm this unequivocally. Hopane is distinctly more dominant than moretane (parameter 1), 22*S* isomers are more abundant than the corresponding 22*R* isomers (parameters 2 and 3), C_{27}-18α(H)-trisnorneohopane (Ts), a typical geoisomer, is present in a lower concentration than Tm, but is still present (parameter 4; Table IV).

A similar judgment can be made for steranes (Figure 3b) where the geolipid isomers that are formed from the biolipid isomers, C_{27}–C_{29} 14α(H),17α(H)(20*R*), are found with them in ratios that are typical for oil. This can be said for 20*S* isomers (parameter 5; Table IV), $\beta\beta$ isomers (parameter 6), as well as for diasteranes. As expected, the concentration of $C_{27}\beta\alpha$(20*S*) disterane is lower than C_{27} $\alpha\alpha$(20*R*) sterane. However, the ratio of relative concentrations of these two isomers in the Rusanda sample is typical for mature organic matter (parameter 7; Table IV).

The distributions of terpane and sterane isomers in the Bujanovac and Vranje samples are not identical to those in the Rusanda sample. However, their fingerprints (*m*/*z* 191 and 217, Fig. 3) are typical petroleum. The ratios of geolipid isomers, thermodynamically stable, and the corresponding biolipids from which they were formed during maturation processes, shown through parameters 1–7 from Table IV, unequivocally confirm this.

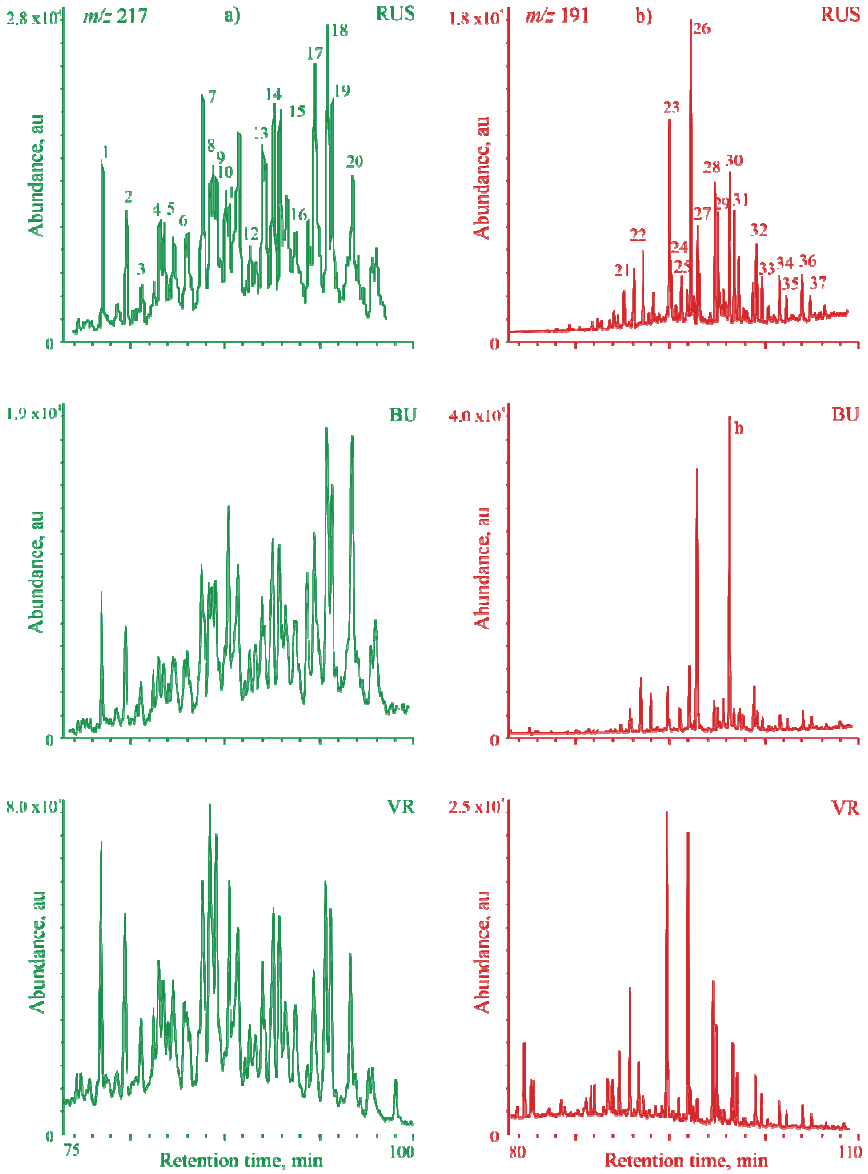

Fig. 3. Fragmentograms of steranes (*m*/*z* 217, a) and terpanes (*m*/*z* 191, b) obtained by GC–MS analysis of isolated saturated hydrocarbon fractions.

Analysis of biomarkers in the solid parts of peloids showed that *n*-alkanes have distributions that are characteristic of immature sediments (Fig. 1). This is an expected result considering that these sediments were not exposed to the temperatures and pressures that are characteristic for the creation of mature forms of the organic matter, e.g., the bitumen of the source rocks for oil or oil itself.

TABLE II. Identification of peaks from Fig. 3a

Peak	Compound
1	C_{27} 13β(H)17α(H)20(*S*)-diasterane
2	C_{27} 13β(H)17α(H)20(*R*)-diasterane
3	C_{27} 13α(H)17β(H)20(*S*)-diasterane
4	C_{27} 13α(H)17β(H)20(*R*)-diasterane
5a	C_{28} 13β(H)17α(H)20(*S*)24(*S*)-diasterane
5b	C_{28} 13β(H)17α(H)20(*S*)24(*R*)-diasterane
6a	C_{28} 13β(H)17α(H)20(*R*)24(*S*)-diasterane
6b	C_{28} 13β(H)17α(H)20(*R*)24(*R*)-diasterane
7	C_{28} 13α(H)17β(H)20(*S*)-diasterane + C_{27} 14α(H)17α(H)20(*S*)-sterane
8	C_{29} 13β(H)17α(H)20(*S*)-diasterane + C_{27} 14β(H)17β(H)20(*R*)-sterane
9	C_{28} 13α(H)17β(H)20(*R*)-diasterane + C_{27} 14β(H)17β(H)20(*S*)-sterane
10	C_{27} 14α(H)17α(H)20(*R*)-sterane
11	C_{29} 13β(H)17α(H)20(*R*)-diasterane
12	C_{29} 13α(H)17β(H)20(*S*)-diasterane
13	C_{28} 14α(H)17α(H)20(*S*)-sterane
14	C_{29} 13α(H)17β(H)20(*R*)-diasterane + C_{28} 14β(H)17β(H)20(*R*)-sterane
15	C_{28} 14β(H)17β(H)20(*S*)-sterane
16	C_{28} 14α(H)17α(H)20(*R*)-sterane
17	C_{29} 14α(H)17α(H)20(*S*)-sterane
18	C_{29} 14β(H)17β(H)20(*R*)-sterane
19	C_{29} 14β(H)17β(H)20(*S*)-sterane
20	C_{29} 14α(H)17α(H)20(*R*)-sterane

TABLE III. Identification of peaks from Fig. 3b

Peak	Compound
21	C_{27} 18α(H),22,29,30-trisnorhopane, Ts
22	C_{27} 17α(H),22,29,30-trisnorhopane, Tm
23	C_{29} 17α(H)21β(H)-hopane
24	C_{29} 18α(H),30-norhopane
25	C_{29} 17β(H)21α(H)-moretane
26	C_{30} 17α(H)21β(H)-hopane
27	C_{30} 7β(H)21α(H)-moretane
28	C_{31} 17α(H)21β(H)22(*S*)-hopane
29	C_{31} 17α(H)21β(H)22(*R*)-hopane
h	C_{30} hopene
30	C_{32} 17α(H)21β(H)22(*S*)-hopane
31	C_{32} 17α(H)21β(H)22(*R*)-hopane
32	C_{33} 17α(H)21β(H)22(*S*)-hopane
33	C_{33}17α(H)21β(H)22(*R*)-hopane
34	C_{34} 17α(H)21β(H)22(*S*)-hopane
35	C_{34} 17α(H)21β(H)22(*R*)-hopane
36	C_{35} 17α(H)21β(H)22(*S*)-hopane
37	C_{35} 17α(H)21β(H)22(*R*)-hopane

TABLE IV. Sterane and terpane maturation parameters

Sample	Terpanes (hopanes)				Steranes (diasteranes)		
	C_{30} moretane / C_{30} hopane	$C_{31}(22S)$ / $C_{31}(22R)$	$C_{31}(22S)$ / $C_{31}(22R)$	Ts / Tm	$C_{29}\alpha\alpha(20S)$ / $C_{29}\alpha\alpha(20R)$	$C_{29}\beta\beta(20R)$ / $C_{29}\alpha\alpha(20R)$	$C_{27}\beta\alpha(20S)$ disterane / $C_{27}\alpha\alpha(20R)$ sterane
Rus	0.19	1.24	1.44	0.76	1.98	1.54	0.36
Bu	0.23	1.32	1.69	0.75	0.84	1.01	0.45
Vr	0.13	1.40	1.34	0.54	1.25	1.29	0.63
Parameter	1	2	3	4	5	6	7

However, the distributions of terpanes and steranes in all three examined samples are surprising. These biomarkers have distributions that are characteristic of mature organic matter of old sedimentary formations (Fig. 3; Table IV) despite insufficiently high temperatures and pressures and, most likely, insufficiently long geological time.

The investigated samples characterize the significant presence of clay minerals (Fig. 1). The conclusion is that illite, smectite and kaolinite, with their strong catalytic effect, actually compensated for all other missing factors, and, as a result, gave terpanes and steranes with distributions that are characteristic even for oil, as the most mature form of organic matter in the geosphere.

CONCLUSION

The composition of *n*-alkane, sterane and terpane biomarkers in the organic matter of sediments used as medicinal mud (peloids) in the Serbian spas of Rusanda, Vranje and Bujanovac was investigated. These sediments are clays that do not belong to formations located at greater geological depths, and therefore were not exposed to high temperatures and pressures. Therefore, it was assumed that the catalytic influence of minerals on changes in biomarkers could be effectively evaluated based on the distribution of their biolipid and thermodynamically more stable geolipid structural and stereoisomers.

Quartz, illite, montmorillonite, plagioclase and chlorite were identified in the samples. Previous tests have shown that all identified minerals in the investigated samples, except quartz, can catalyze the maturation changes of organic matter in sediments.

Analysis of biomarkers in solid parts of peloids showed that *n*-alkanes have distributions that are characteristic of immature sediments. Based on these results, it could be concluded that the identified minerals do not have an obvious catalytic effect on the maturation processes of normal alkanes. Instead, they indicate the precursor biomass from which they originated. Terpanes and steranes in all three examined samples, Rusanda, Bujanovac and Vranje, have distributions characteristic of mature organic matter in old sedimentary formations. Based on this result, it can be concluded that illite, kaolinite, smectite and chlorite, with their strong catalytic effect, actually compensated for all other missing factors

(heat, pressure and most likely, geological time), and as a result gave terpanes and steranes with distributions that are characteristic even for oil, as the most mature form of organic matter in the geosphere.

Acknowledgements. This research has been financially supported by the Ministry of Science, Technological Development and Innovation of Republic of Serbia (Contract No: 451--03-66/2024-03/200026, 451-03-66/2024-03/200168 and 451-03-66/2024-03/200126) and the Science Fund of the Republic of Serbia, Grant No. 11015, Peloids in Serbia: Geochemical characterization, quality assessment and ecosystem services of peloid-rich areas – PELAS.

ИЗВОД

МАТУРАЦИОНЕ ПРОМЕНЕ УГЉОВОДОНИКА У ЧВРСТОМ ДЕЛУ ПЕЛОИДА СРПСКИХ БАЊА – КАТАЛИТИЧКИ УТИЦАЈ МИНЕРАЛА ГЛИНЕ

ЗЛАТКО НИКОЛОВСКИ[1], АЛЕКСАНДРА ШАЈНОВИЋ[2], ГОРДАНА ГАЈИЦА[2], НИКОЛА БУРАЗЕР[2], ИЛИЈА БРЧЕСКИ[1], ПРЕДРАГ ДАБИЋ[3] и БРАНИМИР ЈОВАНЧИЋЕВИЋ[1]

[1]Универзитет у Београду, Хемијски факултет, Студентски трг 12–16, 11001 Београд, [2]Универзитет у Београду, Институт за хемију, технологију и металургију, Национални институт Републике Србије, Његошева 12, 11001 Београд и [2]Универзитет у Београду, Рударско-геолошки факултет, Ђушина 7, 11120 Београд

Проучаван је састав биомаркера типа нормалних алкана, стерана и терпана у органској супстанци седимената који се употребљавају као лековито блато (пелоиди) у српским бањама Русанда, Врање и Бујановац. Пошло се од претпоставке да би се каталитички утицај минерала на промене биомаркера ефикасно могао да се процени на основу расподела њихових биолидних, и термодинимачки стабилнијих геолипидних структурних и стереохемијских изомера. У узорцима су рендгено–дифракционом анализом идентификовани кварц, илит, плагиоклас, монтморионит и хлорит. Гаснохроматографско–масеноспектрометријском техником у чврстим деловима пелоида анализирани су нормални алкани, терпани и стерани. У узорцима из Русанде и Бујановца идентификовани су нормални алкани са расподелама које су карактеристичне за нематурисане седименте. Закључено је да идентификовани минерали немају очигледно каталитичко дејство на матурационе процесе нормалних алкана. Терпани и стерани у сва три испитивана узорка имају расподеле које су карактеристичне за матурисане органске супстанце старих седиментних формација. Закључено је да су илит, каолинит, смектит и хлорит каталитичким дејством заправо надокнадили све друге недостајуће факторе (топлота, притисак и највероватније, геолошко време), и као резултат дали терпане и стеране са расподелама које су карактеристичне чак и за нафту, као најматурисанији облик органске супстанце геосфере.

(Примљено 12. септембра, ревидирано 12. новембра, прихваћено 1. децембра 2024)

REFERENCES

1. B. P. Tissot, D. H. Welte, *Petroleum Formation and Occrrence*, 2nd ed., Springer-verlag, Heidelbarg, 1984 (ISBN: 0-387-08698-6)
2. D. Waples, *Geochemistry in Petroleum Exploration*, International Human Resources Development Corporation, Boston, MA, 1985 (ISBN: 90-277-208-8)

3. R. P. Philp, *Fossil Fuel Biomarkers. Applications and Spectra*, Elsevier, Amsterdam, 1985 (ISBN: 0444424717)
4. K. E. Peters, C. C. Walters, J. M. Moldowan, *The biomarker Guide, Vol. 2: Biomarkers and Isotopes in Petroleum Exploration and Earth History*, Camridge University Press, Cambridge, 2005 (ISBN: 0-521-83763-4)
5. J. Schwarzbauer, B. Jovančićević, *Fundamentals in Organic Geochemistry – Fossil Matter in the Geosphere*, Springer, Heidelberg, 2015 (ISBN: 978-3-319-27241-2)
6. B. Jovančićević, D. Vitorović, M. Šaban, H. Wehner, *Org. Geochem*. **18** (1992) 511 (https://doi.org/10.1016/0146-6380(92)90114-D)
7. D. Vučelić, V. Marković, V. Vučelić, D. Spiridonović, B. Jovančićević, D. Vitorović, *Org. Geochem*. **19** (1992) 445 (https://doi.org/10.1016/0146-6380(92)90011-L)
8. B. Jovančićević, D. Vučelić, M. Šaban, H. Wehner, D. Vitorović, *Org. Geochem*. **20** (1993) 69 (https://doi.org/10.1016/0146-6380(93)90082-M)
9. C. Gomes, M. Isabel Carretero, M. Pozo, F. Maraver, P. Cantista, F. Armijo, J. L. Legido, F. Teixeira, M. Rautureau, R. Delgado, *Appl. Clay Sci.* **75**–**76** (2013) 28 (https://doi.org/10.1016/j.clay.2013.02.008)
10. M. Pozo, M. I. Carretero, F. Maraver, E. Pozo, I. Gómez, F. Armijo, J. A. M. Rubí, *Appl. Clay Sci.* **83**–**84** (2013) 270 (https://doi.org/10.1016/j.clay.2013.08.034)
11. M. Centini, M. R. Tredici, N. Biondi, A. Buonocore, R. Maffei Facino, C. Anselmi, *Int. J. Cosmet. Sci.* **37** (2015) 339 (https://doi.org/10.1111/ics.12204)
12. M. V. Fernández-González, J. M. Martín-García, G. Delgado, J. Párraga, M. I. Carretero, R. Delgado, *Appl. Clay Sci.* **135** (2017) 465 (https://doi.org/10.1016/j.clay.2016.10.034)
13. C. Tolomio, C. Ceschi-Berrini, F. De Apollonia, L. Galzigna, L. Masier, I. Moro, E. Moschin, *Algol. Stud.* **105** (2002) 11 (https://doi.org/10.1127/algol_stud/105/2002/11)
14. C. Tolomio, F. De Apollonia, I. Moro, C. Ceschi-Berrini, *Algol. Stud.* **111** (2004) 145 (https://doi.org/10.1127/1864-1318/2004/0111-0145) x
15. M. L. Mourelle, C. P. Gómez, J. L. Legido, *Mar. Drugs* **19** (2021) 666 (https://doi.org/10.3390/md19120666)
16. S. R. Manning, *Curr. Opin. Biotechnol.* **74** (2022) 1 (https://doi.org/10.1016/j.copbio.2021.10.018)
17. M. Suárez Muñoz, N. V. Martínez Villegas, P. González Hernández, C. Melián Rodríguez, J. Barrios Cossio, R. Hernández Díaz, J. R. Fagundo Catillo, O. Díaz Rizo, C. Díaz López, A. Pérez Gramatges, *Rev. Int. de Contam. Ambient.* **34** (2018) 121 (https://doi.org/10.20937/2018.34.M6ISSM)
18. N. Martínez-Villegas, M. Suarez Munoz, P. González-Hernández, C. Melián Rodríguez, J. Barrios Cossio, R. Hernández Díaz, J.R. Fagundo Castillo, A. Gelen Rudnikas, C. Diaz Lopez, A. Pérez-Gramatges, O. Diaz Rizo, *Environ. Sci. Pollut. Res.* **27** (2020) 15944 (https://doi.org/10.1007/s11356-019-04790-2)
19. C. B. Fox, *Molecules* **14** (2009) 3286 (https://doi.org/10.3390/molecules14093286)
20. A. E. Ardiles, A. González-Rodríguez, M. J. Núñez, N. R. Perestelo, V. Pardo, I. A. Jiménez, A. M. Valverde, I. L. Bazzocchi, *Phytochemistry* **84** (2012) 116 (https://doi.org/10.1016/j.phytochem.2012.07.025)
21. I. Popa, N. Băbeanu, N. Băbeanus, S. Nita, O. Popa, *Farmacia* **62** (2014) 840 (https://farmaciajournal.com/wp-content/uploads/2014-05-art-03-Popa_Ovidiu_840-862.pdf)

22. M. Suárez, P. González, R. Domínguez, A. Bravo, C. Melián, M. Pérez, I. Herrera, D. Blanco, R. Hernández, J. R. Fagundo, *J. Altern. Complement. Med.* **17** (2011) (https://doi.org/10.1089/acm.2009.0587)
23. A. Suresh, R. Praveenkumar, R. Thangaraj, F. Lewis-Oscar, D. Dhanasekaran, N. Thajuddin, *Asian Pac. J. Trop. Dis.* **4** (2014) 930 (https://doi.org/10.1016/S2222-1808(14)60769-6)
24. G. T. Ventura, F. Kenig, C. M. Reddy, G. S. Frysinger, R. K. Nelson, B. Van Mooy, R. B. Gaines, *Org. Geochem.* **39** (2008) 846 (https://doi.org/10.1016/j.orggeochem.2008.03.006).

Journal of the Serbian Chemical Society
JSCS@tmf.bg.ac.rs • www.shd.org.rs/JSCS
J. Serb. Chem. Soc. *89* (12) 1571–1585 (2024)
JSCS–5807
Original scientific paper
Published 26 December, 2024

Sustainable synthesis of samarium molybdate nanoparticles: a simple electrochemical tool for detection of environmental pollutant metol

TIJANA MUTIĆ[1], VESNA STANKOVIĆ[1], JADRANKA MILIKIĆ[2], DANICA BAJUK-BOGDANOVIĆ[2], KURT KALCHER[3], ASTRID ORTNER[4], DRAGAN MANOJLOVIĆ[5] and DALIBOR STANKOVIĆ[5]*

[1]University of Belgrade, Institute of Chemistry, Technology and Metallurgy, National Institute of the Republic of Serbia, Njegoševa 12, 11000 Belgrade, Serbia, [2]University of Belgrade, Faculty of Physical Chemistry, Studentski trg 12–16, 11158 Belgrade, Serbia, [3]Institute of Chemistry, Analytical Chemistry, Karl-Franzens University, Universitaetsplatz I/I, 8010 Graz, Austria, [4]University of Graz, Institute of Pharmaceutical Sciences, Department of Pharmaceutical Chemistry, Schubertstraße 1, 8010 Graz, Austria and [5]University of Belgrade, Faculty of Chemistry, Studentski Trg 12–16, 11158 Belgrade, Serbia

(Received 13 September, revised 7 October, accepted 2 December 2024)

Abstract: This study focused on creating a highly effective sensor for detecting and quantifying the nitrogen-organic pollutant metol (MTL). For this purpose, samarium molybdate ($Sm_2(MoO_4)_3$) nanoparticles were synthesized using an eco-friendly, organic solvent-free and cost-effective hydrothermal method. These nanoparticles were used as a modifier of carbon paste electrodes (CPE), showing exceptional catalytic efficiency. Electrochemical measurements revealed that the developed electrode facilitates electron transfer processes and enhances the catalytic response. The resulting $Sm_2(MoO_4)_3$/CPE sensor exhibited a broad linear range of 0.1–100 and 100–300 μM of MTL, with low detection and quantification limits of 0.047 and 0.156 μM, respectively, at pH 3 in a Britton–Robinson buffer solution (BRBS) as the supporting electrolyte. The findings from the analysis of real water samples from various sources using this sensor were encouraging, suggesting that this method could offer a cost-effective, rapid and sensitive sensor for ambient MTL monitoring.

Keywords: environmental analysis; carbon paste electrode; organic pollutants; rare earth nanoparticles; electrochemical sensor.

INTRODUCTION

In photographic processes, photosensitive materials are used by photographers to convert latent images into visible ones.[1] Among other photographic

* Corresponding author. E-mail: dalibors@chem.bg.ac.rs
https://doi.org/10.2298/JSC240913102M

developers, metol (MTL) has been used as a monochrome photographic chemical for more than 100 years in Europe.[2,3] MTL, chemically *N*-methyl-*p*-aminophenol sulphate with formula $[HOC_6H_4NH_2(CH_3)]_2SO_4$, is also used as a corrosion inhibitor, antioxidant and antimicrobial agent, and it serves as an intermediary for the medication diloxanide and dyes for fur and hair.[4,5] Since it is used in the photographic industry, it is released into the water, contaminating ground, and household water.[6] It can be easily found in different water bodies such as rivers, lakes, ponds and seas.[1] MTL was found to be a cancerogenic organic pollutant with a significant impact on human health, the environment, animals, plants, and water sources.[7] MTL is non-biodegradable and can accumulate in biotic organisms. It is also related to numerous environmental issues, even in low concentrations.[2] Furthermore, a larger dose of MTL is necessary to have a substantial effect on several health problems, such as cancer, irritable eyes, slowed heartbeat, skin allergies and harm to the body's internal blood supply.[8] Therefore, developing a straightforward, quick, affordable, sensitive and practical method for MTL detection in aquatic bodies is imperative.

Various methods for MTL detection were reported, such as spectrophotometry,[9,10] ceric oximetry,[11] photolysis[12] and liquid chromatography–mass spectrometry.[7] Besides that, a few works using electroanalytical methods for MTL detection were reported.[13–15] Despite the incredible accuracy of these analytical techniques, they are costly, time-consuming, and require complex sample preparation procedures.[5,16] On the other hand, electrochemical methods have many advantages over conventional analytical techniques, such as low cost, ease of sample preparation, wide detection range, improved sensitivity and selectivity, facilitated device miniaturization, *in vivo* and *in vitro* process monitoring and they are user-friendly.[5,16–18] Several problems were solved with an electrode modification, such as slow electron transfer kinetics and gradual passivation of the surface, a higher transfer of electrons, enhanced conductivity, and surface area.[19] The application of modified electrodes as working in a three-electrode system for the electrochemical detection allows trace-level analysis[20,21] and increased the sensitivity of detection.[22]

In this work, $Sm_2(MoO_4)_3$ nanoparticles were synthesized using the hydrothermal method to modify the carbon paste electrode as a working electrode in electrochemical measurements. The morphological characteristics of synthesized material were investigated through X-ray diffraction (XRD), scanning electron microscope (SEM) and transmission electron microscope (TEM). The electrochemical properties of modified electrodes were studied by cyclic voltammetry (CV) and electrochemical impedance spectroscopy (EIS). differential pulse voltammetry (DPV) and square wave voltammetry (SWV) were compared and optimized for the selective and sensitive electrochemical detection of MTL. The real

sample application of the developed sensor was tested using the SWV method under the optimized working conditions.

EXPERIMENTAL

Materials and methods

All chemicals used in this study were purchased by Sigma Aldrich, which had the highest purity and were used without further purification. For $Sm_2(MoO_4)_3$ nanoparticles synthesis, samarium (III) nitrate hexahydrate ($Sm(NO_3)_3{\cdot}6H_2O$; 99.9 %), ammonium molybdate tetrahydrate ($(NH_4)_6Mo_7O_{24}{\cdot}4H_2O$; 99.98%), nitric acid (65 %), and ammonia solution (25 %) were used. The solution of analyte metol (4-(methylamino)phenol sulphate; ≥98.0 %) was freshly prepared before every measurement. As the supporting electrolyte, Britton–Robinson buffer solution (BRBS) was used (0.04 M mixture of boric acid, acetic acid and phosphoric acid) and pH value was adjusted by using the NaOH solution. The electrochemical characterization of electrodes was performed in 5 mM $Fe^{2+/3+}$ solution (potassium hexacyanoferrate (II) trihydrate ($K_4[Fe(CN)_6]{\cdot}3H_2O$ and potassium hexacyanoferrate (III) ($K_3[Fe(CN)_6]$) in 0.1 M KCl). The organic compound solutions (vitamins B6, B1, C, sucrose and glucose) were used to investigate potential interferents, and gallic acid, hydroquinone and bisphenol A solutions were used for the selectivity study. As a real sample, tap, and pond water were used.

Jeol JSM 7001 F (JEOL, Ltd., Japan) electron microscope was used for the analysis of the surface morphology of the $Sm_2(MoO_4)_3$ sample. Additionally, the Rigaku Optima IV powder diffractometer (Rigaku, Japan) was used for the examination of its phase composition and structure. The survey was recorded in the range of 2θ angles from 5 to 90° at a survey rate of 2°/min by using radiation from a CuKα copper tube (λ = 1.541 Å) at an accelerating voltage of 40 kV. The FTIR spectra of the sample, dispersed in KBr and compressed into pellets, were recorded using an FTIR Spectrometer Thermo Nicolet iS20 (Thermo Fisher Scientific) in the range of 4000–400 cm^{-1} at 64 scans per spectrum at 4 cm^{-1} resolution. The Raman spectra, excited with a diode-pumped solid-state high-brightness li laser (532 nm) were collected on a Thermo Scientific DXR Raman microscope (Thermo Fisher Scientific), equipped with a research optical microscope and CCD detector. The laser beam was focused on the sample placed on the *X*–*Y* motorized sample stage using objective magnification ×10. The scattered light was analyzed by the spectrograph with a grating of 900 lines mm^{-1}. The laser power was kept at 0.1 mW on the samples.

A PalmSens4 analyzer (Houten, Utrecht, The Netherlands) running PSTrace voltammetry software (version 5.8) was used for all electrochemical measurements. Unmodified and modified carbon paste electrodes were applied as working electrodes, Ag/AgCl was applied as the reference electrode, and a platinum wire was used as a counter electrode in a three-electrode system at room temperature.

Synthesis of $Sm_2(MoO_4)_3$ nanoparticles and electrodes preparation

Samarium (III) nitrate hexahydrate (0.1 mol; *Mr* = 444.47) and ammonium molybdate tetrahydrate (0.1 mol; *Mr* = 1235.86) were dissolved in 2 mL HNO_3 (2 M) and 2 mL deionized water at room temperature, followed by stirring. The pH value of the solution was adjusted to 6 using ammonia NH_3 solution (25 %). The solution was stirred for 30 min and then transferred to a hydrothermal autoclave for 24 h at 180 °C. The precipitate was filtrated, washed with water, ethanol and acetone, and dried overnight at room temperature.

A bare carbon paste electrode (CPE) was prepared by hand-mixing graphite powder and paraffin oil in a mass ratio of 70:30 (graphite powder/paraffin oil), in an agate mortar with a

pestle, until a homogenous paste was achieved. The obtained paste was pressed into a homemade Teflon electrode body with the inner diameter of 2 mm and smoothed on paper to get a uniform surface. The modified carbon paste electrodes were prepared following the same procedure, but with the addition of different percentages of synthesized material. $Sm_2(MoO_4)_3$ nanoparticles were added to paste in 5, 10, 15 and 20 wt. %.

RESULTS AND DISCUSSION

Morphological properties of synthesized $Sm_2(MoO_4)_3$ nanoparticles

The SEM images of $Sm_2(MoO_4)_3$ are presented in Fig. 1A and B, recorded at different sizes of magnitudes. Namely, the aggregated granular-like morphology was obtained for $Sm_2(MoO_4)_3$. A similar kind of morphology of $Sm_2(MoO_4)_3$ was obtained by S. Behvandi *et al.*[23] The EDS spectrum of $Sm_2(MoO_4)_3$ confirmed the presence of Sm, Mo and O elements in Fig. 1C. The mapping images of Sm, Mo and O exhibited their uniform distribution.

Fig. 1D shows the XRD pattern of the $Sm_2(MoO_4)_3$ which contains the diffraction peaks at 28.65, 34.04 and 46.74° corresponding to the reflection from (111), (221) and (100) crystal planes of $Sm_2(MoO_4)_3$.[23–25] These obtained results confirmed the good crystallinity[26] of the synthesized sample. Irrespective of its environment, the stretching and bending internal modes of the molybdate ion appear in the region 950–775 cm^{-1} and 425–275 cm^{-1}, respectively. On the other hand, the frequency of the external modes strongly depends on the nature of the cation.[27] Fig. 1E shows the FTIR spectrum of the $Sm_2(MoO_4)_3$. All the ν_1 and ν_3 stretching vibrational modes fall in the broad contour from 1000 to 600 cm^{-1}.[27] The bending region shows one band centred at 429 cm^{-1}.[27] In the Raman spectrum, Fig. 1F, one can see that the modes are observed in two well-separated regions, *i.e.*, 1000–700 and 400–300 cm^{-1}. The bands located below 300 cm^{-1} are attributed to external vibrations of the MoO_4 anions and translational modes of cations.[28]

All of these results confirmed that the synthesized sample is samarium molybdate.[23]

Electrochemical properties of the prepared electrode

EIS and CV were used for electrochemical investigations of the prepared electrodes in 5 mM $[Fe(CN)_6]^{3-/4-}$ and 0.1 M KCl solution. Fig 2A shows Nyquist plots observed for bare CPE and 5,10, 15 and 20 wt. % modified carbon paste electrodes. A straight line can be seen in the low-frequency part of the graph, which is related to the diffusion transfer of ions into the electrode material (Warburg diffusion). In contrast, a semicircle can be seen in the high-frequency zone, corresponding to the charge transfer process.[29] The *Rct* value is the diameter of the semicircle, representing the quantitative measure of the resistance to charge transfer.[29] The electrochemical performance of the electrode is strongly related to the *Rct* value.[30,31] The *Rct* value of the 15 wt. % modified electrode is 285.5 Ω, and

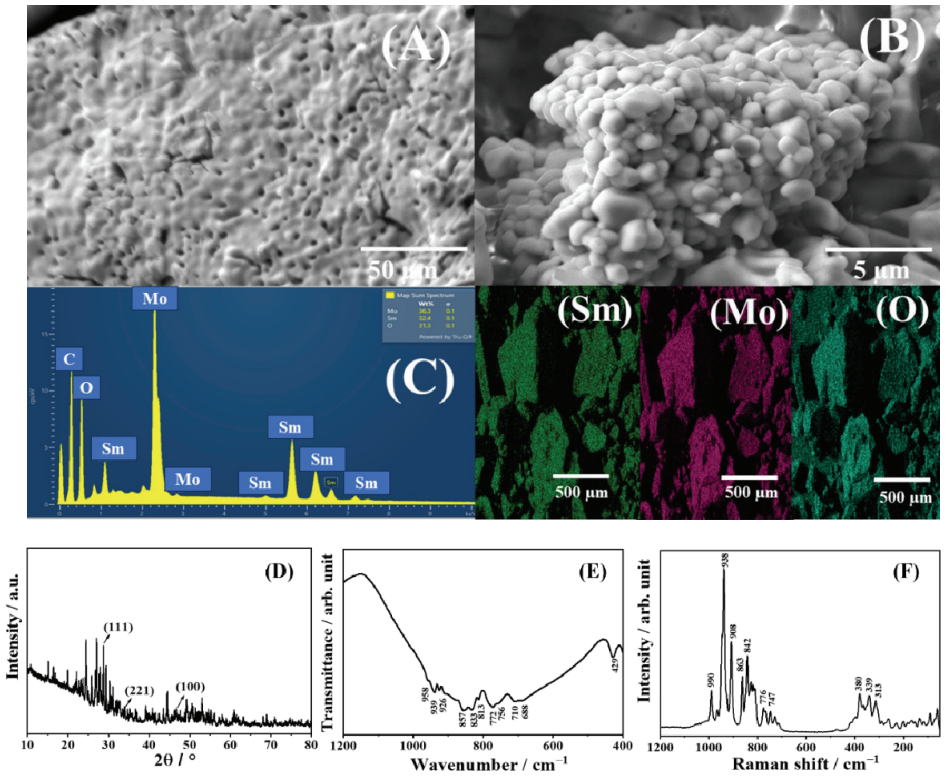

Fig. 1. A, B) SEM images of $Sm_2(MoO_4)_3$ at different magnifications with the corresponding EDS spectrum (C) and mapping images of Sm, Mo and O; D) XRD pattern; E) FTIR and F) Raman spectra of $Sm_2(MoO_4)_3$.

it is lower compared to the *Rct* values of bare CPE and 5, 10 and 20 wt. % modified electrodes, which *Rct* values are 3647.9, 313.5, 430.8 and 367.1 Ω, respectively. Much lower charge transfer resistance of the 15 wt. % modified CPE indicates that $Sm_2(MoO_4)_3$ nanoparticles efficiently promote the electron transfer processes, increasing the flow rate of ferricyanide species toward the electrode surface. These results confirm that the electron transfer kinetics of the modified electrode is quite excellent. From the straight line in the low-frequency plots, the diffusion coefficient could be estimated using the following equation:[31]

$$D = (RT)^2/(2A^2n^4F^4C^2\sigma^2) \quad (1)$$

where R is the universal gas constant (8.314 J mol^{-1} K^{-1}), T corresponds to temperature (K), A denotes electroactive surface area (cm^2), n is the number of electrons transferred, F symbolizes Faraday constant (96485 C mol^{-1}), C is the concentration, and σ is the Warburg factor related to Z'. The Warburg factor σ could be obtained by linearly fitting the relationship curve between Z' and the angular

frequency reciprocal square root, shown for all electrodes in Fig. S-1 of the Supplementary material to paper.

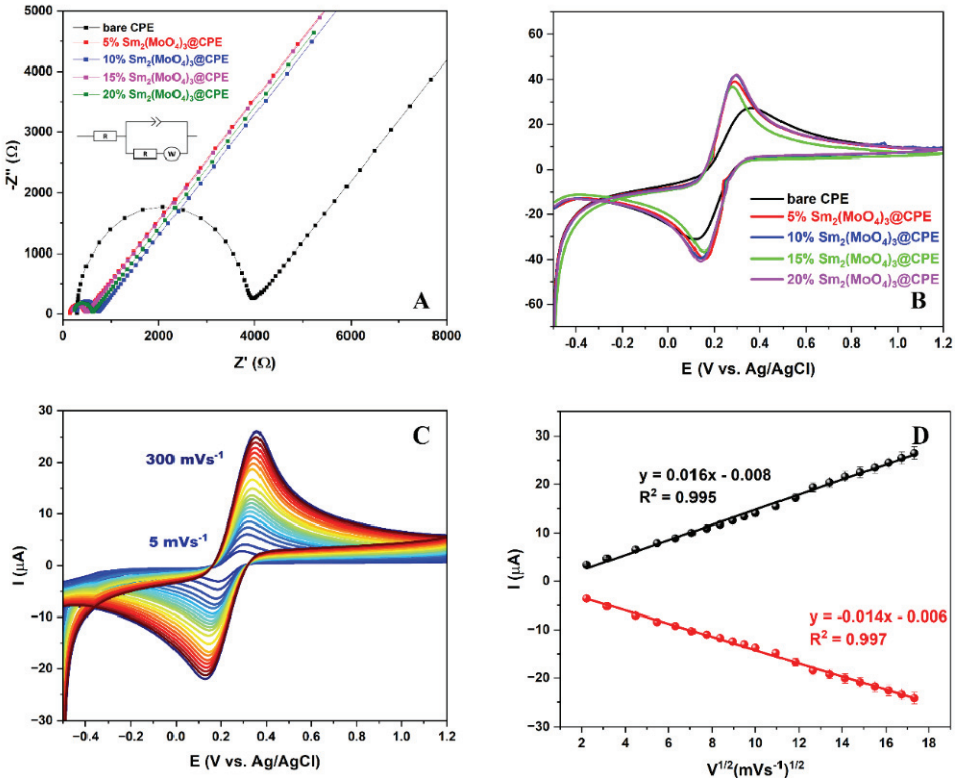

Fig. 2. A) Nyquist plots and B) CV studies of bare CPE and 5, 10, 15 and 20 wt. % modified CPEs in 5 mM $[Fe(CN)_6]^{3-/4-}$ and 0.1 M KCl solution; C) CV curves of 15 wt. % modified CPE at different scan rates in a range from 5 to 300 mV s^{-1}; D) dependence of redox peak currents on the square root of the scan rate.

In the same solution, CV measurements were performed in the potential range from –0.5 to 1.2 V. As shown in Fig. 2B, redox peak currents of bare CPE (27.29 μA for oxidation and –34.05 μA for reduction) are much lower when compared to 5, 10, 15 and 20 wt. % modified electrodes whose peak currents are 40.82, 46.18, 41.98 and 47.46 μA for oxidation, respectively, and –40.62, –42.33, –39.76 and –45.56 μA for reduction, respectively. The 15 wt. % modified electrode showed the lowest peak-to-peak separation value (ΔE = 0.120V) compared to bare CPE, 5, 10 and 20 wt. % modified electrodes with values of 0.232, 0.141, 0.151 and 0.157 V, respectively. For all prepared electrodes, the electrochemical behavior of $Fe^{2+/3+}$ at different scan rates was investigated and presented in Fig. S-2 of the Supplementary material. Fig. 2C shows the impact of the scan rate on

redox peaks of $Fe^{2+/3+}$ over 15 wt. % modified CPE. With increasing scan rate, the redox peak currents also increase with the linear dependence of redox peak currents on the square root of the scan rate, shown in Fig. 2D, and this dependence for all other electrodes is shown in Fig. S-3 of the Supplementary material. From these results, the electroactive surface areas of all electrodes were calculated using the Randles–Sevcik equation:[32]

$$I_p = 2.69\times10^5 n^{3/2} A D^{1/2} C V^{1/2} \quad (2)$$

where I_p is peak current (A), n denotes transferred electrons, D signifies diffusion coefficient ($cm^2\ s^{-1}$), C is the concentration of solution (mol cm^{-3}), and V is the scan rate ($V\ s^{-1}$). All of the modified electrodes have higher values of the electroactive surface area than the bare CPE, indicating that incorporating synthesized material into the carbon paste improved the electron transport capacity and accelerated the electron transfer rates. All calculated values are presented in Table S-I of the Supplementary material. Considering all mentioned above, the electrode with a 15 wt. % modifier was chosen for further electrochemical measurements.

Detection of MTL and optimization of pH of the supporting electrolyte

The CV measurements (Fig. 3A) were performed in 100 μM MTL solution in BRBS pH 3 as supporting electrolyte over bare carbon paste electrode and 15 wt. % $Sm_2(NO_3)_3$ modified electrode, since it showed the best electrocatalytic behaviour in $Fe^{2+/3+}$ solution. The modified electrode shows better MTL response with peak currents of 5.37 μA for the oxidation and –5.33 μA for the reduction than bare CPE, whose peak values are 5.00 and –4.90 μA for the oxidation and the reduction, respectively. A lower value of peak-to-peak separation was obtained with modified CPE, 59 mV, compared to bare CPE, 67 mV. These results indicate that the $Sm_2(NO_3)_3$ modified electrode has outstanding electrocatalytic activity and a quick electron transfer mechanism.

A significant role in developing sensitive and selective sensor plays the pH value of supporting electrolyte. Fig. 3B represents cyclic voltammograms of 100 μM MTL solution at 50 mV s^{-1} at different pH values of BRBS, in the range from 2 to 9. With the increasing pH value of the supporting electrolyte, a significant potential shift to lower values can be seen. This shifting is linear, and the relationship between potential and pH values is presented in Fig. 3C. The dependence of peak potential on pH value is linear for the oxidation and reduction processes with the equations: $y = -0.062x + 0.565$ and $y = -0.064x + 0.517$ with linear regression coefficients R^2 0.993 and 0.996, respectively. Since the slopes of curves are 62 and 65 mV, and both are very close to the theoretical value of 59 mV, it was proved that the mechanism of oxidation involves an equal number of electrons and protons (m/n), using the following equation:[2]

$$E_p = (0.059m/n)\text{pH} + b \quad (4)$$

Fig. 3D represents the relationship between the supporting electrolyte's peak current and pH value. For both oxidation and reduction processes, the highest peak current of the signal was obtained on pH 3, which is selected for all further measurements.

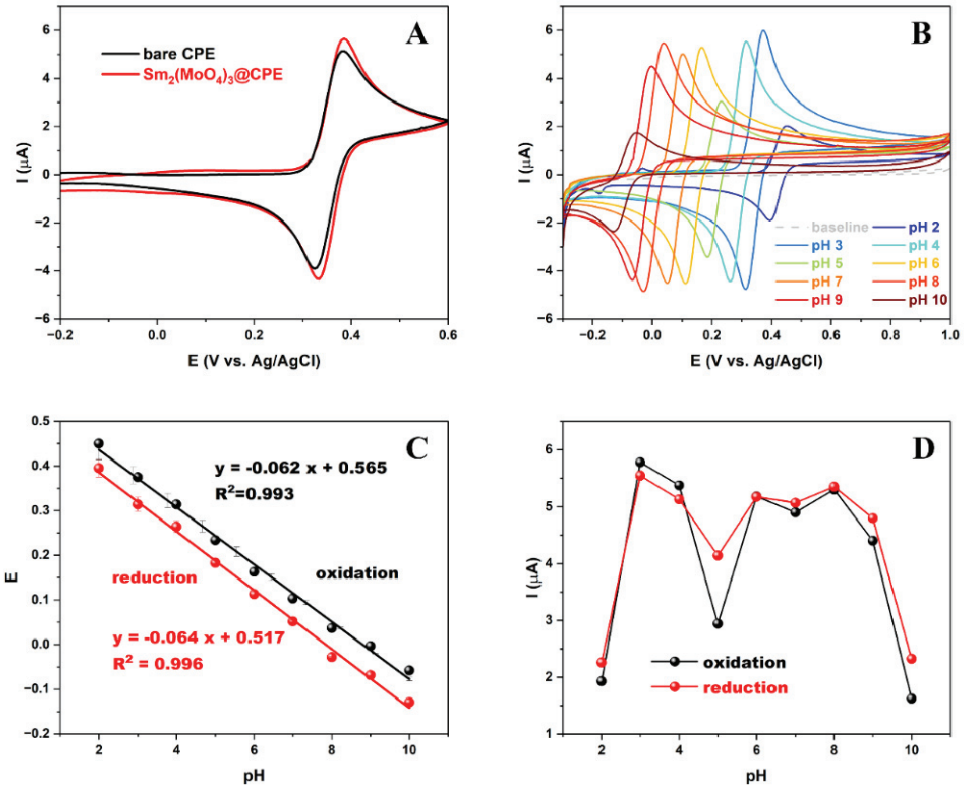

Fig. 3. A) Cyclic voltammogram (CV) of bare carbon paste electrode and 15 wt. % $Sm_2(MoO_4)_3$ modified electrode in 100 μM MTL solution at pH 3; B) CV measurements of 100 μM MTL solution at 50 mV s^{-1} at different pH values of BRBS in the range from 2 to 9; C) dependence of peak potential on pH value of supporting electrolyte in the range from 2 to 9; D) dependence of peak current on pH value of supporting electrolyte in the range from 2 to 9.

Electrochemical behavior of MTL at different scan rates over $Sm_2(MoO_4)_3$/CPE sensor

The electrochemical behaviour of MTL was investigated through CV measurements at different scan rates ranging from 2 to 300 mV s^{-1} in 100 μM MTL solution over a 15 wt. % modified $Sm_2(MoO_4)_3$/CPE electrode. As shown in Fig. 4A, the peak current increases with the scan rate values, implying that the redox reaction of MTL is scan rate dependent. This relationship is shown in Fig. 4B for

both oxidation and reduction peaks. The dependence of redox peak currents is linear on the square root of the scan rate with equations $y = 0.763x - 0.071$ with R^2 0.999 and $y = -0.857x + 0.619$ with R^2 0.999 for the oxidation and the reduction, respectively, indicating that the MTL redox reaction is a diffusion-controlled process. This statement was also proved by the linear dependence of log I on $log\ V$ (Fig. 4C) with a slope of 0.499 for the oxidation and –0.502 for the reduction peak, which is very close to the theoretical slope of 0.5 for diffusion--controlled processes.[8] Furthermore, the redox peak potential is linearly dependent on the natural logarithm of the scan rate (Fig. 4D) and the linear regression plot as $y = 0.031x + 0.347$ with R^2 0.96, and $y = -0.029x + 0.354$ with R^2 0.90 for oxidation and reduction, respectively. The number of electrons participating in the MTL redox reaction was calculated using the following equations:[34]

$$E_p = E_0' + (2.303RT/\alpha nF)\log(RTk_0/\alpha nF) + (2.303RT/\alpha nF)\log V \quad (5)$$

$$E_{p/2} - E_p = 1.857RT/\alpha F \quad (6)$$

where α, k_0, n, V, E_0' and $E_{p/2}$ are the transfer coefficient, the standard heterogeneous rate constant of the reaction, the number of electrons, scan rate, formal

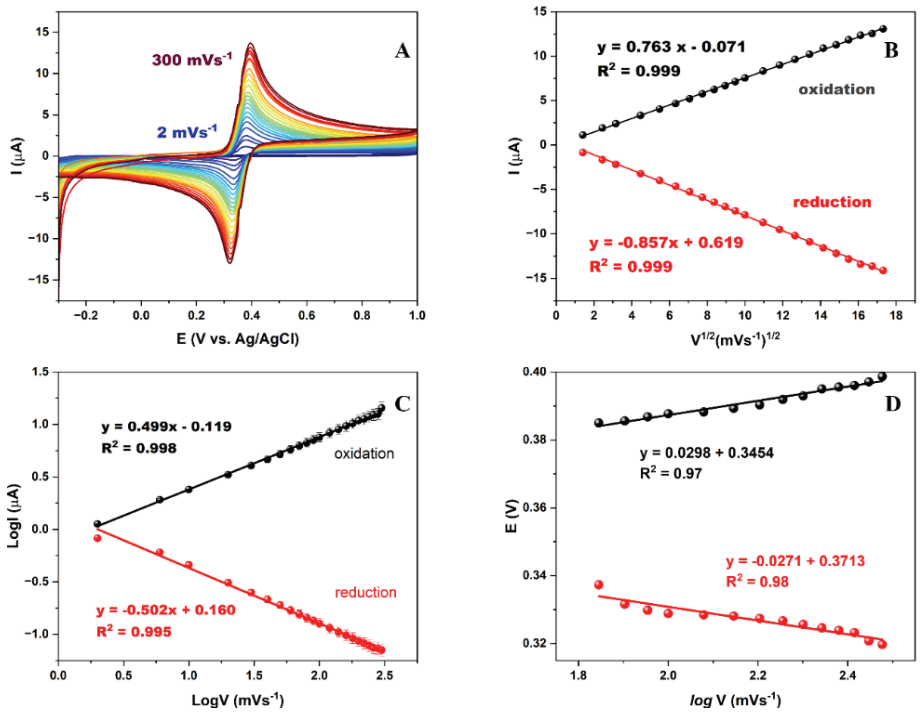

Fig. 4. A) CV curves of the 100 μM MTL solution over 15 wt. % modified CPE at different scan rates in a range from 2 to 300 mV s^{-1}; B) the dependence of the redox peak currents on the square root of the scan rate; C) dependence of the log I on the log V for redox peaks; D) dependence of the potential value on the logV for redox peaks.

redox potential and the potential when the current is at half of the peak value, respectively. Other symbols have their common meanings. The values of α and n are calculated to be 0.4072 and 2.3, which is close to 2. The mechanism of the MTL redox reaction was confirmed with everything mentioned above, where two electrons and two protons participate in this reaction, which follows previously reported works.

Quantification of MTL

The pulse methods were tested to develop sensitive and selective methods for quantification of MTL. We compared DPV and SWV, and the comparison between these two techniques is shown in Fig. 5A. The obtained peak currents with SWV are 15.37 and 15.70 μA for the oxidation and the reduction, respectively, while the values achieved using the DPV method are 6.97 and 6.93 μA for the oxidation and the reduction, respectively. Comparing peaks, a well-shaped peak is obtained using the SWV method, with higher peak currents for the oxid-

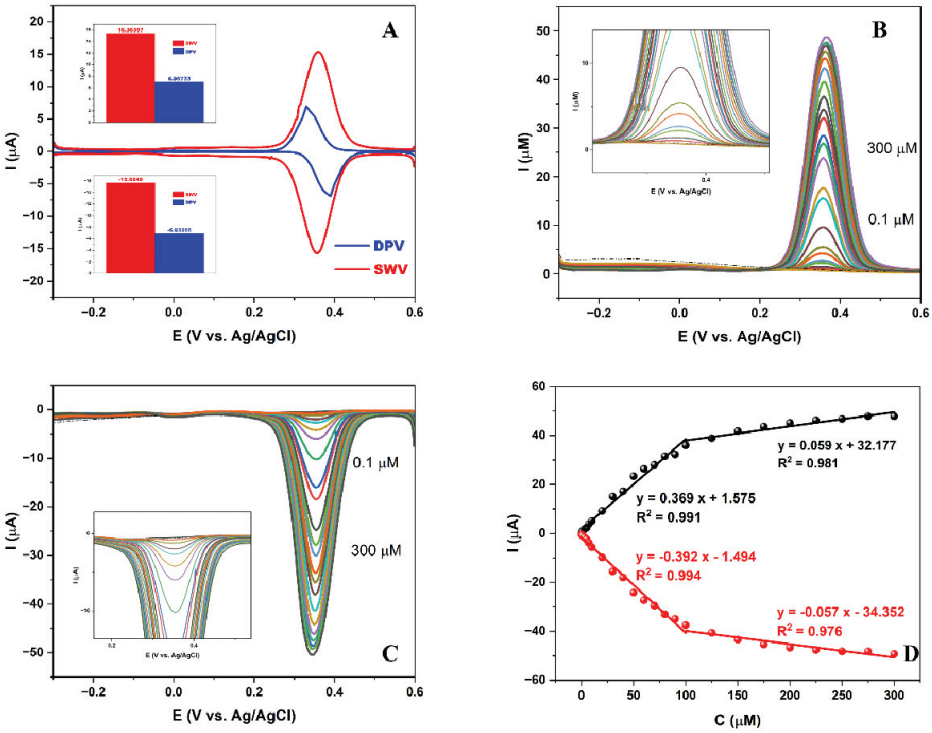

Fig. 5. A) Voltammograms of 100 μM MTL solution in BRBS at pH 3 obtained using DPV and SWV methods; B) anodic peak of the 15 wt. % $Sm_2(MoO_4)_3$ modified electrode at different concentrations of MTL in BRBS at pH 3; C) cathodic peak of the 15 wt. % $Sm_2(MoO_4)_3$ modified electrode at different concentrations of MTL in BRBS at pH 3; D) calibration plot derived from SWV measurements as a function of MTL concentration.

ation and the reduction. Considering all the above, the SWV method was optimized and applied for MTL quantification. The working parameters are optimized and shown in Fig. S-4 of the Supplementary material. The chosen values for further measurements were 30 mV for amplitude and 10 Hz for frequency. Under the optimized parameters, the effect of higher concentrations of MTL on peak current was investigated, shown in Fig. 5B for the oxidation and Fig. 5C for the reduction peak. The measurements were performed at a potential range from –0.3 to 0.6 V, with the addition of MTL solution from 0.1 to 300 μM. The relationship between peak currents and MTL concentrations is shown in Fig. 5D. The dependence of the peak current on the concentration of MTL is linear in two regions: from 0.1 to 100 μM with equations $y = 0.369x + 1.575$ and R^2 0.99 for oxidation and $y = –0.392x – 1.494$ with R^2 0.99 for reduction and from 100 to 300 μM with equations $y = 0.059x + 32.177$ with R^2 0.98 for oxidation and $y = = –0.057x – 34.352$ with R^2 0.98 for reduction. The limit of detection (*LOD*) and limit of quantification (*LOQ*) for the developed method were calculated as 3σ/S and 10σ/S, respectively, where σ signifies the blank's standard deviation, and *S* stands for the calibration curve's slope. *LOD* for oxidation is 0.059 and 0.047 μM for reduction, and *LOQ* values are 0.196 and 0.156 μM for the oxidation and the reduction, respectively. The sensitivity of the developed sensor was calculated as the slope/surface area of the electrode, and the values are 76.01 μA μM^{-1} cm^{-2} for the oxidation and 80.63 μA μM^{-1} cm^{-2} for the reduction. Table S-II of the Supplementary material compares the prepared $Sm_2(MoO_4)_3$/CPE sensor to the other differently modified electrodes.

Interference and selectivity study

A 100 μM solution of MTL and 100 μM of vitamins B6, B1, C, sucrose and glucose were prepared for interference measurements. The SWV measurements were performed under optimized working parameters ranging from –0.3 to 0.6 V (Fig. S-5 of the Supplementary material). All of the species had less than 5 % influence on the peak of MTL, besides glucose, which is considered a potential interferent for MTL detection. The selectivity study was performed with 100 μM solutions of other phenolic compounds, such as gallic acid, hydroquinone (HQ), and bisphenol A. The results of SWV measurements of 100 μM solution of MTL with the addition of phenolic compounds were shown in Fig. S-6 of the Supplementary material. Neither of the tested phenolic compounds significantly impacted MTL redox peak currents, which means that the developed sensor can be used as an excellent tool for MTL detection in real samples.

Real samples application

A developed sensor for sensitive and selective MTL detection and quantification was employed in tap and pond water. SWV measurements were per-

formed in a potential range from –0.3 to 0.6 V. The pH values of the real samples were adjusted using BRBS pH 3, and the measured pH values of the real samples were 3.09 and 3.11 for tap water and pond water, respectively. Fig. 6A and B represents voltammograms of the real sample solutions and the solutions with spiked 5, 10, 15 and 20 μM concentrations of MTL. Added and found concentrations of MTL are given in Table I for both real samples and for the determination in both oxidation and reduction processes. According to the findings of these real-world sample investigations, the $Sm_2(MoO_4)_3$ modified carbon paste electrode shows excellent precision and reliability regarding the real-time MTL detection from water samples.

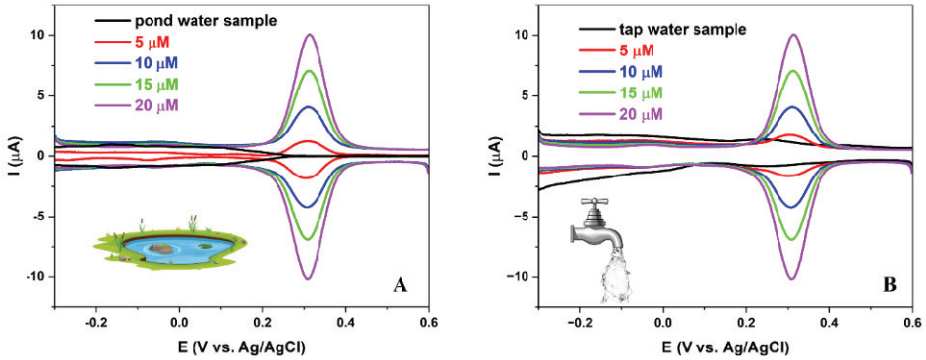

Fig. 6. SWV measurements of: A) pond water sample and B) tap water sample, with spiked 5, 10, 20 and 25 μM of MTL.

TABLE I. Real sample analysis of MTL in pond water and tap water samples

Sample	Added μM	Found μM	Recovery %	Reduction	Added μM	Found μM	Recovery %
Tap water	4.97	4.94	99.40	Tap water	4.97	4.66	93.76
	9.90	9.82	99.19		9.90	9.94	100.40
	14.78	14.86	100.54		14.78	14.79	100.07
	19.61	19.41	98.98		19.61	20.14	102.70
Pond water	4.97	4.95	99.60	Pond water	4.97	4.63	93.16
	9.90	9.76	98.59		9.90	9.82	99.19
	14.78	14.98	101.35		14.78	14.84	100.41
	19.61	19.47	99.29		19.61	20.41	104.08

CONCLUSION

To conclude, we developed a very efficient technique for detecting and quantifying the nitrogen-organic pollutant metol by employing samarium molybdate nanomaterial as a modifier for the carbon paste electrode. We carefully evaluated the morphological characteristics of the nanomaterial using methods including TEM, SEM and XRD. With a detection and quantification limit of 0.047

and 0.156 μM and a wide linear range of 0.1–100 and 100–300 μM, the SWV method over the fabricated electrodes showed remarkable results. Since real sample analyses, such as those of tap and pond water, gave excellent results, this improved method can be easily applied in everyday research.

SUPPLEMENTARY MATERIAL

Additional data and information are available electronically at the pages of journal website: https://www.shd-pub.org.rs/index.php/JSCS/article/view/13044, or from the corresponding author on request.

Acknowledgement. This work was financially supported by the Ministry of Science, Technological Development and Innovation of Republic of Serbia, contracts No: 451-03-66/ /2024-03/200168 and 451-03-66/2024-03/200026.

И З В О Д

ОДРЖИВА СИНТЕЗА НАНОЧЕСТИЦА САМАРИЈУМ-МОЛИБДАТА: ЈЕДНОСТАВАН ЕЛЕКТРОХЕМИЈСКИ АЛАТ ЗА ДЕТЕКЦИЈУ ЗАГАЂИВАЧА ЖИВОТНЕ СРЕДИНЕ МЕТОЛА

ТИЈАНА МУТИЋ[1], ВЕСНА СТАНКОВИЋ[2], ЈАДРАНКА МИЛИКИЋ[2], ДАНИЦА БАЈУК-БОГДАНОВИЋ[2], KURT KALCHER[3], ASTRID ORTNER[4], ДРАГАН МАНОЈЛОВИЋ и ДАЛИБОР СТАНКОВИЋ[5]

[1]Универзитет у Београду, Институт за хемију, технологију и металургију, Његошева 12, 11000 Београд, [2]Универзитет у Београду, Факултет за физичку хемију, Студентски трг 12–16, 11158 Београд, [3]Institute of Chemistry, Analytical Chemistry, Karl-Franzens University, Universitaetsplatz I/I, 8010 Graz, Austria, [4]University of Graz, Institute of Pharmaceutical Sciences, Department of Pharmaceutical Chemistry, Schubertstraße 1, 8010 Graz, Austria и [5]Универзитет у Београду, Хемијски факултет, Студентски трг 12–16, 11158 Београд

Ова студија је фокусирана на развој високо ефикасног сензора за детекцију и квантификацију органског загађивача метола. У ту сврху, наночестице самаријум-молибдата су синтетисане применом еколошки прихватљиве и јефтине хидротермалне методе, без коришћења органских растварача. Ове наночестице су примењене као модификатор електрода од угљеничне пасте због своје изузетне каталитичке ефикасности. Електрохемијска мерења су открила да развијен сензор олакшава процесе преноса електрона и побољшава каталитички одговор електроде. Добијени сензор је показао широк линеарни опсег од 0,1–100 и 100–300 μM метола, са ниским границама детекције и квантификације од 0,047 и 0,156 μM, редом, при pH 3 у Бритон–Робинсоновом пуферском раствору као помоћном електролиту. Анализом реалних узорака воде из различитих извора помоћу овог сензора добијени су задовољавајући резултати, што сугерише да би овај сензор могао да се примењује у рутинским анализама, као брз, исплатив и осетљив метод.

(Примљено 13. септембра, ревидирано 7. октобра, прихваћено 2. децембра 2024)

REFERENCES

1. S. S. Rex Shanlee, R. Sundaresan, S. M. Chen, R. Balaji, T. Jeyapragasam, J. Y. Peng, A. I. Jothi, *Surf. Interf.* **40** (2023) 103020 (https://doi.org/10.1016/j.surfin.2023.103020)
2. K. Venkatesh, B. Muthukutty, S. M. Chen, P. Karuppasamy, A. S. Haidyrah, C. Karuppiah, C. C. Yang, S. K. Ramaraj, *J. Ind. Eng. Chem.* **106** (2022) 287 (https://doi.org/10.1016/j.jiec.2021.11.005)

3. W. Sun, Q. Jiang, Y. Wang, K. Jiao, *Sensors Actuators, B* **136** (2009) 419 (https://doi.org/10.1016/j.snb.2008.10.003)
4. X. Niu, L. Yan, X. Li, A. Hu, C. Zheng, Y. Zhang, W. Sun, *Int. J. Electrochem. Sci.* **11** (2016) 1720 (https://doi.org/10.1016/S1452-3981(23)15955-4)
5. K. Mariappan, S. Sakthinathan, S.-M. Chen, S. Alagarsamy, T.-W. Chiu, *J Electrochem. Soc.* **170** (2023) 126505 (https://doi.org/10.1149/1945-7111/ad1551)
6. S. Samanta, R. Srivastava, *J. Electroanal. Chem.* **777** (2016) 48 (https://doi.org/10.1016/j.jelechem.2016.07.024)
7. L. Lunar, *Water Res.* **34** (2000) 3400 (https://doi.org/10.1016/S0043-1354(00)00089-0)
8. C. Koventhan, V. Vinothkumar, S.-M. Chen, T.-W. Chen, A. Sangili, K. Pandi, V. Sethupathi, *Int. J. Electrochem. Sci.* **15** (2020) 7390 (https://doi.org/10.20964/2020.08.43)
9. C. S. P. Sastry, T. E. Divakar, U. Viplava Prasad, *Talanta* **33** (1986) 164 (https://doi.org/10.1016/0039-9140(86)80034-0)
10. R. R. Krishna, C. S. P. Sastry, *Fresenius' Zeitsch. Anal. Chem* **296** (1979) 46 (https://doi.org/10.1007/BF00481172)
11. W. Sun, Q. Jiang, K. Jiao, *J. Solid State Electrochem.* **13** (2009) 1193 (https://doi.org/10.1007/s10008-008-0646-8)
12. R. Andreozzi, *Water Res.* **34** (2000) 463 (https://doi.org/10.1016/S0043-1354(99)00183-9)
13. X. Hu, J. Qian, J. Yang, X. Hu, Y. Zou, N. Yang, *J. Electroanal. Chem.* **947** (2023) 117756 (https://doi.org/10.1016/j.jelechem.2023.117756)
14. M. M. Stanley, A. Sherlin V, S.-F. Wang, B. Sriram, J. N. Baby, M. George, *J. Environ. Chem. Eng.* **11** (2023) 110185 (https://doi.org/10.1016/j.jece.2023.110185)
15. B. Mutharani, P. K. Gopi, S.-M. Chen, H.-C. Tsai, F. Ahmed, A. S. Haidyrah, P. Ranganathan, *Ecotoxicol. Environ. Saf.* **220** (2021) 112373 (https://doi.org/10.1016/j.ecoenv.2021.112373)
16. K. Mariappan, D. D. F. Packiaraj, T.-W. Chen, S.-M. Chen, S. Sakthinathan, S. V. Alagarsamy, A. M. Al-Mohaimeed, W. A. Al-onazi, M. S. Elshikh, T.-W. Chiu, *New J. Chem.* **48** (2024) 6438 (https://doi.org/10.1039/D3NJ06004G)
17. F. Packiaraj Don Disouza, S. Alagarsamy, T.-W. Chen, S.-M. Chen, W.-C. Liou, B.-S. Lou, W. A. Al-onazi, M. Ajmal Ali, M. S. Elshikh, *J. Ind. Eng. Chem.* **135** (2024) 406 (https://doi.org/10.1016/J.JIEC.2024.01.052)
18. T. Mutić, D. Stanković, D. Manojlović, D. Petrić, F. Pastor, V. V. Avdin, M. Ognjanović, V. Stanković, *Electrochem.* **5** (2024) 45 (https://doi.org/10.3390/electrochem5010003)
19. N. Nataraj, T.-W. Chen, S.-M. Chen, T. Kokulnathan, F. Ahmed, T. Alshahrani, N. Arshi, *J. Taiwan Inst. Chem. Eng.* **156** (2024) 105348 (https://doi.org/10.1016/j.jtice.2024.105348)
20. S. Knežević, M. Ognjanović, V. Stanković, M. Zlatanova, A. Nešić, M. Gavrović-Jankulović, D. Stanković, *Biosensors (Basel)* **12** (2022) 705 (https://doi.org/10.3390/bios12090705)
21. M. Ognjanović, D. M. Stanković, Ž. K. Jaćimović, M. Kosović-Perutović, J. F. M. L. Mariano, S. Krehula, S. Musić, B. Antić, *Electroanalysis* **34** (2022) 1431 (https://doi.org/10.1002/elan.202100602)
22. T. Mutić, M. Ognjanović, I. Kodranov, M. Robić, S. Savić, S. Krehula, D. M. Stanković, *Anal. Bioanal. Chem.* **415** (2023) 4445 (https://doi.org/10.1007/s00216-023-04617-70
23. S. Behvandi, A. Sobhani-Nasab, M. A. Karimi, E. Sohouli, M. S. Karimi, M. R. Ganjali, F. Ahmadi, M. Rahimi-Nasrabadi, *Polyhedron* **180** (2020) 114424 (https://doi.org/10.1016/j.poly.2020.114424)

24. K. P. Mani, V. G., P. R. Biju, C. Joseph, N. V. Unnikrishnan, M. A. Ittyachen, *ECS J. Solid State Sci. Technol.* **4** (2015) R67 (https://doi.org/10.1149/2.0131505jss)
25. Z. Rezapoor-Fashtali, M. R. Ganjali, F. Faridbod, *Biosensors (Basel)* **12** (2022) 720 (https://doi.org/10.3390/bios12090720)
26. M. V. Raskina, V. A. Morozov, A. V. Pavlenko, I. G. Samatov, I. V. Arkhangel'Skii, S. Stefanovich, B. I. Lazoryak, *Russ. J. Inorg. Chem.* **60** (2015) 84 (https://doi.org/10.1134/S0036023615010118)
27. S. S. Saleem, G. Aruldhas, H. D. Bist, *Spectrochim. Acta, A* **39** (1983) 1049 (https://doi.org/10.1016/0584-8539(83)80124-X)
28. W. Dridi, M. F. Zid, M. Maczka, *Adv. Mat. Sci. Eng.* **2017** (2017) 1 (https://doi.org/10.1155/2017/6123628)
29. Z. Zhang, X. Liu, Y. Wu, H. Zhao, *J. Solid State Electrochem.* **19** (2015) 469 (https://doi.org/10.1007/s10008-014-2624-7)
30. H. Zhao, B. Chen, C. Cheng, W. Xiong, Z. Wang, Z. Zhang, L. Wang, X. Liu, *Ceram. Int.* **41** (2015) 15266 (https://doi.org/10.1016/j.ceramint.2015.07.213)
31. H. Zhao, N. Hu, R. Xu, H. Liu, J. Liu, Q. Ran, *Ceram. Int.* **46** (2020) 21805 (https://doi.org/10.1016/j.ceramint.2020.05.256)
32. V. Stanković, S. Đurđić, M. Ognjanović, G. Zlatić, D. Stanković, *Sensors* **24** (2024) 705 (https://doi.org/10.3390/s24020705)
33. V. C. Valsalakumar, S. Vasudevan, *Langmuir* **39** (2023) 15730 (https://doi.org/10.1021/acs.langmuir.3c02303)
34. A. Afkhami, F. Soltani-Felehgari, T. Madrakian, H. Ghaedi, *Biosens. Bioelectron.* **51** (2014) 379 (https://doi.org/10.1016/j.bios.2013.07.056)
35. S. P. Thangavelu, T.-W. Chen, S.-M. Chen, K. Thangavelu, B.-S. Lou, T. saad Algarni, W. A. Al-onazi, M. S. Elshikh, *Carbon N.Y.* **223** (2024) 119026 (https://doi.org/10.1016/j.carbon.2024.119026)
36. S. Alagarsamy, R. Sundaresan, T.-W. Chen, S.-M. Chen, B.-S. Lou, B. Ramachandran, S. K. Ramaraj, M. Ajmal Ali, M. S. Elshikh, J. Yu, *Microchem. J.* **193** (2023) 108960 (https://doi.org/10.1016/j.microc.2023.108960)
37. S. Jose, A. George, A. R. Cherian, A. Varghese, *Surfaces Interf.* **35** (2022) 102416 (https://doi.org/10.1016/j.surfin.2022.102416).

Journal of the Serbian Chemical Society
JSCS@tmf.bg.ac.rs • www.shd.org.rs/JSCS
J. Serb. Chem. Soc. 89 (12) S514–S519 (2024)
Supplementary material

SUPPLEMENTARY MATERIAL TO

Sustainable synthesis of samarium molybdate nanoparticles: a simple electrochemical tool for detection of environmental pollutant metol

TIJANA MUTIĆ[1], VESNA STANKOVIĆ[1], JADRANKA MILIKIĆ[2], DANICA BAJUK-BOGDANOVIĆ[2], KURT KALCHER[3], ASTRID ORTNER[4], DRAGAN MANOJLOVIĆ[5] and DALIBOR STANKOVIĆ[5]*

[1]*University of Belgrade, Institute of Chemistry, Technology and Metallurgy, National Institute of the Republic of Serbia, Njegoševa 12, 11000 Belgrade, Serbia,* [2]*University of Belgrade, Faculty of Physical Chemistry, Studentski trg 12–16, 11158 Belgrade, Serbia,* [3]*Institute of Chemistry, Analytical Chemistry, Karl-Franzens University, Universitaetsplatz I/I, 8010 Graz, Austria,* [4]*University of Graz, Institute of Pharmaceutical Sciences, Department of Pharmaceutical Chemistry, Schubertstraße 1, 8010 Graz, Austria and* [5]*University of Belgrade, Faculty of Chemistry, Studentski Trg 12–16, 11158 Belgrade, Serbia*

J. Serb. Chem. Soc. 89 (12) (2024) 1571–1585

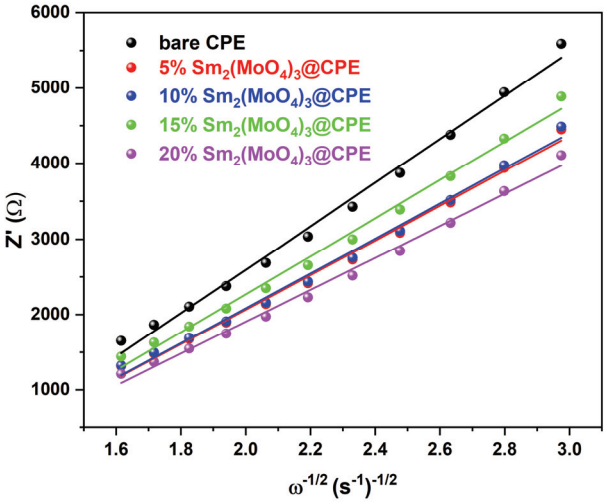

Figure S-1. Dependence of real Z' part of the impedance on the angular frequency for bare CPE, and 5, 10, 15, and 20% $Sm_2(MoO_4)_3$ modified CPE

* Corresponding author. E-mail: dalibors@chem.bg.ac.rs

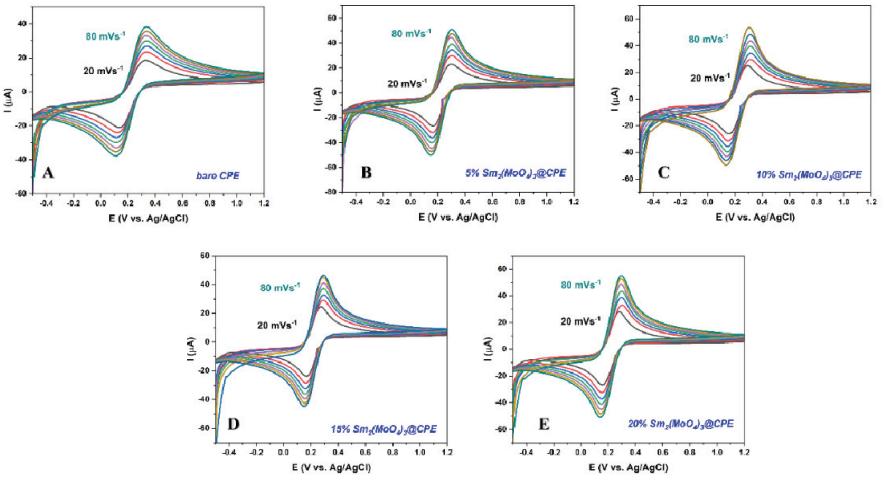

Figure S-2. CV curves of (A) bare CPE; (B) 5% $Sm_2(MoO_4)_3$ modified CPE; (C) 10% $Sm_2(MoO_4)_3$ modified CPE; (D) 15% $Sm_2(MoO_4)_3$ modified CPE; (E) 20% $Sm_2(MoO_4)_3$ modified CPE in 5 mM $[Fe(CN)_6]^{3-/4-}$ and 0.1M KCl solution at different scan rates in a range from 20 to 80 mVs^{-1}.

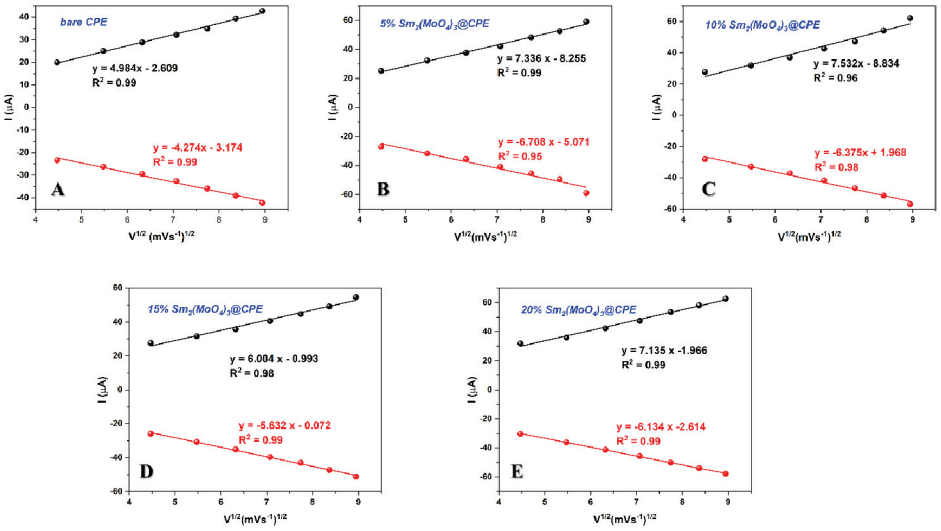

Figure S-3. Dependence of redox peak currents on the square root of the scan rate in 5 mM $[Fe(CN)_6]^{3-/4-}$ and 0.1M KCl solution over (A) bare CPE; (B) 5% $Sm_2(MoO_4)_3$ modified CPE; (C) 10% $Sm_2(MoO_4)_3$ modified CPE; (D) 15% $Sm_2(MoO_4)_3$ modified CPE; (E) 20% $Sm_2(MoO_4)_3$ modified CPE.

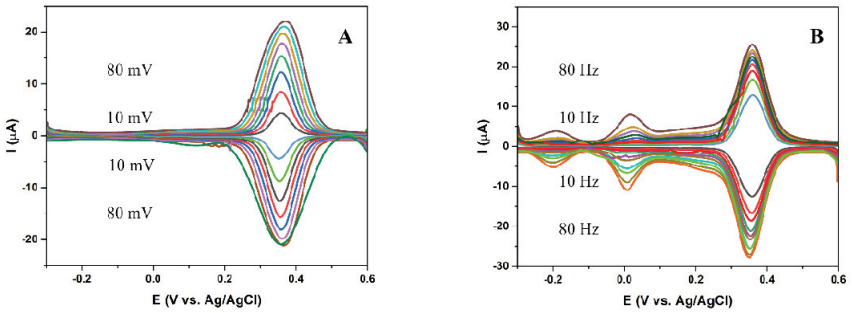

Figure S-4. Optimization of working parameters: (A) Amplitude; (B) Frequency for SWV method.

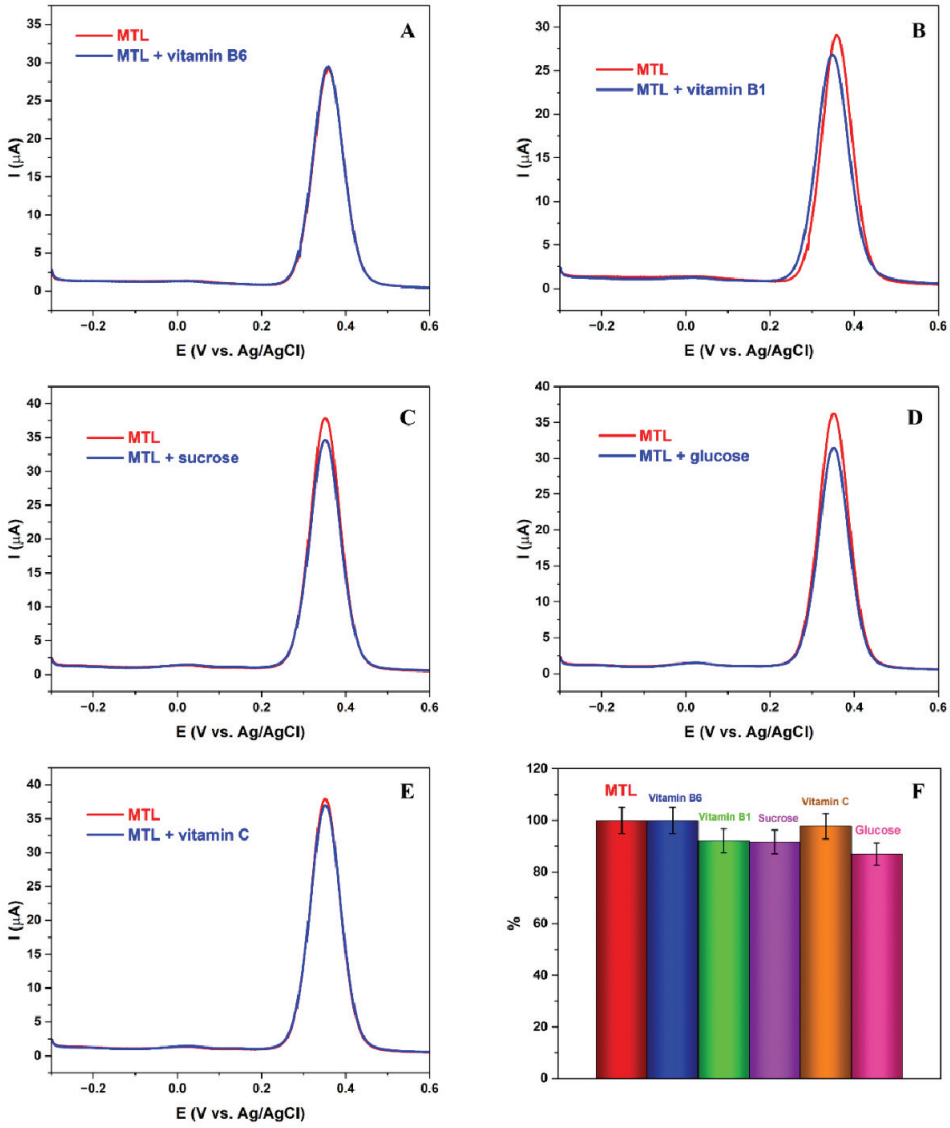

Figure S-5. SWV measurements of MTL in the presence of potential interfering species: (A) Vitamin B6; (B) Vitamin B1; (C) Sucrose; (D) Glucose; (E) Vitamin C; (F) Comparison of current peaks between MTL and potential interfering species.

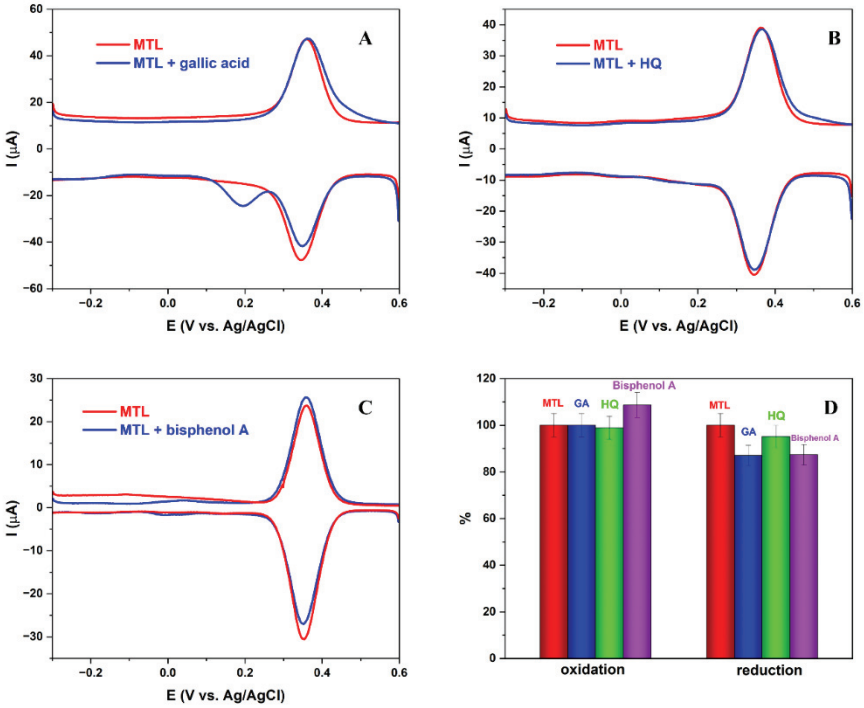

Figure S-6. SWV measurements of MTL in the presence of other phenolic compounds (Selectivity study): (A) Gallic acid; (B) Hydroquinone – HQ; (C) Bisphenol A; (D) Comparison of redox current peaks between MTL and other phenolic compounds.

Table S-I. Calculated values of electroactive surface area of electrodes (A); resistance (Rct), Warburg coefficient (σ), and diffusion-coefficient (D) for bare CPE and 5,10,15, and 20% modified electrodes.

Electrode	A (cm^2)	Rct (Ω)	σ (Ω cm^2 $s^{-1/2}$)	D (cm^2/s)
bare CPE	0.0151	3647.97	2880.27	7.49E-07
5% $Sm_2(MoO_4)_3$	0.0223	313.52	2294.30	5.41E-07
10% $Sm_2(MoO_4)_3$	0.0229	430.07	2314.12	5.04E-07
15% $Sm_2(MoO_4)_3$	0.0182	285.53	2520.75	6.73E-07
20% $Sm_2(MoO_4)_3$	0.0217	367.12	2117.21	6.71E-07

Table S-II. Comparison table of electrochemical MTL developed sensor $Sm_2(MoO_4)_3$/CPE vs previous results

Working electrode	Technique	pH	Linear range (μM)	LOD (μM)	Sensitivity (μA•$μM^{-1}$•cm^{-2})	Ref.
MOF@COF	DPV	7	0.1-200	0.03	/	13
Fe@C/CB/SPCE	DPV	7	0.01-27; 27-142	0.003	12.948	35
CoMn2O4@RGO/SPCE	DPV	7	0.01-137.65	0.05	3.77	2
MoS_2/SPCE	DPV	7	0.2-1211	0.01	/	8
$CuCo_2O_4$/GCE	DPV	7	0.02–1000	0.006	/	6
GdM/RGO/GCE	DPV	7	0.01-1792	0.0039	1.34	36
Co-Pi/PTAA/CFP	DPV	7	0.06-0.8	0.002	/	37
$Sm_2(MoO_4)_3$/CPE	SWV	3	0.1-100; 100-300	0.047	80.63	This work

Journal of the Serbian Chemical Society
JSCS@tmf.bg.ac.rs • www.shd.org.rs/JSCS
J. Serb. Chem. Soc. *89* (12) 1587–1601 (2024)
JSCS–5808
Original scientific paper
Published 27 December, 2024

Removal of pharmaceutically active substance ibuprofen from aqueous solution using TiO_2/ZSM-5 zeolite hybrid photocatalysts

SRNA J. STOJANOVIĆ[1], MARIJA Z. RISTIĆ[2], DANINA R. KRAJIŠNIK[3], VLADISLAV A. RAC[4] and LJILJANA S. DAMJANOVIĆ-VASILIĆ[1]*

[1]University of Belgrade – Faculty of Physical Chemistry, Studentski trg 12–16, 11000 Belgrade, Serbia, [2]University of Belgrade – ICTM, Department of Catalysis and Chemical Engineering, Njegoševa 12, 11000 Belgrade, Serbia, [3]University of Belgrade – Faculty of Pharmacy, Vojvode Stepe 450, 11221 Belgrade, Serbia, and [4]University of Belgrade-Faculty of Agriculture, Nemanjina 6, 11080 Belgrade, Serbia

(Received 18 October, revised 9 November, accepted 1 December 2024)

Abstract: The removal of pharmaceutically active substance ibuprofen (IBU) from aqueous solution was studied using TiO_2/ZSM-5 zeolite hybrid photocatalysts synthesized from 20 wt. % TiO_2 P25 nanoparticles and ZSM-5 zeolites with different Si/Al ratio (11.5, 15, 25, 40 and 140). The hybrid materials were prepared by a simple and economic ultrasound assisted solid-state dispersion method and characterized by X-ray powder diffraction, Fourier transform infrared spectroscopy and ultraviolet-visible diffuse reflectance spectroscopy. Among them, the hybrid photocatalyst containing TiO_2 and ZSM-5 zeolite with a Si/Al = 40 (denoted as TZ(40)) showed the highest removal efficiency, achieving 85 % IBU removal after 80 min under UV irradiation. The optimal condition for the removal of IBU from deionized water was found to be at a natural pH 4.5. Moreover, the removal of IBU from bottled drinking water in the presence of TZ(40) hybrid material was tested. Only 32 % IBU removal was achieved because change in pH value of reaction suspension decreased efficiency of IBU removal.

Keywords: ibuprofen; photocatalytic degradation; titanium dioxide; ZSM-5 zeolite.

INTRODUCTION

The pharmaceuticals represent an important group of emerging pollutants that cause major concern in recent years. These compounds are widely used in human medicine, veterinary medicine and aquaculture.[1] They often enter the aquatic ecosystems through various sources such as municipal wastewater, inap-

* Corresponding author. E-mail: ljiljana@ffh.bg.ac.rs
https://doi.org/10.2298/JSC241018098S

propriate disposition of expired medicines, human and animal excretions in livestock farming.[2,3] Currently, numerous pharmaceutically active substances can be found in various water sources at concentrations ranging from ng L^{-1} to μg L^{-1}. These pollutants are widespread in the environment because the traditional methods for water treatment are insufficiently effective for their removal.[4,5] Long-term exposure to these compounds can cause harmful effects on aquatic organisms and human beings.[1]

Among the most widely used pharmaceuticals in the world are non-steroidal anti-inflammatory drugs (NSAIDs), such as ibuprofen (IBU), which are often detected in the environment.[6] In a study conducted in Serbia, alongside pharmaceuticals such as diclofenac, codeine, valsartan, acetaminophen and carbamazepine derivatives, IBU was detected in municipal wastewater at a concentration of 20.1 μg L^{-1}.[7] Similarly, in Tehran, Iran, a study analysed NSAIDs and found that IBU was the most prevalent, with concentrations of 1.05 μg L^{-1} in municipal wastewater influents and lower levels in tap water, including the maximum values of 47 ng L^{-1} for IBU.[5]

Given the pressing need for development of technologies for removal of these contaminants, the methodologies involving advanced oxidation processes (AOPs) which are known to be very effective towards mineralization of organic compounds, offer a promising solution. Among semiconductor materials, titanium dioxide has been investigated for the removal of IBU, demonstrating its effectiveness in degrading this pharmaceutical.[8,9] Its unique properties, such as high stability, large specific surface area, non-toxicity, and high activity, make it an effective material for degrading organic pollutants.[10]

However, because of the tendency of TiO_2 nanoparticles to agglomerate and the high costs associated with filtration, certain constraints exist, regarding its widespread practical implementation. To address these challenges, the immobilization of TiO_2 nanoparticles on various supports with high surface area (such as zeolites, clay, carbon, etc.) has been proposed, which could enhance the removal process and facilitate easier recovery of the photocatalytic material from treated water.[11–13]

Zeolites are microporous hydrated aluminosilicates with a three-dimensional framework consisting of tetrahedral SiO_4 and AlO_4 units, with the silicon to aluminium ratio significantly influencing their structure and properties like hydrophobicity, acidity, catalytic activity, thermal and hydrothermal stability.[14] Although zeolites are known for their great adsorption properties and are widely used in the studies related to removal of different pharmaceuticals,[15] these materials have also proven to be appropriate support for semiconductor photocatalysts such as TiO_2, improving their performance in pollutant degradation.[16] Furthermore, the zeolites' transparency above 240 nm makes them ideal for UV light excitation of TiO_2.[16]

The materials based on TiO_2 and zeolites have been investigated for the removal of pharmaceuticals such as acetaminophen, codeine and cefazolin from aquatic environment.[17,18] In our previous study the removal of atenolol, a *β*--blocker, was investigated using nanosized TiO_2 and various zeolites, with the highest removal efficiency achieved by TiO_2/ZSM-5 zeolite hybrid photocatalyst.[19] Only few studies assessed the removal of IBU using Pd-TiO_2/ZSM-5 catalyst[20] and UV/H_2O_2/zeolite–titanate photocatalyst system.[21,22]

The aim of this study was to investigate the photocatalytic performance of TiO_2/ZSM-5 zeolite hybrid photocatalysts for the removal of IBU from aqueous solution. The synthetic ZSM-5 zeolite, used as one component of hybrid material, consists of interconnected channels with 10-membered openings (5.1 Å×5.5 Å and 5.3 Å×5.6 Å). These channels intersect and form the opening with size of approximately 8.5–9.0 Å.[23] The commercial nanoparticles TiO_2 P25 was used as another component. The hybrid photocatalysts were prepared using a facile and economical ultrasound assisted solid-state dispersion (USSD) method and characterized by X-ray powder diffraction (XRPD), Fourier transform infrared (FTIR) spectroscopy and ultraviolet–visible diffuse reflectance (UV–Vis DR) spectroscopy. The influence of different Si/Al ratio of ZSM-5 zeolite in the prepared TiO_2/ZSM-5 hybrid materials on the IBU removal process was evaluated, along with the effects of varying pH values. Furthermore, the influence of different water matrix such as commercial bottled drinking water and water spiked with bicarbonate ions to the removal of IBU were also studied.

EXPERIMENTAL

Materials

IBU was provided by the pharmaceutical company Galenika a.d., Serbia. This active substance was of pharmacopoeial (Ph. Eur.) grade. The structural formula of IBU is shown in Fig. S-1 of the Supplementary material to this paper. The ZSM-5 zeolites with Si/Al ratio of 11.5, 15, 25, 40 and 140 from Zeolyst were used. TiO_2 nanoparticles (≥ 99.5 %, Evonik Aeroxide® TiO_2 P25, primary particle size of 21 nm), were obtained from Aldrich. The other chemicals used in this study included ethanol (> 99.8 %, Fisher Scientific), sodium hydrogen carbonate ($NaHCO_3$, >99.5 %, Lachema), sodium hydroxide (NaOH, ≥99 %, Emsure®, Merck), hydrochloric acid (35 %, p. a., Lachner) and KBr (≥99.5 %, Emsure®, Merck).

Preparation of TiO_2/ZSM-5 zeolite materials

Beside ZSM-5 zeolite with Si/Al = 15 which was purchased in hydrogen form, all other used ZSM-5 zeolites were converted from their ammonium to hydrogen form by calcination at 500 °C for 5 h. ZSM-5 zeolites were denoted as Z(11.5), Z(15), Z(25), Z(40) and Z(140), where Z represents the used zeolite, and the number in parentheses indicates Si/Al ratio. TiO_2/ZSM-5 zeolite hybrid photocatalysts were prepared using an ultrasound assisted solid--state dispersion (USSD) method described in our earlier work.[24] A 20 wt. % of TiO_2 was thoroughly mixed with the starting zeolite in an agate mortar using a pestle, and the mixture was ultrasonically dispersed in ethanol (10:1 ethanol (mL) to solid powder (g) ratio) for 15 min at 80 °C using an ultrasonic bath (Bandelin Sonorex RK52H, 35 Hz and 240 W). The

samples were subsequently dried at 80 °C and then calcined in air at 500 °C for 5 h. The prepared samples were labelled as TZ(11.5), TZ(15), TZ(25), TZ(40) and TZ(140), where T represents TiO_2 P25 and Z(11.5) the zeolite and its Si/Al ratio.

Methods

The XRPD patterns of the TiO_2 P25, starting zeolites and TiO_2/ZSM-5 zeolite hybrid materials were recorded using a Rigaku Ultima IV diffractometer in Bragg–Brentano geometry. CuKα radiation (λ = 1.54178 Å) was used, with measurements taken over 2θ range from 4 to 50°, using a step of 0.020° and an acquisition rate of 1° min^{-1}.

FTIR spectra of all investigated materials were recorded using a Thermo Scientific Nicolet Avatar 370 FTIR spectrophotometer. The measurements were conducted in the range of 4000–400 cm^{-1} with a resolution of 4 cm^{-1} and 64 acquisitions. KBr pellets were prepared by mixing 1.5 mg of the sample with 150 mg of KBr.

UV–Vis DR spectra were obtained using an Agilent Cary UV–Vis NIR 5000 spectrophotometer equipped with an integration sphere in the range from 200 - 600 nm, with a data interval of 1 nm and a scan rate of 600 nm min^{-1}. Polytetrafluoroethylene (PTFE) was used as a white reference standard for measuring base line.

Photodegradation procedure

The photocatalytic performance of the starting materials and TiO_2/ZSM-5 zeolite hybrid materials was evaluated in a 50 mL glass reactor. A glass reactor had a water-cooling jacket which was used to retain room temperature (25±2 °C). The experiments were carried out using 40 mL of aqueous solution of IBU (C_0 = 30 mg L^{-1}) with 1 g L^{-1} of catalyst under constant stirring and illumination from a HPR 125 Philips high vapour pressure mercury lamp (125 W; emission bands in the UV region at 313, 334.2, 365.5 and 390.6 nm, with the maximum emission at 365.5 nm). The investigated concentration of IBU was higher than those usually detected in wastewaters, with the aim of detecting changes in the process within measurable time scale with used analytical technique.

The lamp was positioned at a distance of 25 cm from the experimental suspension. To reach adsorption–desorption equilibrium, the suspensions were stirred for 15 min in the dark. At predetermined time intervals, 1 mL aliquots were withdrawn and centrifuged at 12,000 rpm for 15 min to separate the particles from the supernatant. The changes of IBU (λ_{max} = 221 nm) concentrations in the supernatant were determined from absorbance spectra recorded on a Thermo Scientific Evolution 220 UV–Vis spectrophotometer in the range from 200 to 400 nm. The photocatalytic experiments were conducted in triplicate to confirm the reproducibility of the data and the mean of the acquired results is presented together with the standard deviation (as error bars in the figures).

Furthermore, to evaluate the practical applicability of the most efficient hybrid photocatalysts for the removal of IBU, photocatalytic experiments were conducted in bottled drinking water. For these experiments, IBU was dissolved in commercial bottled water with the following composition: HCO_3^- = 42.7 mg L^{-1}, NO_3^- = 1.46 mg L^{-1}, SO_4^{2-} = 5.2 mg L^{-1}, Cl^- = < 1 mg L^{-1}, Ca^{2+} = 9.6 mg L^{-1}, Mg^{2+} = 0.82 mg L^{-1}, Na^+ = 2.7 mg L^{-1}, K^+ < 1 mg L^{-1}, and conductivity = 69.5 μS cm^{-1} and pH 7.5. Subsequently, to determine the influence of bicarbonate anions on the photocatalytic activity of TiO_2/ZSM-5 zeolite hybrid photocatalysts, aqueous solution of IBU was spiked with HCO_3^- = 42.7 mg L^{-1}.

For the studies of pH influence on the removal of IBU from aqueous solution, the pH values of solutions were adjusted by adding HCl or NaOH. The pH measurements were conducted using a PC5 multiparameter tester (XS Instruments).

RESULTS AND DISCUSSION

XRPD analysis

The XRPD patterns of TiO_2 P25, the starting ZSM-5 zeolites and TiO_2/ /ZSM-5 zeolite hybrid materials are shown in Fig. 1. The XRPD pattern of TiO_2 P25 revealed reflections corresponding to the anatase phase (2θ of 25.3, 37.0, 37.8, 38.6 and 48.1°; JCPDS 89-4921) and the rutile phase (2θ of 27.4 and 36.1°; JCPDS 89-8304). The XRPD patterns of all starting ZSM-5 zeolites exhibited the characteristic reflections of the MFI structure at 2θ of 7.9, 8.9, 23.9, 29.9°.[25] In the diffractograms of TiO_2/ZSM-5 zeolite hybrid materials, the reflections from both ZSM-5 zeolite and TiO_2 phases (anatase: 2θ of 25.3, 37.8 and 48.1°; JCPDS 89-4921 and rutile: 2θ = 27.4°; JCPDS 89-8304) are detected. These results confirm the successful loading of TiO_2 nanoparticles on the starting zeolites and the preservation of zeolite structure.

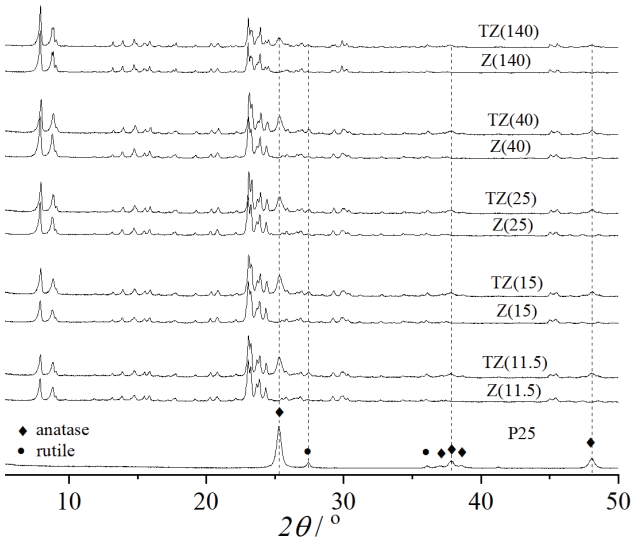

Fig. 1. XRPD patterns of TiO_2 P25, the starting zeolites and TiO_2/ZSM-5 zeolite hybrid photocatalysts. Vertical dashed lines are at 25.3, 27.4, 37.8 and 48.1°.

FTIR spectroscopy

The FTIR spectra of TiO_2 P25, the starting ZSM-5 zeolites and TiO_2/ZSM-5 zeolite hybrid materials are shown in Fig. 2. In these spectra, the characteristic bands originating from the vibrations of ZSM-5 zeolite framework are present. The band at ~453 cm^{-1} corresponds to the bending vibrations of T–O bonds (T is Si, Al). The band positioned at ~545 cm^{-1} is attributed to the external stretching vibrations of double 6-member rings (D6R), while the band at ~794 cm^{-1} corresponds to the external symmetric stretching vibrations of T–O bonds.[24] The band

at ~1095 cm^{-1} is related to the asymmetric stretching vibrations of T–O–T bonds and the band at ~1221 cm^{-1} is attributed to the external asymmetric stretching vibrations of T–O–T bonds.[26]

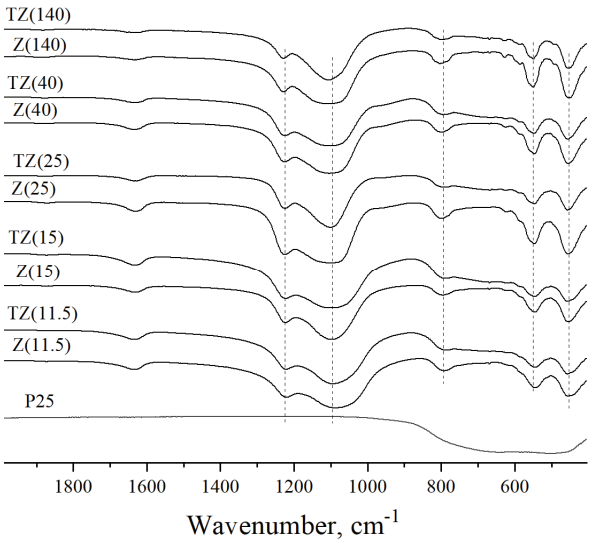

Fig. 2. FTIR spectra of TiO_2 P25, starting zeolites and TiO_2/ZSM-5 zeolite hybrid photocatalysts. Vertical dashed lines are at 1221, 1095, 794, 545 and 453 cm^{-1}.

The FTIR spectra of TiO_2 P25 is characterized by broad band below 1000 cm^{-1} consisting of two signals originating from Ti–O and Ti–O–Ti stretching vibrations.[27] In the case of all investigated hybrid materials, a broadening of the bands in the 400– 600 cm^{-1} range was observed, attributed to the overlapping of the bands originating from the zeolite and TiO_2.

Since there were no significant changes in the FTIR spectra of the starting zeolites and TiO_2/ZSM-5 zeolite hybrid materials, it can be concluded that the zeolite structure was preserved, which aligns with the XRD results. The absence of a band present at about 960 cm^{-1} in FTIR spectra of TiO_2/ZSM-5 zeolite hybrid materials, typically associated with the asymmetric stretching vibration of Ti–O–Si bonds, suggests that Ti species are immobilized on the external surface of the zeolite, rather than being incorporated into the internal structure.[28]

UV–Vis DR spectroscopy

The light absorption properties of TiO_2/ZSM-5 zeolite hybrid materials were evaluated using UV–Vis DR spectroscopy. The obtained results together with the UV–Vis DR spectra of the starting materials are presented in Fig. 3. As observed from the spectra, all TiO_2/ZSM-5 zeolite hybrid materials exhibited characteristic absorption in the UV region, corresponding to the optical absorbance ability of

TiO_2 nanoparticles dispersed on the ZSM-5 zeolites. No significant shift in the absorption edges was observed when comparing the TiO_2 P25 and the TiO_2/ /ZSM-5 zeolite hybrid photocatalysts which indicate that the optical properties of TiO_2 were preserved after the preparation of these materials. Furthermore, these results confirm the successful loading of TiO_2, which is consistent with the XRPD and FTIR spectroscopy findings.

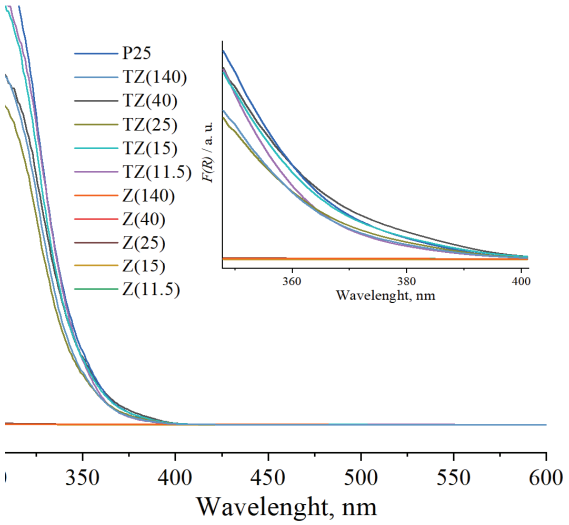

Fig. 3. UV–Vis DR spectra of TiO_2 P25, starting zeolites and TiO_2/ZSM-5 zeolite hybrid photocatalysts.

The efficiency of TiO_2/ZSM-5 zeolite hybrid photocatalysts for IBU removal from aqueous solution

The results of photocatalytic removal of IBU from aqueous solution in the presence of starting ZSM-5 zeolites with different Si/Al ratios and TiO_2/ZSM-5 zeolite hybrid materials are shown in Fig. 4. IBU has two characteristic bands with absorption maxima at 221 nm and 264 nm in the UV–Vis spectra, related to benzene ring.[8] In this study, the concentration of IBU was monitored based on absorbance at 221 nm.

Initially, the photolysis of IBU was investigated, and the results showed that there were no changes in the UV–Vis spectra after 120 min of UV irradiation (Fig. S-2 of the Supplementary material) demonstrating that IBU remains stable under the investigated conditions. Subsequently, the adsorption in the dark and photocatalytic ability of the starting ZSM-5 zeolites with different Si/Al ratio was investigated, and obtained results are presented in Fig. 4a. The findings reveal that during 15 min of stirring in the dark, the concentration of IBU decreased due to adsorption on the initial zeolites. Upon turning on the lamp, the IBU concen-

tration remains unchanged, confirming that ZSM-5 zeolites do not act as photocatalysts.

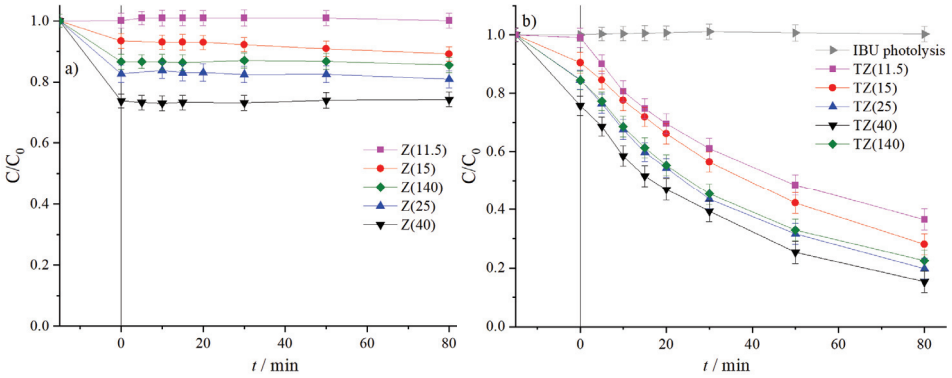

Fig. 4. Adsorption in the dark and photodegradation of IBU in the presence of: a) starting ZSM-5 zeolites with different Si/Al ratio and b) TiO_2/ZSM-5 zeolite hybrid photocatalysts with 20 wt. % of TiO_2; photolysis of IBU is shown for comparison. (Experimental conditions: C_0 = 30 mg L^{-1}, 1 g L^{-1} catalyst; initial pH values of IBU solution in the presence of pure zeolites and hybrid photocatalysts are similar varying between 4.0 and 4.3).

The results showed (Fig. 4a) that Z(11.5), the most acidic zeolite, did not adsorb IBU. An increase in the Si/Al ratio led to higher IBU adsorption, with Z(15) removing 11, Z(25) 19 and Z(40) removing 26 %, which is in accordance with literature, *i.e.*, increase of Si/Al ratio results in an increase in hydrophobicity for the same zeolite framework type and consequently in higher adsorption of organic micro-pollutants.[29] Despite having the highest Si/Al ratio, Z(140) exhibited a decrease in IBU adsorption, achieving only the removal of 15 %, which can be explained by competition between water and IBU molecules for the same adsorption sites with increased hydrophobicity.[29]

The photodegradation of IBU in the presence of TiO_2/ZSM-5 zeolite hybrid photocatalysts is shown in Fig. 4b. Among the TiO_2/ZSM-5 zeolite hybrid materials, TZ(40) was the most efficient, removing 85 % of IBU after 80 min of irradiation. The UV–Vis spectra of IBU photodegradation in the presence of TZ(40) hybrid photocatalyst after 5, 10, 15, 20, 30, 50 and 80 min of UV irradiation are shown in Fig. S-3a of the Supplementary material. This was followed by TZ(25), which removed 80 % of IBU, TZ(140) 77 % of IBU, TZ(15) 72 % of IBU and TZ(11.5) 64 % of IBU. For TZ(11.5), the removal of IBU from aqueous solution was achieved solely through photocatalytic degradation. In contrast, for the other TiO_2/ZSM-5 zeolite hybrid materials, the removal resulted from a combination of adsorption and photocatalytic degradation, which enhanced the overall removal efficiency.

The kinetics of photocatalytic IBU degradation can be modelled using the Langmuir–Hinshelwood equation, which at low concentration is converted to pseudo-first-order kinetic model represented by the following equation: ln (C_o/C) = = $k_{app}t$, where k_{app} is the rate constant, C_o is the initial concentation of IBU, C is the concentration at different irradiation time t.[30] The pseudo-first-order rate constants were determined as slope from linear plot of ln (C_o/C) *versus* irradiation time (t) for investigated hybrid photocatalysts and the results are shown in Table I. Besides the highest IBU adsorption, the highest rate constant has been determined for TZ(40). Thus, the combined adsorption and photocatalytic efficiency result in the highest removal efficiency for IBU using TZ(40).

TABLE I. Values of rate constant determined based on fit of UV–Vis experimental data to pseudo-first-order kinetic model

Sample	k_{app} / min^{-1}	R^2
TZ(11.5)	0.0135±0.0007	0.9911
TZ(15)	0.0151±0.0003	0.9982
TZ(25)	0.0188±0.0007	0.9988
TZ(40)	0.0209±0.0006	0.9957
TZ(140)	0.0177±0.0007	0.9948

For comparison, in the presence of pure TiO_2 P25 nanoparticles, using the amount of TiO_2 which corresponded to 20 wt. % of catalyst loading in composites, band at 221 nm in UV spectra (Fig. S-4 of the Supplementary material) strikingly disappears after 10 min of irradiation proving fast photocatalytic degradation of IBU, whereas intensity of band at 260 nm increases for 20 min and then decreases. According to the literature, band at 260 nm originates from the formation of temporary photodegradation products which can be degraded with prolonged irradiation.[8,22] It is interesting to note that band at 260 nm has significantly smaller intensity when TZ(40) is used as photocatalyst compared to pure TiO_2 (Figs. S-3a and S-4), indicating lower concentration of photodegradation products in the reaction mixture, which can be explained either by different degradation mechanism or by adsorption of degradation products by TZ(40).

Among limited number of studies investigating removal of IBU form aqueous solution in the presence of hybrid photocatalysts based on zeolites, Pd-TiO_2/ZSM-5 catalyst achieved 80 % removal of IBU after 300 min of UVC irradiation (with low power) using a lower initial IBU concentration of 10 ppm and a smaller catalyst dose of 0.17 g L^{-1},[20] whereas TZ(40), catalyst dose 1 g L^{-1}, achieved higher removal efficiency in a much shorter time (80 min) despite the higher IBU concentration (30 mg L^{-1}). Similarly, an another study reported the highest removal efficiency of 97.5 % of IBU using zeolite-titanate photocatalyst prepared by sol–gel method (under experimental conditions: IBU concentration 100 mg L^{-1}, 6W UVC lamp, pH 7, 0.7 mL H_2O_2, catalyst dose 1.67 g L^{-1} 100

min sonication).[21] In a follow-up study, the zeolite-titanate photocatalyst was tested for IBU removal from different media and achieved 77.82 % removal of IBU from tap water and 96.48 % of IBU from deionized water (under experimental conditions: IBU concentration 100 mg L^{-1}, pH 5, 0.05 mM H_2O_2, 1 g L^{-1} catalyst, 6W UVC, 100 min sonication).[22] Unlike these studies, where chemicals such as H_2O_2 are used as well as sonication, TZ(40) achieved comparable performance without such enhancements. This highlights its superior efficiency and the potential for cost-effective practical applications in water purification. Moreover, combined TiO_2 and zeolites result in an efficient hybrid photocatalyst which can be easily separated from aqueous media. In addition, in our previous work the reusability of TZ(40) was tested, revealing that TiO_2 is firmly immobilized on zeolite and that the calcination process can recover initial activity of TZ(40).[19]

Since the TZ(40) demonstrated the highest efficiency among the investigated hybrid photocatalysts for the removal of IBU, it was further tested.

Influence of pH on the removal of IBU from aqueous solution

The pH of the solution is a crucial factor that can significantly influence the efficiency of pollutant removal during heterogeneous catalysis, as it affects both the surface properties of the catalyst and the ionization state of the pollutants.[4,31] Therefore, the removal process of IBU from aqueous solution was investigated at different pH values in the presence of TZ(40) and the results are shown in Fig. 5. The natural pH of the IBU aqueous solution was 4.3, and the pH of the reaction suspension with hybrid material was 4.5. As reported in the literature, the pK_a of IBU is 4.4.[32] At pH values below pK_a, IBU will predominantly exists in its molecular (protonated) form, while at pH values above pK_a, it will be present in its deprotonated form (IBU^-).[33] In our previous work, the isoelectric point of TZ(40) has been determined to be at pH 3.3.[19] Meaning, at this pH the surface charge of TZ(40) is neutral, while at pH values higher than 3.3 the surface becomes negatively charged, and at pH values lower than 3.3 it becomes positively charged.

The highest removal percentage of IBU (85 %) was achieved at the natural pH of suspension. However, when the pH was adjusted to 3, 7 and 10, the removal efficiency decreased to 70, 29 and 27 %, respectively. Although at pH 3 the adsorption in the dark was higher (32 %) compared to the adsorption at natural pH (24 %), the photodegradation was reduced. At pH 7 as well as at pH 10, there was no adsorption of IBU in the dark in the presence of hybrid material. These findings can be explained by the surface charge interactions between the hybrid material and IBU at different pH values. At the alkaline conditions (pH 10) and at the neutral conditions (pH 7) the surface of TZ(40) is negatively charged, and IBU is predominantly in its deprotonated form (IBU^-), which leads to the electro-

static repulsion between the catalyst and the pollutant. This repulsion likely explains the absence of adsorption in the dark and the reduced photocatalytic degradation. In the case of acidic conditions (pH 3), the surface of TZ(40) becomes positively charged, while IBU exists in its neutral, molecular form. The lack of significant interaction between the positively charged surface and neutral IBU results in lower photocatalytic degradation, despite the increased adsorption observed in the dark.

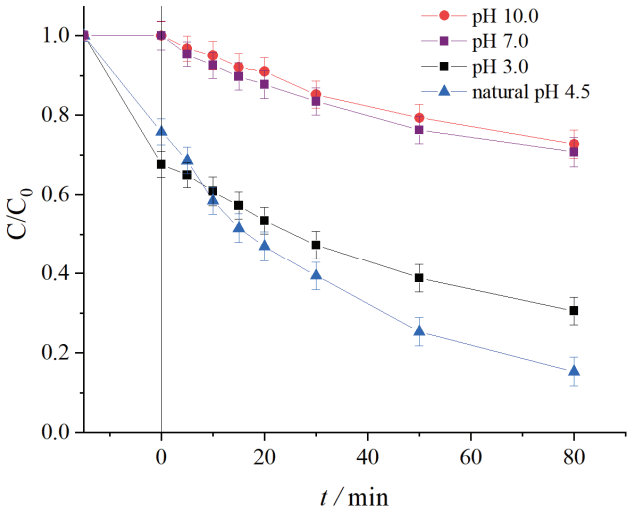

Fig. 5. Effect of pH on IBU removal in the presence of TZ(40) hybrid photocatalyst. (Experimental conditions: C_0 = 30 mg L^{-1}, 1 g L^{-1} catalyst).

Similar findings were observed in a study where the removal of IBU was less efficient at pH 3 and 9 compared to pH 7, using TiO_2 P25 catalyst (isoelectric point: 6) under UV–Vis irradiation, with 10 mg L^{-1} of IBU and 20 mg L^{-1} of catalyst.[8]

Influence of water media on the removal of IBU

The effectiveness of TZ(40) hybrid material for the removal of IBU in bottled drinking water was also evaluated, considering its potential for practical application. The results of IBU removal in the presence of TZ(40) hybrid material in different water media are shown in Fig. 6.

After 80 min of irradiation in the presence of TZ(40), 85 % of IBU was successfully removed. In contrast, the removal efficiency of IBU was significantly reduced in bottled drinking water, achieving only 32 % removal. This decrease can be attributed to the presence of various inorganic ions commonly found in drinking water, which may interfere with the photocatalytic degradation. Notably, the bicarbonate ions are known to act as radical scavengers, reacting with

hydroxyl radicals to form less reactive carbonate radicals, thereby reducing the availability of reactive oxygen species needed for the degradation of organic pollutants.[34,35] Given that bicarbonate ions were present at the highest concentration among other ions in used bottled drinking water, an additional experiment was conducted, where IBU was dissolved in deionized water with bicarbonates added at the same concentration as in the bottled water. The results showed that the presence of bicarbonate ions significantly slowed the degradation process. However, the addition of bicarbonate ions changed pH of reaction suspension from 4.5 (IBU solution in deionized water in the presence of TZ(40)) to 7. As shown in Fig. 5, decrease in the IBU removal has been obtained without bicarbonate ions in this reaction suspension at pH 7. Thus, the decrease in the IBU removal is due to the change of pH of the reaction suspension, not the presence of bicarbonates. Consequently, a longer period of irradiation would be necessary for the IBU removal from drinking water in the presence of TZ(40).

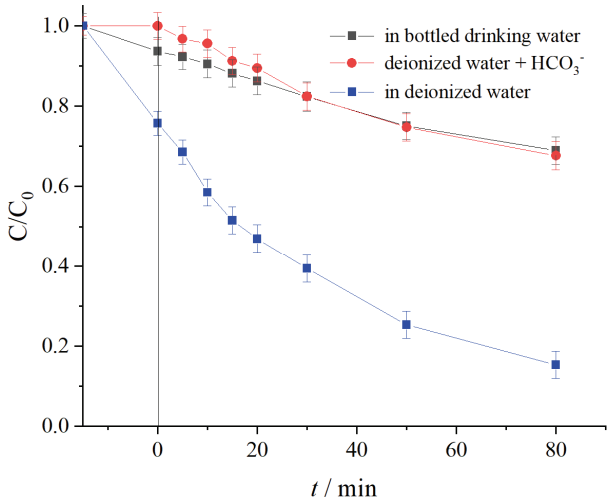

Fig. 6. Removal of IBU in the presence of TZ(40) hybrid material in deionized water, bottled drinking water and deionized water with addition of bicarbonates (42.7 mg L^{-1}). (Experimental conditions: C_0 = 30 mg L^{-1}, 1 g L^{-1} catalyst; initial pH values before irradiation of reaction suspensions were: 4.5 in deionized water; 7 in deionized water + HCO_3^-; 6.4 in bottled drinking water).

CONCLUSION

This study demonstrated the successful preparation of TiO_2/ZSM-5 zeolite hybrid photocatalysts based on TiO_2 P25 nanoparticles and ZSM-5 zeolites with different Si/Al ratio, using a facile ultrasound assisted solid-state dispersion method. The photocatalytic results showed that the hybrid material containing TiO_2 and ZSM-5 zeolite with a Si/Al = 40 (TZ(40)) achieved the highest effi-

ciency in removal of IBU (85 %) from aqueous solution after 80 min of irradiation, through a combination of adsorption and photocatalytic degradation. The optimal condition for IBU removal in the presence of TZ(40), was natural pH (4.5), while reduced efficiency was observed at pH 7 and 10. Additionally, the removal of IBU from bottled drinking water decreased significantly (32 % removal), due to the changes of pH of reaction suspension. These findings suggest that TiO_2/ZSM-5 zeolite hybrid photocatalyst could be used for the effective removal of pharmaceutical contaminates like NSAIDs IBU from aqueous environments.

SUPPLEMENTARY MATERIAL

Additional data and information are available electronically at the pages of journal website: https://www.shd-pub.org.rs/index.php/JSCS/article/view/13085, or from the corresponding author on request.

Acknowledgements. The authors acknowledge the financial support from the Ministry of Science, Technological Development and Innovation of the Republic of Serbia (contracts no. 451-03-65/2024-03/200146, 451-03-66/2024-03/200026, 451-03-65/2024-03/ 200161, 451--03-66/2024-03/ 200161 and 451-03-65/2024-03/200116). This research was supported by the Science Fund of the Republic of Serbia, #Grant No 7309, Project acronym: ZEOCOAT.

ИЗВОД

УКЛАЊАЊЕ ФАРМАЦЕУТСКИ АКТИВНЕ СУПСТАНЦЕ ИБУПРОФЕНА ИЗ ВОДЕНЕ СРЕДИНЕ У ПРИСУСТВУ TiO_2/ZSM-5 ЗЕОЛИТ ХИБРИДНИХ ФОТОКАТАЛИЗАТОРА

СРНА Ј. СТОЈАНОВИЋ[1], МАРИЈА З. РИСТИЋ[2], ДАНИНА Р. КРАЈИШНИК[3], ВЛАДИСЛАВ А. РАЦ[4] и ЉИЉАНА С. ДАМЈАНОВИЋ-ВАСИЛИЋ[1]

[1]Универзитет у Београду – Факултет за физичку хемију, Студентски трг 12–16, 11000 Београд, [2]Универзитет у Београду – ИХТМ, Центар за катализу и хемијско инжењерство, Његошева 12, 11000 Београд, [3]Универзитет у Београду – Фармацеутски факултет, Војводе Степе 450, 11221 Београд и [4]Универзитет у Београду – Пољопривредни факултет, Немањина 6, 11080 Београд

Уклањање фармацеутски активне супстанце ибупрофена (IBU) из водене средине је испитивано у присуству TiO_2/ZSM-5 зеолит хибридних фотокатализатора синтетисаних коришћењем 20 мас. % наночестичног TiO_2 P25 и ZSM-5 зеолита са различитим Si/Al односом (11,5, 15, 25, 40 и 140). Хибридни материјали су добијени једноставном и економски исплативом методом дисперзије у чврстој фази потпомогнутој ултразвуком, а затим карактерисани методама дифракције рендгенских зрака на праху, инфрацрвеном спектроскопијом са Фуријеовом трансформацијом и дифузно рефлексионом спектроскопијом. Највећу ефикасност у уклањању IBU је показао хибридни фотокатализатор добијен од TiO_2 и ZSM-5 зеолита са Si/Al = 40 (ознака TZ(40)), одстрањивањем 85% IBU из воденог раствора након 80 min излагања UV зрачењу. Утврђено је да су оптимални услови за уклањање IBU из дестиловане воде на pH 4,5, што је pH вредност воденог раствора IBU у присуству TZ(40). Додатно, испитивано је и уклањање IBU из флаширане воде за пиће у присуству TZ(40) хибридног материјала. Из раствора добијеног са флашираном водом уклоњено је само 32 % IBU, јер је промена pH реакционе суспензије резултовала смањењем ефикасности одстрањивања IBU.

(Примљено 18. октобра, ревидирано 9. новембра, прихваћено 1. децембра 2024)

REFERENCES

1. A. L. Moreno Ríos, K. Gutierrez-Suarez, Z. Carmona, C. G. Ramos, L. F. Silva Oliveira, *Chemosphere* **291** (2022) 132822 (https://doi.org/10.1016/j.chemosphere.2021.132822)
2. Y. Li, G. Zhu, W. J. Ng, S. K. Tan, *Sci. Total Environ.* **468**–**469** (2014) 908 (https://doi.org/10.1016/j.scitotenv.2013.09.018)
3. P. Bottoni, S. Caroli, A. B. Caracciolo, *Toxicol. Environ. Chem.* **92** (2010) 549 (https://doi.org/10.1080/02772241003614320)
4. J. Rivera-Utrilla, M. Sánchez-Polo, M. Á. Ferro-García, G. Prados-Joya, R. Ocampo--Pérez, *Chemosphere* **93** (2013) 1268 (https://doi.org/10.1016/j.chemosphere.2013.07.059)
5. A. Eslami, M. M. Amini, A. R. Yazdanbakhsh, N. Rastkari, A. Mohseni-Bandpei, S. Nasseri, E. Piroti, A. Asadi, *Environ. Monit. Assess.* **187** (2015) 1 (https://doi.org/10.1007/s10661-015-4952-1)
6. A. Romeiro, M. E. Azenha, M. Canle, V. H. N. Rodrigues, J. P. Da Silva, H. D. Burrows, *Chem. Select* **3** (2018) 10915 (https://doi.org/10.1002/slct.201801953)
7. M. Petrović, B. Škrbić, J. Živančev, L. Ferrando-Climent, D. Barcelo, *Sci. Total Environ.* **468**–**469** (2014) 415 (https://doi.org/10.1016/j.scitotenv.2013.08.079)
8. J. Choina, H. Kosslick, C. Fischer, G. U. Flechsig, L. Frunza, A. Schulz, *Appl. Catal., B Environ.* **129** (2013) 589 (https://doi.org/10.1016/j.apcatb.2012.09.053)
9. N. Jallouli, L. M. Pastrana-Martínez, A. R. Ribeiro, N. F. F. Moreira, J. L. Faria, O. Hentati, A. M. T. Silva, M. Ksibi, *Chem. Eng. J.* **334** (2018) 976 (https://doi.org/10.1016/j.cej.2017.10.045)
10. D. Chen, Y. Cheng, N. Zhou, P. Chen, Y. Wang, K. Li, S. Huo, P. Cheng, P. Peng, R. Zhang, L. Wang, H. Liu, Y. Liu, R. Ruan, *J. Clean. Prod.* **268** (2020) 121725 (https://doi.org/10.1016/j.jclepro.2020.121725)
11. Y. Xu, C. H. Langford, *J. Phys. Chem., B* **101** (1997) 3115 (https://doi.org/10.1021/jp962494l)
12. M. Gar Alalm, A. Tawfik, S. Ookawara, *J. Environ. Chem. Eng.* **4** (2016) 1929 (https://doi.org/10.1016/j.jece.2016.03.023)
13. A. Mishra, A. Mehta, S. Basu, *J. Environ. Chem. Eng.* **6** (2018) 6088 (https://doi.org/10.1016/j.jece.2018.09.029)
14. Lj. Damjanovic, A. Auroux, , in *Zeolite Characterization and Catalysis*, A. W. Chester, E. G. Derouane, Eds., Springer, Dordrecht, 2009, p. 107 (https://doi.org/10.1007/978-1-4020-9678-5)
15. A. Grela, J. Kuc, T. Bajda, *Materials* **14** (2021) 4994 (https://doi.org/10.3390/ma14174994)
16. G. Hu, J. Yang, X. Duan, R. Farnood, C. Yang, J. Yang, W. Liu, Q. Liu, *Chem. Eng. J.* **417** (2021) 129209 (https://doi.org/10.1016/j.cej.2021.129209)
17. S. Behravesh, N. Mirghaffari, A. A. Alemrajabi, F. Davar, M. Soleimani, *Environ. Sci. Pollut. Res.* **27** (2020) 26929 (https://doi.org/10.1007/s11356-020-09038-y)
18. K. K. Abbas, K. M. Shabeeb, A. A. A. Aljanabi, A. M. H. A. Al-Ghaban, *Environ. Technol. Innov.* **20** (2020) 101070 (https://doi.org/10.1016/j.eti.2020.101070)
19. S. Stojanović, M. Vranješ, Z. Šaponjić, V. Rac, V. Rakić, L. Ignjatović, L. Damjanović--Vasilić, *Int. J. Environ. Sci. Technol.* **20** (2023) 1 (https://doi.org/10.1007/s13762-022-04305-6)
20. T. F. Ferens, L. J. Visioli, A. T. Paulino, H. Enzweiler, *Int. J. Environ. Sci. Technol.* (2024) (https://doi.org/10.1007/s13762-024-06076-8)
21. N. Farhadi, T. Tabatabaie, B. Ramavandi, F. Amiri, *Ultrason. Sonochem.* **67** (2020) 105122 (https://doi.org/10.1016/j.ultsonch.2020.105122)

22. N. Farhadi, T. Tabatabaie, B. Ramavandi, F. Amiri, *Environ. Res.* **198** (2021) 111260 (https://doi.org/10.1016/j.envres.2021.111260)
23. J. Weitkamp, *Solid State Ionics* **131** (2000) 175 (https://doi.org/10.1016/S0167-2738(00)00632-9)
24. S. Stojanović, V. Rac, K. Mojsilović, R. Vasilić, S. Marković, Lj. Damjanović-Vasilić, *Environ. Sci. Pollut. Res.* **30** (2023) 84046 (https://doi.org/10.1007/s11356-023-28397-w)
25. C. Baerlocher, W. M. Meier, D. H. Olson, *Atlas of Zeolite Framework Types*, 5th ed., Elsevier, Amsterdam, Holland, 2001 (https://www.iza-structure.org/books/Atlas_5ed.pdf)
26. H. G. Karge, E. Geidel, in C*haracterization I. Molecular Sieves – Science and Technology*, Vol. 4., H. G. Karge, J. Weitkamp, Eds., Springer, Berlin, 2004, p. 1 (ISBN: 978-3-54-064335-7)
27. J. G. Yu, H.G. Yu, B. Cheng, X-J. Zhao, J. C. Yu, W-K. Ho, *J. Phys. Chem., B* **107** (2003) 13871 (https://doi.org/10.1021/jp036158y)
28. A. N. Ökte, Ö. Yilmaz, *Appl. Catal., A* **354** (2009) 132 (https://doi.org/10.1016/j.apcata.2008.11.022)
29. N. Jiang, R. Shang, S.G.J. Heijman, L.C. Rietveld, *Water Res.* **144** (2018) 145 (https://doi.org/10.1016/j.watres.2018.07.017)
30. X. Zhang, F. Wu, X.W. Wu, C. Pengyu, D. Nansheng, *J. Hazard. Mater.* **157** (2008) 300 (https://doi.org/10.1016/j.jhazmat.2007.12.098)
31. U. I. Gaya, A. H. Abdullah, *J. Photochem. Photobiol., C* **9** (2008) 1 (https://doi.org/10.1016/j.jphotochemrev.2007.12.003)
32. D. Krajišnik, A. Daković, A. Malenović, M. Kragović, J. Milić, *Clay Miner.* **50** (2015) 11 (https://doi.org/10.1180/claymin.2015.050.1.02)
33. P. Iovino, S. Canzano, S. Capasso, A. Erto, D. Musmarra, *Chem. Eng. J.* **277** (2015) 360 (https://doi.org/10.1016/j.cej.2015.04.097)
34. H. Ding, J. Hu, *Chem. Eng. J.* **397** (2020) 125462 (https://doi.org/10.1016/j.cej.2020.125462)
35. N. Negishi, Y. Miyazaki, S. Kato, Y. Yang, *Appl. Catal., B* **242** (2019) 449 (https://doi.org/10.1016/j.apcatb.2018.10.022).

Journal of the Serbian Chemical Society
JSCS@tmf.bg.ac.rs • www.shd.org.rs/JSCS
J. Serb. Chem. Soc. 89 (12) S520–S522 (2024) *Supplementary material*

SUPPLEMENTARY MATERIAL TO

Removal of pharmaceutically active substance ibuprofen from aqueous solution using TiO_2/ZSM-5 zeolite hybrid photocatalysts

SRNA J. STOJANOVIĆ[1], MARIJA Z. RISTIĆ[2], DANINA R. KRAJIŠNIK[3], VLADISLAV A. RAC[4] and LJILJANA S. DAMJANOVIĆ-VASILIĆ[1]*

[1]University of Belgrade – Faculty of Physical Chemistry, Studentski trg 12–16, 11000 Belgrade, Serbia, [2]University of Belgrade – ICTM, Department of Catalysis and Chemical Engineering, Njegoševa 12, 11000 Belgrade, Serbia, [3]University of Belgrade – Faculty of Pharmacy, Vojvode Stepe 450, 11221 Belgrade, Serbia, and [4]University of Belgrade-Faculty of Agriculture, Nemanjina 6, 11080 Belgrade, Serbia

J. Serb. Chem. Soc. 89 (12) (2024) 1587–1601

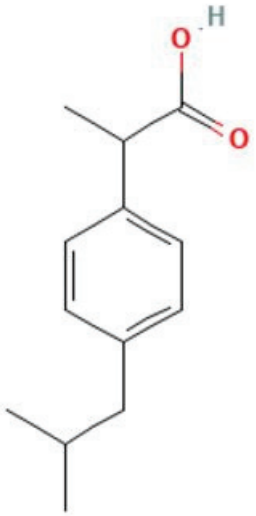

Fig. S-1. Structural formula of IBU ($C_{13}H_{18}O_2$) (PubChem Identifier: CID 3672, https://pubchem.ncbi.nlm.nih.gov/compound/3672, accessed October 1st 2024)

* Corresponding author. E-mail: ljiljana@ffh.bg.ac.rs

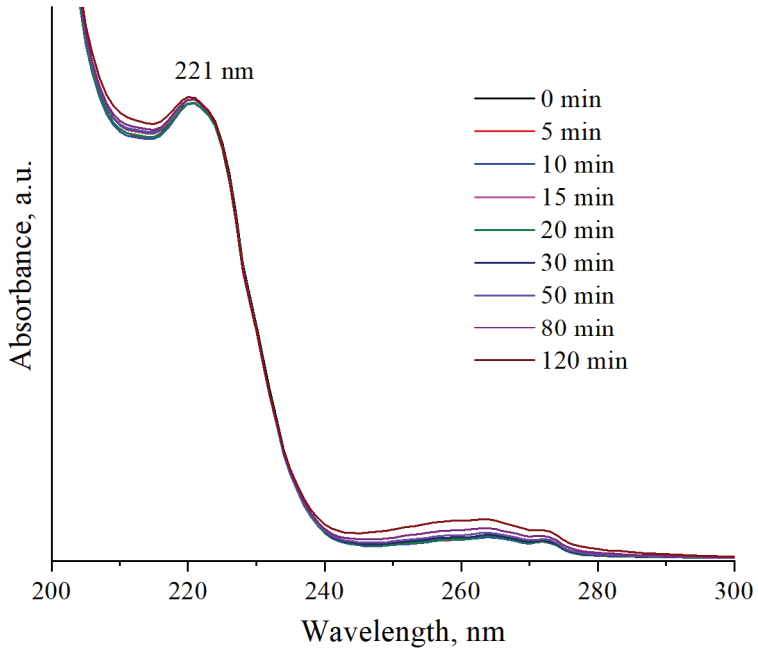

Fig. S-2. UV spectra of IBU aqueous solution after 0, 5, 10, 15, 20, 30, 50, 80 and 120 min of UV irradiation (Experimental conditions: C_0 = 30 mg L^{-1})

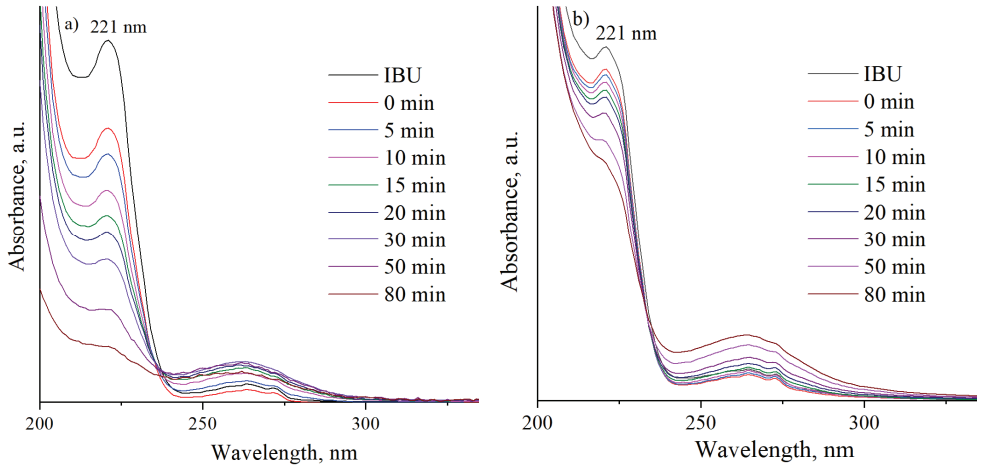

Fig. S-3. UV spectra of IBU in starting solution and in the presence of TZ(40) after 0, 5, 10, 15, 20, 30, 50 and 80 min of UV irradiation in a) deionized water and b) bottled drinking water (Experimental conditions: C_0 = 30 mg L^{-1}, 1 g L^{-1} catalyst)

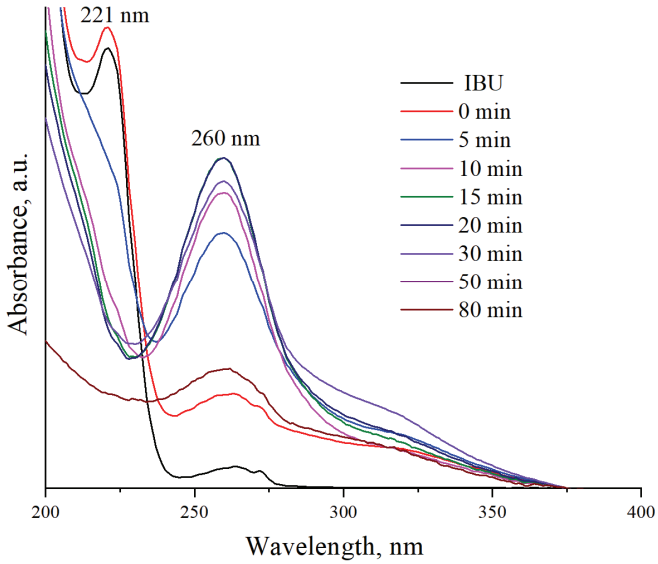

Fig. S-4. UV spectra of IBU in starting solution and in the presence of TiO_2 P25 nanoparticles after 0, 5, 10, 15, 20, 30, 50 and 80 min of UV irradiation in deionized water (Experimental conditions: C_0 = 30 mg L^{-1}, 1 g L^{-1} catalyst).

Journal of the Serbian Chemical Society
JSCS@tmf.bg.ac.rs • www.shd.org.rs/JSCS
J. Serb. Chem. Soc. *89* (12) 1603–1617 (2024)
JSCS–5809
Original scientific paper
Published 27 December, 2024

Potentially toxic elements from different environmental compartments of the River Watershed in Eastern Serbia – Assessment of the human health risk

ALEKSANDRA MIHAJLIDI-ZELIĆ[1]*, SANJA SAKAN[1], LJUBIŠA IGNJATOVIĆ[2], ALEKSANDAR POPOVIĆ[3#] and DRAGANA ĐORĐEVIĆ[1]

[1]University of Belgrade, Institute of Chemistry, Technology and Metallurgy, Centre of Excellence in Environmental Chemistry and Engineering, Njegoševa 12, 11000 Belgrade, Serbia, [2]University of Belgrade, Faculty of Physical Chemistry, Studentski trg 12–16, 11000 Belgrade, Serbia and [3]University of Belgrade, Faculty of Chemistry, Studentski trg 12–16, 11000 Belgrade, Serbia

(Received 2 November, revised 8 November, accepted 2 December 2024)

Abstract: This study assessed human health risks due to exposure to potentially toxic elements (PTE_S) in soil and river water in eastern Serbia. Concentrations of As, Cu, Cd, Zn, Pb, Ni and Cr were measured in soil and river water from the Vlasina watershed area. The concentrations of Cl^-, SO_4^{2-} and NO_3^- were also measured in the river water. According to the Regulation of the Republic of Serbia, the water quality of the investigated rivers corresponds to the surface water quality Class I and II. The content of PTEs in soil was below soil guideline values. Children were more sensitive than adults when exposed to PTE in water and soil. Arsenic was the dominant contributor to the total non-carcinogenic and carcinogenic risks for exposure to PTE in water. For PTE in soil, As had the dominant contribution to non-carcinogenic risks, and Ni to carcinogenic risks. All hazard index (*HI*) values for adults and children are less than 1, which indicates that the impact of PTEs in the examined river water and soil on human health is insignificant. Ingestion route is a major contributor to both total non-carcinogenic and carcinogenic risks.

Keywords: health risk; toxic elements; river water; soil; resident; recreator.

INTRODUCTION

Urbanization, industrial and agricultural activities have led to deterioration of surface water quality and the lack of drinking water sources, especially in developing countries. The quality of water resources, their potential effect on human health, and protection and preservation of sources of clean drinking water are

* Corresponding author. E-mail: mihajlidi.zeljic@ihtm.bg.ac.rs
# Serbian Chemical Society member.
https://doi.org/10.2298/JSC241102103M

extremely important environmental issues. Potentially toxic elements (PTEs) are considered to be among the most hazardous contaminants in aquatic ecosystems and soil because of their toxicity, non-biodegradability, and due to the fact that they can be bioaccumulated.[1] PTEs can occur in soil and surface water as a result of natural processes, but their presence in soil and surface water, often in high concentrations, can be a consequence of human activities. Rock weathering is the major natural source of PTEs in soil, while for surface water, additionally, erosion of soil is the important natural source of PTEs. Regarding anthropogenic sources of PTEs, mining, industrial and agricultural activities are their main sources. Once in these environmental compartments, PTEs can enter the food chain and, as a result of chronic exposure, they can pose a health risk to humans, even in low concentrations.[2] PTE pollution of soil and surface water has become a significant worldwide problem.[3,4] For that reason, methods for the estimation of threats that PTEs pose to human health have been developed. Health risk assessment indices have been introduced to assess the threatening effects of PTEs on human health.[5] For the assessment of both carcinogenic and non-carcinogenic risks that PTEs in soil and surface water pose to human health, the methodology developed by USEPA is widely used.[6]

In the present study, river water and soil samples were taken in the Vlasina River Watershed area and analyzed for PTEs. Additionally, anion concentrations were determined in water samples. The objectives of this research are: 1) to investigate distribution characteristics of PTE in river water and soil, 2) to estimate contamination levels of PTEs by comparison with surface water and soil quality standards and 3) to assess the impacts of PTEs on human health through ingestion and dermal contact pathways for exposure to water, and ingestion, dermal contact and inhalation pathways for exposure to soil. Non-carcinogenic and carcinogenic risks associated with human exposure to As, Cu, Cr, Ni and Zn in the river water, and As, Cu, Cr, Ni, Pb, Zn and Cd in soil were estimated in this research. The results obtained in this study could provide valuable information for drinking water source management and the protection of human health.

EXPERIMENTAL

Collection of river water and soil samples

Water samples (17) of the river Vlasina, important components in its watershed (Gradska River, Tegošnička River, Ljuberađa, Pusta River, Bistrička River, Rastavnica) and Zelenička River were collected in August 2018. Soil samples (15) were taken near the river water sampling locations. Details regarding the study area and sampling can be found in the Supplementary material to this paper.

Chemical analysis

For soil samples, the optimized BCR (Community Bureau of Reference) three-step sequential extraction procedure[7-9] was applied and subsequently, the residue was digested with *aqua regia*. In this study, presented results on element content are the sums of element content ext-

racted in all three steps of BCR extraction procedure and *aqua regia* digestion step.[10,11] Analytical techniques of inductively coupled plasma-optical emission spectrometry (ICP-OES, Thermo Scientific ICP-OES iCap 6500 Duo) and inductively coupled plasma-mass spectrometry (ICP-MS, Thermo Scientific ICP-MS iCap Q) were used for the measurement of the element concentrations in water samples and the obtained soil extracts, while ion chromatography technique (Metrohm 761 Compact IC) was applied for the determination of anions in river water. Further information on analytical measurements can be found in the Supplementary material.

Human health risk assessment

Humans can be exposed to pollutants in soil through ingestion, dermal contact and inhalation, while the main exposure pathways for humans to pollutants in water are ingestion and dermal contact. In this paper, potential health risks for humans due to exposure to PTE in soil and river water were assessed according to US Environmental Protection Agency (USEPA) guideline documents.[6,12-14] Human exposure to PTEs was estimated through the calculation of average daily dose (*ADD*), followed by the calculation of hazard quotients (*HQ*s) and hazard indices (*HI*s), as a sum of *HQ*s, for the assessment of non-carcinogenic health risks, while the carcinogenic health risks are assessed by calculating cancer risks (*CR*s) and their sum – total cancer risks (*TCR*).

Details regarding the health risk assessment procedure applied in this study are given in the Supplementary material.

RESULTS AND DISCUSSION

Concentrations of the investigated elements and anions in river water and comparison with surface water quality standard

The concentrations of investigated elements (Zn, As, Cr, Ni, Cu) and anions, representatives of salinity (Cl^-, SO_4^{2-}) and nutrients (NO_3^-), in the investigated rivers located in the Vlasina River catchment area, are presented in Fig. 1. The concentration values ranged from: <*DL* to 6.40 μg L^{-1} for Zn, 0.236–3.05 μg L^{-1} for As, 0.039–0.194 μg L^{-1} for Cr, 0.128–0.486 μg L^{-1} for Ni, <*DL* to 1.05 μg L^{-1} for Cu, 10.34–39.92 mg L^{-1} for Cl^-, <*DL* to 9.66 mg L^{-1} for NO_3^- and 10.03––21.00 mg L^{-1} for SO_4^{2-}. The concentrations of Pb, Cd and PO_4^{3-} were below the detection limit in all investigated samples. The values of detection limits are given in the Supplementary material. The chosen set of anions represent the major anions in river water which are often used in the assessment of water quality. Also, the selected elements are frequently used for the assessment of river water and sediment pollution status, and health risks due to human exposure to PTE in water and soil. Higher concentrations of Zn, compared to other water samples of the Vlasina watershed investigated rivers, were found in sample 5 – Tegošnica River (near the village Doroviš, downriver from the stone pit) and sample 15 – Vlasina River (upstream of the intake for water supply). The highest concentrations of As (Fig. 1) were found in Ljuberađa River (samples 7–9), whose upper course is mostly made from karst springs' waters, and in the lower course Ljuberađa River formed a gorge through lower cretaceous carbonate rocks.[15] Our previous paper[16] rev-

ealed that As in the rivers of the Vlasina watershed was strongly correlated with Ca and Sr. Higher concentrations of As (up to 17 μg L^{-1}) have already been found in karst springs in Greece where carbonate formations are in contact with metamorphic and metavolcanic formations.[17] For Cr, the highest concentrations were detected in Rastavnica River (sample 14) and Vlasina River, downriver from Vlasotince (sample 16). Among investigated rivers, the highest concentrations of Cu were found in Gradska River (sample 2), also higher concentrations of Cu than in other investigated river water samples, were found in sample 1 – Vlasina River (before receiving Gradska River), sample 2 – Gradska River, sample 5 – Tegošnička River (near the village Doroviš), sample 10 (Vlasina, after receiving Ljuberađa) and sample 16 (Vlasina River, downriver from Vlasotince).

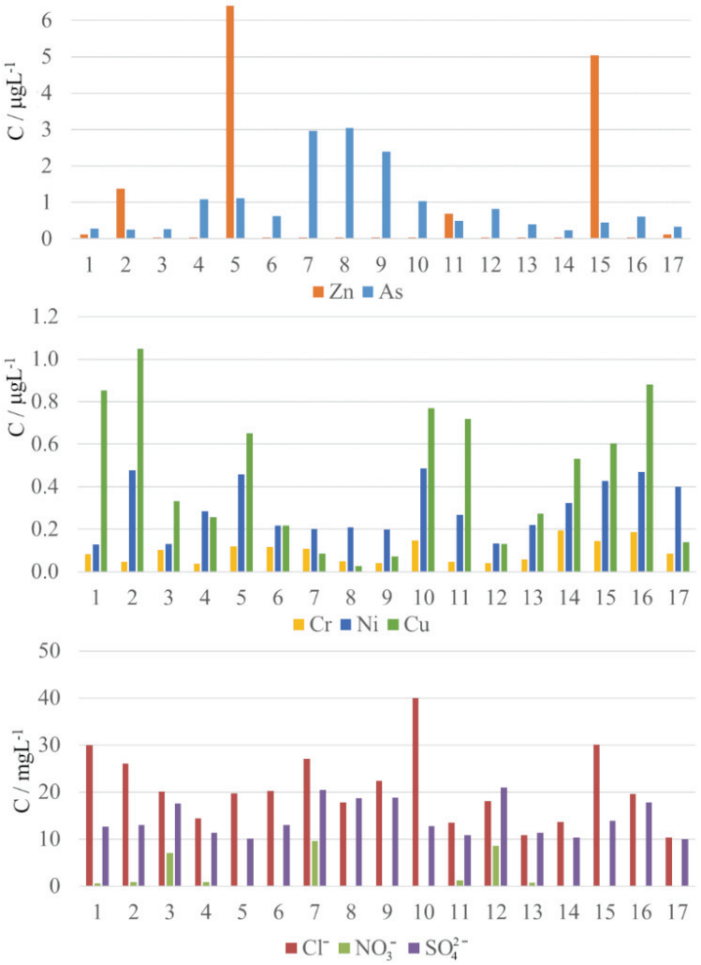

Fig. 1. Concentration of Zn, Cr, Ni, Cu, As, chlorides, nitrates and sulphates in river water.

The concentrations of elements, and anions (nutrient content and salinity indicators) in the investigated river water samples (Fig. 1) were compared with the limit values for pollutants in surface waters (Table S-V of the Supplementary material) prescribed by the Regulation on limit values for pollutants in surface and ground waters and sediment and deadlines for their achievement.[18] Excluding the values of nitrate content in river water samples of Ljuberađa – middle course, sample 7 (2.181 mg NL^{-1}), Vlasina – downstream of the confluence with Pusta River, sample 12 (1.953 mg NL^{-1}), Vlasina – upstream of the confluence with Tegošnička River, sample 3 (1.586 mg NL^{-1}), which correspond to the Class II surface water quality, the values of the measured parameters in the rest of the examined river water samples are in the ranges that are characteristic for surface water quality Class I. Surface waters of Class I and II quality can be used for drinking water supply with prior filtration and disinfection treatment, bathing and recreation, irrigation, industrial use (process and cooling water).

Content of the investigated elements in soil and comparison with soil quality standards

The content of Zn, Ni, Cu, Cr, Pb, Cd and As in studied soils are shown in Fig. 2 and Table I.

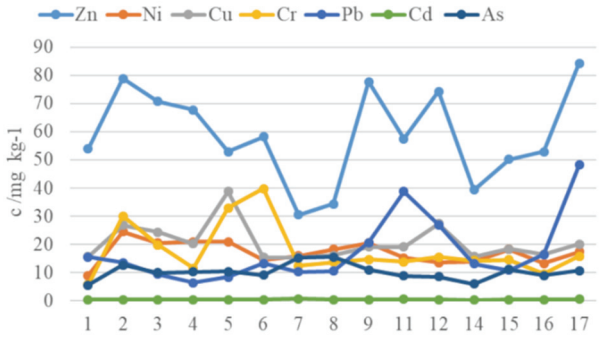

Fig. 2. Content of elements in studied soil.

TABLE I. Contents of PTEs in the soils in this study, other worldwide soils and quality standards; V – Vlasina soil

Sample	Zn	Ni	Cu	Cr	Pb	Cd	As
Mean V	58.9	17.1	20.6	17.6	17.5	0.44	10.2
Max V	84.29	24.50	38.79	39.76	48.17	0.66	15.49
Srem[24]	65.9	51.6	28	49.3	21.6	0.36	6.55
ŠS[21]	n.d.	47.6	37.6	59.8	82.0	1.6	n.a.
EAS[23]	45	15.0	15	20.0	16	0.18	5.5
Belgrade[22]	268	124	122	70.2	350	8.90	n.a.
EU[19]	150–300	30–75	50–140	n.a.	50–300	1–3	n.a.
EIL[20]	200	60.0	100	400	600	3.00	20.0

Based on the results of the comparison of the Cd, Ni, Pb, Cu and Zn, total content with the limits for the element content prescribed by the European Union directive 86/278/EEC[19] and ecological investigation levels (EIL), defined by the Assessment Level for Soil, Sediment and Water (Government of Western Australia)[20], it can be concluded that the mean values (Mean V, Table I), as well as the maximum contents of all studied toxic elements (Max V, Table I) are lower than the values which are defined by this legislation.

When comparing the mean content of elements in the soil from Vlasina region with the element content in Šabac[21] and Belgrade soil[22] it is possible to see that all values of the mean content of the studied elements in Vlasina region soils are lower than the average value of element content in other localities. In relation to results for European agricultural soils (EAS),[23] similar values were observed for Ni, Cu, Cr and Pb, and slightly higher values were observed for Zn, Cd and As.

As a result of comparing our results with the soil content from the Srem locality,[24] it is possible to conclude that similar contents were observed for Zn, Pb, Cd and Cu, lower for Ni and Cr, and slightly higher for As.

Health risk assessment

Non-carcinogenic risk for exposure to PTE in river water. Hazard index (*HI*) values for As, Cr, Zn, Ni and Cu from human exposure to river water, and their sum, representing non-carcinogenic health hazards of all PTEs combined from all exposure pathways, for different receptors are shown in Fig. 3. The values of *HI*s for all receptors were in the following descending order: As > Cr > Ni > Cu > Zn. The highest values of hazard indices were calculated for As in Ljuberađa River (samples 7–9) for both residential receptors (0.33–0.42 for children and 0.22–0.28 for adults) and recreational receptors (0.0076–0.0098 for children and 0.0019––0.0025 for adults, Fig. 3).

Average values of hazard quotients (*HQ*s), hazard indices of individual PTE, representing non-carcinogenic health risks of PTE from combined exposure through ingestion of water and dermal contact with water, hazard indices of all PTE combined for each exposure pathway, and total hazard indices (*THI*) as hazard indices of all PTEs combined from all exposure pathways are presented in TABLES S-VI and S-VII, for residential receptors and recreational receptors, respectively.

THI for resident receptors (Fig. 3a and b) were from 0.039 to 0.42 (mean value 0.14, Table S-VI of the Supplementary material) for children, and from 0.025 to 0.28 (mean value 0.091, Table S-VI) for adults. The corresponding values of *THI* for recreational children and adults (Fig. 3c and d) were from 0.00097 to 0.0098 (mean value 0.0033, Table S-VII of the Supplementary material), and from 0.00031 to 0.0025 (mean value 0.0009, Table S-VII), respectively. The obtained results indicate that the potential for non-carcinogenic health effects is higher for

residential receptors than recreational receptors and that children, compared to adults, are more sensitive to developing non-carcinogenic health effects as a result of exposure to PTE in water, and this is in accordance with findings of other studies.[1,3,25]

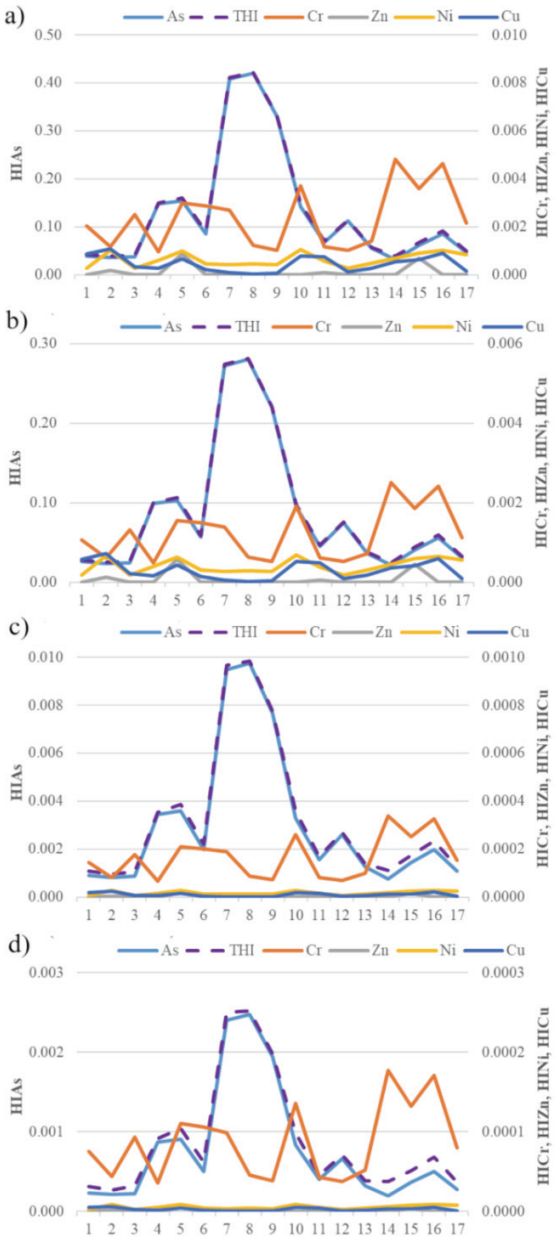

Fig. 3. Non-carcinogenic risks (*HI*) from exposure to PTE in river water: a – residential children, b – residential adults, c – recreational children and d – recreational adults.

Among investigated rivers, the highest *THI* values were calculated for Ljuberađa River (samples 7–9), for both residential receptors (0.33–0.42 for children and 0.22–0.28 for adults) and recreational receptors (0.0077–0.0098 for children and 0.0020–0.0025 for adults, Fig. 3). Given that hazard index values for both residential and recreational receptors were < 1 (Tables S-VI and S-VII, Fig. 3), detrimental non-carcinogenic effects on human health from PTE in the investigated rivers of the Vlasina watershed, through water ingestion and dermal contact with water, are not expected.

The contributions (%) of individual PTE to the total non-carcinogenic health risk (risks of all potentially toxic elements combined from all exposure pathways, THI) are presented in Fig. 4a and b for residential children and adults, and in Fig. 4c and d for recreational children and adults. Arsenic was the dominant contributor to *THI* for both residential children (97 %) and adults (98 %) (Table S-VI and Fig. 4a and b), and recreational children (94%) and adults (87%) (Table S-VII and Fig. 4c and d). A high contribution of As to *THI* was also observed for exposure to PTE in surface waters in Turkey.[1]

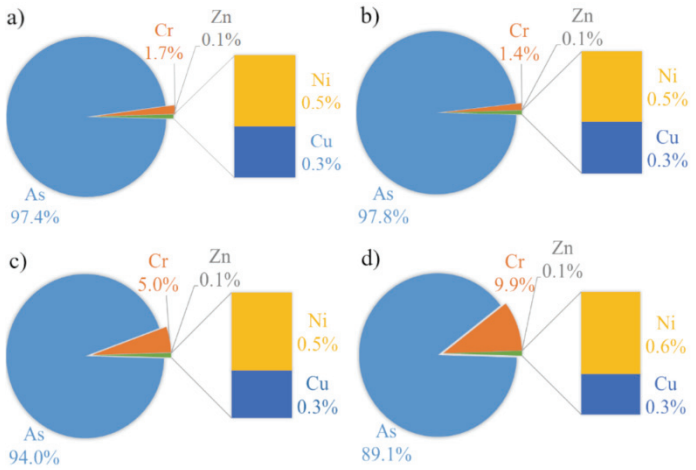

Fig. 4. Contributions of non-carcinogenic risks (*HI*) of individual PTEs to the total non-carcinogenic risk: a – residential children, b – residential adults, c – recreational children and d – recreational adults.

Average *HI* values as a result of exposure to all PTE *via* water ingestion for residential children and adults were 0.13 and 0.090, respectively, and from dermal absorption of PTE in water were 0.0025 and 0.00084 for children and adults, respectively (Table S-VI). For recreational receptors, average non-carcinogenic risks of all PTE combined, through ingestion of river water and dermal contact with river water were 0.0030 and 0.00070 (children and adults), and 0.00032 and 0.00018 (children and adults, Table S-VII). For all receptors, and both exposure

pathways, the values of *HQ*s calculated for investigated PTE decreased in the following order: As > Cr > Ni > Cu > Zn.

Obtained results of the assessment of non-carcinogenic risk of all PTE combined from each exposure pathway (Tables S-VI and S-VII) show that the water ingestion pathway has a dominant contribution to the potential occurrence of non--carcinogenic health effects for all receptors – 98 % for residential children, 99 % for and residential adults and 79 and 90 % for recreational children and adults, respectively. Also, for both exposure pathways, non-carcinogenic risk of all PTE is higher for children than adults, which is in agreement with the results of the previous studies.[1,3–5,25] Regarding water ingestion pathway for both residential and recreational receptors, the highest *HQ* values of all PTE, by far, were for As, which contributed 98 % to non-carcinogenic health risks via water ingestion. The largest contribution to non-carcinogenic health risks through dermal contact with water for both residential and recreational receptors was from As (55 %) and Cr (43 %). For Cr, the dermal contact pathway contributes much more to *HI* than for other PTE, 45 % for residential children, 29 % for residential adults and 83 and 92 % for recreational children and adults, respectively. Similar was observed in the other studies.[1,3,25]

Carcinogenic risk for exposure to PTE in river water. Potentially toxic elements that have cancer slope factors were used to assess carcinogenic risks, As and Cr. Average values of carcinogenic risks for exposure to PTE in river water through ingestion ($CR_{ingestion}$) and dermal contact (CR_{dermal}) and the total carcinogenic risks (*TCR*) for residential and recreational receptors are presented in Tables II and III.

As can be noticed in Tables II and III, values of *TCR* of both elements were lower than the target risk (1×10^{-4}) for both residential receptors (6.00×10^{-5} and 4.00×10^{-5} for As, for children and adults, respectively, and 3.54×10^{-6} and 1.84×10^{-6} for Cr, for children and adults, respectively) and recreational receptors (1.39×10^{-6} and 3.53×10^{-7} for As, for children and adults, respectively, and 1.64×10^{-6} and 1.30×10^{-7} for Cr, for children and adults, respectively).

TABLE II. Average values ($\times10^6$) of carcinogenic risks for exposure to PTE in river water through ingestion ($CR_{ingestion}$) and dermal contact (CR_{dermal}) pathways and total carcinogenic risks (*TCR*); residential receptors

Element	Child			Adult		
	$CR_{ingestion}$	CR_{dermal}	*TCR*	$CR_{ingestion}$	CR_{dermal}	*TCR*
As	59.4	0.612	60.0	39.8	0.207	40.0
Cr	1.94	1.60	3.54	1.30	0.542	1.84
All elements	61.3	2.21	63.5	41.0	0.750	41.8

Results of the carcinogenic risk assessment presented in Tables II and III indicate that, for residential and recreational receptors, As was the predominant

contributor to the total carcinogenic risk of Cr and As combined. The contribution is higher for residential children and adults (94 and 96 %) than for recreational children and adults (85 and 73 %). Results of the assessment of carcinogenic risks of Cr and As for different exposure pathways show that the water ingestion pathway contributes more than the dermal pathway to *TCR* for all receptors (Tables II and III). For both As and Cr values of *CR via* water ingestion and dermal contact with water were higher for residents than recreators. For both exposure pathways carcinogenic risk of As and Cr are higher for children than adults (Tables II and III). Arsenic was the predominant contributor to the *CR* through water ingestion pathway for residential and recreational receptors (97 %). Conversely, Cr contributed 72 % to the *CR via* dermal contact with water for residents and recreators.

TABLE III. Average values ($\times 10^7$) of carcinogenic risks for exposure to PTE in river water through ingestion ($CR_{ingestion}$) and dermal contact (CR_{dermal}) pathways and total carcinogenic risks (*TCR*); recreational receptors

Element	Child			Adult		
	$CR_{ingestion}$	CR_{dermal}	*TCR*	$CR_{ingestion}$	CR_{dermal}	*TCR*
As	13.1	0.787	13.9	3.07	0.460	3.53
Cr	0.428	2.06	2.48	0.100	1.20	1.30
All elements	13.5	2.84	16.4	3.17	1.66	4.83

Non-carcinogenic risk for exposure to PTE in soil. *HQ* trend (Table S-VIII of the Supplementary material) in both, adults and children was found in order: *HQ*ing > *HQ*derm > *HQ*inh, except for Cd in children where the following trend was observed: *HQ*der > *HQ*ing > *HQ*inh. It should be noted that the differences between the values of HQder and *HQ*ing for Cd were not large. *HI* values for adults were from: 0.0255 to 0.0714 for As; 0.0031 to 0.0221 for Cr; 0.0026 to 0.0194 for Pb; 0.0006 to 0.0017 for Ni; 0.0007 to 0.0013 for Cd; 0.0005 to 0.0013 for Cu and 0.0001 to 0.0004 for Zn (Fig. 5). HI values for children were from: 0.2370 to 0.6782 for As; 0.0276 to 0.2649 for Cr; 0.0251 to 0.1891 for Pb; 0.0066 to 0.00180 for Cd; 0.0058 to 0.0163 for Ni; 0.0051 to 0.0128 for Cu and 0.0004 to 0.0010 for Zn, Fig. 6).

All *HI* values for adults and children are less than 1, which indicates that the impact of PTEs is insignificant in the examined soils. For children, the highest *HI* values were observed for As, Cr, Pb, Cd, Ni, Cu and the lowest for Zn. For adults, the highest *HI* values are for As, Cr, Pb, Ni, Cd = Cu, and the lowest for Zn. Many *HI* values are 10 times higher for children than for adults. This trend was also observed in Alarifi[26] and the mentioned scientists explained that noncarcinogenic risks of heavy metal exposure for children are higher than for adults due to their physiological characteristics. The highest values of *HI* for children and adults were observed in the soil at the sampling sites 8 and 7 for As, and for Pb at sites 17 and 11.

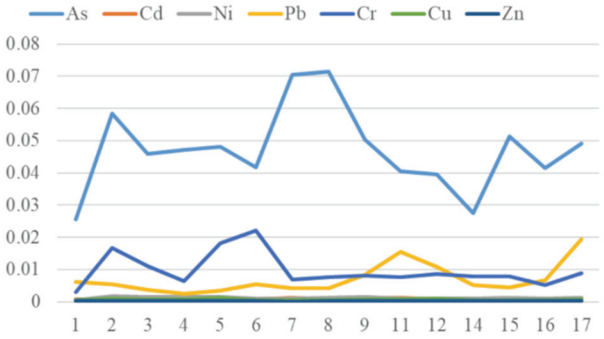

Fig. 5. Hazard index (*HI*) for non-carcinogenic risk in adults.

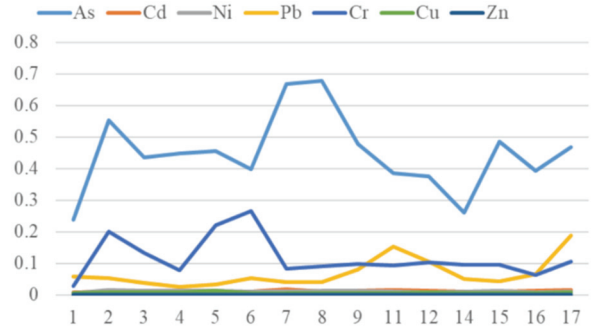

Fig. 6. Hazard index (*HI*) for non-carcinogenic risk in children.

Carcinogenic risk for exposure to PTE in soil. Carcinogenic human health risk values (*CR* and *TCR*) are shown in Tables S-IX and S-X of the Supplementary material, and Figs. 7 and 8. *TCR* values for adults were from: 3.22×10^{-5} to 1.15×10^{-4} for As; 2.85×10^{-6} to 5.56×10^{-6} for Cd; 2.30×10^{-5} to 6.28×10^{-5} for Ni; 7.49×10^{-8} to 5.64×10^{-7} for Pb; and 4.55×10^{-6} to 3.19×10^{-5} for Cr. *CR* values for children were from: 1.07×10^{-4} to 3.05×10^{-4} for As; 2.68×10^{-5} to 5.23×10^{-5} for Cd; 2.09×10^{-4} to 6.82×10^{-4} for Ni; 7.04×10^{-7} to 5.29×10^{-6} for Pb; and 4.04×10^{-5}

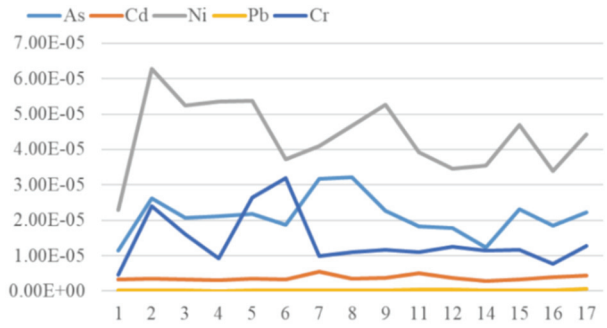

Fig. 7. Carcinogenic risk value for adults.

to 3.69×10^{-4} for Cr. The *TCR* values, for adults and children, were in the following descending order: Ni, Cr, As, Cd, Pb and Ni, As, Cr, Cd, Pb, respectively. The highest *CR* values were observed at sites 7 and 8 (for As), site 2 (for Ni), and site 6 (for Cr). For adults, all *TCR* values belong to the acceptable and no-risk category. Regarding children, the *TCR* values for As, Cr and Ni are greater than 10^{-4}, excluding values for Cr at two localities (1 and 16). As can be seen in Table S-X of the Supplementary material, the ingestion route is a major contributor to *TCR* followed by dermal and inhalation pathways. Also, *TCR* values for children were higher than for adults and therefore children are more at risk than adults in this study area.

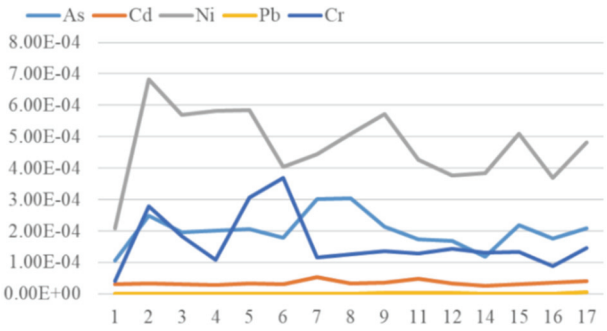

Fig. 8. Carcinogenic risk value for children.

CONCLUSION

Taking into account the globally spread problem of river water and soil pollution and the scarcity of adequate quality drinking water sources, the investigation of water resources is a critical topic. In this study, PTEs in river water and soil in the Vlasina River drainage basin were studied in relation to contamination and human health risk assessment. Regarding studied elements, nutrient content and salinity indicators, the water quality of the investigated rivers corresponds to surface water quality Class I and Class II. Results of the comparison with limit values for PTE in soil indicate that the studied region is not under significant anthropogenic influence. According to the results of non-carcinogenic risk assessment, adverse non-carcinogenic effects of PTE in river water (As, Cu, Cr, Ni and Zn) and soil (As, Cu, Cr, Ni, Pb, Zn and Cd) on human health are not expected. The *TCR* values of all considered PTE (As and Cr) for exposure to river water were below the target risk. Regarding exposure to PTE in soil, all *TCR* values for adult receptors belong to the acceptable and no-risk category. For children, the *TCR* values of As, Cr and Ni were slightly higher than the acceptable limit of 1×10^{-4}. The results of the health risk assessment indicate that children are more susceptible to the detrimental effects of PTE on health. Arsenic was a predominant contributor to non-carcinogenic risk for exposure to PTE in water and soil. Dominant contribution to carcinogenic risks was from As for exposure to water, and from Ni for

exposure to soil. These are the first results of the assessment of human health risks posed by PTEs in river water and soil in the Vlasina River basin. We believe that the results of this study could be beneficial for the protection of human health and drinking water source management.

SUPPLEMENTARY MATERIAL

Additional data and information are available electronically at the pages of journal website: https://www.shd-pub.org.rs/index.php/JSCS/article/view/13105, or from the corresponding author on request.

Acknowledgement. This research has been financially supported by the Ministry of Science, Technological Development and Innovation of the Republic of Serbia (Contract No: 451-03-66/2024-03/200026).

ИЗВОД

ПОТЕНЦИЈАЛНО ТОКСИЧНИ ЕЛЕМЕНТИ У ВОДАМА РЕЧНОГ СЛИВА И ОКОЛНОМ ЗЕМЉИШТУ У ИСТОЧНОЈ СРБИЈИ – ПРОЦЕНА РИЗИКА ПО ЉУДСКО ЗДРАВЉЕ

АЛЕКСАНДРА МИХАЈЛИДИ-ЗЕЛИЋ[1], САЊА САКАН[1], ЉУБИША ИГЊАТОВИЋ[2], АЛЕКСАНДАР ПОПОВИЋ[3] и ДРАГАНА ЂОРЂЕВИЋ[1]

[1]Центар изузетних вредности за хемију и инжењеринг животне средине, Универзитет у Београду, Институт за хемију, технологију и металургију, Његошева 12, 11000 Београд, [2]Универзитет у Београду, Факултет за физичку хемију, Студентски трг 12–16, 11000 Београд и [3]Универзитет у Београду, Хемијски факултет, Студентски трг 12–16, 11000 Београд

У овој студији су процењени ризици по здравље људи услед изложености потенцијално токсичним елементима (PTE) у земљишту и речним водама у источној Србији. Садржај As, Cu, Cd, Zn, Pb, Ni и Cr мерен је у водама река из слива Власине и околном земљишту. Концентрације Cl^-, SO_4^{2-} и NO_3^- су такође мерене у речној води. Према Уредби Републике Србије, квалитет воде истраживаних река одговара квалитету површинских вода класе I и II. Садржаји PTE у земљишту су нижи од граничних вредности прописаних међународним правилницима. Резултати процене ризика по здравље показују да су деца осетљивија од одраслих када су изложена PTE у води и земљишту. За изложеност људи PTE у води, доминантан допринос укупним неканцерогеним и канцерогеним ризицима потиче од As. За PTE у земљишту, As је имао доминантан допринос не-канцерогеним ризицима, а Ni канцерогеним ризицима. Све вредности *HI* за одрасле и децу су мањи од 1, што указује да је утицај PTE у испитиваној речној води и земљишту на људско здравље занемарљив.

(Примљено 2. новембра, ревидирано 8. новембра, прихваћено 2. децембра 2024)

REFERENCES

1. Ö. Canpolat, M. Varol, Ö. Ö. Okan, K. K. Eriş, M. Çağlar, *Environ. Res.* **190** (2020) 110012 (https://doi.org/10.1016/j.envres.2020.110012
2. S. M. Shaheen, V. Antoniadis, E. Kwon, H. Song, S-L. Wang, Z-Y. Hseu, J. Rinklebe, *Environ. Poll*. **262** (2020) 114312 (https://doi.org/10.1016/j.envpol.2020.114312)
3. M. S. Islam, *Environ. Earth Sci*. **28** (2021) 2987 (https://doi.org/10.1007/s11356-021-12541-5)
4. C. Tokatli, F. Ustaoglu., *Environ. Earth Sci.* **79** (2020), 426 (https://doi.org/10.1007/s12665-020-09171-4)

5. C. Tokatli, *Environ. Earth Sci.* **80** (2021) 156 (https://doi.org/10.1007/s12665-021-09467-z)
6. U.S. EPA, *Risk assessment guidance for Superfund. Volume I: Human Health Evaluation Manual (Part A). Interim Final. Office of Emergency and Remedial Response. EPA/540/1-89/002*, 1989
7. E. de Andrade Passos, J. C. Alves, I. S. dos Santos, J. P. H Alves, C. A. B. Garcia, C. S. Costa, *Microchem. J.* **96** (2010) 50 (https://doi.org/10.1016/j.microc.2010.01.018)
8. R.A. Sutherland, *Anal. Chim. Acta* **680** (2010) 10 (https://doi.org/10.1016/j.aca.2010.09.016)
9. S. Sakan, A. Popović, I. Anđelković, D. Đorđević, *Environ. Geochem. Health* **38** (2016) 855 (https://doi.org/10.1007/s10653-015-9766-0)
10. A. Facchinelli, E. Sacchi, L. Mallen, *Environ. Pollut.* **14** (2001) 313 (https://doi.org/10.1016/S0269-7491(00)00243-8)
11. S. Sakan, I. Gržetic, D. Đorđević, *Environ. Sci. Pollut. Res. Int.* **14** (2007) 229 (https://doi.org/10.1065/espr2006.05.304)
12. U.S.EPA, *Risk Assessment Guidance for Superfund Volume I: Human Health Evaluation Manual (Part E, Supplemental Guidance for Dermal Risk Assessment) Final. OSWER 9285.7-02EP*, 2004
13. U.S.EPA, *Exposure Factors Handbook 2011 Edition (Final Report). U.S. Environmental Protection Agency, Washington, DC, EPA/600/R-09/052F*, 2011
14. U.S.EPA, 2024. *Regional Screening Level (RSL) Summary Table (TR=1E-06 THQ=1.0)*, https://semspub.epa.gov/work/HQ/404463.pdf (accessed 12 October 2024)
15. Miladinović, B., Đokanović, S., *Pirotski zbornik* **44** (2019) 147 (https://nbpi.org.rs/wordpress/wp-content/uploads/2019/11/Pirotski-zbornik-44.pdf) (in Serbian)
16. S. Sakan, A. Mihajlidi-Zelic, S. Frančišković-Bilinski, D. Đordević, *Front. Environ. Sci.* **10** (2022) 909858 (https://doi.org/10.3389/fenvs.2022.909858)
17. L. Li Vigni, K. Daskalopoulou, S. Calabrese, L. Brusca, S. Bellomo, C. Cardellini, K. Kyriakopoulos, F. Brugnone, F. Parello, W. D'Alessandro, *Sci. Rep.* **13** (2023) 11191 (https://doi.org/10.1038/s41598-023-38349-6)
18. *Regulation on limit values of pollutants in surface and ground waters and sediment and deadlines for their achievement*, *Off. Gaz. Rep. Serbia* **50** (2012) (in Serbian)
19. Council of the European Communities (CEC), *The protection of the environment, and in particular of the soil, when sewage sludge is used in agriculture. Council Directive of 12 june 1986*, *Off. J. Eur. Communities* **181**, Issue 6 (1986)
20. Government of Western Australia*, Assessment levels for Soil, Sediment and Water*, Department of Environment and Conservation, 2010
21. M. Antonijević Nikolić, J. Đuričić Milanković, Đ. Nikolić, *Zaštita Materijala* **62** (2021) 83. (https://doi.org/10.5937/zasmat2102083A) (in Serbian)
22. I. Gržetić, R. H. A. Ghariani, *J. Serb. Chem. Soc.* **73** (2008) 923 (https://doi.org/10.2298/JSC0809923G)
23. C. Reimann, K. Fabian, M. Birke, P. Filmozer, A. Demetriades, P. Negrél, K. Oorts, J. Matschullat, P. Caritat, *Appl. Geochem.* **88** (2018) 302 (https://doi.org/10.1016/j.apgeochem.2017.01.021)
24. M. Poznanović Spahić, D. Manojlović, P. Tančić, Ž. Cvetković, Z. Nikić, R. Kovačević, S. Sakan, *Environ. Monit. Assess.* **191** (2019) 133 (https://doi.org/10.1007/s10661-019-7268-8)

25. L. Li, J. Wu, J. Lu, K. Li, X. Zhang, X. Min, C. Gao, J. Xu, *Ecotoxicol. Environ. Saf.* **241** (2022) 113775 (https://doi.org/10.1016/j.ecoenv.2022.113775)
26. S. S. Alarifi, A. S. El-Sorogy, K. Al-Kahtany, S. A. Hazaea, *J. King Saud Univ. Sci.* **35** (2023) 102826 (https://doi.org/10.1016/j.jksus.2023.102826).

Journal of the Serbian Chemical Society
JSCS@tmf.bg.ac.rs • www.shd.org.rs/JSCS
J. Serb. Chem. Soc. *89* (12) S523–S532 (2024) *Supplementary material*

SUPPLEMENTARY MATERIAL TO

Potentially toxic elements from different environmental compartments of the River Watershed in Eastern Serbia – Assessment of the human health risk

ALEKSANDRA MIHAJLIDI-ZELIĆ[1]*, SANJA SAKAN[1], LJUBIŠA IGNJATOVIĆ[2], ALEKSANDAR POPOVIĆ[3] and DRAGANA ĐORĐEVIĆ[1]

[1]University of Belgrade, Institute of Chemistry, Technology and Metallurgy, Centre of Excellence in Environmental Chemistry and Engineering, Njegoševa 12, 11000 Belgrade, Serbia, [2]University of Belgrade, Faculty of Physical Chemistry, Studentski trg 12–16, 11000 Belgrade, Serbia and [3]University of Belgrade, Faculty of Chemistry, Studentski trg 12–16, 11000 Belgrade, Serbia

J. Serb. Chem. Soc. *89* (12) (2024) 1603–1617

STUDY AREA

Vlasina River is located in southeastern Serbia, flowing around 70 km from Vlasina Lake to South Morava River, belonging to the Dunav River watershed (Fig. S-I). Vlasina River basin covers a surface of around 1,000 km^2. The area is mostly hilly-mountainous (up to 1700 m a.s.l.) covered by forests, pastures, and agricultural crops. One of the main activities of the inhabitants of Vlasina is mountain cattle breeding (sheep, cattle and horses), mountain agriculture (rye, barley, oats, potatoes),[1] and also Vlasotince is the centre of the wine-growing region.[2] Lower quality arable land occupies a significant area in the Vlasina River basin, while around Vlasotince alluvial sediments in the Vlasina River valley are rich in humus. The majority of the area of the Vlasina River basin belongs to the Vlasina unit, which is a part of the vast Serbo-Macedonian Unit, stretching from the Panonian Basin in the north to the Aegean Sea in the south, in Serbia encompassing its central and southeastern parts, originating from the Carbon – Permian period (Paleozoic). Metamorphic rocks dominate the southern and western parts of the research area, while tertiary clastic sediments, Mesozoic carbonate rocks and flysch make the most of the eastern and northern parts.[3]

COLLECTION OF RIVER WATER AND SOIL SAMPLES

River water samples were taken at the following sampling sites (Fig. S-I): (1) Vlasina (upstream of the confluence Gradska river); (2) Gradska River (before its

* Corresponding author. E-mail: mihajlidi.zeljic@ihtm.bg.ac.rs

confluence with Vlasina); (3) Vlasina (upstream of the confluence with Tegošnička River); (4) Tegošnička River (stone pit); (5) Tegošnička River (near village Dobroviš); (6) Vlasina (downstream of the confluence with Tegošnička River, near village Gornji Orah); (7) Ljuberađa (middle course); (8) Ljuberađa (measuring profile); (9) Ljuberađa (confluence with Vlasina); (10) Vlasina (after receiving Ljuberađa); (11) Pusta River; (12) Vlasina (downstream of the confluence with Pusta River); (13) Bistrička River; (14) Rastavnica River; (15) Vlasina (upstream of the intake for water supply); (16) Vlasina (downriver from Vlasotince); (17) Zelenička River. Soil samples were taken at 15 sampling locations, close to the river water sampling locations. The soil was not sampled on locations (10) Vlasina after receiving Ljuberađa and (13) Bistrička River.

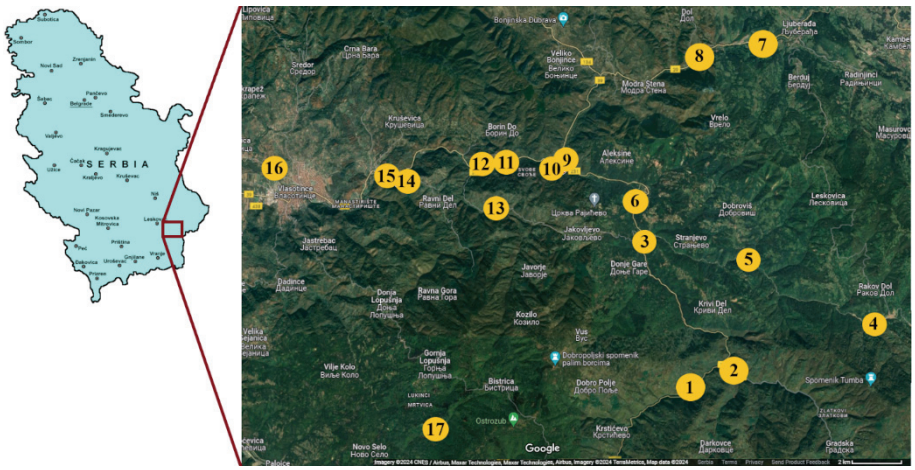

Fig. S-1. Location of the research area in Serbia and sampling sites in the Vlasina region.

Water grab samples were taken at around 10 cm beneath the water surface and filtered through 0.2 μM nylon syringe filters into the high-density polyethylene bottles. Aliquot of each sample for the analysis of elements was subsequently acidified with HNO_3 to a pH below 2 and all samples were stored at 4°C until.[3-5]

Soil samples were collected into polyethylene bottles with a plastic spatula/shovel [7-9] and transported to the laboratory. Stones and plant debris were removed from the samples in the laboratory, the samples were subsequently homogenized and kept in the refrigerator at 4° C. Samples were air dried for 8 days before analysis.[10, 11]

DETERMINATION OF ELEMENT CONCENTRATIONS IN RIVER WATER SAMPLES AND SOIL EXTRACTS BY ICP-OES AND ICP-MS

Element concentrations in river water and soil extracts obtained at each of BCR extraction steps were determined using techniques of Inductively Coupled Plasma-Optical Emission spectrometry (Thermo Scientific ICP-OES iCap 6500

Duo) and Inductively Coupled Plasma-Mass spectrometry (Thermo Scientific ICP-MS iCap Q). The analytical data quality was controlled by using laboratory quality assurance and quality control methods, including the use of standard operating procedures, calibration with standards, and analysis of both reagent blanks and replicates.[12] The blank solutions were prepared in the same way as the samples during the extraction procedure. The quality of data was assessed by estimations of accuracy and precision. The accuracy and precision of the obtained results were checked by analyzing sediment reference material (BCR 701) for three-step sequential extraction. Acceptable accuracy (80–120%) and precision (≤20%) of metals was achieved for all steps of sequential extraction. Values of detection limits (μgL^{-1}) for elements in river water were: 0.09 for Zn, 0.025 for Ni, 0.055 for Cu, 0.006 for Cr, 0.021 for As, 0.056 for Pb, and 0.029 for Cd.

DETERMINATION OF ANION CONCENTRATION IN RIVER WATER BY ION CHROMATOGRAPHY

The concentrations of anions (Cl^-, NO_3^-, SO_4^{2-} and PO_4^{3-}) were measured by ion chromatograph Metrohm 761 Compact IC, with a conductometric detector, Metrosep A Supp 1-250 column (particle size 7 µm, column dimensions 4.6 x 250 mm) and guard precolumn Metrosep A Supp 1 Guard. The used eluent was 3 mM Na_2CO_3 (Fluka, Switzerland). Every analytical run started with calibration standards in order of increasing concentration, followed by water blank and samples. Reagent blank, which followed all procedure steps as samples, was also analyzed. The check calibration standard was analyzed after every ten analyses. Detection limit values (mgL^{-1}) for anions in river water were: 0.02 for Cl, NO_3^-, SO_4^{2-} and PO_4^{3-}.

HEALTH RISK ASSESSMENT

Human health risks of PTEs via ingestion and dermal absorption of river water, which represent the main routes of exposure, were assessed for residential receptors (direct ingestion of water, dermal absorption during showering) and recreational receptors (incidental water ingestion and dermal contact with water during swimming), both adults and children. Although direct ingestion of river water is the less probable route of exposure, assessing health risks by direct ingestion in this study is justified because the river Vlasina is the source of raw water for the water supply of Vlasotince town and this assessment can offer information on requirements for drinking water treatment. To estimate human exposure to PTE through ingestion and dermal contact with river water average daily doses (ADDs) were calculated. Non-cancer health risks of individual PTE in river water for every considered exposure pathway and receptor were assessed through the calculation of hazard quotients (HQs). Non-cancer risks due to exposure to all PTE in river water for each exposure scenario were assessed by calculating the sum of HQs of individual PTE. Non-cancer risks for different

receptors caused by all routes of exposure were assessed using hazard index (HI), which is calculated as a sum of HQs. Cancer health risks (CR) for each exposure pathway and receptor were calculated for elements having cancer slope factors, which in the case of this study are Cr and As. Summation of CR of all exposure routes for each receptor yielded the total cancer risks (TCR).

To assess the human health risk of PTE in soil, ingestion, dermal contact and inhalation exposure pathways were considered. Following the health risk assessment methodology applied for river water, hazard quotients (HQs), hazard indices (HI), cancer risks (CR) and total cancer risks (TCR) were calculated.

Values of HQ and HI > 1 indicate that detrimental non-carcinogenic effects on human health could be expected.[13] If the values of CR and TCR are < 10^{-6}, there is generally no concern for increased cancer risk, values in the range 10^{-6} - 10^{-4} indicate potential risk, while values > 10^{-4} are considered unacceptably high risk.[14]

The following equations were used for the assessment of the health risk of PTEs in river water for residential (res) or recreational (rec) receptors:

$$ADDw_{ingestion\ res/rec} = \frac{C_w \times IRw_{res/rec} \times EF_{res/rec} \times ED}{BW \times AT} \quad (1)$$

$$ADDw_{dermal\ res/rec} = \frac{C_w \times SA \times K_p \times ET_{res/rec} \times EF_{res/rec} \times ED}{BW \times AT_{res/rec} \times 10^3} \quad (2)$$

$$HQw_{ingestion\ res/rec} = \frac{ADDw_{ingestion\ res/rec}}{RfD_o \times 10^3} \quad (3)$$

$$HQw_{dermal\ res/rec} = \frac{ADDw_{dermal\ res/rec}}{RfD_o \times GIABS \times 10^3} \quad (4)$$

$$HIw = HQw_{ingestion} + HQw_{dermal} \quad (5)$$

$$CRw_{ingestion\ res/rec} = \frac{ADDw_{ingestion\ res/rec} \times CSF_o}{10^3} \quad (6)$$

$$CRw_{dermal\ res/rec} = \frac{ADDw_{dermal\ res/rec} \times CSF_o}{GIABS \times 10^3} \quad (7)$$

$$TCRw = CRw_{ingestion} + CRw_{dermal} \quad (8)$$

The calculation of the human health risk of TE in soil, caused by ingestion, dermal contact and inhalation of soil, was as follows:

$$ADDs_{ing} = \mathrm{C} \times \frac{I_{ing}R \times EF \times ED}{BW \times AT} \times \mathrm{CF} \quad (9)$$

$$ADDs_{dermal} = \mathrm{C} \times \frac{AF \times SA \times ABS \times EF \times ED}{BW \times AT} \times CF \quad (10)$$

$$ADDs_{inhalation} = \mathrm{C} \times \frac{I_{inh}R \times EF \times ED}{PEF \times BW \times AT} \quad (11)$$

$$\mathrm{HQ} = \frac{ADD}{RfD} \quad (12)$$

$$\mathrm{HI} = \mathrm{NCR} = \sum HQ = \mathrm{HQ_{ing}} + \mathrm{HQ_{der}} + \mathrm{HQ_{inh}} \quad (13)$$

$$\mathrm{CR} = \mathrm{ADD} \times \mathrm{CSF} \quad (14)$$

$$\mathrm{TCR} = \mathrm{CR_{total}} = \mathrm{CR_{ing}} + \mathrm{CR_{der}} + \mathrm{CR_{inh}} \quad (15)$$

The values of exposure factors and chemical specific and toxicity associated parameters related to assessment of human exposure to PTE in river water and soil are given in TABLES S-I and S-II, and TABLES S-III and S-IV, respectively.

TABLE S-I. Exposure factors and their values used in the assessment of exposure to PTE through water ingestion and dermal contact with water for residential (res) and recreational (rec) receptors[15-20]

Parameters	Unit	Adult	Children
C_{water}: Element concentration in water	μgL^{-1}	/	/
IRw_{res}: Resident water ingestion rate	$Lday^{-1}$	2	0.64
IRw_{rec}: Recreator water ingestion rate	$Lday^{-1}$	0.11	0.12
EFw_{res}: Exposure frequency	day $year^{-1}$	350	350
EFw_{rec}: Exposure frequency	day $year^{-1}$	45	45
ED: Resident/recreator exposure duration	years	24	6
BW: Body weight	kg	70	15
AT: Averaging time	days	8760	2190
SA: Resident/recreator skin surface area	cm^2	18000	6600
ET_{res}: Resident exposure time	h day^{-1}	0.58	1
ET_{rec}: Recreator exposure time	h day^{-1}	1	1

TABLE S-II. Chemical specific and toxicity-associated parameter values for trace elements used for health risk assessment (exposure pathway - ingestion and dermal absorption of water): dermal permeability coefficient (K_p), reference dose oral (RfD_o), cancer slope factor oral (CSF_O) and gastrointestinal absorption coefficient (GIABS) [20, 21]

Element	K_p (cm h^{-1})	RfD_o (mg $kg^{-1}day^{-1}$)	CSF_O (mg $kg^{-1}day^{-1}$) $^{-1}$	GIABS (unitless)
Cr	0.002	0.003	0.5	0.025
Ni	0.0002	0.02		0.04
Cu	0.001	0.04		1
Zn	0.0006	0.3		1
As	0.001	0.0003	1.5	1

TABLE S-III. Parameters of health risk assessment for exposure to PTE in soil [17, 22-28]

Parameters	Unit	Adult	Children
Ir_{inh}: Inhalation Intake rate	$m^3 \cdot day^{-1}$	12.8	7.63
BW: Body weight	kg	70	15
AT: Averaging time	days	8760	2190
EF: Exposure frequency	day · $year^{-1}$	350	350
ED: Exposure duration	years	24	6
PEF: particle Emission factor	$m^3 \cdot kg^{-1}$	1.36E+09	1.36E+09
SL(AF): Skin Adherence Factor	mg · $cm^{-2} \cdot day^{-1}$	0.07	0.2
SA: Skin Area	$cm^2 \cdot day^{-1}$	5700	2800
ABS: Dermal absorption factor	Unitless	0.001	0.001
IngR	mg · day^{-1}	100	200
InhR	$m^3 \cdot day^{-1}$	20	7.65
CF	Unitless	0.000001	0.000001

TABLE S-IV. Reference dose (RfD) and cancer slope factor (CSF) of potentially toxic metals via the three main pathways of human exposure to soil [24, 25 28, 29]

Reference dose (RfD)			
	RfD_{ing}	RfD_{der}	RfD_{inh}
Cr	3.00E-03	6.00E-05	2.86E-05
Ni	2.00E-02	5.40E-03	2.06E-02
Cu	4.00E-02	1.20E-02	4.02E-02
Zn	3.00E-01	6.00E-02	3.00E-01
As	3.00E-04	1.23E-04	3.00E-04
Cd	1.00E-03	1.00E-05	1.00E-03
Pb	3.50E-03	5.25E-04	3.52E-03
Cancer slope factor (CSF)			
	CSF_{ing}	CSF_{der}	CSF_{inh}
Cr	5.00E-01	2.00E+01	4.20E+01
Ni	1.70E+00	4.25E+01	8.40E-01
As	1.50E+00	3.66E+00	1.51E+01
Cd	6.10E+00	6.10E+00	6.30E+00
Pb	8.50E-03	8.50E-03	4.20E-02

TABLE S-V. Pollutant limit values for surface water quality classes[30]

	Surface water quality classes according to the Regulation Off. Gaz. RS 50/2012				
	I	II	III	IV	V
	Limit values				
Fe / μg L^{-1}	200	500	1000	2000	>2000
Cr / μg L^{-1}	25 (or natur. level)	50	100	250	>250
Mn / μg L^{-1}	50	100	300	1000	>1000
Ni / μg L^{-1}	4		34		>34
Cu / μg L^{-1}	5 (H=10)[a] 22 (H=50) 40 (H=100) 112 (H=300)	5 (H=10)[a] 22 (H=50) 40 (H=100) 112 (H=300)	500	1000	>1000
Zn / μg L^{-1}	30 (H=10)[a] 200 (H=50) 300 (H=100) 500 (H=500)	300 (H=10)[a] 700 (H=50) 1000 (H=100) 2000 (H=500)	2000	5000	>5000
As / μg L^{-1}	<5 (or natur. level)	10	50	100	>100
Cd / μg L^{-1}*	0.08(H<40)[a] 0.08(H=40-50) 0.09(H=50-100) 0.15(H=100-200) 0.25 (H≥200)		0.45(H<40)[a] 0.45(H=40-50) 0.6(H=50-100) 0.9(H=100-200) 1.5(H≥200)		>0.45(H<40)[a] > 0.45(H=40-50) > 0.6(H=50-100) > 0.9(H=100-200) > 1.5(H≥200)
Pb / μg L^{-1}*	1.2		14		>14
Cl^- / mg L^{-1}	50 (or natur. level)	100	150	250	>250
NO_3^- / mgN L^{-1}	1.0-1.5	3.0	6	15	>15
PO_4^{3-} / mgP L^{-1}	0.02	0.05-0.10	0.2	0.5	>0.5
SO_4^{2-} / mg L^{-1}	50 (or natur. level)	100	200	300	>300

[a]H – water hardness / mgL^{-1} CaCO3.

TABLE S-VI. Average values of HQ and HI for PTE in the investigated rivers (residential receptors)

	Child			Adult		
	$HQ_{ingestion}$	HQ_{dermal}	HI	$HQ_{ingestion}$	HQ_{dermal}	HI
As	0.1319131	0.0013604	0.1332735	0.0883347	0.0004611	0.0887958
Cr	0.0012925	0.0010663	0.0023587	0.0008655	0.0003614	0.0012269
Zn	0.0001142	0.0000007	0.0001149	0.0000764	0.0000002	0.0000767
Ni	0.0006060	0.0000312	0.0006372	0.0004058	0.0000106	0.0004164
Cu	0.0004567	0.0000047	0.0004614	0.0003058	0.0000016	0.0003074
All elements	0.1343825	0.0024633	0.1368458	0.0899883	0.0008350	0.0908232

TABLE S-VII. Average values of HQ, and HI for PTE in the investigated rivers (recreational receptors)

	Child			Adult		
	$HQ_{ingestion}$	HQ_{dermal}	HI	$HQ_{ingestion}$	HQ_{dermal}	HI
As	0.0029150	0.0001749	0.0030899	0.0006814	0.0001022	0.0007837
Cr	0.0000286	0.0001371	0.0001657	0.0000067	0.0000801	0.0000868
Zn	0.0000025	0.0000001	0.0000026	0.0000006	0.0000001	0.0000006
Ni	0.0000134	0.0000040	0.0000174	0.0000031	0.0000023	0.0000055
Cu	0.0000101	0.0000006	0.0000107	0.0000024	0.0000004	0.0000027
All elements	0.0029696	0.0003167	0.0032863	0.0006942	0.0001851	0.0008793

TABLE S-VIII. Average hazard quotients (HQ) for non-carcinogenic risk in adults and children due to exposure (inhalation, dermal, and ingestion) of various PTEs in studied soils

	Adults			Children		
	HQing	HQder	HQinh	HQing	HQder	HQinh
As	0.046763	0.00045508	6.88E-06	0.4364558	0.011601	1.23E-05
Cd	0.000606	0.00024199	8.92E-08	0.0056606	0.006053	1.59E-07
Ni	0.001173	1.7333E-05	1.67E-07	0.0109470	0.000442	2.99E-07
Pb	0.006846	0.00018212	1.67E-07	0.0639005	0.004560	1.79E-06
Cr	0.008042	0.00160448	1.24E-04	0.0750633	0.041359	2.21E-04
Cu	0.008042	0.00160448	1.24 E-05	0.0065923	0.000209	1.84E-07
Zn	0.008042	0.00160448	1.24 E-05	0.0005378	0.000134	7.06E-07

TABLE S-IX. Average hazard index values (HI) and the total cancer risk (TCR) through PTE consumption in the studied soils.

PTE	HI		TCR	
	Adults	Children	Adults	Children
As	0.0472	0.4481	2.13E-05	2.02E-04
Cd	0.0008	0.0117	3.71E-06	3.49E-05
Ni	0.0012	0.0114	4.39E-05	4.74E-04
Pb	0.0070	0.0685	2.05E-07	1.92E-06
Cr	0.0098	0.1166	1.41E-05	1.62E-04
Cu	0.0007	0.0068	-	-
Zn	0.0003	0.0007	-	-

TABLE S-X. Mean values of carcinogenic human health risk (CR) for adults and children via inhalation, dermal, and ingestion

	Adults			Children		
	CRing	CRder	CRinh	CRing	CRder	CRinh
As	2.10E-05	2.05E-07	3.12E-08	1.96E-04	5.22E-06	5.56E-08
Cd	3.70E-06	1.48E-08	5.62E-10	3.45E-05	3.69E-07	1.00E-09
Ni	3.99E-05	3.98E-06	2.90E-09	3.72E-04	1.01E-04	5.17E-09
Pb	2.04E-07	8.13E-10	1.48E-10	1.90E-06	2.03E-08	2.64E-10
Cr	1.21E-05	1.93E-06	1.49E-07	1.13E-04	4.96E-05	2.66E-07

REFERENCES

1. M. Savić, Regional-geographical overview of Vlasina and Krajina [Master Thesis], University of Niš Niš, Serbia. 2019.
2. J. Čvoro, P. Golubović, Geography of Yugoslavia, University of Niš, Faculty of Science, Niš, Serbia, 2001.
3. U. Durlević, A. Momčilović, V. Ćurić, M. Dragojevic, Bull. Serbian. Geograph. Soc. 99 (2019) 17 https://doi.org/10.2298/GSGD2101049D
4. B. Batsaikhan, J-S. Kwon, K-H. Kim,Y-J. Lee, J-H. Lee, M. Badarch, S-T. Yun,. Environ. Sci. Pollut. Res **24** (2017) 2019 https://doi.org/10.1007/s11356-016-7895-3
5. P. Piroozfar, S. Alipour, S. Modabberi, D. Cohen. Environ. Monit. Assess. **193**, (2021) 564 https://doi.org/10.1007/s10661-021-09363-w
6. N. T. Thuong, M. Yoneda, M. Ikegami, M. Takakura, Environ. Monit. Assess. **185**, (2013) 8065 https://doi.org/10.1007/s10661-013-3155-x
7. S. Sakan, I. Gržetić, D. Đorđević, Environ. Sci. Pollut. Res. Int. 14 (2007) 229 https://doi.org/10.1065/espr2006.05.304
8. P. Patel, N. J. Raju, B. C. S. R. Reddy, U. Suresh, D. B. Sankar, T. V. K. Reddy, Environ. Geochem. Health 40 (2018) 609 https://doi.org/10.1007/s10653 017-0006-7
9. D. Đorđević, S. Sakan, S. Trifunović, S. Škrivanj, D. Finger, Water 13, (2021) 1928 https://doi.org/10.3390/w13141928
10. M. B. Arain, T. G. Kazi, M. K. Jamali N. Jalbani, H. I. Afridi, J. A. Baig, J. Hazard. Mater. 154 (2008) 998 https://doi.org/10.1016/j.jhazmat.2007.11.004
11. M. K. Jamali, T. G. Kazi, M. B, Arain, H. I. Afridi, N. Jalbani, G. A. Kandhro, et al. Procedure. J. Hazard. Mater. 163 (2009) 1157 https://doi.org/10.1016/j.jhazmat.2008.07.071
12. S. Sakan, A. Popović, I. Anđelković, D. Đorđević, Environ. Geochem. Health 38 (2016) 855 https://doi.org/10.1007/s10653-015-9766-0
13. USEPA, Risk assessment guidance for Superfund. Volume I: Human health evaluation manual (Part A), Interim Final, EPA/540/1-89/002, Office of Emergency and Remedial Response, U.S. Environmental Protection Agency, Washington, DC, 1989
14. USEPA, Residual Risk Report to Congress, EPA-453 R-99-001, U.S. Environmental Protection Agency, Washington, DC, 1999
15. C. Tokatli, Environ. Earth Sci. 80 (2021) 1 https://doi.org/10.1007/s12665-021-09467-z
16. J. Wang, G. Liu, H. Liu, P. K. Lam, Sci. Total Environ. 583 (2017) 421 https://doi.org/10.1016/j.scitotenv.2017.01.088
17. USEPA, Exposure Factors Handbook 2011 Edition (Final Report), EPA/600/R-09/052F, U.S. Environmental Protection Agency, Washington, DC, 2011

18. USEPA, Human health evaluation manual, Supplemental Guidance, Standard default exposure factors. OSWER Directive 9285.6-03, Office of Emergency and Remedial Response, U.S. Environmental Protection Agency, Washington, DC, 1991
19. V. Antunović, D. Blagojević, R. Baošić, D. Relić, A. Lolić, Environ. Monit. Assess. 195 (2023) 596 https://doi.org/10.1007/s10661-023-11232-7
20. USEPA, Risk Assessment Guidance for Superfund Volume I: Human Health Evaluation Manual (Part E, Supplemental Guidance for Dermal Risk Assessment) Final, OSWER 9285.7-02EP, Office of Emergency and Remedial Response, U.S. Environmental Protection Agency, Washington, DC, 2004.
21. USEPA, Regional Screening Level (RSL) Summary Table (TR=1E-06 THQ=1.0). https://semspub.epa.gov/work/HQ/404463.pdf, (Accessed 12 October 2024)
22. USEPA, Risk Assessment Guidance for Superfund: Volume I – Human health Evaluation manual (Part B, development of Risk-based Preliminary Remediation Goals), EPA/540/R-92/003, U.S. Environmental Protection Agency, Washington, DC, 1991
23. USEPA, Supplemental guidance for developing soil screening levels for superfund sites, Office of Emergency and Remedial Response, U.S. Environmental Protection Agency, Washington, DC, 2002
24. USEPA, Integrated Risk Information System of the US Environmental Protection Agency, 2012
25. E. De Miguel, I., Iribarren, E. Chacon, A. Ordonez, S. Charlesworth, Chemosphere 66 (2007) 505 https://doi.org/10.1016/j.chemosphere.2006.05.065
26. Z. Li, Z. Ma, T.J. van der Kuijp, Z. Yuan, L. Huang, Sci. Tot. Environ. 468 (2014) 843 https://doi.org/10.1016/j.scitotenv.2013.08.090
27. F. Khelifi, A. G. Caporale, Y. Hamed, P. Adamo, J Environ. Manage. 279 (2021)111634 https://doi.org/10.1016/j.jenvman.2020.111634
28. B. Boumaza, R. Kechiched, T. Vladimirovna Chekushina, N. Benabdeslam, K. Senouci, A. Hamitouche, F. Ait Merzeg, W. Rezgui, N.Y. Rebouh, K. Harizi, J Hazard.Mater. 465 (2024) 133110 https://doi.org/10.1016/j.jhazmat.2023.133110
29. USEPA, Supplemental Guidance for Developing Soil Screening Levels for Superfund Sites, US Environmental Protection Agency, Washington, DC, USA, 2001
30. Regulation on limit values for pollutants in surface and ground waters and sediments and deadlines for their achievement, Off Gaz. Rep. Serbia, 50 (2012) (https://pravno-informacioni-sistem.rs/eli/rep/sgrs/vlada/uredba/2012/50/1).

Journal of the Serbian Chemical Society
JSCS-info@shd.org.rs • www.shd.org.rs/JSCS
J. Serb. Chem. Soc. *89* (12) 1619–1628 (2024)
JSCS–5810
Original scientific paper
Published 18 December, 2024

Adsorption analysis of PFOA on activated carbon and ion-exchange resin: A comparative study using four isotherm models

KRISTINA B. KASALICA[1#*], NATALIJA PETRONIJEVIĆ[2], JELENA RADULOVIĆ[3], LATINKA SLAVKOVIĆ BEŠKOSKI[3], MARIJA B. LJEŠEVIĆ[1#], BOJANA MARKOVIĆ[1] and VLADIMIR P. BEŠKOSKI[2#**]

[1]*University of Belgrade – Institute of Chemistry, Technology and Metallurgy, National Institute of the Republic of Serbia, Njegoševa 12, Belgrade, Serbia,* [2]*University of Belgrade – Faculty of Chemistry, Studentski trg 12–16, Belgrade, Serbia and* [3]*Anahem LTD, Belgrade, Serbia*

(Received 20 November, revised 26 November, accepted 1 December 2024)

Abstract: Per- and polyfluoroalkyl substances (PFAS), known as "forever chemicals", are highly persistent environmental pollutants due to their strong carbon–fluorine bonds. Widely used across industries and consumer products, PFAS have accumulated in the environment, raising concerns about their bioaccumulation, toxicity and mobility. Adsorption, particularly using activated carbon and ion exchange resins, is a suitable technique for PFAS removal from contaminated water. This study evaluates the sorption efficiency of granular and powdered activated carbon and two ion exchange resins to identify the most effective materials for remediation. All tested sorbents showed great performance, however Amberlite IRA 402, and powdered activated carbon K/B were the most efficient. Based on the isotherm models used, it is suggested that physisorption is a dominant process, where the multilayer adsorption on a heterogeneous surface is being favoured.

Keywords: immobilization; PFAS; water remediation.

INTRODUCTION

Per- and polyfluoroalkyl substances (PFAS), often known as "forever chemicals", are a group of manmade compounds currently under intense scrutiny. PFAS comprise thousands of individual chemicals, valued for their unique commercial properties, such as heat resistance and water- and grease-repellent qualities.[1] In the last several decades, PFAS are widely used across industries, inc-

* Corresponding authors. E-mail: (*)kristina.kasalica@ihtm.bg.ac.rs; (**)vbeskoski@chem.bg.ac.rs
# Serbian Chemical Society member.
https://doi.org/10.2298/JSC241120097K

luding construction, electronics, oil and gas, mining, semiconductors, recycling and transportation. They are also integral to producing ceramics, nanostructures, explosives, firefighting foams, medical devices, plastics, rubbers and refrigerants. In daily life, PFAS are present in adhesives, cleaning products, coatings, paints, cosmetics, personal care items, food packaging, pesticides, fertilizers and textiles. Their extensive use underscores their essential role in modern society, necessitating closer investigation of their production and environmental impact.[2] However, despite the highly valuable and important properties that have led to the widespread use of these compounds, one characteristic stands out in particular – their persistence in the environment. Namely, due to the strength of their carbon-fluorine bonds, all PFAS exhibit environmental persistence, with many being bioaccumulative, highly mobile and toxic. Their widespread use has led to their presence across various environmental compartments, complicating efforts to manage them.[3] Significant efforts are being made to regulate the use of PFAS compounds in industry,[4] but at the same time it is essential to focus on the environment where these compounds have already accumulated.

One of the most studied methods for PFAS removal from water is adsorption. Adsorption involves the physical or chemical interaction between a solid surface (adsorbent) and a solute (adsorbate), where the adsorbate in this context is a pollutant in an aqueous solution. This technique enables the efficient treatment of large volumes of water in a straightforward and compact manner, with manageable costs.[5] Adsorption of PFAS could be performed using carbon-based materials (activated carbon, carbon nanotubes), ionic surfactants, anion exchange resins, composite materials but the overall efficacy depends on PFAS that are present in the environment, matrix characteristics as well as the properties of material used.[6,7] Sorbents bind PFAS mainly through hydrophobic and electrostatic interactions, and their effectiveness often depends on surface area and porosity.[8,9] In addition to adsorption, ion exchange process using ion exchange resins (IER) has received a lot of attention in the past couple of years.[8] The immobilization of PFAS onto a sorbent has proven to be very efficient and easy to apply, however this method does not destroy PFAS, opening the question of safe disposal or possible reuse of the sorbent after the sorption process. However, given the very low concentrations of PFAS in the environment, the immobilization could serve as an effective preliminary step for other remediation technologies that are unsuitable for addressing low-level contamination in terms of their associated remediation costs.[10]. Hence the aim of this study was to evaluate the sorption efficiency of granular and powdered activated carbon, along with two ion exchange resins, to identify the most effective sorbent for future research on treating contaminated materials. Additionally, sorption behaviour of the sorbents that were most efficient in adsorbing of PFOA used as PFAS model compound was investigated. Removing PFAS from water not only reduces their mobility

and bioavailability but also promotes the desorption of PFAS from sediments, facilitating sediment purification and contributing to a comprehensive remediation strategy for contaminated environments.

EXPERIMENTAL

Chemicals

Perfluorooctanoic acid (PFOA) was purchased from Sigma–Aldrich, Cat. No. 171468. Two types of activated carbon obtained from Trayal Corporation, Serbia, were used, granular activated carbon (KRF), as activated carbon in grain with particle size 0.25–1.0 mm, produced from carbonized coconut shell, activated by the water steam in static furnace, and powdered activated carbon (K/B powder), screen size of 0.080 mm at max. 70 %, produced from the same material and activated by the water steam in static furnace. Ion exchange resins: Amberlite® IRA402 chloride form, product number: 06466, batch number: bccg5078, brand: SIAL, CAS number: 52439-77-7, particle size: 600–750 μm, was purchased from Supelco and Amberlite® IRA67 free base – gel form, 16–50 mesh (wet), product number: A9960, batch number: SLCB3374, brand: SIGMA, CAS number: 65899-87-8, MDL number: MFCD00145567, was purchased from Sigma–Aldrich. Native perfluorooctanoic acid standard and labelled standard of perfluoro-*n*-(^{13}C8) octanoic acid, M8PFOA were purchased from Wellington Laboratories Inc.

Study design

A batch test to assess the adsorption of PFOA was performed by weighing 50 mg each of Amberlite IRA 402, Amberlite IRA 67 ionic exchange resin (activated overnight in distilled water) KRF and K/B powder into 50 mL vials and 25 mL of 100 mg/L PFOA. The experiment was conducted at the rotary shaker with 200 rpm during 24 h, after which an aliquot of 5 mL was filtered through 0.22 μm PP syringe filter and stored at 4 °C until analysis where the remaining concentration of PFOA was determined.

Additional batch tests were set up similarly to determine the behaviour of most efficient sorbents on different temperatures and with varying concentration of PFOA (5–35 ppm). The experiment was conducted at two temperatures, 4 and 28 °C, at the rotary shaker with 200 rpm during 24 h, after which an aliquot of 5 mL was filtered through 0.22 μm PP syringe filter and stored at 4 °C until analysis.

Isotherm models

The collected equilibrium data were analyzed using Langmuir, Freundlich, Temkin and Dubinin–Radushkevich isotherm models to identify the mechanisms that control the PFOA adsorption process.[11] The Langmuir adsorption isotherm model treats the adsorption process as a chemical phenomenon, assuming that adsorption occurs on a homogeneous surface of the adsorbent and is limited to the formation of a monolayer. On the other hand, the Freundlich isotherm model describes multilayer adsorption on a heterogeneous adsorbent surface. The Temkin isotherm assumes that the heat of adsorption for all molecules on the adsorbent surface decreases linearly with coverage due to adsorbate–adsorbent interactions. This model is characterized by multilayer adsorption with a uniform distribution of binding energies. The Dubinin–Radushkevich model can describe adsorption on heterogeneous surfaces and provides valuable insights into the energy distribution and nature of the adsorption process. The OriginPro 2021 Software was used for the isotherms' linear regression analyses. Two error functions, the coefficient of determination (R^2) and chi-square (χ^2) test, were used to ensure

accurate and consistent estimations for fitting the experimental data to the investigated isothermal models.[12]

Liquid chromatography coupled to tandem mass spectrometry

Quantitative analysis of PFOA was performed using a Thermo Scientific Accela high performance liquid chromatograph (HPLC) with a triple quadrupole mass analyser TSQ Quantum Access MAX (Thermo Fisher Scientific, USA). The column used was a Waters Acquity UPLC BEH Shield RP18 Column, (130 Å, 1.7 μm, 2.1 mm×100 mm, Waters, USA) equipped with security guard ultra holder for UHPLC Columns (2.1 to 4.6 mm, Phenomenex, USA) with SecurityGuard ULTRA cartridges for EVO-C18 and elution was performed using a mobile phase consisting of ultrapure water, 0.1 % HCOOH, 5 mM $HCOONH_4$ (solution A) and MeOH, 0.1 % HCOOH, 5 mM $HCOONH_4$ (solution B) as follows: 0 min: 72 % A, 28 % B; 4.5 min: 15 % A, 85 % B; 4.6 min: 1 % A, 99 % B; 10 min: 1 % A, 99 % B; 12 min: 72 % A, 28 % B. The column flow was 250 μL/min and column temperature 40 °C. The ionization was performed in H-ESI mode. The mass spectrometer operated in negative ionization mode. M8PFOA was used as an injection standard. Parameters of MS/MS analysis are given in the Table I. Prior to injection, the samples were filtered through 0.22 μm PP syringe filters, previously rinsed with methanol. Data analyses were performed using Thermo Xcalibur 3.0.63, 2014 software (Thermo Fisher Scientific, USA).

TABLE I. MS/MS parameters for PFOA analysis

Parameter	PFOA	M8PFOA
Standard type	Native standard	Injection standard
Retention time, min	4.21	4.21
Parent ion (*m*/*z*)	413	421
Quantification ion (*m*/*z*)	369	376
Confirmation ion (*m*/*z*)	169	172
Cone voltage, eV	10	10
Collision energy Q1, eV	17	18
Collision energy Q2, eV	10	10
Scan time, s	0.05	0.05
Scan width (*m*/*z*)	0.2	0.2

RESULTS AND DISCUSSION

Batch test for assessing the adsorption efficacy of four different sorbents was investigated, and the results are shown in the Table II. The PFOA concentrations remaining after the incubation period adsorption onto activated carbons are extremely low, with the adsorption efficiency reaching over 95 % for all tested activated carbons. Ion exchange resins were also very effective in the PFOA adsorption, with over 90 % adsorption with IRA 67 and 99 % with IRA 402.

Since the best adsorption results were obtained using IRA 402 and K/B powder, these two sorbents were investigated in more detail. Four commonly used isotherm models, Langmuir, Freundlich, Temkin and Dubinin–Radushkevich, were applied to analyse and discusse experimentally obtained data. The values of the calculated isotherm parameters and the corresponding error functions for PFOA on K/B and IRA 402 are given in Tables III and IV, respectively.

TABLE II. Results of the batch adsorption test using different sorbents

Sorbent	PFOA concentration, mg/L	Adsorption of PFOA, %
KRF	4.65	95.35
K/B powder	1.05	98.95
IRA 67	9.02	90.98
IRA 402	0.34	99.66

TABLE III. Parameters of the Langmuir, Freundlich, Temkin and Dubinin–Radushkevich isotherm models of PFOA adsorption on K/B

Isotherm	Parameter	Value	
Langmuir	t / °C	28	4
	$q_{m,L}$ / mg g^{-1}	12.75	11.74
	K_L / L mg^{-1}	5.98	16.71
	R_L	1.10×10^{-2}	3.99×10^{-3}
	R^2	0.827	0.685
	χ^2	1.107	2.150
	$q_{m,L}$ / mg g^{-1}	12.75	11.74
Freundlich	K_F / dm^3 g^{-1}	9.34	10.46
	n	2.95	3.51
	R^2	0.949	0.922
	χ^2	0.527	0.703
	K_T / dm^3 g^{-1}	56,61	162.10
	b_T / kJ mol^{-1}	0.96	1.03
Temkin	R^2	0.969	0.937
	χ^2	0.268	0.540
Dubinin–Radushkevich	$q_{m,DR}$ / mg g^{-1}	12.43	12.37
	K_{DR} / mol^2 J^{-2}	2.58×10^{-8}	1.81×10^{-8}
	E / kJ mol^{-1}	4.40	5.26
	R^2	0.811	0.775
	χ^2	1.312	1.585
	C3a	D3	30

As can be seen from Fig. 1, the Langmuir adsorption isotherms for K/B and IRA 402 showed good agreement with experimental data at low initial concentration values (5–20 ppm). At higher initial concentrations of PFOA, the experimental data show a deviation from the Langmuir model, which indicates that the adsorption process continues even after the formation of a monolayer on the active sites. The Langmuir constant (K_L) is a measure of the adsorption energy. Lower K_L values for IRA 402 adsorbent (0.02 L/mg for 28 °C and 3.73×10^{-3} L/mg for 4 °C) indicate that physisorption is more dominant than chemisorption during PFOA adsorption. The value of the dimensionless separation factor (R_L), indicates the adsorption nature as favourable ($0 < R_L < 1$), linear ($R_L = 1$) or irreversible ($R_L = 0$). R_L values for K/B and IRA 402 range from 3.99×10^{-3} to 0.93 indicating that adsorption is favoured.

TABLE IV. Parameters of the Langmuir, Freundlich, Temkin and Dubinin-Radushkevich isotherm models of PFOA adsorption on IRA 402

Isotherm	Parameter	Value	
Langmuir	t / °C	28	4
	$q_{m,L}$ / mg g^{-1}	51.28	123.45
	K_L / L mg^{-1}	0.02	3.73×10^{-3}
	R_L	0.71	0.93
	R^2	0.859	0.767
	χ^2	1.509	1.389
	$q_{m,L}$ / mg g^{-1}	51.28	123.45
Freundlich	K_F / dm^3 g^{-1}	1.41	0.61
	n	1.30	1.17
	R^2	0.862	0.775
	χ^2	1.236	1.252
	K_T / dm^3 g^{-1}	0.81	0.48
	b_T / kJ mol^{-1}	0.62	0.73
Temkin	R^2	0.871	0.808
	χ^2	0.828	0.760
Dubinin–Radushkevich	$q_{m,DR}$ / mg g^{-1}	9.39	6.58
	K_{DR} / mol^2 J^{-2}	1.77×10^{-6}	4.34×10^{-6}
	E / kJ mol^{-1}	0.53	0.34
	R^2	0.818	0.743
	χ^2	0.935	0.962
	C3a	9.39	6.58

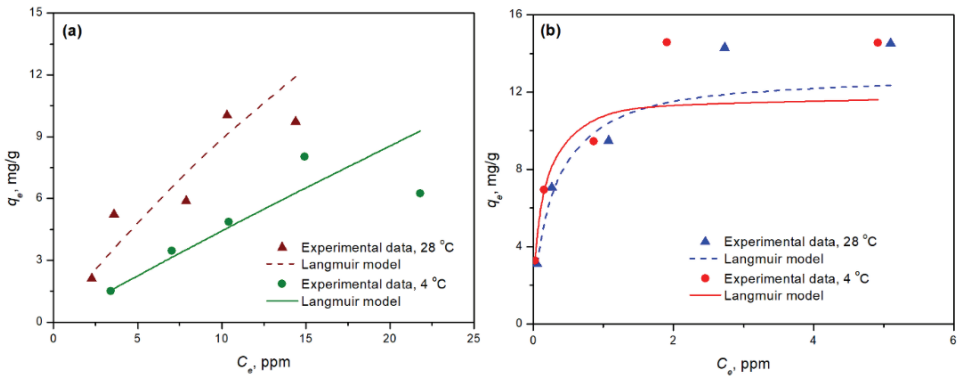

Fig. 1. Langmuir adsorption isotherms for: a) IRA 402 and b) K/B at 28 and 4 °C (conditions: C_o, 5– 35 ppm, m_{ads} = 50 mg, V = 25 ml, τ = 24 h).

The low values of the coefficient of determination and high values of the chi-square test for the Langmuir isotherm model mean that the applied isotherm could not be used to predict the PFOA adsorption process on both adsorbents. Therefore, linear fitting of the Freundlich adsorption isotherm model was applied to the experimental data. The results are shown in Fig. 2.

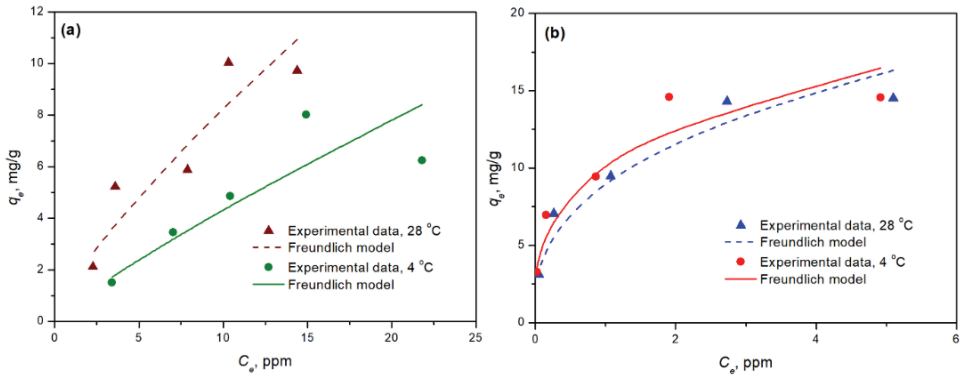

Fig. 2. Freundlich adsorption isotherms for: a) IRA 402 and b) K/B at 28 and 4 °C (conditions: C_o, 5–35 ppm, m_{ads} = 50 mg, V = 25 ml, τ = 24 h).

Based on the R^2 and χ^2 values for the Freundlich adsorption isotherm, the adsorption isotherms show a slightly better agreement with the experimental results compared to the Langmuir model on both materials and at both tested temperatures, which indicates that the adsorption takes place on a heterogeneous surface through multilayer adsorption. The Freundlich constant (K_F) indicates the adsorption strength. Based on the obtained results for K_F values, it can be concluded that a higher adsorption capacity is achieved with K/B adsorbent than with IRA 402, which is in accordance with the experimentally obtained data. Likewise, based on the $1/n$ value, which is in the range of 0.28 to 0.85, it can be concluded that the analysed adsorption processes on K/B and IRA 402 adsorbent are favoured.[11] The heterogeneous nature of adsorption increases with decreasing temperature because the value of $1/n$ is lower at lower temperatures, as can be seen from Tables III and IV.

Further, the experimental data were also analysed by the Temkin adsorption isotherm model. Graphic representations of experimental results fitted with a linearized form of the Temkin isotherm model for PFOA adsorption on K/B and IRA 402 are shown in Fig. 3. Based on the obtained results shown in Tables III and IV for R^2 and χ^2, it can be concluded that the mentioned model best describes the adsorption processes at both investigated temperatures for K/B and IRA 402 adsorbents. The b_T values are greater than 0, which indicates exothermmic adsorption processes. The higher K_T values for the K/B adsorbent at both investigated temperatures suggest a greater adsorption capacity for PFOA compared to that of IRA 402.

The Dubinin–Radushkevich adsorption isotherm model was used to determine the type of adsorbate–adsorbent interaction during the adsorption process. Fig. 4 shows the fitting curves of linear regression for PFOA adsorption onto IRA 402 and K/B adsorbents. The values of the Dubinin–Radushkevich constant

(K_{DR}) for K/B adsorbent were 2.58×10^{-8} and 1.81×10^{-8} mol^2/J^2, while for IRA 402 amounted to 1.77×10^{-6} and 4.34×10^{-6} mol^2/J^2 at 28 and 4 °C, respectively. Based on the obtained K_{DR} values, the energies of the adsorption processes (E) were determined. The values of E for the PFOA adsorption on K/B and IRA 402 adsorbents range from 0.34 to 5.26 kJ/mol, which corresponds to physisorption ($E < 8$ kJ/mol).[13]

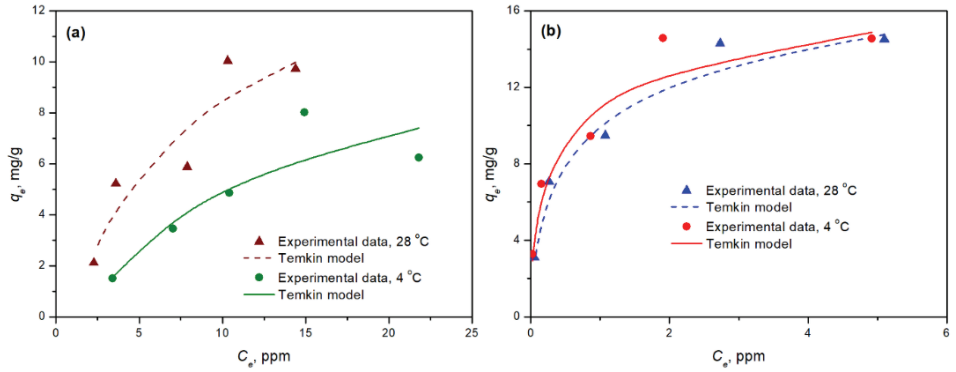

Fig. 3. Temkin adsorption isotherms for: a) IRA 402 and b) K/B at 28 and 4 °C (conditions: C_o, 5–35 ppm, m_{ads} = 50 mg, V = 25 ml, τ = 24 h).

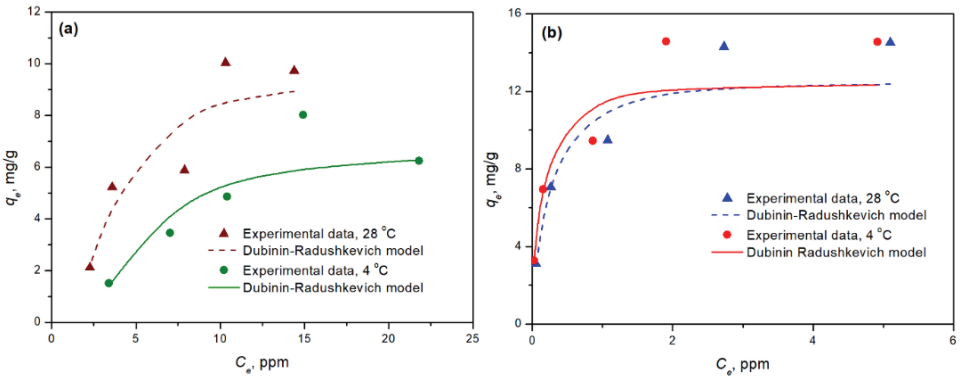

Fig. 4. Dubinin–Radushkevich adsorption isotherms for: a) IRA 402 and b) K/B at 28 and 4 °C (conditions: C_o, 5–35 ppm, m_{ads} = 50 mg, V = 25 ml, τ = 24 h).

CONCLUSION

This study applied four well-known two-parameter isotherm models to better understand the PFOA adsorption mechanism onto K/B and IRA 402 adsorbents. The Langmuir isotherm model showed compatibility with experimental data at low PFOA concentrations, supporting monolayer adsorption on a homogeneous surface. However, deviations at higher concentrations, indicated by low R^2 values and high chi-square values, suggest multilayer adsorption or interactions

beyond a single monolayer. The Freundlich model provided a slightly better fit, suggesting multilayer adsorption on a heterogeneous surface, as supported by the Freundlich constant (K_F) and $1/n$ values (0.28–0.85), which indicate favourable adsorption, especially at lower temperatures. This temperature dependence further highlights the heterogeneous nature of the adsorption sites. The Temkin model best described the adsorption processes for both adsorbents at all temperatures, indicating exothermic and multilayer adsorption, as reflected in the positive b_T values. The higher K_T values for the K/B adsorbent indicate a greater adsorption capacity for PFOA compared to that of IRA 402. Lastly, the Dubinin–Radushkevich model helped confirm that the adsorption process primarily involves physisorption, as the energy values (E) were consistently below 8 kJ/mol. In conclusion, PFOA adsorption on K/B and IRA 402 follows a predominantly physisorption process, with multilayer adsorption on a heterogeneous surface being favoured, particularly for K/B. This understanding of adsorption mechanisms and affinities across isotherm models can form more effective adsorbent selection and optimization for PFOA removal in future applications.

Acknowledgements. This research was supported by Project "VISION" funded by the company Solvay Specialty Polymers Italy S.p.A. The activated carbons were obtained from the Trayal Corporation, Serbia.

ИЗВОД

АНАЛИЗА АДСОРПЦИЈЕ PFOA НА АКТИВНОМ УГЉЕНИКУ И ЈОНОИЗМЕЊИВАЧКИМ СМОЛАМА: УПОРЕДНА СТУДИЈА НА ОСНОВУ ЧЕТИРИ МОДЕЛА ИЗОТЕРМИ

КРИСТИНА Б. КАСАЛИЦА[1], НАТАЛИЈА ПЕТРОНИЈЕВИЋ[2], ЈЕЛЕНА РАДУЛОВИЋ[3], ЛАТИНКА СЛАВКОВИЋ БЕШКОСКИ[3], МАРИЈА Б. ЉЕШЕВИЋ[1], БОЈАНА МАРКОВИЋ[1] и ВЛАДИМИР П. БЕШКОСКИ[2]

[1]Универзитет у Београду – Институт за хемију, технологију и металургију, Институт од националног значаја за Републику Србију, Његошева 12, Београд, [2]Универзитет у Београду – Хемијски факултет, Студентски трг 12–16, Београд и [3]Анахем доо, Београд

Пер- и полифлуороалкилна једињења (PFAS), позната као „вечне хемикалије", представљају дуготрајне загађујуће супстанце услед присуства јаких угљеник–флуор веза. Ова једињења су нашла широку употребу у индустрији и роби широке потрошње те су тако ослобођена и у животну средину, што је довело до забринутости због њихове биоакумулације, токсичности и мобилности. Адсорпција, посебно коришћењем активног угља и јоноизмењивачких смола, представља погодну технику за уклањање PFAS из контаминиране воде. У овој студији процењена је ефикасност сорпције гранулисаног и прашкастог активног угља, као и две јоноизмењивачке смоле, како би се идентификовали најефикаснији материјали за ремедијацију. Сви тестирани сорбенти показали су одличне резултате, али су Amberlite IRA 402 и прашкасти активни угаљ K/B били најефикаснији. На основу примењених изотермских модела, закључак је да је физисорпција доминантан процес, при чему је фаворизована мултислојна адсорпција на хетерогеној површини.

(Примљено 20. новембра, ревидирано 26. новембра, прихваћено 1. децембра 2024)

REFERENCES

1. Z. Wang, A. M. Buser, I. T. Cousins, S. Demattio, W. Drost, O. Johansson, K. Ohno, G. Patlewicz, A. M. Richard G. W. Walker, G. S. White, E. Leinala, *Environ. Sci. Technol*. **55** (2021) 15575 (https://doi.org/10.1021/acs.est.1c06896)
2. L. G. T. Gaines, *Am. J. Ind. Med*. **66** (2023) 353 (https://doi.org/10.1002/ajim.23362)
3. I. J. Neuwald, D. Hübner, H. L. Wiegand, V. Valkov, U. Borchers, K. Nödler, M. Scheurer, S. E. Hale, H. P. H. Arp, D. Zahn, *Environ*. *Sci. Technol.* **56** (2022) 6380 (https://doi.org/10.1021/acs.est.1c07949)
4. ECHA, https://echa.europa.eu/hot-topics/perfluoroalkyl-chemicals-pfas (accssed 15.11.2024)
5. I. Ali, M. Asim, T.A. Khan, *J. Environ. Manage*. **113** (2012) 170 (https://doi.org/10.1016/j.jenvman.2012.08.028)
6. N. Bolan, B. Sarkar, Y. Yan, Q. Li, H. Wijesekara, K. Kannan, D.C.W. Tsang, M. Schauerte, J. Bosch, H. Noll, Y. S. Ok, K. Scheckel, J. Kumpiene, K. Gobindlal, M. Kah, J. Sperry, M. B. Kirkham, H. Wang, Y. F. Tsang, D. Hou, J. Rinklebe, *J. Hazard. Mater*. **401** (2021) 123892 (https://doi.org/10.1016/j.jhazmat.2020.123892)
7. R. Mahinroosta, L. Senevirathna, *J. Environ. Manage*. **255** (2020) 109896 (https://doi.org/10.1016/j.jenvman.2019.109896)
8. F. Dixit, R. Dutta, B. Barbeau, P. Berube, M. Mohseni, *Chemosphere* **272** (2021) 129777 (https://doi.org/10.1016/j.chemosphere.2021.129777)
9. E. Barth, J. McKernan, D. Bless, K. Dasu, *J. Environ. Manage*. **296** (2021) 113069 (https://doi.org/10.1016/j.jenvman.2021.113069)
10. V. Beškoski, M. Ljević, B. Jiménez, J. Muñoz-Arnanz, P. Colomer-Vidal, H. Inui, T. Nakano, in *Soil Remediation Science and Technology. The Handbook of Environmental Chemistry*, Vol 130, J. J. Ortega-Calvo, F. Coulon, Eds., Springer Nature, Cham, 2024, p.332 (https://doi.org/10.1007/698_2023_1070)
11. E. E. Jasper, V. O. Ajibola, J.C. Onwuka, *Appl. Water. Sci.* **10** (2020) 132 (https://doi.org/10.1007/s13201-020-01218-y)
12. A. Nastasović, B. Marković, Lj. Suručić, A. Onjia, *Metals* **12** (2022) 814 (https://doi.org/10.3390/met12050814)
13. M. Shafiq, A. A. Alazba, M. T. Amin, *Sustainability* **13** (2021) 3785 (https://doi.org/10.3390/su13073785).

Journal of the Serbian Chemical Society
JSCS-info@shd.org.rs • www.shd.org.rs/JSCS
J. Serb. Chem. Soc. *89* (12) 1629–1645 (2024)
JSCS–5811
Original scientific paper
Published 11 November, 2024

Assessment of the concentration of toxic metals (aluminum, cadmium and manganese) in the soil and evergreen plant species at the Sastavci surface mine and its vicinity

MILICA TOMOVIĆ[1]*, JOVANA GRAHOVAC[2], JELENA DODIĆ[2], MARIJA RADOJKOVIĆ[2#], NATAŠA ELEZOVIĆ[1] and KRSTIMIR PANTIĆ[1]

[1]*University of Priština in Kosovska Mitrovica, Faculty of Technical Sciences, Knjaza Miloša 7, 38220 Kosovska Mitrovica and* [2]*Faculty of Technology Novi Sad, University of Novi Sad, Bulevar cara Lazara 1, 21000 Novi Sad, Serbia*

(Received 1 April, revised 30 April, accepted 18 June 2024)

Abstract: The study aims to determine the concentration of Al^{3+}, Cd^{2+} and Mn^{2+} in the soil and parts of evergreen plant species – juniper and white pine – at the surface mine Sastavci (Badanj) and its vicinity in order to determine the possibility of using evergreen plants as an ecological indicator or for phytoremediation. Globally, as a result of various anthropogenic activities such as traffic, agricultural activities, waste incineration, industrial production, mining, *etc*., it represents a serious problem leading to pollution with toxic and potentially toxic metal cations. One of the more innovative techniques used for the remediation of mining areas is phytoremediation. By applying phytoremediation, certain plant species in polluted areas have the ability to act as accumulators or hyperaccumulators, absorbing toxic metals from the soil through the plant roots and transporting them to the upper parts. This research has been conducted to determine the concentration of Al^{3+}, Cd^{2+} and Mn^{2+} at the surface mine itself and its surroundings, as well as to monitor the distribution of metal cations in the system of roots, branches, needles, and fruits of the evergreen plant species – white pine and juniper. The results showed that the sampled soil was contaminated with Cd in zones I and II for both plant species, since the concentrations exceeded the limit values, while the concentration of Cd in zone III, as well as in the control zone was below the determination limits for both plant species. The concentration of Mn in the soil from the white pine and juniper zone was above the world average in all three zones, as well as in the control zone itself. The soil was most enriched with the analysed elements in the surface mine of zonec I and II. According to the analysis of elements in the parts of white pine, roots, branches, needles and fruits, the highest concentration of Al was detected in the root in zone I, while the lowest concentration was recorded in the fruit

* Corresponding author. E-mail: milica.tomovic@pr.ac.rs
# Serbian Chemical Society member.
https://doi.org/10.2298/JSC240401063T

(cones) in the control zone, an increased concentration of Cd was recorded in the branches in zones I and II, and the highest concentration of Mn was recorded in needles in zone II. The highest Al concentration was recorded in the juniper root in zone I and the lowest in the juniper fruit in the control zone, the Cd concentration was the highest in the juniper root zone I, and the lowest in the juniper fruit and the highest Mn concentration was recorded in the juniper needles in zone I. Based on the obtained values of the coefficient of biological absorption, it can be concluded that white pine is not suitable for phytoextraction or phytostabilization of the tested elements. The analysis of biological factors (bioconcentration, translocation and bioaccumulation factor) indicated a possible usage of juniper in phytoextraction for Cd only.

Keywords: trace elements; ICP-OES; ICP-MS; juniper; white pine; phytoremediation.

INTRODUCTION

The quantity of heavy metals originating from natural sources is almost negligible, when compared to the quantity of heavy metals generated as a result of anthropogenic activities. Trace elements – heavy metals, represent pollutants of significant concern due to their potentially harmful effects on the environment.[1–3] Long-term and excessive intake of these elements can burden the environment, as they enter and circulate within biogeochemical cycles. Due to their inability to degrade, these elements accumulate through the food chain, and depending on their concentration and toxicity, they pose a risk to human health as well as to ecosystems.[3–5] Heavy metals cannot be degraded through physical or biological processes, which makes them more persistent in soil. These metals can remain in the soil for extended periods, accumulating and causing harmful effects on ecosystems and human health.[6] For the removal of heavy metals from contaminated areas, people employ various techniques. These techniques can often be combined, depending on the specific contamination conditions and the goals of remediation. Phytoremediation has proven to be one of the best solutions, as technological methods have shown to be ineffective and uneconomical.[7] Phytoremediation is an ecological method that applies plant species to remove or reduce the contamination of heavy metals from soil. The plant species used in phytoremediation have the ability to accumulate heavy metals from the soil through processes such as phytoextraction or phytostabilization.[8] Different plant species have varying abilities to absorb pollutants from the soil, including heavy metals. These diverse capabilities of plants to absorb pollutants play a crucial role in preserving the environment from the harmful effects of pollutants.[9,10] Some heavy metals pose a significant problem worldwide due to their toxicity and ability to induce cytotoxic and mutagenic effects on all living organisms, including plants.[11–17] Some plant species have developed tolerance and resistance to high concentrations of heavy metals. They can absorb and accumulate large amounts of heavy metals in their

tissues without significant negative effects on their growth and development.[18–20] For the subject of investigation in this study, two evergreen plant species were selected - juniper and white pine. Juniper belongs to the group of long-lived plant species, as its needle-like leaves function throughout the year. Previous research has shown that juniper is a promising candidate for phytoremediation.[21] The use of juniper as a plant for phytoremediation and the restoration of contaminated soil has proven to be promising. Juniper possesses specific properties of heavy metal accumulation, meaning it can uptake and concentrate large amounts of these metals from the environment into its tissues. Juniper is also known for its rapid biomass growth, which is an additional advantage in its use for phytoremediation.[22] Juniper is ideal for phytostabilization of contaminated soil due to its deep root system, high tolerance to heavy metals, and ability to grow in nutrient-poor soils.[23] The second evergreen plant species examined in this study is the white pine. White pine is widely distributed and often used to monitor changes in the environment due to its extensive prevalence compared to its relatives.[24] White pine is a conifer that thrives on various types of soil, including dry, moist, rocky, and sandy soils, as well as marshy areas. It grows in diverse conditions, ranging from fertile to dry and infertile habitats.[25,26] The needles of the white pine have the ability to absorb and retain heavy metal cations from the surrounding environment, making them important indicators of environmental conditions. By studying the content of heavy metals in the needles of the white pine, we can obtain information about the degree of pollution and the quality of the environment. White pine is known for its efficient abilities in absorbing heavy metals from the soil.[27,28] Establishing surface mines represents one of the greatest sources of changes in the natural environment. This can lead to catastrophic consequences, including the release of heavy metals into the environment.[29–31] The aim of the research was to evaluate the content of elements (Al^{3+}, Cd^{2+} and Mn^{2+}) in soil and parts of white pine and juniper (root, branches, needles and fruits) in order to study their potential use in phytoremediation and the possibility of using evergreen plants as an ecological indicator.

EXPERIMENTAL

Description of the investigated area

Since the 1920s, the first explorations of lead-zinc ore deposits began in the vicinity of Raška. Mining has a long history in this part of Serbia. In the medieval period, mining was one of the most significant economic activities in the territory of present-day Serbia, and Mount Kopaonik was known for its rich mineral deposits. The lead–zinc ore deposit of Sastavci (Badanj) is located at the source of the Radišićka River, on the slopes of Mount Karač (916 m) and Šanac (1098 m), in an altitude zone ranging from 720 to 905 m above sea level. The estimates determine that this deposit contains approximately 364,000 tons of ore with an average content of 2.05 % lead and 5.59 % zinc. On the mine site, a high content of Au was discovered, but the content of As was also high, leading to the cessation of exploitation. Although mining is no longer a dominant industry in this region, one of the problems that remains as a consequence of exploitation is tailings, an unusable material that remains as residual toxic waste after ore pro-

cessing. Mine tailings can contain various harmful substances and metals that pose a potential threat to the surrounding soil and water systems. While surface mines lead to soil degradation, they often contain heavy metal cations that accumulate through the food chain, causing toxicity and posing a serious threat to animals and human populations.

Sampling of soil and plant material

White pine and juniper, which were used for the purpose of this research, were selected for sampling based on several criteria. These plant species are perennial and are adapted to different living conditions, which allows them to survive and thrive. When it comes to long--term anthropogenic pollution, these plants can provide some useful information since they are perennial plants and have the ability to accumulate pollutants over time. This means that the presence of certain toxic elements in white pine and juniper tissues may indicate the presence or history of pollution in the area. White pine and juniper have an important role in human nutrition and medicine. If white pine and juniper grow in polluted areas, there is a risk that toxic elements accumulate in their tissues. If these plants are used for food or medicinal purposes, there is a possibility that toxic elements can be transferred to the human body, which can be harmful to health.

Description of the zones and places of sampling of soil and plant material for the Sastavci (Badanj) surface mine and its vicinity

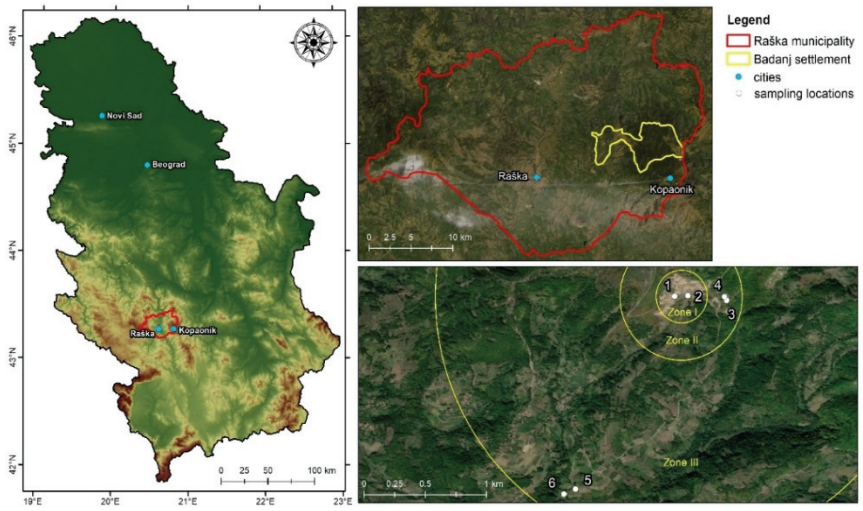

Fig. 1. Map of the surveyed area with sampling locations of soil and plant material by zones of the Sastavci (Badanj) surface mine (points 1, 3 and 5 are samples of white pine; points 2, 4 and 6 are samples of juniper).

The sampling of soil and plant material was conducted in three different zones (6 sampling sites) with varying degrees of contamination. The sampling locations were selected based on the assumption that the concentration of metal cations would decrease with the distance from Sastavci (Badanj) surface mine. For soil sampling, a stainless-steel probe was used, and soil samples were taken from a depth of 20 cm, where the highest concentration of roots was observed. After the composite samples were collected, the removal of leaves, stones, twigs, and other visible impurities was performed. The sampling locations of plant material and soil (Fig.

1) are divided into different sampling zones. Samples were collected at the primary source of pollution, *i.e.*, at the surface mine, Zone I. This part represents the most polluted area. The samples were collected in the immediate vicinity of the surface mine, representing a secondary source of pollution, Zone II. A lower degree of pollution is expected in this zone, when compared to Zone I. Samples collected in the tertiary zone are located at a distance of 1,700 m from the surface mine, Zone III. Here, the degree of pollution is expected to be lower compared to the previous two zones. The control sampling zone is located 5 km straight-line distance from the Pb-Zn surface mine near the village of Kneževići. This zone is considered uncontaminated.

Description of the sampling procedure of plant material and soil

The indigenous plant species used for analysis were in good condition, without the presence of visible signs of disease or pests, which was important in order to ensure quality and representative samples for analysis. These precise measures were taken to ensure maximum accumulation of metal cations in the selected plant species and to obtain accurate analysis results. Soil samples were collected at a depth of 20 cm and weighed approximately 500 g. At the same depth, roots up to 1 cm in diameter were sampled. For juniper, samples were collected at a height of 50–70 cm, and for white pine at a height of approximately 1.50–1.80 cm. Samples were collected from different sides of each plant and weighed 4–5 g. When it comes to sampling mature juniper berries and pine cones, those with similar shape and colour were selected. Samples for both plant species were collected from the same branches. Sampling procedure was applied according to the given protocol, whereby soil and various parts of plants (roots, branches, needles and fruits) were prepared as composite samples (Fig. 2).[32] This sampling methodology was used to ensure the representativeness of samples for the detection of concentrations of metal cations in soil and various parts of plants.

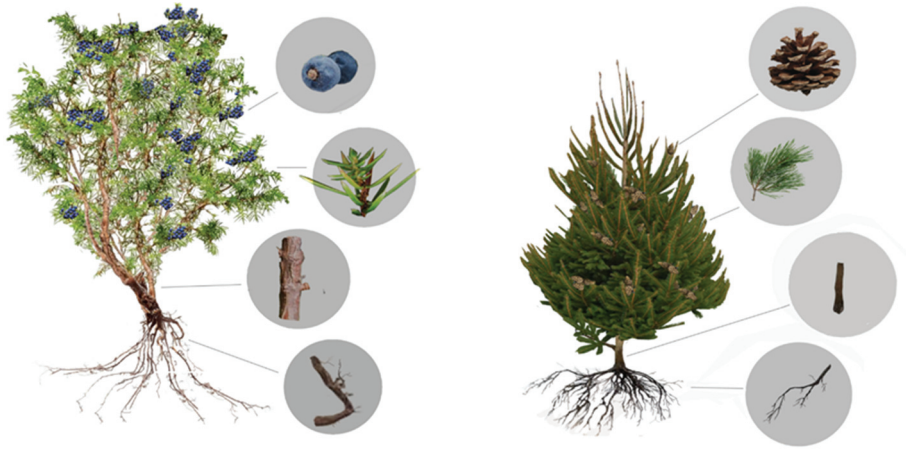

a) b)

Fig. 2. Sampling scheme (roots, branches, needles and (fruits) cones); a) juniper and b) white pine.

Materials and methods

For the investigation of this locality and the investigation of the persistence of toxic elements in the soil and parts of white pine and juniper, sampling was carried out that was

adapted to the morphology of the terrain and wild plant species, whereby a total of 6 soil samples and 24 samples, parts of white pine and juniper (roots, branches, needles and (fruits) cones) in three different zones. Microwave dissolution of soil and plant material samples was performed at the Faculty of Chemistry in Belgrade. The content of major elements in traces was determined using two analysis methods: inductively coupled plasma-optical emission spectrometry (ICP--OES) and inductively coupled plasma-mass spectrometry (ICP-MS). These methods enable precise measurement of concentrations of various elements in the samples, which is crucial for assessing contamination. Microwave digestion was performed in SpeedWave XPERT instrument, manufactured by Berghof. About 0.4 g of sample was measured in Teflon cuvettes. 6 ml of purified nitric acid and 2 ml of hydrogen peroxide (30 %, Fluka) were added. Purified nitric acid was made through purification of HNO_3 (65 % p.a., Sigma Aldrich), on Berghof-purification apparatus-BSB-939-IR. Degradation of samples was performed according to Microwave Digestion of Soil according to EPA 3051A, Application Note Environment & Geology, Digestion, Berghof (https://www.berghof-instruments.com/en/application/microwave-digestion-of-soilaccording-to-epa-3051a/). After completion of the program and cooling of the cuvettes, the samples were quantitatively transferred and diluted with ultra-pure water (Milli Q water, Thermo Scientific, UK) in volumetric flasks of 50 ml. All samples were filtered with Syringe filters (25 mm, PTFE membrane 0.45 μm). 3 elements were analysed in samples. On ICP-OES (ICP-OES, iCAP 6500 Duo, Thermo Scientific, UK) Al was analysed, and on ICP-MS (ICP--MS, iCAP Qc, Thermo Scientific, UK) Cd and Mn were analysed. Standard series were made from internal standards of 1000 μg L^{-1}, and diluted with ultra-pure water to appropriate concentration. The data on the concentration of each element were obtained on the basis of three measurements. For the analyses, calibration solutions were made from the standard stocks (Multi--Element Plasma Standard Solution 4, Specture®, Alfa Aesar; Major Elements Stock, EPA Method Standard, VHG Labs, Merck). The determination of soil pH values, both active (pH (H_2O)) and potential acidity of the soil (pH (KCl)), was conducted in accordance with ISO standard 10390:2005.[33] For this purpose, the Orion Star A221 instrument by Thermo Scientific was used. The determination of pH values was carried out in a suspension of 1g soil and 100 ml distilled water or 1g soil and 1 mol L^{-1} solution of KCl, using the Orion Star A221 instrument, Thermo Scientific. It is important that the soil has an optimal pH value between 6.5 and 7.8 because this provides ideal conditions for the absorption of nutrients, access to water, and good root ventilation, contributing to a healthy and improved plant growth.[34,35] The attached soil samples were dried at a temperature of 105±5 °C in a drying oven, to a constant mass. The gravimetric method of mass loss (*LOI* – loss on ignition) was used to determine the content of organic matter in the soil after drying. The samples were weighed on an analytical balance, brand KERN model ABJ-NM/ABS-N, then they were transferred to porcelain containers and placed in an annealing furnace (high-temperature furnace, VTP-1,2, Elektron), where the soil samples were annealed for of 2 h in which the temperature gradually increased to 440 °C. In soil samples, the content of organic matter was determined based on mass loss at high temperature.[36] Organic matter in soil originates from various residues, including animal and plant materials, and plays a crucial role in maintaining soil quality and the circulation of nutrients within it. The content of organic matter in the soil has a great influence on maintaining the biological productivity of the soil.[37] The enrichment factor is a method used to estimate the degree of contamination of soil and plant material in the investigated area compared to an uncontaminated area.[32,38,39] To determine the degree of soil contamination, there are five categories, each of which represents a different degree of enrichment, $EF < 2$ no or minimal enrichment, $2 \leq EF < 5$ moderately enriched, $5 \leq EF < 20$ significant enrichment, $20 \leq EF < 40$ very

high enrichment and $EF > 40$ extremely high soil enrichment.[40] The value of the bioconcentration factor (*BCF*) is defined as the ratio of the concentration of elements in the roots of the plant to the concentration of elements in the soil. It is considered that the accumulation of elements from the soil in the roots occurs when the *BCF* value is > 1.[41-44] Biological absorption coefficient (*BAC*) is defined as the ratio of the concentration of elements in plant leaves to the concentration of elements in the soil. *BAC* values are classified into five groups: *BAC*, 10–100 (intense absorption), *BAC*, 1–10 (strong absorption), *BAC*, 0.1–1 (medium absorption), *BAC*, 0.01–0.1 (weak absorption) and *BAC*, 0.001–0.01 (very weak absorption).[45] The translocation factor (*TF*) is defined as the ratio of the total concentration of elements in the root and the concentration in the aerial part of the plant. It is considered that the translocation of elements is efficient from the roots to the aerial part of the plant when the value is >1.[42,43,46–48]

RESULTS AND DISCUSSION

In Table I, the data on the content of organic matter in the root zone of the evergreen plant species of white pine and juniper in the researched area are presented. One of the key factors is the OM content influencing the capacity of soils to sustain biological productivity and to maintain the environmental quality.[49] The organic matter content in the soil ranged from 4.78 to 15.96 %. Based on these results, it can be concluded that the highest percentage of soil had a moderate content of organic matter, while three sampled soil locations had a high content of organic matter.[50] The highest concentration of organic matter in the soil was recorded in the root zone of white pine sample 5, while the lowest concentration of organic matter was in the root zone of juniper sample 2.

TABLE I. Organic matter content (*OM*) in soil from the root zone of white pine and juniper in the researched area

Sampling zone	Sampling number	Organic matter, *OM* / %	Average
I	S 1 (White pine)	11.13	7.955
	S 2 (Juniper)	4.78	
II	S 3 (White pine)	6.95	7.515
	S 4 (Juniper)	8.08	
III	S 5 (White pine)	15.96	14.09
	S 6 (Juniper)	12.22	

Table II presents the pH values of active and potential soil acidity from the root zone of white pine and juniper. Soil pH plays the most important role in determining metal morphology, mineral surface solubility, migration and ultimate bioavailability.[51,52] One of the most frequently measured parameters is soil pH, considering its influence on behaviour and condition bioavailability of elements in soil.[53] In the 6 to 7 range, soil pH is generally optimal for plant growth because more plant nutrients are readily available in this pH range.[54] According to the acidity classification categories of soil,[54] the sampled soil can be classified as very strongly acidic to slightly acidic. Based on the comparison of soil pH values in the investigated area, we can see that the highest soil acidity was in the I zone, sample

2, while the least acidity was in III zone, sample 6. Samples 1, 4 and 6 had a ΔpH value ($pH(H_2O) - pH(KCl)$) slightly above 1 at the sampling sites, indicating a tendency of soil acidification at these sampling locations.

TABLE II. Soil acidity from the root zone of white pine and juniper in the studied area; ΔpH = $pH(H_2O) - pH(KCl)$

Sampling zone	Sampling number	$pH(H_2O)$	pH (KCl)	ΔpH
I	S 1 (White pine)	5.77	4.72	1.05
	S 2 (Juniper)	4.72	4.01	0.71
II	S 3 (White pine)	6.07	5.43	0.64
	S 4 (Juniper)	6.11	5.03	1.08
III	S 5 (White pine)	6.16	5.29	0.87
	S 6 (Juniper)	6.33	5.19	1.14

Fig. 3 shows the concentrations of elements Al^{3+}, Cd^{2+} and Mn^{2+} in the root zone soil of white pine and juniper and they are also presented in the Table III. The obtained concentrations of the examined elements were compared with the corresponding remediation values and threshold values prescribed by the Regulation of the Republic of Serbia.[55]

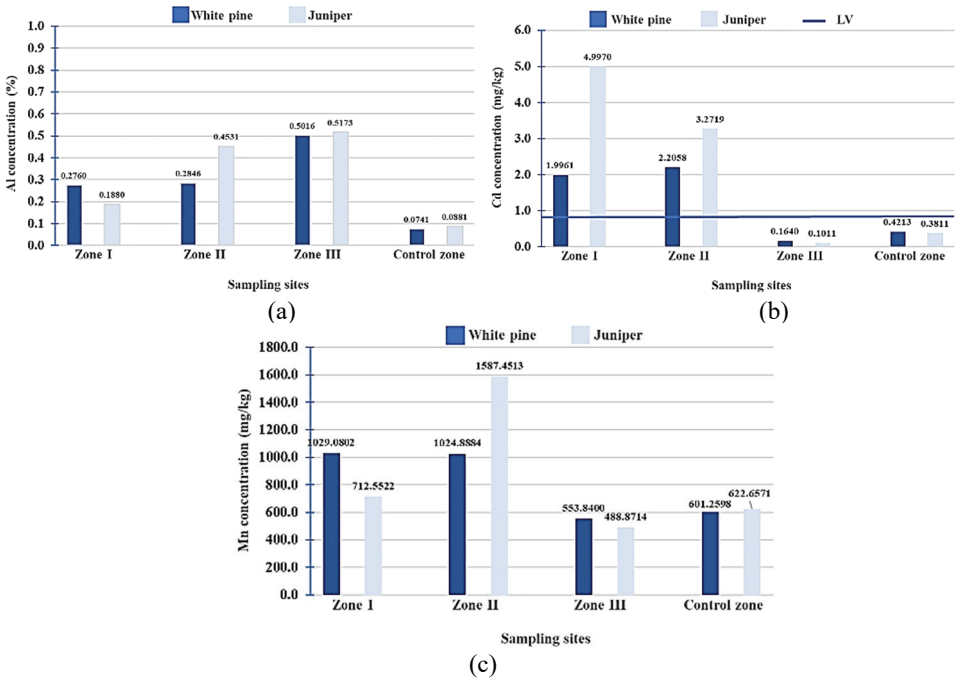

Fig. 3. Concentrations of metal cations a) Al, b) Cd and c) Mn in the root zone of white pine and juniper at 6 sampled locations (solid line represents the threshold value according to the Regulation of Serbia (Regulation No. 30/2018-50, 2018)).

TABLE III. The concentrations (mg kg^{-1})of elements Al^{3+}, Cd^{2+} and Mn^{2+} in the root zone soil of white pine and juniper

Sampling zone	Sampling number	Al	Cd	Mn
I	S 1 (White pine)	0.2760	1.9961	1029.0802
	S 2 (Juniper)	0.1880	4.9970	712.5522
II	S 3 (White pine)	0.2846	2.2058	1024.8884
	S 4 (Juniper)	0.4531	3.2719	1587.4513
III	S 5 (White pine)	0.5016	0.1640	553.8400
	S 6 (Juniper)	0.5173	0.1011	488.8714
Control	White pine	0.0741	0.4213	601.2598
	Juniper	0.0881	0.3811	62.6571

The concentrations of aluminium in the soil from the root zones of the analysed plant species are lower than the average values (1–5 %), indicating a relatively low concentration of aluminium in the soil or the presence of factors that reduce these concentrations. Slightly higher aluminium values were observed in Zone III for both plant species. Fig. 3b shows the concentration of cadmium in the soil from the root zone of white pine and juniper. The prescribed limit values for cadmium in the soil according to the Regulation of the Republic of Serbia are 0.8 mg kg^{-1}.[55] The world average concentration of cadmium in the soil is 0.41 mg kg^{-1}.[56] Cd concentrations that exceeded the limit values were recorded for both plant species in zones I and II, while in soil samples from zone III as from the control zone, the Cd concentration was below the determination limits for both plant species. There are no defined limits and remediation values for manganese in the soil according to the Regulation of the Republic of Serbia, while the world average concentration of manganese in the soil is from 411 to 550 mg kg^{-1}.[56] The concentrations of manganese in the soil from the root zones of white pine and juniper were above the global average in all three zones, as well as in the control zone.

The values of enrichment factors for Al^{3+}, Cd^{2+} and Mn^{2+} in the soil of white pine and juniper are presented in Table IV. The enrichment factors for aluminium were greater than 2, indicating enrichment or contamination of soil with aluminium. The presence of aluminium can be considered anthropogenic at all sampling locations, although there are differences in aluminium concentrations depending on the sampling location. Enrichment of soil with cadmium was observed for both plant species in Zones I and II, while there was no soil enrichment with cadmium for white pine and juniper in Zone III. Most soil samples belong to the category of moderate to significant enrichment with cadmium. The enrichment factor values indicate no soil enrichment for most samples, while moderate enrichment with manganese was observed in juniper soil in Zone II. Table V presents a literature review of the range of element concentrations in plant leaves.

Analysis of the concentration of Al, Cd and Mn (Fig. 4 and Table VI) was conducted on various parts of the white pine at the surface mine Sastavci (Badanj)

and its vicinity. The highest concentrations of Al were detected in the roots of the white pine in Zone I, while the lowest concentration was observed in the fruit (cone) in the control zone. For most samples of plant material, the concentration of Cd was below the detection limit (< 0.2 mg kg^{-1}). The World Health Organization (WHO) has established permissible levels for Cd herbal materials, which amount to 0.3 mg kg^{-1}.[58] The content of these metals in unwashed pine needles was 0.1-2.4 mg kg^{-1} for Cd.[59] However, an increased concentration of Cd was observed in the branches of the white pine in Zone I and Zone II. Regarding Mn, the highest concentrations were found in the needles of the white pine in Zone II, while the lowest concentrations were observed in the control zone.

TABLE IV. Enrichment factor for soil in the White Pine and Juniper Zone Sastavci (Badanj)

Element	Zone I		Zone II		Zone III	
	Sample 1	Sample 2	Sample 3	Sample 4	Sample 5	Sample 6
Al	3.7249	2.1341	3.8403	5.1431	6.7695	5.8713
Cd	4.7380	13.1120	5.2357	8.5854	0.3893	0.2653
Mn	1.7115	1.1444	1.7046	2.5495	0.9211	0.7851

TABLE V. Concentration ranges of the elements in mature leaves (mg kg^{-1} dw);[57] dw – dry weight basis, and „-“ not defined

Element	Deficient	Sufficient or normal	Excessive or toxic	Tolerable in agronomic crops
Cd	–	0.05–0.2	5–30	0.05–0.5[a]
Mn	10-30	30-300	400-1000	300

[a]Fresh weigh basis

TABLE VI. Concentration (mg kg^{-1}) of Al, Cd and Mn in parts of the white pine

Sampling zone	Sampling number	Al	Cd	Mn
I	Root	593.1935	1.0142	93.3293
	Branch	307.7305	3.7611	96.8308
	Needle	183.2863	0.9624	301.8593
	Strobilus	221.4027	0.7828	65.0804
II	Root	63.6972	1.7570	56.3886
	Branch	192.7475	3.8288	164.2559
	Needle	120.9598	1.7201	738.1713
	Strobilus	112.0603	0.2243	64.8791
III	Root	135.0197	0.1560	9.7610
	Branch	216.4097	0.2316	88.7822
	Needle	449.4844	0.0512	602.5080
	Strobilus	506.1707	0.0930	123.9799
Control	Root	82.0100	0.2200	22.7200
	Branch	70.9300	0.3400	30.7000
	Needle	110.9300	0.4100	35.6100
	Strobilus	33.0900	0.1100	25.1200

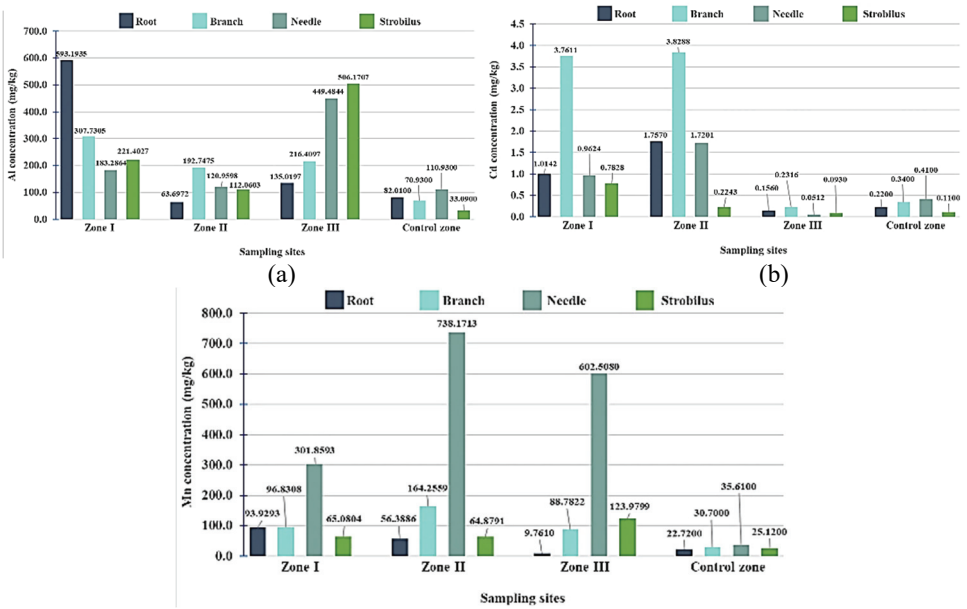

Fig. 4. Concentration (mg kg^{-1}) for a) Al, b) Cd and c) Mn in the root and above-ground parts of the white pine.

In the examined area, concentrations of Al vary in the juniper (roots, branches, needles, and fruit). The highest concentration of aluminium was observed in the roots of juniper in the first zone, while the lowest was in the juniper fruit in the control zone. Concentrations of Cd in the juniper, examined both at the open pit and its immediate surroundings, also vary. The highest concentration of Cd was found in the roots of spruce in Zone I, while the lowest was in the juniper fruit in zone III. Regarding Mn, the highest concentrations were observed in the juniper needles in the first zone of the examined area, while the lowest concentrations were detected in the control zone (Fig. 5 and Table VII).

Table VIII displays the values of biological factors for white pine. It can be observed that for Al, Cd and Mn, the criterion BCF > 1 and TF > 1 does not exist in any zone or sample. When it comes to aluminium, cadmium and manganese, we can conclude that white pine is not suitable for phytoextraction or phytostabilization of the examined elements, under the given conditions of the Sastavci (Investigation area) surface mine and its immediate vicinity.

Based on the tabular data for juniper in phytoextraction (Table IX), the criterion BCF > 1 and TF > 1 is fulfilled only for Cd, sample 6, zone III. Based on the BAC values, which were less than 1, it can be concluded that juniper excludes the examined elements. In the case of Cd and Mn, the BAC value was greater than 1, indicating the potential accumulation of these elements in juniper needles.

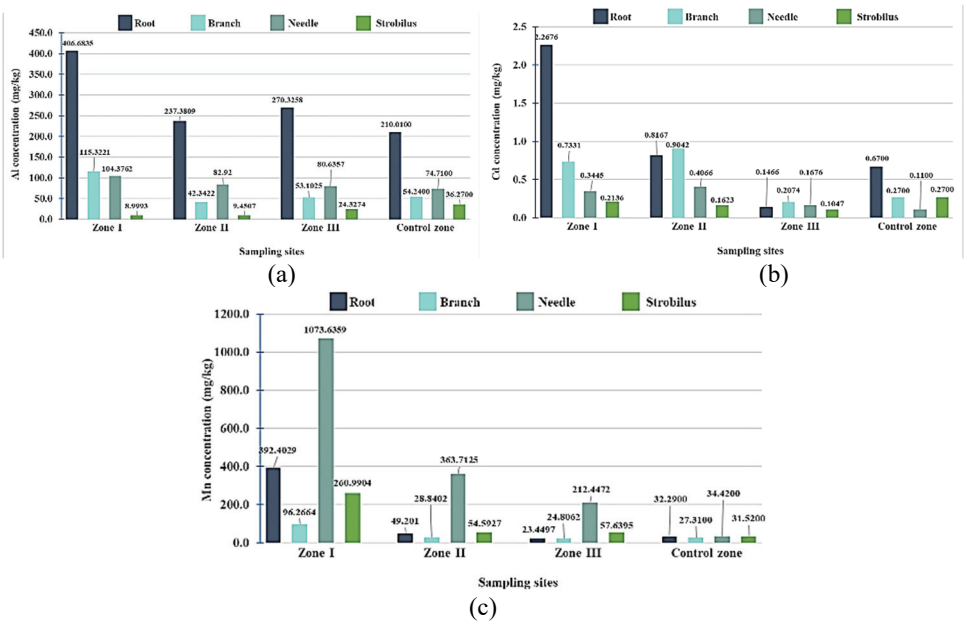

Fig. 5. Concentration (mg kg^{-1}) of: a) Al, b) Cd and c) Mn in parts of the juniper.

TABLE VII. Concentration (mg kg^{-1}) of Al, Cd and Mn in parts of the juniper

Sampling zone	Sampling number	Al	Cd	Mn
I	Root	406.6835	2.2676	392.4029
	Branch	115.3221	0.7331	96.2664
	Needle	104.3762	0.3445	1073.6359
	Strobilus	8.9993	0.2136	260.9904
II	Root	237.3809	0.8167	49.201
	Branch	42.3422	0.9042	28.8402
	Needle	82.92	0.4066	363.7125
	Strobilus	9.4507	0.1623	54.5927
III	Root	270.3258	0.1466	23.4497
	Branch	53.1025	0.2074	24.8062
	Needle	80.6357	0.1676	212.4472
	Strobilus	24.3274	0.1047	57.6395
Control	Root	210.0100	0.6700	32.2900
	Branch	54.2400	0.2700	27.3100
	Needle	74.7100	0.1100	34.4200
	Strobilus	36.2700	0.2700	31.5200

TABLE VIII. Bioconcentration factor (BCF), translocation factor (TF), and biological absorption coefficients (BAC) for white pine

Factor	Sampling site	Al	Cd	Mn
BCF	Sample 1	0.2149	0.5081	0.0913
	Sample 3	0.0224	0.7965	0.0550

TABLE VIII. Continued

Factor	Sampling site	Al	Cd	Mn
BCF	5	0.0269	0.9512	0.0176
TF	1	0.3090	0.9489	**3.2137**
	3	**1.8990**	0.9790	**13.0908**
	5	**3.3290**	0.3282	**61.7261**
BAC	1	0.0664	0.4821	0.2933
	3	0.0425	0.7798	0.7202
	5	0.0896	0.3122	**1.0879**

TABLE IX. Bioconcentration factor (*BCF*), translocation factor (*TF*) and biological absorption coefficients (*BAC*) for juniper

Factor	Sampling site/Elements	Al	Cd	Mn
BCF	2	0.2163	0.4538	0.5507
	4	0.0524	0.2496	0.0310
	6	0.0523	**1.4500**	0.0037
TF	2	0.2567	0.1519	**2.7361**
		0.3493	0.4979	**7.3924**
		0.2983	**1.1432**	**9.0597**
BAC	2	0.0378	0.1726	1.0433
	4	0.0291	0.1843	0.3549
	6	0.0161	**1.0220**	0.3836

CONCLUSION

The exploitation of natural resources can have significant negative consequences on soil, plant and animal life, and the environment in general. The results indicate that there have been exceedances of the threshold values for elements in the soil, particularly for Cd in zones I and II for both plant species. Enrichment factors, which were mostly in the categories of moderate and significant enrichment, were observed in most soil samples from the root zones of white pine and juniper for Al, Cd, and Mn (only one sampled location). We conclude that Al, Cd and Mn in the soil from the root zones of white pine and juniper originate from the exploitation process of Pb–Zn ore. The natural origin was determined for manganese, while the enrichment was detected in only one sample, indicating that the exploitation contributed to the increase in the concentration of this element. For the Sastavci (Badanj) surface mine, the values of the bioconcentration factor (*BCF*) for the examined elements were <1, indicating very low uptake of elements from the soil through the roots of white pine. Based on the values of the bioconcentration factor for juniper, *BCF* >1 was observed for Cd, while for other elements, the bioconcentration factor value was <1. Based on the obtained values of the biological absorption coefficient, the absorption intensity ranged from very weak to strong intensity for Mn in white pine needles, while for juniper, the absorption of elements

from the soil to the juniper needles was observed for Cd and Mn. The criteria for the possibility of using juniper in the phytoextraction process, $BCF > 1$ and $TF > 1$, were achieved only for Cd. Given that the research was conducted on a surface mine of lead-zinc ore, there is a possibility that an increased concentration of other toxic elements may be found on the surface mine, as well as in its immediate surroundings. Given that for this research we used wild evergreen plant species, which belong to the group of tolerant plants, which managed to develop and survive in the polluted area and which did not prove to be good candidates for phytoremediation of the investigated elements, further research can be carried out in order to examination of some other wild plant species such as wild cherry, fern, oak, since these plant species also survive in such a polluted area. The final research should provide a scientific contribution to the assessment and/or rehabilitation of such areas, using appropriate plant species for the phytoremediation process in the form of erosion reduction, reforestation and environmental preservation.

ИЗВОД

ПРОЦЕНА КОНЦЕНТРАЦИЈЕ ТОКСИЧНИХ МЕТАЛА (АЛУМИНИЈУМ, КАДМИЈУМ И МАНГАН) У ЗЕМЉИШТУ И ЗИМЗЕЛЕНИМ БИЉНИМ ВРСТА НА ПОВРШИНСКОМ КОПУ САСТАВЦИ И ОКОЛИНИ

МИЛИЦА ТОМОВИЋ[1], ЈОВАНА ГРАХОВАЦ[2], ЈЕЛЕНА ДОДИЋ[2], МАРИЈА РАДОЈКОВИЋ[2], НАТАША ЕЛЕЗОВИЋ[1] и КРСТИМИР ПАНТИЋ[1]

[1]Универзитет у Приштини са привременим седиштем у Косовској Митровици, Факултет техничких наука, Ул. Кнеза Милоша 7, 38220 Косовска Митровица, [2]Технолошки факултет Нови Сад, Универзитет у Новом Саду, Булевар цара Лазара 1, 21000 Нови Сад

У раду је спроведено истраживање у циљу утврђивања концентрације Al^{3+}, Cd^{2+} и Mn^{2+} у земљишту и деловима зимзелених биљних врста – клеке и белог бора – на површинском копу Саставци (Бадањ) и његовој околини и његовој околини у циљу утврђивања могућност коришћења зимзелених биљака као еколошког индикатора или за фиторемедијацију. На глобалном нивоу, као резултат различитих антропогених активности као што су саобраћај, пољопривредне активности, спаљивање отпада, индустријска производња, рударење, итд., представља озбиљан проблем који доводи до загађења токсичним и потенцијално токсичним катјонима метала. Једна од иновативнијих техника која се користи за санацију рударских подручја је фиторемедијација. Применом фиторемедијације одређене биљне врсте на загађеним подручијима имају способност да делују као акумулатори или хиперакумулатори, апсорбују токсичне метале из земљишта кроз корен биљке и транспортује их у горње делове. Ово истраживање је спроведено у циљу одређивања концентрације Al^{3+}, Cd^{2+} и Mn^{2+} на самом површинском копу и његовој околини, као и праћења дистрибуције металних катјона у систему корен, гране, иглице и плодови зимзелених биљних врста – бели бор и клека. Резултати су показали да је узорковано земљиште контаминирано Cd у зони I и II за обе биљне врсте, јер су концентрације прелазиле граничне вредности, док је концентрација Cd у зони III као и у контролној зони била испод граница одређивања за обе биљне врсте. Концентрација Mn у земљишту из зоне белог бора и клеке била је изнад светског просека у све три зоне, као и у самој контролној зони. Земљиште је највише обогаћено анализираним елементима у површинском копу I и II зоне. Анализом елемената у деловима белог бора, корену, гранама, иглицама и плодовима, највећа концентрација Al је откривена у корену у зони I, док је најмања концентрација забележена у плоду (шишаркама) у контролној зони,

повећана концентрација Cd забележена је у гранама у зонама I и II, а највећа концентрација Mn забележена је у иглицама у зони II. Највећа концентрација Al забележена је у корену клеке у зони I, а најмања у плоду клеке у контролној зони, концентрација Cd је највећа у зони корена клеке I, а најмања у плоду клеке и највећа концентрација Mn забележена је у иглицама клеке у зони I. На основу добијених вредности коефицијента биолошке апсорпције, може се закључити да бели бор није погодан за фитоекстракцију или фитостабилизацију испитиваних елемената. Анализа биолошких фактора (биоконцентрација, транслокација и фактор биоакумулације) указала је на могућу употребу клеке у фитоекстракцији само за Cd.

(Примљено 1. априла, ревидирано 30. априла, прихваћено 18. јуна 2024)

REFERENCES

1. L. Järup, *Brit. Med. Bull.* **68** (2003) 167 (https://doi.org/10.1093/bmb/ldg032)
2. B. Wei, L. Yang, *Microchem. J.* **94** (2010) 99 (https://doi.org/10.1016/j.microc.2009.09.014)
3. N. B. Milosavljević, M. Đ. Ristić, A. A. Perić-Grujić, J. M. Filipović, S. B. Štrbac, Z. Lj. Rakočević, M. T. Kalagasidis Krušić, *J. Haz. Mat.* **192** (2011) 846 (https://doi.org/10.1016/j.jhazmat.2011.05.093)
4. Z. Cong, S. Kang, Y. Zhang, X. Li, *App. Geochem.* **25** (2010) 1415 (https://doi.org/10.1016/j.apgeochem.2010.06.011)
5. V. D. Nica, M. Bura, I. Gergen, M. Harmanescu, D-M. Bordean, *Chem. Cent. J.* **6** (2012) 55 (https://doi.org/10.1186/1752-153x-6-55)
6. J. Suman, O. Uhlik, J. Viktorova, T. Macek, *Front. Plant Sci.* **1476** (2018). (https://doi.org/10.3389/fpls.2018.01476)
7. A. S. Mussina, G. U. Baitasheva, M. S. Kurmanbayeva, G. J. Medeuova, A. A. Mauy, E. M. Imanova, A. Zh. Kurasbaeva, Z. S. Rachimova, Y. S. Nurkeyev, K. Orazbayev, *Israel J. Ecol. Evol.* **64** (2018) 35 (http://doi.org/10.1163/22244662-06303005)
8. S. Adiloğlu, *Heavy Metal Removal with Phytoremediation*. in *Advances in Bioremediation and Phytoremediation*, Ed. N. Shiomi, InTech, (2018). (https://doi.org/10.5772/intechopen.70330)
9. Y. Hu, Z. Nan, J. Su, N. Wang, *Env. Sci. Poll. Res.* **20** (2013) 7194 (https://doi.org/10.1007/s11356-013-1711-0)
10. E. Osma, M. Elveren, G. Karakoyun, *Air Qual. Atm. Health* **10** (2017) 85 (https://doi.org/10.1007/s11869-016-0410-7)
11. M. P. Waalkes, *Mut. Res. – Fund. Mol. Mech. Mutagen.* **533** (2003) 107 (https://doi.org/10.1016/j.mrfmmm.2003.07.011)
12. J. Ding, G. He, W. Gong, W. Wen, W. Sun, B. Ning, S. Huang, K. Wu, C. Huang, M. Wu, W. Xie, H. Wang, *Can. Epid. Biomark. Prevent.* **18** (2009) 1720 (https://doi.org/10.1158/1055-9965.EPI-09-0115)
13. H. Chen, N. C. Giri, R. Zhang, K. Yamane, Y. Zhang, M. Maroney, M. Costa, *J. Biol. Chem.* **285** (2010) 7374 (https://doi.org/10.1074/jbc.M109.058503)
14. T. Schwerdtle, F. Ebert, C. Thuy, C. Richter, L. H. F. Mullenders, A. Hartwig, *Chem. Res. Tox.* **23** (2010) 432 (https://doi.org/10.1021/tx900444w)
15. Y. Asara, J. A. Marchal, E. Carrasco, H. Boulaiz, G. Solinas, P. Bandiera, M. A. Garcia, C. Farace, A. Montella, R. Madeddu, *Int. J. Mol. Sci.* **14** (2013) 16600 (https://doi.org/10.3390/ijms140816600)
16. M. Ovečka, T. Takáč, *Biotec. Adv.* **32** (2014) 73 (https://doi.org/10.1016/j.biotechadv.2013.11.011)

17. M. E. Morales, R. S. Derbes, C. M. Ade, J. C. Ortego, J. Stark, P. L. Deininger, A. M. Roy-Engel, *PLoS One* **11** (2016) e0151367 (https://doi.org/10.1371/journal.pone.0151367)
18. H. Jia, D. Hou, D. O'Connor, S. Pan, J. Zhu, N.S. Bolan, J. Mulder, *J. Haz. Mat.* **389** (2020) 121849 (https://doi.org/10.1016/j.jhazmat.2019.121849)
19. L. Wang, D. Hou, Z. Shen, J. Zhu, X. Jia, Y.S. Ok, F. M. G. Tack, J. Rinklebe, *Crit. Rev. Env. Sci. Tech.* **50** (2020) 2724 (https://doi.org/10.1080/10643389.2019.1705724)
20. D. O'Connor, X. Zheng, D. Hou, Z. Shen, G. Li, G. Miao, S. O'Connell, M. Guo, *Env. Int.* **130** (2019) 104945 (https://doi.org/10.1016/j.envint.2019.104945)
21. L. Ahrens, M. Shoeib, T. Harner, S. C. Lee, R. Guo, E. J. Reiner, *Env. Sci. Techn.* **45** (2011) 8098 (https://doi.org/10.1021/es1036173)
22. Li X. Zhang, X, Li, B, Wu, Y, Sun, H, Yang, Y. *Env. Sci. Poll. Res.* **24** (2017) 21660 (https://doi.org/10.1007/s11356-017-9781-z)
23. I. D. Pulford, C. Watson, *Env. Int.* **29** (2003) 529 (https://doi.org/10.1016/s0160-4120(02)00152-6)
24. E. Baltrenaite, P. Baltrenas, D. Butkus, A. Lietuvninkas, *Phytoremediation* (2015) 21 (https://doi.org/10.1007/978-3-319-10395-2_2)
25. C. Kole, Genome Mapping and Molecular Breeding in Plants, Springer, Berlin, 2007.
26. R. Muilu-Mäkelä, J. Vuosku, E. Läärä, M. Saarinen, J. Heiskanen, H. Häggman, T. Sarjala, *Plant Physiol. Biochem.* **88** (2015) 70 (https://doi.org/10.1016/j.plaphy.2015.01.009)
27. M. Pajak, W. Halecki, M. Gąsiorek, *Chemosphere* **168** (2017) 851 (https://doi.org/10.1016/j.chemosphere.2016.10.125)
28. M. Mleczek, P. Goliński, B. Waliszewska, A. Mocek, M. Gąsecka, M. Zborowska, Z. Magdziak, W.J. Cichy, B. Mazela, T. Kozubik, A. Mocek-Płóciniak, W. Moliński, P. Niedzielski, *J. Env. Sci. Health, Part A* **53** (2018) 1029 (https://doi.org/10.1080/10934529.2018.1471116)
29. A. Aidosov, G. Aidosov, N. Zaurbekov, N. Zaurbekova, G. Zaurbekova, I. Zaurbekov, *Ekoloji* **28** (2019) 349
30. G. Cheloni, V. I. Slaveykova, *Environments* **5** (2018) 1 (https://doi.org/10.3390/environments5120138)
31. FAO, Status of the World's Soil Resources. Google Scholar, (2015).
32. M. D. Mingorance, B. Valdés, S. R. Oliva, *Env. Int.* **33** (2007) 514 (http://dx.doi.org/10.1016/j.envint.2007.01.005)
33. ISO 2005, International Organisation for Standardisation, Soil Quality: Determination of pH, 10390:2005. ISO, Geneva.
34. N. S. Eash, T. J. Sauer, D. O'Dell, E. Odoi, Soil Science Simplified. Sixth edition. John Wiley & Sons, Inc., Hoboken, New Jersey (2016)
35. A. Zseni, H. Goldie, I. Bárány-Kevei, *Acta Carsologica* **32/1**(5), (2003) 57 (https://doi.org/10.3986/ac.v32i1.364)
36. K. R. Reddy, Organic matter determination. In: Engineering properties of soils based on laboratory testing, Illinois, Chicago. Chicago, Illinois: Department of Civil and Materials Engineering University of Illinois at Chicago, (2002) 13-19
37. Y. Mao, S. Sang, S. Liu, J. Jia, *Comptes Rendus Biologies* **337** (2014) 332 (https://doi.org/10.1016/j.crvi.2014.02.008)
38. S. R. Oliva, A .J. F. Espinosa, *Microchem. J.* **86** (2007) 131 (https://doi.org/10.1016/j.microc.2007.01.003)
39. E. O. Fagbote, E. O. Olanipekun, *Am.–Euras. J. Sci. Res.* **5** (2010) 241 (https://idosi.org/aejsr/5(4)10/4.pdf)

40. A. Enuneku, E. Biose, L. Ezemonye, *J. Env. Chem. Eng.* **5** (2017) 2773 (https://doi.org/10.1016/j.jece.2017.05.019)
41. A. Christou, C. P. Theologides, C. Costa, I. K. Kalavrouziotis, S. P. Varnavas, *J. Geochem. Exp.* **178** (2017) 16 (https://doi.org/10.1016/j.gexplo.2017.03.012)
42. R. E. Mendoza, I. V. García, L. de Cabo, C. F. Weigandt, A. F. de Iorio, *Sci. Tot. Env.* **505** (2015) 555 (https://doi.org/10.1016/j.scitotenv.2014.09.105)
43. J. Nouri, B. Lorestani, N. Yousefi, N. Khorasani, A. H. Hasani, F. Seif, M. Cheraghi, *Env. Earth Sci.* **62** (2011) 639 (https://doi.org/10.1007/s12665-010-0553-z)
44. A. A. Radojevic, S. M. Serbula, T. S. Kalinovic, J. V. Kalinovic, M. M. Steharnik, J. V. Petrovic, J. S. Milosavljevic, *Env. Sci. Poll. Res.* **24** (2017) 10326 (https://doi.org/10.1007/s11356-017-8520-9)
45. P. J. C. Favas, J. Pratas, M. N. V. Prasad, *Int. J. Env. Sci. Tech.* **10** (2013) 809 (https://doi.org/10.1007/s13762-012-0115-x)
46. D. Yildirim, A. Sasmaz, *J. Geochem. Expl.* **182** (2017) 228 (https://doi.org/10.1016/j.gexplo.2016.11.005)
47. D. Marbaniang, S. S. Chaturve*, Int. J. Sci. Res. Manag. (IJSRM)*, **2** (2014) 965 (https://ijsrm.net/index.php/ijsrm/article/view/668)
48. S. Shiyab, *Agriculture* **8** (2018) 29 (https://doi.org/10.3390/agriculture8020029)
49. Y. Mao, S. Sang, S. Liu, J. Jia, *Comptes Rendus Biologies* **337** (2014) 332 (https://doi.org/10.1016/j.crvi.2014.02.008)
50. USDA. Soil quality information sheet, Soil quality indicators: Organic matter. Washington D.C.: United States Department of Agriculture (USDA), Natural Resources Conservation Service (NRCS) (1996)
51. G. Du Laing, D. R. J. Vanthuyne, B. Vandecasteele, F. M. G. Tack, M. G. Verloo, *Environ. Pollut.* **147** (2007) 615 (https://doi.org/10.1016/j.envpol.2006.10.004)
52. F. R. Zeng, S. Ali, H. T. Zhang, Y. B. Ouyang, B. Y. Qiu, F. B. Wu, G. P. Zhang, *Environ. Pollut.* **159** (2011) 84 (https://doi.org/10.1016/j.envpol.2010.09.019)
53. S. Bravo, J. A. Amorós, C. Pérez-de-los-Reyes, F. J. García, M. M. Moreno, M. Sánchez-Ormeño, P. Higueras, *J. Geochem. Expl.* **174** (2017) 79 (https://doi.org/10.1016/j.gexplo.2015.12.012)
54. USDA, Soil Quality Indicators: pH. Soil quality information sheet. Natural resources conservation service, U.S. Department of agriculture, (1998)
55. Uredba br. 30/2018-50; UREDBU o graničnim vrednostima zagađujućih, štetnih i opasnih materija u zemljištu 30/2018-50. „Službeni glasnik Republike Srbije" (2018)
56. A. Kabata-Pendias Trace elements in soils and plants (4th ed.) CRC Press, Boca Raton, Florida, (2010) (https://doi.org/10.1201/b10158)
57. A.Kabata-Pendias, H. Pendias, Trace Elements in Soil and Plants (3rd ed.), Boca Raton: CRC Press, (2000) (https://doi.org/10.1201/9781420039900)
58. WHO. WHO guidelines for assessing quality of herbal medicines with reference to contaminants and residues. Geneva: World Health Organization (2007)
59. M. Pająk, W. Halecki, M. Gąsiorek, *Chemosphere* **168** (2017) 851 (https://doi.org/10.1016/j.chemosphere.2016.10.125).

Journal of the Serbian Chemical Society
JSCS-info@shd.org.rs • www.shd.org.rs/JSCS
J. Serb. Chem. Soc. *89* (12) 1647–1659 (2024)
JSCS–5812
Original scientific paper
Published 11 November, 2024

Potentially toxic elements in pikeperch (*Sander lucioperca* L.) from the Gruža reservoir: Health risk assessment related to fish consumption by the general population and fishermen

ALEKSANDRA M. MILOŠKOVIĆ[1]*, MILENA D. RADENKOVIĆ[2], NATAŠA M. KOJADINOVIĆ[2], TIJANA Z. VELIČKOVIĆ[2], SIMONA R. ĐURETANOVIĆ[2] and VLADICA M. SIMIĆ[2]

[1]*University of Kragujevac, Institute for Information Technologies, Department of Sciences, Kragujevac, Serbia and* [2]*University of Kragujevac, Faculty of Sciences, Institute of Biology and Ecology, Kragujevac, Serbia*

(Received 10 January, revised 17 February, accepted 6 April 2024)

Abstract: The aim was to evaluate concentrations of 14 potentially toxic elements in three tissues (muscle, liver and gills) of pikeperch (*Sander lucioperca*) and to assess health risk (the potential non-cancerogenic – tTotal target hazard quotient (*TTHQ*) and cancerogenic – target carcinogenic risk factor (*TR*) health risk) associated with the consumption of pikeperch from the Gruža Reservoir by the general population and fishermen. A value of Fulton's condition factor (*CF*) of less than one in our study indicated the poor general health of pikeperch. According to metal pollution index (*MPI*), the liver was exposed to the highest pressure of metal pollution. Levels of elements were lower than the national levels and international threshold levels, thus suggested a very likely absence of contamination risk of fish with elements in the Gruža Reservoir. Higher *TTHQ* was observed for fishermen (0.25) compared to the general population (0.20). Higher value of *TR* for As compared to *TR* for Pb was detected, both for the general population and for fishermen. In general, there was no risk to human health from pikeperch consumption, but fishermen were at slightly higher health risk to develop cancer if they consume pikeperch meat compared to the general population.

Keywords: water supply reservoir; piscivore fish; fish tissues; Serbia.

INTRODUCTION

Numerous health benefits from consuming fish that provide many essential nutrients such as high-value proteins, various vitamins and minerals and polyunsaturated omega-3 fatty acids, and the danger of excessive intake of potentially

* Corresponding author. E-mail: aleksandra@uni.kg.ac.rs
https://doi.org/10.2298/JSC240110044M

toxic elements, such as arsenic, mercury, cadmium and lead, due to the consumption of contaminated fish meat are in confrontation.[1] Fish and fish products are among the food categories that contribute most to human exposure to dietary contaminants.[2] In an era where the emphasis is on healthier principles in human nutrition based on fish consumption instead of other types of meat, it is important to assess the risk of potentially toxic elements (PTEs) of the fish used in the human diet.

The globally present problem of PTEs water pollution has not bypassed Serbia, and Teodorović[3] highlights a large number of „hot spots“ of extreme pollution. Among aquatic biota, fish species are the most sensitive taxa to the long-term effects of pollution.[4] The uptake and bioaccumulation of PTEs in fish depend on the biological characteristics of fish (*e.g.*, length and weight, age, behaviour or nutrition), the properties of PTEs, as well as properties of aquatic ecosystems.[5,6] Inland waters are sinks for pollutants (urban, industrial, and agricultural runoff), and according to Brönmark and Hansson[7] stagnant waters (reservoirs) are usually impacted by PTEs due to point sources. Lentic ecosystems (*i.e.*, rivers) often carry concentrations of PTEs under detection limits compared to lotic (*i.e.*, reservoirs).[8] The problem of PTEs pollution is more present in reservoirs due to lower self-purification capacity and pollutant dispersion in those ecosystems.[9]

Gruža Reservoir is located in central Serbia. This reservoir was formed by building a dam on the Gruža River in 1984, with the main purpose of supplying drinking water to the city of Kragujevac and its surroundings. Contradictory, the reservoir is also used for recreational purposes. It represents the largest water surface in Central Serbia, with an area of 934 ha. With a low water depth (average reservoir depth of 6.5 m), more than two-thirds of the reservoir has the characteristics of a lowland reservoir.[10] The maximum depth of the reservoir is 31 m. The reservoir suffers a strong anthropogenic influence. It is surrounded by an agricultural area where agricultural measures in the form of pesticides and herbicides are constantly applied. The reservoir also receives unprocessed wastewater from illegally built surrounding touristic settlements.

A study on the accumulation of Fe, Pb, Cd, Cu, Mn, Hg and As in water, sediment, five macrophytes (*Typha angustifolia*, *Iris pseudacorus*, *Polygonum amphybium*, *Myriophyllum spicatum* and *Lemna gibba*) and muscle tissue of five fish species (*Sander lucioperca*, *Abramis brama*, *Carassius gibelio*, *Silurus glanis* and *Arystichtys nobilis*) has already been carried out in order to investigate the level of pollution in the reservoir.[11] The results of this study indicated higher concentrations of all examined elements in sediment than in water. Among the examined fish species, pikeperch (*Sander lucioperca*) showed the highest tendency to accumulate Pb and Hg in muscle tissue. The lack of data on the distribution of PTEs in tissues of pikeperch as the most valuable fish species in Gruža

Reservoir, as well as the potential health risks, is the reason for conducting our research.

Widely distributed in Europe and Asia pikeperch (*Sander lucioperca* L.) is an indigenous fish of the Danube basin.[12] As a common piscivore in fish communities of many European lakes with low water transparency,[13] it also inhabits almost all eutrophic lakes in Serbia. As a member of the first quality group, pikeperch is an extremely valued fish species in Serbia.[12,14] Additionally, pikeperch is highly desirable for human consumption due to its nutritional characteristics, including the composition of proteins and fatty acids and low-fat content (1–2 %) in muscle tissue.[15]

The fish catch by recreational fishermen is 1.5 higher than commercial fishing catch in Serbia.[16] When it comes to pikeperch, there is also a decline in commercial fishing. On the other hand, this species is particularly interesting for recreational fishermen. Illegal fishing of this species is also evident in the Gruža Reservoir, due to the meat's quality and high market price. Pikeperch is an important fish species in the diet, and certainly the entire catch from the Gruža Reservoir is used for human consumption.

Having in mind all of the above, this study aimed to evaluate in more detail concentrations of Al, As, Cd, Co, Cr, Cu, Fe, Hg, Mn, Ni, Pb, Se, Sn and Zn in three tissues (muscle, liver and gills) of pikeperch. Also, the main aim of this study was to assess health risks (the potential non-cancerogenic *TTHQ* and cancerogenic *TR* health risk) associated with the consumption of pikeperch from the Gruža Reservoir by the general population and fishermen.

EXPERIMENTAL

Fish sampling and sample preparation

The field study was conducted at the Gruža Reservoir in central Serbia in the autumn of 2013. The sampling site coordinates are 43.927888 N, 20.678524E (Fig. 1).

Fish (n = 20) were sampled using standing gillnets (50 m–30 mm mesh size, 130 m–50 mm mesh size, 100 m–100 mm mesh size) that were left overnight. Immediately after removing the nets from the water, each pikeperch individual was sacrificed with a quick blow to the head and then dissected. Before dissection, total length (*TL*; to the nearest mm) and body weight (*BW*; to the nearest g) were measured. The evaluation of fish health was done using Fulton's condition factor (*CF*) with the following formula by Ricker:[17]

$$CF = 100BW / TL^3 \quad (1)$$

Fish dissection was done with a decontaminated ceramic knife. Tissue samples (right dorsal muscle below the dorsal fin, right gills – second arch and liver) were washed with distilled water and transported on ice in a portable hand-held refrigerator to the laboratory.

In the laboratory, samples were weighed using an electronic scale (accuracy ±0.01 g) and stored at –20 °C prior to analysis. Before digestion in microwave Christ Alpha 2-4 LD, Harz, Germany, samples were dried in a lyophilizer Christ Alpha 2-4 LD, Harz, Germany, and measured one more time. Dried sample portions between 0.3 and 0.5 g were digested with a mixture of 65 % nitric acid and 30 % hydrogen peroxide (Suprapur®, Merck, Darmstadt, Ger-

many, 10:2 volume ratio) at 200 °C for 20 min. After cooling to room temperature and without filtration, the solution was diluted to a fixed volume of 25 ml with ultrapure water.

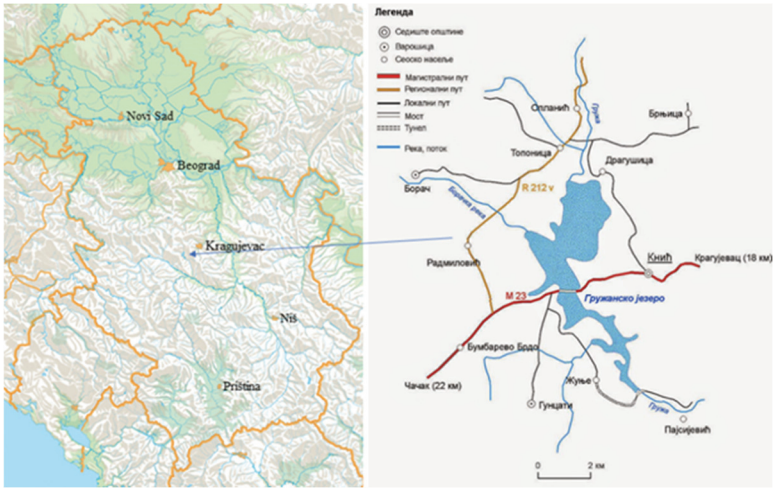

Fig. 1. Map of the sampling site (43.927888N, 20.678524E) at the Gruža Reservoir.

Potentially toxic element analysis

The concentration of elements in tissues of pikeperch was measured using an inductively-coupled plasma optical emission spectrometry (ICP-OES), using a Thermo Fisher Scientific iCAP 6500 Duo ICP (Cambridge, UK). The following wavelengths were used for the ICP-OES analysis (nm): Al 391.402, As 188.032, Cd 226.602, Co 221.618, Cr 204.542, Cu 322.764, Fe 257.921, Hg 183.940, Mn 260.353, Ni 234.606, Pb 222.354, Se 199.093, Sn 245.162 and Zn 207.194. Standard muscle reference material (DORM-4, National Research Council of Canada) was digested and analyzed in triplicate to support quality assurance and control. The following assigned/measured values for DORM-4 reference material in mg kg^{-1} are given in Table I. Recovery ranged from 95.6 to 107.14 %.

TABLE I. Certified values of reference material DORM-4 and values experimentally obtained. Data are mean ± *SD*

Element	Certified values, mg kg^{-1}	Results obtained, mg kg^{-1}	Recovery, %
As	6.80±0.64	6.62±0.48	97.35
Cd	0.306±0.15	0.323±0.019	105.56
Cr	15.9±0.9	15.20±0.4	95.60
Fe	341±27	333.96±25.87	97.93
Pb	0.416±0.053	0.443±0.011	106.49
Hg	0.410±0.055	0.400±0.064	97.56
Ni	1.36±0.22	1.35±0.45	99.26
Se	3.56±0.34	3.61±0.59	101.40
Sn	0.056±0.010	0.060±0.013	107.14

Mean values and standard deviations were calculated for each group, and element concentrations were expressed as mg kg^{-1} dry weight (dw). These concentrations were recal-

culated to wet weight (mg kg^{-1}) element concentrations, which were used to calculate the metal pollution index (*MPI*), compare the concentrations of Cd, Hg, Pb, As, Cu and Zn in fish muscles with maximum permissible concentrations (*MPC*) in fish meat determined by the national legislation of Serbia[18] and the European Union,[19] and to assess the risk to human health. According to these legislations, the MPCs for As, Cd, Cu, Hg, Pb and Zn are 2.0, 0.05, 30.0, 0.50, 0.30, and 100.0 mg kg^{-1} ww, respectively.

*Metal pollution index (*MPI*)*

The *MPI* was calculated to compare the total metals content of fish muscles, gills and liver with each other using the following equation by Usero *et al.*:[20]

$$MPI = (c_1\ c_2\ \cdots c_n)^{1/n} \tag{2}$$

where *c* is the concentration of the metal *n* in the sample (mg kg^{-1}).

Liver/muscle Hg index – L_{Hg}/M_{Hg}

The liver/muscle Hg index was calculated as the ratio of the concentration of Hg in the liver and muscles:[21]

$$L_{\mathrm{Hg}} / M_{\mathrm{Hg}} = CL(\mathrm{Hg}) / CM(\mathrm{Hg}) \tag{3}$$

Se:Hg mole ratio

The Se:Hg mole ratio was calculated using the method of Burger *et al.*[26] The molar concentration of Hg was calculated by dividing the concentration of Hg (in mg kg^{-1}) from muscle tissue by the molecular weight of Hg (200.59). The molar concentration of Se was calculated by dividing the concentration of Se (in mg kg^{-1}) from muscle tissue by the molecular weight of Se (78.9).

Health risk assessments

Target hazard quotient – THQ. The *THQ*, a methodology taken from the US EPA Region III Risk-based Concentration table,[22] is described by the following equation:

$$THQ = 10^{-3} EF \times ED \times FIR \times C / (RFD \times WAB \times TA) \tag{4}$$

where *EF* is the exposure frequency (365 days/year); *ED* is the exposure duration (70 years), equivalent to the average lifetime; *FIR* is the food ingestion rate for freshwater fish for Serbia – 20 g/person per day for the general population and 25 g/person per day for fishermen;[23] *C* is the element concentration in pikeperch (mg kg^{-1}); *RFD* is the oral reference dose (Hg = 0.0005, Cd = 0.001, Pb = 0.004, Cu = 0.04, Zn = 0.3, Cr = 1.5, Mn = 0.14, Al = 0.0004, As = 0.0003, Fe = 0.04, Co = 0.0003, Ni = 0.02 mg kg^{-1} per day);[22,24,25] *WAB* is the average body weight of an adult (70 kg); and *TA* is the average exposure time (365 days/year×*ED*).

Total *THQ* (*TTHQ*) was calculated using the following formula:

$$TTHQ = \Sigma THQ \tag{5}$$

Target carcinogenic risk factor – TR. The target carcinogenic risk factor (*TR*) for arsenic and lead was estimated using the equation:

$$TR = 10^{-3} EF \times ED \times FIR \times C \times CSFo / (WAB \times TA) \tag{6}$$

where *CSFo* is the oral carcinogenic slope factor (mg kg^{-1} per day) which is 1.5 for As and 0.0085 for Pb.[22]

Statistical analysis

All values are expressed as mean(s) ± standard deviation (*SD*). At the beginning of the statistical analysis normality of data was tested using the Shapiro-Wilk test. In cases when data followed a normal distribution, we tested significant differences among groups using the one-way ANOVA, followed by Tukey's HSD posthoc test. On the contrary, we used the non-parametric Kruskal–Wallis *H* test, followed by the Mann–Whitney *U* test to assess differences among investigated groups. The significance level (α) was at 5 %. All analyses were carried out using the SPSS 19.0 statistical package program for Windows (SPSS Inc., Chicago, IL, USA).

RESULTS AND DISCUSSION

The weight of the pikeperch specimens examined was 2,158.00±767.13 g, while the total length was 58.40±7.51 cm. The CF was 0.87±0.16. CF factor, as a measure of fish health, can be considered as a response to the quality of the environment. The *CF* value of less than one in our study indicates the poor general health of pikeperch in the Gruža Reservoir. According to Lafamme *et al.*,[27] Rajotte and Coutre[28] and Zhelev *et al.*[29] *CF* decline was determined at highly contaminated sites. On the other hand, Kroon *et al.*[30] pointed out that *CF* as a biomarker should be examined in terms of its specificity and suitability. Overall, the value of the *CF* factor in this study can be seen as the first warning alarm of poor environmental conditions in the Gruža Reservoir. However, we cannot single out PTEs as the main and only reason for this condition.

The highest concentration of Hg was observed in muscle, the highest concentrations of As, Cd, Co, Cu, Fe, Se and Zn in the liver, while the highest concentrations of Al, Cr, Mn, Ni, Pb and Sn were detected in the gills (Table II). On the contrary, the lowest concentrations of Cd, Co, Cr, Cu, Fe, Mn, Se, Sn and Zn in the muscle, the lowest concentrations of Al, Ni and Pb in the liver, as well as the lowest concentrations of As and Hg in the gills were detected. Statistical tests showed no significant differences between pikeperch tissues in terms of Pb and Cr concentrations. A significant difference was recorded between all pikeperch tissues regarding Co, Cu, Fe, Ni, Se and Zn concentrations (Table II). Muscle tissue contained significantly higher concentrations of Hg and significantly lower concentrations of Mn and Se compared to the other two tissues. Gills contained significantly higher concentrations of Al, and liver had significantly higher concentrations of As and Cd compared to the other two tissues.

Pikeperch muscle was the tissue with the lowest potential for PTEs bioaccumulation, which is confirmed by all, to date, performed studies on pikeperch fish species in Serbia.[15,31–35] According to Meena *et al.*,[36] the reason may be a low level of binding proteins in the muscle tissue. On the other hand, Hg has a high potential for bioaccumulation and biomagnification in food chains.[37,38] Predator fish species show important accumulation and indicator potential for Hg, with the highest concentrations in muscle tissue.[39,40] As the top predator in the

Gruža Reservoir, pikeperch accumulated Hg in significantly higher concentrations in muscle tissue compared to the other two tissues.

TABLE II. Element concentrations (mg kg^{-1} dw) and metal pollution index (*MPI*) in muscle, liver and gills of pikeperch (*Sander lucioperca*) in Gruža Reservoir. Values are presented as mean ± *SD*; different letters in row denote significant differences in element concentrations among the pikeperch tissues, $p < 0.05$

Element	Muscle	Liver	Gills
Al	1.917 ± 0.607^{a}	1.098 ± 0.577^{a}	47.068 ± 26.512^{b}
As	0.766 ± 0.149^{a}	1.798 ± 0.302^{b}	0.630 ± 0.195^{a}
Cd	0.016 ± 0.004^{a}	0.312 ± 0.126^{b}	0.019 ± 0.009^{a}
Co	0.005 ± 0.002^{a}	0.431 ± 0.128^{c}	0.091 ± 0.035^{b}
Cr	0.719 ± 0.318	1.204 ± 0.435	1.283 ± 0.762
Cu	0.438 ± 0.080^{a}	7.947 ± 0.802^{c}	2.465 ± 0.711^{b}
Fe	6.391 ± 3.863^{a}	436.389 ± 212.493^{c}	222.349 ± 80.996^{b}
Hg	0.280 ± 0.090^{b}	0.026 ± 0.021^{a}	0.001 ± 0.001^{a}
Mn	0.359 ± 0.134^{a}	4.613 ± 0.927^{b}	4.657 ± 2.287^{b}
Ni	0.084 ± 0.080^{b}	0.015 ± 0.013^{a}	0.330 ± 0.131^{c}
Pb	0.870 ± 0.438	0.756 ± 0.312	1.005 ± 0.482
Se	1.163 ± 0.191^{a}	3.66 ± 0.494^{c}	1.663 ± 0.383^{b}
Sn	0.020 ± 0.007^{a}	0.697 ± 0.059^{b}	1.226 ± 0.531^{b}
Zn	17.713 ± 3.094^{a}	78.866 ± 9.414^{c}	41.464 ± 9.491^{b}
MPI	0.30	1.31	0.69

Se:Hg mole ratio in pikeperch from Gruža Reservoir was the highest in the gills (4,227.68), followed by the liver (353.85) and the lowest in the muscle tissue (10.35). Additionally, Se:Hg ratio in all three tissues was much higher than 1. This indicated that pikeperches from Gruža Reservoir were protected against Hg toxicity, since Se:Hg molar ratio that is above 1 protects against toxicity of this element.[41,42]

The highest concentrations of Cu, Fe and Zn were found in the liver of pikeperch, which agrees with results from studies by Mazej *et al.*[43] and Kenšová *et al.*[44] On the other hand, lower concentration of Cu, Fe, Zn and Mn in muscle tissue compared to the other two tissues is in accordance with the findings of Subotić *et al.*[45] who stated that low level of these elements reflects the low level of binding proteins in this tissue.

Higher concentrations of Cd in pikeperch liver can be explained by the fact that this element has a very long elimination half-time, and therefore accumulates in large amounts in parenchymatous tissues such as liver.[46] Our results are not in accordance with the findings of Altındağ and Yiğit[47] and Mazej *et al.*,[43] who found no difference between Cd levels in the gills and liver. Given that the Gruža Reservoir is surrounded by agricultural land, our results are in agreement with the observation of Arumugam *et al.*[48] regarding the anthropogenic origin of Cd

and As from agricultural fields, which dissolved in the water column remains for a long time in the environment.

According to Zhou *et al.*[49] and Ruelas-Inzunza *et al.*[50] gills are the organ with the highest tendency to accumulate Pb, which was also confirmed in our study. However the difference between the three tissues was not significant. The presence of Pb in the tissues of *S. lucioperca* is probably due to the traffic on the main road on the bridge that crosses the reservoir and the presence of motor boats on the surface of the reservoir.

Concentrations of Hg and As in the muscle tissue of pikeperch in this study were higher than in the previous study[11] and this can be explained by the fish size because the fish specimens in this study are much larger.[51]

In comparison with the national legislation of Serbia[18] and the legislation of the European Union,[19] concentrations of As, Cd, Cu, Hg, Pb and Zn in muscles of all pikeperch individuals were below the prescribed *MPC*s. The fact that the levels of elements As, Cd, Cu, Hg, Pb and Zn were lower than the national and international threshold levels suggest a very likely absence of risk of contamination of fish with elements in the Gruža Reservoir. In the reservoirs Zlatar,[35] Bovan[32,52] and Garaši[15] concentrations of elements in the muscle of the pikeperch were also below the *MPC*s. A recent study of Nikolić *et al.*[53] reported concentrations of Hg and Cd above the *MPC* in the muscle of pikeperch in some 4^+ age group and emphasized biomagnification of these elements.

According to *MPI*, the liver was exposed to the highest pressure of metal pollution (Table II). The lowest *MPI* value was recorded for muscle tissue. According to *MPI*, the gills were exposed to the higher pressure of metal pollution than muscle tissue, probably due to direct contact of gills with pollutants in the water.[54] This was also recorded for the same species in the Garaši Reservoir.[15,53] The liver of pikeperch was exposed to the highest pressure of metal pollution (highest *MPI*) as seen in pikeperch samples from the Zlatar Reservoir.[35] *MPI* values recorded in this study for all three pikeperch tissues were lower than in the same tissues of pikeperch from the Garaši Reservoir,[15,53] but higher than in the tissues of pikeperch from the Zlatar Reservoir.[35]

Liver/muscle Hg index was 0.093. According to Havelková *et al.*,[21] in fish from heavily contaminated localities, the target organ for Hg accumulation is liver, while in fish from slightly contaminated localities, the main target organ for Hg accumulation is muscle. Consequently, a higher liver/muscle Hg index value is high in heavily contaminated sites. In our study, liver/muscle index value was low, indicating a slightly contaminated site. According to the above, we can conclude that Gruža is still a slightly polluted reservoir with Hg. Compared with pikeperch from the other researched reservoirs in Serbia, the concentration of Hg in the muscle tissue of pikeperch from Gruža Reservoir was higher than in the

muscle tissue of pikeperch from Bovan Reservoir,[32] but lower than in the muscle of pikeperch from Garaši Reservoir[15] and Zlatar Reservoir.[35]

Higher *TTHQ* was observed for fishermen (0.25) compared to the general population (0.20), Fig. 2. Arsenic had the highest contribution to the overall *TTHQ* value, both in the general population and fishermen. The contribution of As to the overall *TTHQ* value was 71.40 %. According to the results of *THQ* for all the elements as well as *TTHQ*, the general population is under lower health risk compared to the fishermen.

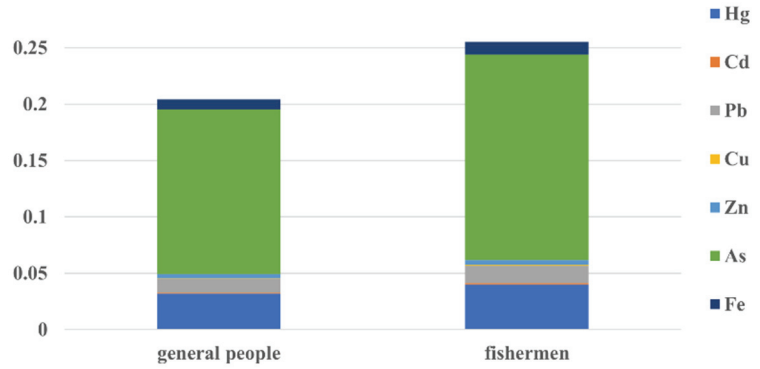

Fig. 2. Total elemental *THQ* values due to consumption of pikeperch for general population and fishermen.

The *TTHQ* values ranged from 0.20 to 0.25, which is much lower than the threshold value (*TTHQ* < 1), indicating the absence of significant noncarcinogenic risk.[55] The values of *TTHQ* in our study were lower than in the study of the Garaši Reservoir, with values above 0.5[15] and the Zlatar Reservoir with values of 0.297 and 0.405.[35] In the two mentioned studies, the major contributor to *TTHQ* was Hg. According to the authors, the reason may be the lower reference dose for this element compared to other elements. In our study, the main contributor to *TTHQ* was As. Since agricultural activities are regularly carried out near the reservoir, we can assume that As originates from the uncontrolled use of pesticides and herbicides.

Higher values of *TR* for As compared to TR for Pb were detected, both for the general population and for fishermen (Table III). Fishermen are more susceptible to develop cancer, if they consume pikeperch meat, compared to the general population.

No cancerogenic risk due to intake of As and Pb from the meat of pikeperch from the Gruža Reservoir was recorded since the TRs for these elements were lower from 10^{-6} or were equal to 10^{-6}.[56] Compared to our results, a lower risk of cancer development due to As and Pb intake from pikeperch meat was recorded

in the Garaši Reservoir.[15] Also, a lower risk of developing cancer due to intake of As from pikeperch meat was recorded in the Zlatar Reservoir.[35]

TABLE III. Target carcinogenic risk factor ($TR \times 10^6$) of As and Pb for the general population and fishermen due to consumption of pikeperch (*Sander lucioperca*)

Group	As	Pb
General population	1.97	4.20
Fishermen	2.46	5.25

CONCLUSION

Based on the obtained results, we can conclude that despite obvious anthropogenic pressure in Gruža Reservoir and elevated concentrations of As and Hg in water,[11] pikeperch did not show contamination with PTEs. *CF* value indicated the poor general health of pikeperches indicating poor water quality. However, none of the elements exceeded *MPC*s and there was no noncancerogenic and cancerogenic risk to humans' health. Meat of pikeperch can be safely used by the general population and fishermen. Still, fishermen are at slightly higher health risk to develop cancer if they consume pikeperch meat compared to the general population. Due to the absences of analysis of age, gender and diet of pikeperch in this study, the conclusions of this study should be viewed with caution. Further studies including this analysis are needed.

Acknowledgement. The study was supported by a Grant (Agreement No. 451-03-66/ /2024-03/200378) funded by the Serbian Ministry of Science, Technological Development and Innovation.

ИЗВОД

ПОТЕНЦИЈАЛНО ТОКСИЧНИ ЕЛЕМЕНТИ У СМУЂУ (*Sander lucioperca* L.) ИЗ АКУМУЛАЦИЈЕ ГРУЖА: ПРОЦЕНА ЗДРАВСТВЕНОГ РИЗИКА ОПШТЕ ПОПУЛАЦИЈЕ И РИБАРА УСЛЕД КОНЗУМАЦИЈЕ

АЛЕКСАНДРА М. МИЛОШКОВИЋ[1], МИЛЕНА Д. РАДЕНКОВИЋ[2], НАТАША М. КОЈАДИНОВИЋ[2], ТИЈАНА З. ВЕЛИЧКОВИЋ[2], СИМОНА Р. ЂУРЕТАНОВИЋ[2] и ВЛАДИЦА М. СИМИЋ[2]

[1]Универзитет у Крагујевцу, Институт за информационе технологије Крагујевац, Департман за природно-математичке науке, Крагујевац и [2]Универзитет у Крагујевцу, Природно–математички факултет, Институт за биологију и екологију, Крагујевац

Циљ ове студије био је да се одреде концентрације 14 потенцијално токсичних елемената у три ткива (мишићи, јетра и шкрге) смуђа (*Sander lucioperca*) и да се процени здравствени ризик (потенцијално неканцерогени ризик – укупни циљни ризик од опасности (енгл. Total target hazard quotient – *TTHQ*) и канцерогени ризик - циљни канцерогени фактор ризика (енгл. Target carcinogenic risk factor – *TR*) повезан са конзумацијом смуђа из акумулације Гружа. Вредност Фултоновог кондиционог индекса мања од један у нашој студији указује на лоше опште здравствено стање смуђа. Према индексу загађења металима (енгл. metal pollution index – *MPI*) јетра је била изложена највишем притиску загађења металима. Концентрације елемената су биле ниже од прописаних националним

и међународним законодавством, указујући на непостојање ризика услед конзумације контаминиране рибе из акумулације Гружа. Примећен је већи *TTHQ* за рибаре (0,25) у односу на општу популацију (0,20). Утврђена је већа вредност *TR* за As у поређењу са *TR* за Pb, како за општу популацију тако и за рибаре. Генерално, није забележен ризик за здравље људи услед конзумације смуђа, али су рибари под незнатно већим здравственим ризиком да развију рак у поређењу са општом популацијом.

(Примљено 10. јануара, ревидирано 17. фебруара, прихваћено 6. априла 2024)

REFERENCES

1. A. C. Bosch, B. O'Neill, G. O. Sigge, S. E. Kerwath, L. C. Hoffman, *J. Sci. Food Agr.* **96** (2015) 32 (https://doi.org/10.1002/jsfa.7360)
2. WHO - World Health Organisation, Brief guide to analytical methods for measuring lead in blood. Inter-Organization Programme for the Sound Management of Chemicals 2011
3. I. Teodorović I, *Environ. Sci. Pollut. Res.* **16** (2009) 123 (https://doi.org/10.1007/s11356-009-0152-2)
4. N. Collin, A. Maceda-Veiga, N. Flor-Arnau, J. Mora, P. Fortuño, C. Vieira, A. de Sostoa, *Ecotox. Environ. Saf.* **132** (2016) 295 (https://doi.org/10.1016/j.ecoenv.2016.06.017)
5. M.G.M. Alam, A. Tanaka, G Allinson, L.J.B. Laurenson, F. Stagnitti, E.T. Snow, *Ecotox. Environ. Saf.* **53** (2002) 348 (https://doi.org/10.1016/S0147-6513(02)00012-X)
6. J. Mwamburi, *Lakes and Reservoirs: Research Management* **18** (2013) 329 (https://doi.org/10.1111/lre.12040)
7. C. Brönmark, L. A. Hansson, *Environ. Conserv.* **29** (2002) 290 (https://doi.org/10.1017/S0376892902000218)
8. E. Has-Schön, I Bogut, R. Vuković, D. Galović, A. Bogut, J Horvatić J, *Chemosphere* **135** (2015) 289 (https://doi.org/10.1016/j.chemosphere.2015.04.015)
9. P. K. Rai, *Int. J. Phytoremediat.* **12** (2010) 226 (https://doi.org/10.1080/15226510903563843)
10. B. Ranković, J. Radulović, I. Radojević, A. Ostojić, LJ. Čomić, *Ecol. Model.* **221** (2010) 1239 (https://doi.org/10.1016/j.ecolmodel.2009.12.023)
11. A. Milošković, S. Branković, V. Simić, S. Kovačević, M. Ćirković, D. Manojlović, *B. Environ. Contam. Tox.* **90** (2013) 563 (https://doi.org/10.1007/s00128-013-0969-8)
12. P. Simonović: *Ribe Srbije*, NNK International, Beograd, Biološki fakultet Univerziteta u Beogradu, Beograd, Zavod za zaštitu prirode Srbije. 2001
13. H. Dörner, S. Berg, L. Jacobsen, S. Hülsmann, M. Brojerg, A. Wagner, *Hydrobiologia* **506** (2003) 427 (https://doi.org/10.1023/B:HYDR.0000008608.22869.99)
14. M. Kottelat, J. Freyhof, *Handbook of European freshwater fishes,* Publications Kottelat, Cornol, Switzerland and Freyhof, Berlin, Germany. 2007
15. D. Nikolić, S. Skorić, V. Poleksić, B. Rašković, *Environ. Sci. Pollut. Res.* **28** (2021) 53700 (https://doi.org/10.1007/s11356-021-14526-w)
16. Statistical Office of the Republic of Serbia, Statistical Yearbook of the Republic of Serbia, 2022 (Accessed on July 20, 2023) (https://publikacije.stat.gov.rs/G2022/PdfE/G20222055.pdf)
17. W.E. Ricker: *Computation and interpretation of biological statistics of fish populations*, *Bulletin,* Fisheries Research Board of Canada (1975) ISBN 0662014405 (https://publications.gc.ca/site/eng/9.581563/publication.html)
18. *Official Gazette of the Republic of Serbia* (2018), Nos. 22/2018 & 90/ 2018
19. EC No. 1881/2006 of 19 December 2006 setting maximum levels for certain contaminants in foodstuffs (Text with EEA relevance), *Official Journal of the European*

Union No. 1881/2006 364 (2006) 5 (Accessed 14.03.2023) (https://eurlex.europa.eu/eli/reg/2006/1881/oj)
20. J. Usero, E. González-Regalado, I. Gracia, *Environ. Int.* **23** (199) 291 (https://doi.org/10.1016/S0160-4120(97)00030-5)
21. M. Havelková, L. Dušek, D. Némethová, G. Poleszczuk, Z Svobodová, *Sensors* **8** (2008) 4095 (https://doi.org/10.3390/s8074095)
22. US EPA, Risk-based concentration table. Philadelphia PA: United States Environmental Protection Agency, Washington DC, 2000
23. FAO (Food and Agriculture Organization), National Aquaculture Sector, 2005 (Accessed 16.03.2023) (http://www.fao.org/fshery/countrysector/en/)
24. US EPA, Mercury study report to Congress health effects of mercury and mercury compounds, vol. V. Washington (DC), United States Environmental Protection Agency, EPA-452/ R-97-007, 1997
25. FAO WHO, *National Research Council Recommended Dietary Allowances 10th Edition*, National Academy Press Washington, DC, 1989
26. J. Burger, C. Jeitner, M. Donio, T. Pittfield, M. Gochfeld, *Sci. Total Environ.* **443** (2013) 278 (https://doi.org/10.1016/j.scitotenv.2012.10.040)
27. J. S. Lafamme, Y. Couillard, G. C. Campbell, A. Hontela, *Can. J. Fish. Aquat. Sci.* **57** (2000) 1692 (https://cdnsciencepub.com/doi/abs/10.1139/f00-118)
28. J. W. Rajotte, P. Couture, *Can. J. Fish. Aquat. Sci.* **59** (2002) 1296 (https://cdnsciencepub.com/doi/abs/10.1139/f02-095)
29. Z. M. Zhelev, S. V. Tsonev, P. S. Boyadziev *Acta Zool. Bulgar.* **70** (2018) 547 (https://www.acta-zoologica-bulgarica.eu/downloads/acta-zoologica-bulgarica/2018/70-4-547-556.pdf)
30. F. Kroon, C. Streten, S. Harries, *PLoS One* **12** (2017) e0174762 (https://doi.org/10.1371/journal.pone.0174762)
31. S. Subotić, S. Spasić, Ž. Višnjić-Jeftić, A. Hegediš, A. Krpo-Ćetković, B. Mićković, S. Skorić, M. Lenhardt, *Ecotox. Environ. Saf.* **98** (2013) 196 (https://doi.org/10.1016/j.ecoenv.2013.08.020)
32. A. Milošković, B. Dojčinović, S. Simić, M. Pavlović, V. Simić, *Fresen. Environ. Bull.* **23** (2014) 1884 (https://hdl.handle.net/21.15107/rcub_cer_1591)
33. A. Milošković, B. Dojčinović, S. Kovačević, N. Radojković, M. Radenković, D. Milošević, V. Simić, *Environ. Sci. Pollut. Res.* **23** (2016) 9918 (https://doi.org/10.1007/s11356-016-6207-2)
34. D. A. Jovanović, R. V. Marković, V. B Teodorović, D. S. Šefer, M. P. Krstić, S. B. Radulović, J. S. Ivanović Ćirić, J. M. Janjić, M. Ž. Baltić, *Environ. Sci. Pollut. Res.* **12** (2017) 11383 (https://doi.org/10.1007/s11356-017-8783-1)
35. D. Nikolić, S. Skorić, B. Mićković, M. Nikčević, M. Smederevac-Lalić, V. Djikanović, *Environ. Sci. Pollut. Res.* **29** (2022) 50271 (https://doi.org/10.1007/s11356-022-19472-9)
36. R. A. A. Meena, P. Sathishkumar, F. Ameen, A. R. M. Yusoff, F. L. Gu, *Environ. Sci. Pollut. Res.* **25** (2018) 4134 (https://doi.org/10.1007/s11356-017-0966-2)
37. T. W. Clarkson, *Environ. Health Persp.* **100** (1993) 31 (https://doi.org/10.1289/ehp.9310031)
38. M. Gochfeld, *Ecotox. Environ. Sa.f* **56** (2003) 174 (https://doi.org/10.1016/S0147-6513(03)00060-5)
39. L. Dušek, Z. Svobodová, D. Janoušková, B. Vykusová, J. Jarkovský, R. Šmíd, P. Pavliš, *Ecotox. Environ. Saf.* **6** (2005) 256 (https://doi.org/10.1016/j.ecoenv.2004.11.007)

40. S. Zrnčić, D. Oraić, M. Ćaleta, Ž. Mihaljević, D. Zanella, N. Bilandžić, *Environ. Monit. Assess.* **185** (2013) 1189 (https://doi.org/10.1007/s10661-012-2625-x)
41. S. A. Peterson, N. V. C Ralston, P. D. Whanger, J. E. Oldfield, W. D. Mosher, *Environmental Bioindicators* **4** (2009) 318 (https://doi.org/10.1080/15555270903358428)
42. A. Cabañero, Y. Madrid, C. Cámara, *Biol. Trace Elem. Res.* **119** (2007) 195 (https://doi.org/10.1007/s12011-007-8007-5)
43. Z. Mazej, S. Sayegh-Petkovšek, B. Pokorny, *Arc. Environ. Con. Tox.* **58** (2010) 998 (https://doi.org/10.1007/s00244-009-9417-5)
44. R. Kenšová, O. Čelechovská, J. Doubravová, Z. Svobodová, *Acta Vet. Brno* **79** (2010) 335 (https://doi.org/10.2754/avb201079020335)
45. S. Subotić, Ž. Višnjić-Jeftić, S. Spasić, A. Hegediš, J. Krpo-Ćetković, M. Lenhardt, *Environ. Sci. Pollut. Res.* **20** (2013) 5309 (https://doi.org/10.1007/s11356-013-1522-3)
46. R. Cornelis, J. Caruso, H. Crews, K. Heumann, *Handbook of Elemental Speciation II. Species in the environment, food, medicine and occupational health*, Wiley, Chichester England, 2005
47. A. Altındağ, S. Yiğit, *Chemosphere* **60** (2005) 552 (https://doi.org/10.1016/j.chemosphere.2005.01.009)
48. A. Arumugam, J. Li, P. Krishnamurthy, Z. X. Jia, Z. Leng, N. Ramasamy, D. Du, *Environ. Sci. Pollut. Res.* **270** (2020) 19955 (https://doi.org/10.1007/s11356-020-08554-1)
49. H. Y. Zhou, R. Y. H. Cheung, K. M. Chan, M. H. Wong, *Water Research* **32** (1998) 3331 (https://doi.org/10.1016/S0043-1354(98)00115-8)
50. J. Ruelas-Inzunza, F. Páez-Osuna, D. García-Flores, *Environ. Monit. Assess.* **162** (2009) 251 (https://doi.org/10.1007/s10661-009-0793-0)
51. E. Zubcov, N. Zubcov, A. Ene, L. Biletchi, *Environ. Sci. Pollut. Res.* **19** (2012) 2238 (https://doi.org/10.1007/s11356-011-0728-5)
52. A. Milošković, V. Simić, *Pol. J. Environ. Stud.* **24** (2014) 199 (https://doi.org/10.15244/pjoes/24929)
53. D. Nikolić, V. Poleksić, A. Tasić, M. Smederevac-Lalić, V. Djikanović, B. Rašković, *Sustainability* **15** (2023) 11321 (https://doi.org/10.3390/su151411321)
54. P. B. Hamilton, G. Rolshausen, T. M. Uren Webster, C. R. Tyler, *Philosophical Transactions of the Royal Society of London Series B* **372** (2017) 20160042 (https://doi.org/10.1098/rstb.2016.0042)
55. N. Zheng, Q. Wang, X. Zhang, D. Zheng, Z. Zhang, S. Zhang, *Sci. Total Environ.* **387** (2007) 96 (https://doi.org/10.1016/j.scitotenv.2007.07.044)
56. M. S. Islam, M. K. Ahmed, M. Habibullah-Al-Mamun, K. N. Islam, M. Ibrahim, S. Masunaga, *Food Additives & Contaminants: Part A* **31** (2014) 1982 (https://doi.org/10.1080/19440049.2014.974686).

Journal of the Serbian Chemical Society
JSCS-info@shd.org.rs • www.shd.org.rs/JSCS
J. Serb. Chem. Soc. *89* (12) 1661–1673 (2024)
JSCS–5813
Original scientific paper
Published 9 November, 2024

Solid-phase extraction of estrogen hormones onto chemically modified carbon cryogel

DANIJELA B. PROKIĆ[1#]*, MARIJA M. VUKČEVIĆ[2#], MARINA M. MALETIĆ[1#], ANA M. KALIJADIS[3], JOVANKA N. PEJIĆ[4#], BILJANA M. BABIĆ[5] and TATJANA M. ĐURKIĆ[2#]

[1]Innovation Center of the Faculty of Technology and Metallurgy, Karnegijeva 4, 11000 Belgrade, Serbia, [2]Faculty of Technology and Metallurgy, University of Belgrade, Karnegijeva 4, 11000 Belgrade, Serbia, [3]Department of Materials, „Vinča" Institute of Nuclear Sciences – National Institute of the Republic of Serbia, University of Belgrade, Mike Petrovića Alasa 12–14, 11000 Belgrade, Serbia, [4]Institute for Chemistry, Technology and Metallurgy, University of Belgrade, Njegoševa 12, 11000 Belgrade, Serbia and [5]Institute of Physics – National Institute of the Republic of Serbia, University of Belgrade, Pregrevica 118, 11080 Belgrade, Serbia

(Received 10 March, revised 7 April, accepted 2 June 2024)

Abstract: This study introduces a novel solid-phase extraction (SPE) method utilizing pristine and chemically treated carbon cryogel (CC) as an adsorbent for the isolation and enrichment of estrogen hormones (estrone, 17*β*-estradiol, and 17*α*-ethinylestradiol) from water samples. High recovery values (82–95 %) were obtained after optimizing the SPE technique, which included adsorbent mass and chemical treatment, sample volume and pH, and elution solvent type and volume. The developed analytical method, based on SPE coupled with liquid chromatography–tandem mass spectrometry (LC–MS/MS), proves to be selective, efficient, and cost-effective for the determination of selected estrogens. The utilization of self-made cartridges with chemically modified CC produced results comparable to those obtained with commercial cartridges while employing significantly less material. Furthermore, the selectivity of the employed materials contributed to minor matrix effects. The optimized method was successfully applied to analyze estrogen hormones in groundwater, surface water, and wastewater samples, with the results highlighting the importance of monitoring these contaminants in the aquatic environment.

Keywords: estrogens; SPE; surface water; groundwater; waste water; liquid chromatography–tandem mass spectrometry.

* Corresponding author. E-mail: dprokic@tmf.bg.ac.rs
# Serbian Chemical Society member.
https://doi.org/10.2298/JSC240313055P

INTRODUCTION

Estrogen hormones are acknowledged as endocrine-disrupting compounds (EDCs) capable of disrupting the endocrine systems of both humans and animals, leading to adverse health effects.[1] Wastewater is the main route by which these hormones get into the environment. Existing wastewater treatment plants (WWTPs) struggle to entirely eliminate hormones, contributing to their pervasive presence in environmental water.[2] The presence of these compounds in the aquatic environment can affect fish sexual development and reproduction.[3,4] Long-term estrogen exposure also has negative effects, such as bioaccumulation in aquatic species, which can eventually reach people through the food chain.[3] Therefore, the removal of these substances from wastewater and their monitoring in the aquatic environment is becoming increasingly important.

Estrogens are generally present in the aquatic environment at very low concentrations (ng dm^{-3}), so their detection requires an efficient isolation and preconcentration method before analysis. This step is of crucial importance for the outcome of further analysis, especially when dealing with complex matrix samples where the components of interest are present at trace concentrations. Solid-phase extraction (SPE) is commonly used to enrich ambient water samples prior to analysis.[4–8] The choice of the adsorbent is essential in the application of the SPE technique since it affects parameters such as affinity, selectivity and extraction capacity.[9]

Due to their well-developed specific surface area, wide porosity range, and consequently high adsorption capacity, numerous carbon-based materials have been used as efficient adsorbents for the removal or extraction of different environmental pollutants from water.[10–12] Additionally, the surface of carbon materials can be easily tailored or modified by various treatments in order to improve the adsorption features of the examined materials for specific water pollutants.[13–15] Due to their easily controllable mesoporosity, carbon cryogel (CC) has become an attractive material for adsorption purposes.[10] By selecting the right precursor material and managing the synthesis settings, it is possible to customize the pore structure of CC.[16] The predominantly mesoporous structure of CC provides a fast transfer of adsorbate through the pore network, so this material has been used as an adsorbent for different organic and inorganic solutes from the liquid phase.[10,14,16]

Previously, it was shown that modified and unmodified CC have high efficiency in the removal of estrone (E1), 17β-estradiol (E2) and 17α-ethinylestradiol (EE2) from water, showing higher Langmuir adsorption capacities for all three hormones in comparison with carbonized and activated hydrothermal carbons, multi-walled carbon nanotubes, and activated carbon cloths.[14,15] The results also demonstrated that the matrix component of surface water, groundwater and

wastewater samples did not significantly affect the adsorption capacity of CC towards E1, E2 and EE2.[14]

The objectives of this study were to assess the possibility of using self-made cartridges packed with pristine and chemically modified CC as SPE adsorbents and to develop a new, reliable, efficient and cost-effective method for the determination of E1, E2 and EE2 from environmental water samples. Also, hormone recoveries obtained using the most efficient CC adsorbent were compared with those obtained by commercially available cartridges. To the best of our knowledge, CC material has not been used as an adsorbent for hormone extraction from water so far. The instrumental method used for hormone detection was liquid chromatography–tandem mass spectrometry (LC–MS/MS) with electrospray ionization. The optimized and validated method was applied to the analysis of real water samples.

EXPERIMENTAL

Material preparation

The CC was manufactured at the Vinča Institute of Nuclear Sciences, and a detailed synthesis procedure is described in the literature.[10] Briefly, a solution of resorcinol (R) and formaldehyde (F) with sodium carbonate as a basic catalyst was poured into a glass tube, sealed and gelled for 7 days. Wet RF gel was washed in t-butanol, pre-frozen (–30 °C) and freeze-dried for 24 h under a vacuum (0.4 mbar). The obtained RF cryogel was finally carbonized to 800 °C under a nitrogen atmosphere with a heating rate of 5 °C min^{-1} and cooled to room temperature. The resulting material was squashed into powder and stored closed in a PVC box.

Chemical modification of CC was carried out by heating a suspension of the material in HNO_3 or KOH water solution, and modified materials were labeled as CC/HNO_3 and CC/KOH, respectively. Applied treatment conditions during the chemical modification process are described in a previous paper.[14] Chemical modification with the mentioned agents leads to the formation and/or alternation of oxygen functional groups.[17,18] An increased amount of oxygen groups may enhance the adsorption efficiency of tested estrogens since these hormones possess hydroxyl groups, which may form hydrogen bonds on the adsorption surface.[15,19]

Solid-phase extraction

In order to obtain high recoveries of the SPE method, the following parameters were optimized: the mass of the adsorbent, the volume and initial pH value of the water samples, and the type and volume of the organic solvent for hormone elution. In addition, the possibility of improving the method through CC modification was investigated.

Initially, spiked water samples were prepared by spiking deionized water with a mixed hormone stock solution (5 mg dm^{-3} of each hormone in methanol) to a concentration of 2.5 μg dm^{-3} per hormone. The SPE cartridges (3 cm^3 volume) were made by packaging a selected amount of CC between two Teflon frits. The cartridges were conditioned by passing 5 cm^3 of a chosen organic solvent followed by 5 cm^3 of pH-adjusted deionized water. After conditioning, spiked water samples of the required volume and pH value were passed through the cartridges. Then, the cartridges were dried under vacuum for 10 min and eluted with a chosen organic solvent until the optimal eluent volume was achieved. The eluents were collected in

glass tubes, evaporated to dryness under N_2, and reconstituted in 1 cm^3 of the mobile phase. After reconstitution, all samples were vortexed and filtered through the polyvinylidene difluoride (PVDF) 0.45 μm filters into glass vials.

The optimal parameters of the extraction procedure were selected based on the highest recovery values obtained. The optimization process involved varying the adsorbent mass, using 20, 50 and 100 mg of material. Subsequently, the optimal volume of water samples was selected based on recoveries obtained by performing the extraction from 25, 50, 100 and 200 cm^3. To find an optimal pH value of water samples, extraction of selected hormones was carried out by using 20 mg of adsorbent and 200 cm^3 of water sample with an initial pH adjusted to 5, 6, 7, 8, 9, 10 and 11. An optimal organic elution solvent was selected according to SPE recoveries gained using methanol (MeOH), acetonitrile (ACN), ethyl acetate (EtOAc), a 1:1 volume ratio mixture of dichloromethane and methanol (DCM/MeOH) and a 1:1 volume ratio mixture of ethyl acetate and methanol (EtOAc/MeOH). Further optimization steps involved determining the appropriate eluent volume, with elution performed using 5, 10 and 15 cm^3 of the optimal organic solvent. In the final optimization step, three types of materials (CC, CC/ /HNO_3 and CC/KOH) were evaluated as potential adsorbents, maintaining the parameters optimized in previous steps. Additionally, recovery values gained using cartridges packed with the most efficient CC material were compared with the recoveries gained using commercially available cartridges: Supelclean Envi Carb, Supelclean Envi-18, Supelclean LC--SCX, Supelclean LC-18 (Sigma–Aldrich) and Oasis HLB (Waters, USA).

LC–MS/MS analysis

The concentrations of the hormones in the final extracts were measured by liquid chromatography coupled with tandem mass spectrometry. The separation of tested hormones was performed using a Surveyor LC system (Thermo Fisher Scientific, USA). The analytical column used for reverse-phase separation was an Agilent Zorbax Eclipse XDB-C18 column (75 mm×4.6 mm×3.5 μm). According to literary sources, a mixture of water, MeOH, and/or ACN is often utilized during LC–MS analysis of E1, E2 and EE2, with NH_4OH as a mobile phase modifier in negative mode and formic acid in positive mode.[7,20,21] During the optimization of the LC–MS method, we obtained the most stable and intense signals in positive mode, with the optimal mobile phase composition of 25 % formic acid (0.1 % water solution) and 75 % methanol. The method was isocratic, with a constant flow rate of 0.3 cm^3 min^{-1}.

For detection and quantification of the hormones, LCQ Advantage (Thermo Fisher Scientific, USA) mass spectrometer with an electrospray ion source and quadrupole ion trap mass analyzer was used. The measurements were conducted in positive ionization mode, with optimal source parameters set at: source voltage, 4.5 kV; sheath gas, 23 au; auxiliary gas, 5 au; capillary temperature, 350 °C. The selected reaction monitoring mode (SRM) was used for quantification purposes. Table S-I of the Supplementary material to this paper lists the selected precursor ion, the optimal collision energy, the most abundant fragment ion, and its isolation width for each hormone, whereas Fig. S-2 of the Supplementary material shows an example of a SRM chromatogram.

Real water samples analysis

The applicability of the optimized SPE method was tested by analyzing selected hormones in groundwater, surface water and wastewater samples. Two groundwater, four surface water, and four wastewater samples were collected. Groundwater samples GW1 and GW2 were collected from observation wells close to the river Danube in the vicinity of Kovin. Surface water samples were collected from the rivers Danube (locations Novi Sad and Kladovo,

labeled SW1 and SW2, respectively), the Velika Morava (location 1 km from the confluence with the Danube, labeled SW3) and the Pek (location 8 km from the confluence with the Danube, labeled SW4). Two wastewater samples were taken from Belgrade (WW1, sampled at discharge into the Danube near the confluence of the Sava into the Danube, and WW2, sampled at discharge near Belgrade Fair), while two samples were from the entrance and exit of the wastewater treatment plant (WWTP) Aranđelovac (WW3 and WW4). Water samples were stored in 1 dm^3 plastic bottles and stored in a freezer. Prior to the SPE procedure, the water samples were filtered through 1–3 μm glass fiber filters (Whatman GmbH, Dassel, Germany).

RESULTS AND DISCUSSION

Optimization of solid-phase extraction

The initial step in optimizing the SPE method for hormone analysis from water samples was to determine an adequate adsorbent mass. The influence of the adsorbent mass on the extraction efficiency is demonstrated in Fig. 1a. Results showed that recoveries of all three investigated hormones increased as the mass of CC decreased. It can be assumed that the increase in adsorbent mass leads to a decrease in the homogeneity of close-packed material, preventing satisfactory contact between the adsorbent particles and solution. The highest recovery values, ranging from 65 to 70 %, were obtained for the adsorbent mass of 20 mg. Therefore, 20 mg of adsorbent was chosen for further experiments.

Choosing the appropriate volume of the water sample is an important step in the SPE optimization process. Low sample loading volumes are advantageous when considering potential matrix effects and extraction times, yet extraction efficacy and pre-concentration factors generally increase as sample volume is increased.[22] Fig. 1b illustrates the SPE method's recoveries for all tested hormones. Recoveries increase with sample volume, yet volumes above 200 cm^3 weren't tested due to analysis time constraints. Thus, 200 cm^3 was chosen as optimal. The effect of the initial pH value of the water sample was also investigated by varying the initial pH values in the range from 5 to 11. Recoveries obtained for all selected hormones (Fig. 1c) in the tested pH range were high and acceptable (72–85 %). As pH did not have a significant influence on extraction efficiency, the neutral pH value was selected for further experiments. Additionally, at a neutral pH value, the highest recoveries for EE2 were achieved.

Fig. 1d shows the effects of different eluents on extraction efficiency. The experiment was done under the following conditions: material mass was 20 mg, sample volume was 200 cm^3 and initial pH value was 7. The elution conditions were chosen based on the optimization of the parameters in the previous steps. The tested elution solvents were MeOH, ACN, EtOAc, DCM/MeOH and EtOAc/MeOH. All tested solvents used individually yielded low recoveries, with ACN providing the lowest recovery. When using DCM/MeOH and EtOAc/MeOH mixtures, high and acceptable recoveries for all tested hormones were obtained.

Even though the DCM/MeOH mixture produced slightly higher recoveries than the EtOAc/MeOH mixture, the latter was chosen as a suitable elution solvent due to its lower toxicity when compared to DCM.[23,24]

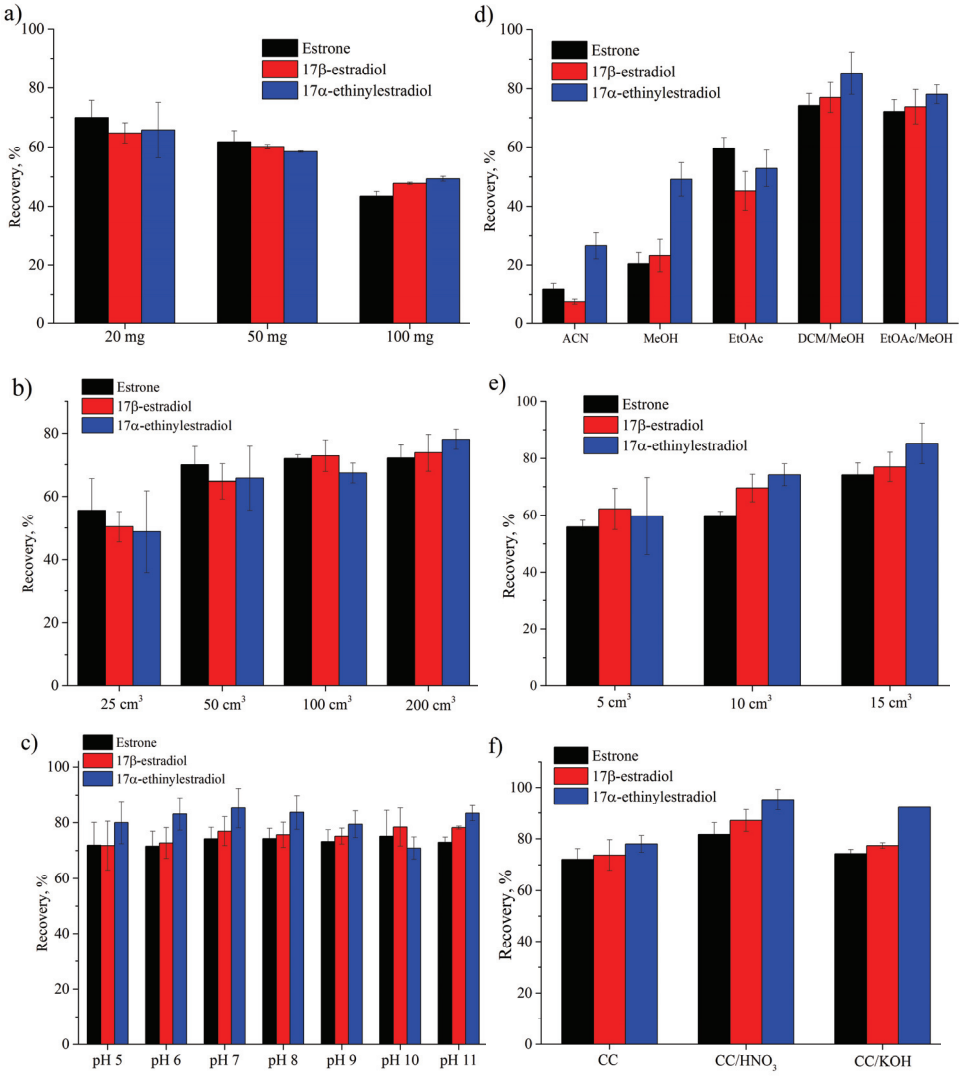

Fig. 1. Recoveries of selected hormones obtained using different a) adsorbent masses, b) sample volumes, c) initial pH values of the sample, d) elution solvents, e) eluent volumes and f) unmodified and chemically modified CCs.

In the next step, the eluent volume was optimized. As shown in Fig. 1e, the recoveries of the tested hormones consistently improved with the increase in elu-

ent volume. A 15 cm^3 eluent volume proved to be adequate, providing satisfactory recoveries for all observed hormones (74-85%). Therefore, this volume was selected as the optimal choice for subsequent analyses.

The final step in SPE optimization was the selection of the material modification method that would provide the highest efficiency of CC for the extraction of tested hormones. The obtained results (Fig. 1f) show that after the chemical modification of CC, modest variations in recovery values were found. However, utilizing CC/HNO_3 as an adsorbent produced better results for all three hormones with high recoveries (82–95 %), hence CC/HNO_3 was chosen for real water sample analysis. In our previous study, we found that modifying the material with HNO_3 resulted in an increase of carboxyl functional groups.[14] In the present study, it is observed that functionalization leads to a slight increase in the recovery values of the tested hormones, possibly due to the prevalence of hydrogen bonds in the mechanism of adsorption, which is a consequence of the increase in oxygen surface groups.[25] The final optimized analysis procedure was as follows: the 3 cm^3 cartridge, packed with 20 mg CC/HNO_3, was conditioned with 5 cm^3 of EtOAc/MeOH (1:1) mixture followed by 5 cm^3 of deionized water; 200 cm^3 of the water sample, with the initial pH adjusted to 7, was passed through the preconditioned cartridge; the cartridge was dried under vacuum for 10 min, and analytes were eluted with EtOAc/MeOH mixture (1:1) until 15 cm^3 of extract was collected in a glass test tube; the extract was evaporated to dryness, reconstituted with 1 cm^3 of mobile phase, and the final extract was filtered through a PVDF filter (0.45 μm) into the glass vial and analyzed.

Method validation

In order to determine the applicability of the developed analytical method for the extraction of observed hormones from real water samples, the linearity, repeatability, matrix effect, limit of detection (*LOD*) and limit of quantification (*LOQ*) were estimated. Details related to method validation are given in Supplementary material. The calibration curves based on six calibration levels ranging from 5 to 500 μg dm^{-3} showed good linearity, with determination coefficients (R^2) of 0.9981 for E1, 0.9909 for E2 and 0.9971 for EE2. The calibration curves are presented in Fig. S-3 of the Supplementary material. The relative standard deviation (*RSD*) was in the range of 3.2–5.9 %, indicating good repeatability. For all observed hormones, the calculated values of *LOD* and *LOQ* were in the range of 2.63–6.36 and 8.77–21.19 ng dm^{-3}, respectively. The recoveries, *RSD*, *LOD*, *LOQ* and R^2 values are given in Table S-II of the Supplementary material. The *LOD* values of our method are lower than the corresponding values obtained in some studies[20–27] and comparable to some recently published studies.[1,7] Glineur *et al*.[28] developed an analytical method in which lower *LOD* and *LOQ* were

achieved, but that method requires more time because an additional sample purification technique is necessary.

The existence of certain co-extracted substances, including natural organic matter and other contaminants, in environmental samples has the potential to impact the signal intensity of LC–MS/MS through either suppression or enhancement of the signal. Hence, assessing the matrix effect becomes crucial for a comprehensive understanding of the analytical results. The results presented in Table S-II show that the matrix effect has no significant influence on the determination in this case. In all studied matrices, the deviation of the results was less than 20 %, indicating the strong selectivity of CC/HNO_3 for the investigated hormones. However, in order to improve accuracy, the standard addition method was used to analyze real water samples.

By comparing recoveries gained using commercially obtained cartridges and cartridges packed with CC/HNO_3 (Fig. 2), it was demonstrated that CC/HNO_3 could be successfully used as a solid-phase adsorbent for the analysis of tested hormones in water samples. According to the results presented in Fig. 2, it is evident that recoveries obtained using cartridges packed with CC/HNO_3 were comparable to the recoveries gained by commercial cartridges. The performance of the proposed method also was on par with a few previously documented methods,[7,29] which utilized expensive commercial cartridges. Notably, our cartridges utilized a significantly smaller amount of material, 20 mg as opposed to 200–500 mg in the referenced studies, underscoring the cost-effectiveness of this approach.

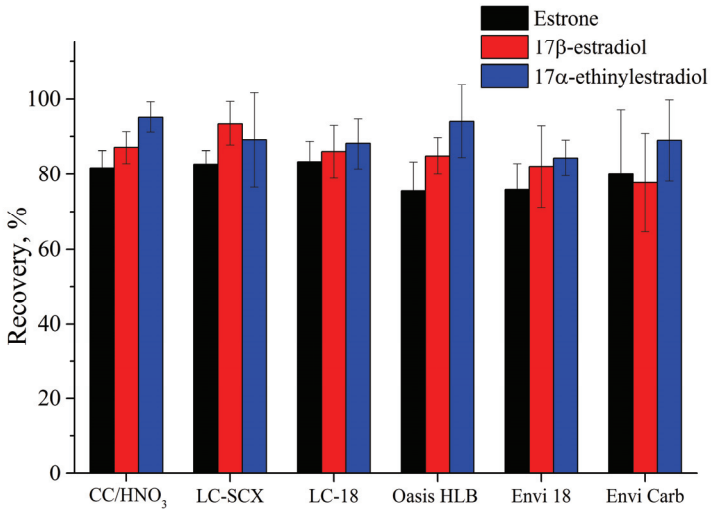

Fig. 2. Recoveries of selected hormones obtained using commercial cartridges and CC/HNO_3.

Real water samples

In Table I, detected concentrations of examined hormones in groundwater, surface water, and wastewater samples are presented. At least one hormone was found in eight, out of the ten samples that were tested, indicating a considerable prevalence of these compounds in the aquatic environment.

TABLE I. Hormone concentrations (ng dm^{-3}) detected in ground, surface and wastewater samples

Sample	Location	Hormone		
		E1	E2	EE2
Groundwater				
GW1	Kovin 1	< *LOQ*[a]	< *LOQ*	< *LOQ*
GW2	Kovin 2	–[b]	< *LOQ*	–
Surface water				
SW1	Danube, Novi Sad	36.2	10.1	–
SW2	Danube, Kladovo	–	–	–
SW3	Velika Morava	–	8.8	–
SW4	Pek	22.8	10.2	9.6
Wastewater				
WW1	Belgrade, Confluence	99.3	–	–
WW2	Belgrade, Belgrade Fair	71.3	–	–
WW3	WWTP Aranđelovac, influent	163.5	101.8	91.0
WW4	WWTP Aranđelovac, efluent	–	–	–

[a](< *LOQ*) detected, but below *LOQ*; [b](–) not detected

In GW samples, only trace amounts of the studied hormones were detected, below *LOQ* levels, which is in accordance with results obtained in some previous studies.[30,31] Higher concentrations were detected in GW samples in Poland (≤ 43 ng dm^{-3} for estrone and ≤ 48 ng dm^{-3} for 17*β*-estradiol).[32] None of the tested hormones were found in the SW2 sample collected from the Danube, Kladovo, while in the remaining SW samples, hormone concentrations ranged from 8.8 to 36.2 ng dm^{-3}, which was comparable with hormone concentrations obtained in previous studies in Italy,[33] Poland,[34] China,[29] Indonesia[35] and Malaysia (river Pahang).[36]

Higher concentrations, up to 820 ng dm^{-3} were recorded in the Bacanga River in Brazil.[1] This river is positioned in an area affected by urbanization, burning, deforestation, water contamination, and siltation, which may explain the high concentration of the selected compounds detected in the water samples of that river.[1] Zhang et al. detected observed hormones in river water in Switzerland at concentrations up to 3.7 ng dm^{-3},[37] which was lower than the results obtained in the present study. Rocha *et al*. determined estrone, 17*β*-estradiol, and 17*α*-ethinylestradiol in a river estuary in Portugal at concentrations ≤ 16, ≤ 18 and ≤ 11 ng dm^{-3}, respectively.[38] As anticipated, wastewater samples contained the high-

est quantities of the hormones. Concentrations of E1, E2 and EE2 in the present work were up to 163.5, 101.8, and 91.0, respectively. The relatively high concentrations of E1 can be explained by the conversion of E2 and EE2 into E1 before it can be transformed further.[39] The highest concentrations of hormones were detected in sample WW3, from the inlet of WWTP Aranđelovac, while there was no detectible amount left in the sample from the exit of the same WWTP. Concentrations of E1 in sample WW3 were comparable with obtained E1 concentrations of wastewater influents in France and Slovenia.[40,41] The concentration of E2 in the WW3 sample was also comparable with the E2 concentration of influent wastewater in Malaysia,[42] while higher levels of E1 and EE2 were recorded in wastewater influents in Brazil.[39]

Taking into account the obtained results, it can be concluded that the developed method was efficiently applied for the selective determination of trace estrogens in complex environmental water samples.

CONCLUSION

In the present study, pristine and chemically modified CC was used as a new solid-phase extraction adsorbent for the determination of estrogen hormones in environmental water samples. An efficient SPE method was developed by optimizing the adsorbent mass (20 mg), volume (200 cm^3) and initial pH value (pH 7) of the water sample, the type and volume of elution solvent (15 cm^3 of EtOAc/MeOH 1:1 mixture), and by selecting HNO_3 treated CC as an adsorbent. The optimized SPE method provided high recovery values for all tested hormones (82–95 %), comparable with the recoveries obtained using commercially available cartridges. Notably, our method used significantly less material than is customary, demonstrating the cost-effectiveness of this approach. The developed SPE/LC–MS/MS method was successfully applied to the analysis of ground, surface and wastewater samples, whereby the matrix effect of examined water samples did not have a significant impact on method accuracy. The highest concentrations of tested hormones were found in wastewater samples. However, the fact that the tested hormones were detected and quantified in most of the tested samples indicates the significant presence of these pollutants in the aquatic environment, which requires further monitoring.

SUPPLEMENTARY MATERIAL

Additional data and information are available electronically at the pages of journal website: https://www.shd-pub.org.rs/index.php/JSCS/article/view/12844, or from the corresponding author on request.

Acknowledgement. The authors wish to thank the Ministry of Science, Technological Development and Innovation of the Republic of Serbia (Contract Nos. 451-03-65/2024-03/ /200135 and 451-03-66/2024-03/200287).

И З В О Д

ЕКСТРАКЦИЈА ЕСТРОГЕНИХ ХОРМОНА НА ХЕМИЈСКИ МОДИФИКОВАНОМ УГЉЕНИЧНОМ КРИОГЕЛУ

ДАНИЈЕЛА Б. ПРОКИЋ[1], МАРИЈА М. ВУКЧЕВИЋ[2], МАРИНА М. МАЛЕТИЋ[1], АНА М. КАЛИЈАДИС[3], ЈОВАНКА Н. ПЕЈИЋ[4], БИЉАНА М. БАБИЋ[5] и ТАТЈАНА М. ЂУРКИЋ[2]

[1]Иновациони Центар Технолошко–металуршког факултета, Карнегијева 4, 11000 Београд, [2]Технолошко–металуршки факултет, Универзитет у Београду, Карнегијева 4, 11000 Београд, [3]Лабораторија за материјале, Институт за нуклеарне науке Винча – Институт, од националног значаја Републике Србије, Универзитет у Београду, Мике Петровића Аласа 12–14, 11000 Београд, [4]Институт за хемију, технологију и металургију, Универзитет у Београду, Његошева 12, 11000 Београд и [5]Институт за физику – Институт од националног значаја Републике Србије, Универзитет у Београду, Прегревица 118, 11080 Београд

У овом раду је представљена нова метода екстракције на чврстој фази, коришћењем немодификованог и хемијски модификованог угљеничног криогела (енгл. carbon cryogel, CC) као адсорбента за изоловање и предконцентрисање естрогених хормона (естрона, 17β-естрадиола и 17α-етинилестрадиола) из узорака воде. Након оптимизације методе, која је обухватила оптимизацију масе и хемијског третмана адсорбента, запремине и pH-вредности узорка и типа и запремине растварача за елуирање, добијене су високе вредности приноса (82–95 %). Развијена аналитичка метода, базирана на SPE екстракцији и течној хроматографији–тандем масеној спектрометрији, показала се селективном, ефикасном и економичном за одређивање одабраних естрогених хормона. Коришћењем кертрица са модификованим CC постигнути су резултати који су били упоредиви са резултатима добијеним при употреби комерцијалних кертрица, уз коришћење знатно мање масе материјала. Поред тога, селективност одабраног материјала је допринела малом ефекту матрице. Оптимизована метода је успешно примењена за анализу естрогених хормона у подземним, површинским и отпадним водама, при чему резултати указују на важност праћења ових загађујућих материја у воденој средини.

(Примљено 13. марта, ревидирано 7. априла, прихваћено 2. јуна 2024)

REFERENCES

1. E. M. L. Sousa, R. A. S. Dias, E. R. Sousa, N. M. Brito, A. S. Freitas, G. S. Silva, L. K. Silva, D. L. D. Lima, V. I. Esteves, G. S. Silva, *Water. Air. Soil. Pollut.* **231** (2020) 172 (https://dx.doi.org/10.1007/s11270-020-04552-8)
2. C. L. S. Vilela, J. P. Bassin, R. S. Peixoto, *Environ. Pollut*. **235** (2018) 546 (https://dx.doi.org/10.1016/j.envpol.2017.12.098)
3. M. Bilal, D. Barceló, H. M. N. Iqbal, *Sci. Total Environ*. **800** (2021) 149635 (https://dx.doi.org/10.1016/j.scitotenv.2021.149635)
4. A. González, J. Avivar, F. Maya, C. Palomino Cabello, G. Turnes Palomino, V. Cerdà, *Anal. Bioanal. Chem.* **409** (2017) 225 (https://dx.doi.org/10.1007/s00216-016-9988-8)
5. E. Simon, A. Duffek, C. Stahl, M. Frey, M. Scheurer, J. Tuerk, L. Gehrmann, S. Könemann, K. Swart, P. Behnisch, D. Olbrich, F. Brion, S. Aït-Aïssa, R. Pasanen-Kase, I. Werner, E. L. M. Vermeirssen, *Environ. Int.* **159** (2022) 107033 (https://dx.doi.org/10.1016/j.envint.2021.107033)
6. J. Wang, Y. Zhu, *Enviromen. Toxicol. Pharmacol.* **52** (2017) 69
7. (https://dx.doi.org/10.1016/j.etap.2017.03.018)

8. Y. Li, L. Yang, H. Zhen, X. Chen, M. Sheng, K. Li, W. Xue, H. Zhao, S. Meng, G. Cao, *J. Chromatogr. B.* **1168** (2021) 122559 (https://dx.doi.org/10.1016/j.jchromb.2021.122559)
9. J. Zhang, L. Zang, T. Wang, X. Wang, M. Jia, D. Zhang, H. Zhang, *Food Chem.* **333** (2020) 127529 (https://dx.doi.org/10.1016/j.foodchem.2020.127529)
10. D. Mutavdžić Pavlović, S. Babić, A. J. M. Horvat, M. Kaštelan-Macan, *Trends Anal. Chem.* **26** (2007) 1062 (https://dx.doi.org/10.1016/j.trac.2007.09.010)
11. T. Z. Minović, J. J. Gulicovski, M. M. Stoiljkovic, B. M. Jokic, Lj. S. Živković, B. Z. Matović, B. M. Babić, *Micropor. Mesopor. Mater.* **201** (2015) 271 (https://dx.doi.org/10.1016/j.micromeso.2014.09.031)
12. L. Wang, G. Chen, H. Shu, X. Cui, Z. Luo, C. Chang, A. Zeng, J. Zhang, Q. Fu, *J. Chromatogr. A* . **1638** (2021) 461889 (https://dx.doi.org/10.1016/j.chroma.2021.461889)
13. M. Tagliavini, F. Engel, P. G. Weidler, T. Scherer, A. I. Schäfer, *J. Hazard. Mater.* **337** (2017) 126 (https://dx.doi.org/10.1016/j.jhazmat.2017.03.036)
14. B. Lalović, T. Đurkić, M. Vukčević, I. Janković-Častvan, A. Kalijadis, Z. Laušević, M. Laušević, *Environ. Sci. Pollut. Res.* **24** (2017) 20784 (https://dx.doi.org/10.1007/s11356-017-9748-0)
15. D. Prokić, M. Vukčević, A. Mitrović, M. Maletić, A. Kalijadis, I. Janković-Častvan, T. Đurkić, *Environ. Sci. Pollut. Res.* **29** (2022). (https://dx.doi.org/10.1007/s11356-021-15970-4)
16. D. Prokić, M. Vukčević, A. Kalijadis, M. Maletić, B. Babić, T. Đurkić, *Fibers Polym.* **21** (2020) 2263 (https://dx.doi.org/10.1007/s12221-020-9758-2)
17. A. Celzard, V. Fierro, G. Amaral-Labat, *Adsorption by Carbon Gels*, in *Novel Carbon Adsorbents*, J.M.D. Tascón, Ed., Elsevier, Amsterdam, The Netherlands, 2012, p. 207 (https://dx.doi.org/10.1016/B978-0-08-097744-7.00007-7)
18. B. Jiang, Y. Wang, D. Wang, M. Yao, C. Fan, J. Dai, *Water Sci. Technol*. **80** (2019) (https://dx.doi.org/10.2166/wst.2020.072)
19. J. H. Kim, S. Y. Hwang, J. E. Park, G. B. Lee, H. Kim, S. Kim, B. U. Hong, *Carbon Lett.* **29** (2019) 281 (https://dx.doi.org/10.1007/s42823-019-00024-0)
20. L. H. Jiang, Y. G. Liu, G. M. Zeng, F. Y. Xiao, X. J. Hu, X. Hu, H. Wang, T. T. Li, L. Zhou, X. F. Tan, *Chem. Eng. J.* **284** (2016) 93 (https://dx.doi.org/10.1016/j.cej.2015.08.139)
21. L. H. G. Coelho, T. A. DeJesus, M. Y. Kohatsu, G. T. Poccia, V. Chicarolli, K. Helwig, C. Hunter, J. Roberts, P. Teedon, O. Pahl, *Water. Air. Soil Pollut.* **231** (2020) 150 (https://dx.doi.org/10.1007/s11270-020-04477-2)
22. M. E. Valdés, D. J. Marino, D. A. Wunderlin, G. M. Somoza, A. E. Ronco, P. Carriquiriborde, *Bull. Environ. Contam. Toxicol.* **94** (2014) 29 (https://dx.doi.org/10.1007/s00128-014-1417-0)
23. G. J. Maranata, N. O. Surya, A. N. Hasanah, *Heliyon* **7** (2021) e05934 (https://dx.doi.org/10.1016/j.heliyon.2021.e05934)
24. C. Estevan, E. Vilanova, *Ethyl acetate* in *Encyclopedia of Toxicology*, P. Wexler, Ed., Elsevier, London, UK, 2014, p. 506 (https://dx.doi.org/10.1016/B978-0-12-386454-3.00502-9)
25. C. Pacheco, R. Magalhães, M. Fonseca, P. Silveira, I. Brandão, *J. Acute Med.* **6** (2016) 43 (https://dx.doi.org/10.1016/j.jacme.2016.03.008)
26. M. O. Barbosa, R. S. Ribeiro, A. R. L. Ribeiro, M. F. R. Pereira, A. M. T. Silva, *Sci. Rep.* **10** (2020) 22304 (https://doi.org/10.1038/s41598-020-79244-8)

27. X. Zhu, Y. Zhang, P. Liu, X. Bai, N. Chen, Y. Zhang, *J. Chem.* **2021** (2021) 9970518 (https://dx.doi.org/10.1155/2021/9970518)
28. A. González, K. J. Kroll, C. Silva-Sanchez, P. Carriquiriborde, J. I. Fernandino, N. D. Denslow, G. M. Somoza, *Sci. Total Environ*. **743** (2020) 140401 (https://dx.doi.org/10.1016/j.scitotenv.2020.140401)
29. A. Glineur, K. Nott, P. Carbonnelle, S. Ronkart, G. Purcaro, *J. Chromatogr. A.* **1624** (2020) 461242 (https://dx.doi.org/10.1016/j.chroma.2020.461242)
30. S. Liu, G. G. Ying, J. L. Zhao, F. Chen, B. Yang, L. J. Zhou, H. J. Lai, *J. Chromatogr. A.* **1218** (2011) 1367 (https://dx.doi.org/10.1016/j.chroma.2011.01.014)
31. E. Vulliet, L. Wiest, R. Baudot, M. F. Grenier-Loustalot, *J. Chromatogr. A.* **1210** (2008) 84 (https://dx.doi.org/10.1016/j.chroma.2008.09.034)
32. E. W. Peterson, L. A. Hanna, *Environ. Earth Sci.* **75** (2016) 384 (https://dx.doi.org/10.1007/s12665-016-5259-4)
33. J. Kapelewska, U. Kotowska, K. Wiśniewska, *Environ. Sci. Pollut. Res.* **23** (2016) 1642 (https://dx.doi.org/10.1007/s11356-015-5359-9)
34. E. Pignotti, M. Farré, D. Barceló, E. Dinelli, *Environ. Sci. Pollut. Res.* **24** (2017) 21153 (https://dx.doi.org/10.1007/s11356-017-9756-0)
35. B. Woźniak, A. Klopot, I. Matraszek-Zuchowska, K. Sielska, J. Zmudzki, *J. Vet. Res.* **58** (2014) 603 (https://dx.doi.org/10.2478/bvip-2014-0093)
36. T. Hadibarata, R. A. Kristanti, A. H. Mahmoud, *J. Water Health.* **18** (2020) 38 (https://dx.doi.org/10.2166/wh.2019.100)
37. T. H. Nazifa, R. A. Kristanti, M. Ike, M. Kuroda, T. Hadibarata, *Toxicol. Environ. Health Sci.* **12** (2020) 65 (https://dx.doi.org/10.1007/s13530-020-00036-8)
38. K. Zhang, Y. Zhao, K. Fent, *Sci. Technol.* **51** (2017) 6498 (https://dx.doi.org/10.1021/acs.est.7b01231)
39. M. J. Rocha, C. Cruzeiro, M. Reis, M. Â. Pardal, E. Rocha, *Env. Monit Assess.* **186** (2014) 3337 (https://dx.doi.org/10.1007/s10661-014-3621-0)
40. G. P. Pessoa, N. C. de Souza, C. B. Vidal, J. A. C. Alves, P. I. M. Firmino, R. F. Nascimento, A. B. dos Santos, *Sci. Total Environ.* **490** (2014) 288 (https://dx.doi.org/10.1016/j.scitotenv.2014.05.008)
41. V. Gabet-Giraud, C. Miège, J. M. Choubert, S. M. Ruel, M. Coquery, *Sci. Total Environ.* **408** (2010) 4257 (https://dx.doi.org/10.1016/j.scitotenv.2010.05.023)
42. M. Česen, D. Heath, M. Krivec, J. Košmrlj, T. Kosjek, E. Heath, *Environ. Pollut.* **242** (2018) 143 (https://dx.doi.org/10.1016/j.envpol.2018.06.052)
43. T. Y. Fang, S. M. Praveena, A. Z. Aris, S. N. S. Ismail, I. Rasdi, *Chemosphere* **215** (2019) 153 (https://dx.doi.org/10.1016/j.chemosphere.2018.10.032).

Journal of the Serbian Chemical Society
JSCS-info@shd.org.rs • www.shd.org.rs/JSCS
J. Serb. Chem. Soc. ***89*** (12) S533–S536 (2024) *Supplementary material*

SUPPLEMENTARY MATERIAL TO

Solid-phase extraction of estrogen hormones onto chemically modified carbon cryogel

DANIJELA B. PROKIĆ[1]*, MARIJA M. VUKČEVIĆ[2], MARINA M. MALETIĆ[1], ANA M. KALIJADIS[3], JOVANKA N. PEJIĆ[4], BILJANA M. BABIĆ[5] and TATJANA M. ĐURKIĆ[2]

[1]Innovation Center of the Faculty of Technology and Metallurgy, Karnegijeva 4, 11000 Belgrade, Serbia, [2]Faculty of Technology and Metallurgy, University of Belgrade, Karnegijeva 4, 11000 Belgrade, Serbia, [3]Department of Materials „Vinča" Institute of Nuclear Sciences - National Institute of the Republic of Serbia, University of Belgrade, Mike Petrovića Alasa 12-14, 11000 Belgrade, Serbia, [4]Institute for Chemistry, Technology and Metallurgy, University of Belgrade, Njegoševa 12, 11000 Belgrade, Serbia, and [5]Institute of Physics – National Institute of the Republic of Serbia, University of Belgrade, Pregrevica 118, 11080 Belgrade, Serbia.

J. Serb. Chem. Soc. 89 (12) (2024) 1661–1673

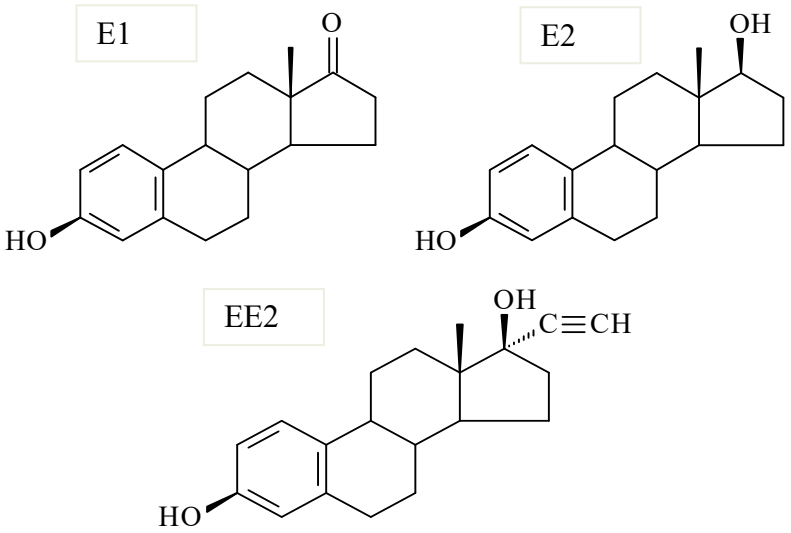

Fig. S-1. Chemical structures of E1, E2 and EE2

* Corresponding author. E-mail: dprokic@tmf.bg.ac.rs

The most abundant ions from each hormone MS spectra were selected as precursor ions: the protonated molecule for E1 (m/z 271.0) and the dehydrated protonated molecules for E2 and EE2 (m/z 255.0 and 279.0, respectively). The most intense product ions resulting from the fragmentation of the selected precursor ions were chosen for quantitative analysis (Table S-I).

TABLE S-I. MS-MS quantification parameters for selected hormones

Hormone	Retention time, min	Precursor ion m/z	Collision energy, %	Fragment ion m/z	Isolation width
E1	6.34	271.0	24	253.0	2
E2	6.10	255.0	27	159.1	2
EE2	5.80	279.0	33	133.2	2

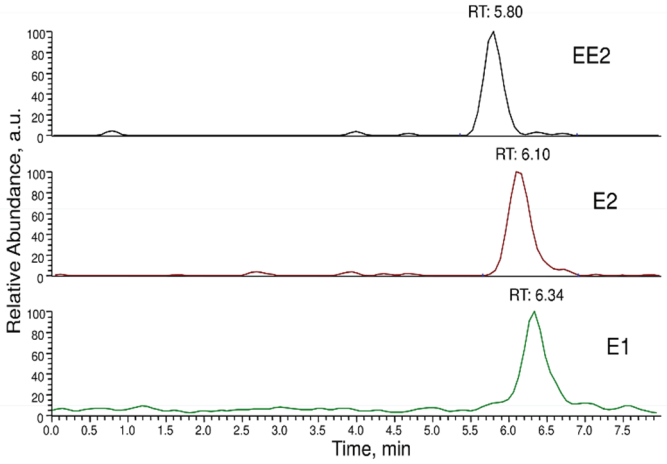

Fig. S-2. SRM chromatograms of selected estrogen hormones from extract of water sample spiked at 0.5 μg dm^{-3}

METHOD VALIDATION

The linearity of the method was estimated by a calibration curve with six concentrations ranging from 5 to 500 μg dm^{-3} (which corresponds to the concentration range of 25–2500 ng dm^{-3} in the water sample). The repeatability of the method was estimated by calculating the relative standard deviation (*RSD* / %) of samples measured in the triplicates (n = 3). The limit of detection (*LOD*) and limit of quantitation (*LOQ*) were calculated as the minimal quantity of analyte necessary to produce a signal-to-noise ratio of 3 and 10, respectively.[1,2]

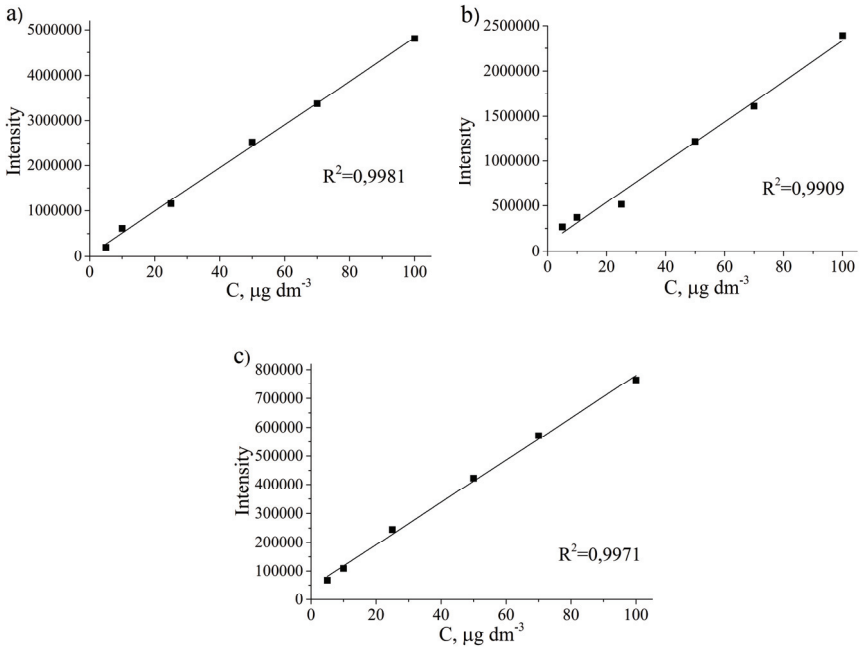

Fig. S-3. Calibration curves of a) E1, b) E2 and c) EE2

In order to estimate the suppression or enhancement of the analyte signal in the matrix solution, spiked and blank extracts of groundwater, surface water, and wastewater samples were prepared and analyzed. The matrix effect (%) was calculated by applying the following equation.[3]

$$\text{Matrix effect} = \frac{Area_{matrix} - Area_{blank}}{Area_{solvent}} \times 100 \quad (1)$$

where $Area_{matrix}$ is the peak area of the analyte in the spiked real water extract, $Area_{blank}$ is the peak area of the analyte in the correspondent nonspiked extract, and $Area_{solvent}$ is the peak area of the analyte in the appropriate working standard solution in methanol. A matrix effect greater than 100% implies ionization enhancement, while a matrix effect less than 100% indicates ionization suppression.

TABLE S–II. Analytical characteristics of the developed method (n = 3)

Compound	Recovery, % (RSD, %)	Linearity, R^2	LOD, ng dm^{-3}	LOQ, ng dm^{-3}	Matrix effect, %		
					GW	SW	WW
E1	82 (4)	0.9981	6.36	21.19	94	89	91
E2	87 (6)	0.9909	2.63	8.77	117	114	119
EE2	95 (3)	0.9971	5.14	17.12	102	103	110

REFERENCES

1. B. Lalović, T. Đurkić, M. Vukčević, I. Janković-Častvan, A. Kalijadis, Z. Laušević, M. Laušević, *Environ. Sci. Pollut. Res.* **24** (2017) 20784 (https://dx.doi.org/10.1007/s11356-017-9748-0)
2. N. H. Tran, J. Hu, S. L. Ong, *Talanta* **113** (2013) 82 (https://dx.doi.org/10.1016/j.talanta.2013.03.072)
3. Matić, S. Grujić, Z. Jauković, M. Laušević, *J. Chromatogr. A.* **1364** (2014) 117 (https://dx.doi.org/10.1016/j.chroma.2014.08.061)

Journal of the Serbian Chemical Society
JSCS-info@shd.org.rs • www.shd.org.rs/JSCS
J. Serb. Chem. Soc. *89* (12) 1675–1687 (2024)
JSCS–5814
Original scientific paper
Published 7 November, 2024

Pyrolysis of corn stalks: the potential of using bio-oil as a fuel

JELENA ISAILOVIĆ[1]*, EMILIJA VUKIĆEVIĆ[2], MALIŠA ANTIĆ[1], JAN SCHWARZBAUER[3], LJUBIŠA IGNJATOVIĆ[4], GORDANA GAJICA[5] and VESNA ANTIĆ[1]

[1]*University of Belgrade – Faculty of Agriculture, Nemanjina 6, 11080 Zemun, Serbia,* [2]*University of Belgrade – Faculty of Chemistry, Studentski trg 12–16, 11158 Belgrade, Serbia,* [3]*Institute for Geology and Geochemistry of Petroleum and Coal, RWTH, Lochnerstr. 4–20, Aachen, Germany,* [4]*University of Belgrade – Faculty of Physical Chemistry, Studentski trg 12–16, 11000 Belgrade, Serbia and* [5]*Institute of Chemistry, Technology and Metallurgy, National Institute of the Republic of Serbia, Njegoševa 12, 11000 Belgrade, Serbia*

(Received 10 January, revised 20 January, accepted 6 April 2024)

Abstract: Due to the increasing consumption of fossil fuels, there is a growing demand for renewable energy resources. At the same time, a significant amount of agricultural waste accumulates, including corn residues, and the efficient management of this waste is a challenge. In this work, the waste biomass, which consisted of the stalks of two types of corn, was characterized and subjected to the pyrolysis process at 400 °C. The physicochemical characterization of the obtained liquid fraction (bio-oil) was performed, and the obtained data were compared with the literature data for liquid biofuel. The calorific value of bio-oil was above 22 MJ kg^{-1}, which indicates the good potential of waste corn biomass as an energy source. With appropriate further changes in the composition of waste, by adding materials with a higher carbon and hydrogen content, corn stalks can represent a significant energy source, with better regulation of disposal and storage of agricultural waste.

Keywords: agricultural biomass; pyrolysis process; physicochemical properties; liquid fraction.

INTRODUCTION

Contemporary society encounters significant challenges due to the rising consumption of fossil fuels and the resulting environmental impacts. Therefore, there is an increasing emphasis on developing alternatives to ensure a more sustainable energy balance and reduce negative environmental impacts. In this context, the present research focuses on using corn biomass as a renewable energy source.[1]

* Corresponding author. E-mail: jelena.isailovic@agrif.bg.ac.rs
https://doi.org/10.2298/JSC240110043I

The global corn production continues to grow and it has reached 1.2 billion tons according to the latest statistics from 2021.[2] In Serbia, the data from 2022 show an annual output of 4,283,293 tons of corn on 952,216 ha of arable land across the country.[3]

After corn harvest, the plant residues such as stalks, leaves, cobs and husks can be partly used as animal feed. Also, parts of plant waste remain on arable land and return to the soil.[4] The remaining amount of biomass, which is not negligible (about 30 %), remains to be used as an energy source. Corn waste biomass is rich in lignocellulose material, with lignin, cellulose, and hemicellulose being the main components of these plant residues.[5] Lignin is a three-dimensional amorphous polymer consisting of aliphatic and aromatic structures, and it is considered a non-nutritive part of biomass. Lignin provides strength and hydrophobicity to plant cell walls, while protecting polysaccharides from microbial degradation. Lignin, cellulose, and hemicellulose can be converted into liquid fuel by the pyrolysis process, effectively managing this waste and yielding a significant amount of bio-oil that can be modified as a substitute for fossil fuel.[6,7] It is important to note that corn biomass is not a significant food source for the animal consumption because it has a low level of nutrients, making it waste.[7,8] Also, agricultural lignocellulosic biomass represents a cheap and readily available source of carbon that can be used.[9]

Traditionally, corn residues are often burned or disposed of as unnecessary waste in many fields worldwide.[10] However, such a practice can have profound implications for the environment, because the burning of such material releases various gases and particles into the atmosphere, contributing to air pollution and negatively impacting the quality of the environment and human health.[11]

Using biomass as an energy source has several advantages because it is renewable and can be replenished faster than used, keeping ecosystems in balance.[8] The biomass-based energy reduces greenhouse gas emissions and contributes to the reduction of the greenhouse effect, which is crucial to the climate change issue.[12] The production of the liquid fuels from biomass can help reduce dependency on fossil fuels, increase the energy independence, and reduce the economic and the geopolitical risks.[1]

This is the first study examining the characteristics of waste stalks from two types of corn, BC 398 and ZP 6263, cultivated in the municipality of Šabac, Serbia. Additionally, it provides a detailed analysis of the physicochemical characteristics of the bio-oil obtained through the pyrolysis of corn residues under the specified conditions. The characterization of the liquid fractions obtained aims to provide a thorough understanding of the potential of this alternative energy approach. The findings of this research are expected to offer valuable insights for the advance of sustainable energy solutions and contributing to the global initiatives aimed considering the climate change.

EXPERIMENTAL

Biomass samples

Two types of corn, BC 398, designated as Kz, and ZP 6263, designated as Kn, were used for this study, collected from the vicinity of Šabac, Serbia, from two different plots. The samples were taken at a height of 5 to 10 cm above the ground surface. Before any analysis, the samples were air-dried for 30 days to achieve a less than 10 % moisture content. Afterward, they were milled to achieve an average particle size ranging between 2 and 5 mm.

Thermogravimetric analysis (TGA)

The thermal degradation of corn stalk samples was studied by thermogravimetric analysis (TGA). TГ was performed on TA Instruments TGA Q500, thermogravimetric analyzer (Delaware, USA). The nitrogen flow was 60 cm^3 min^{-1}. About 10 mg of the sample was placed into the platinum crucible, loaded into the TG furnace, and heated from 25 to 700 °C. The applied heating rate was 5 °C min^{-1}. The signals of weight (%) and deriv. weight (% $°C^{-1}$) were presented by the package TA Advantage Universal Analysis 2000 software, version 4.5 A. The obtained TGA and their DTG curves were used to analyse the thermal properties of the biomass samples.

Pyrolysis

Air-dried samples of corns Kz and Kn, 19.61 g and 19.14 g, respectively, were pyrolyzed in a carbolite tube furnace (MTF 10/15/130, Carbolite, UK) for 30 min at 400 °C under a constant flow of nitrogen (99.999 %) at a rate of 150 cm^3 min^{-1}. The quartz tube was situated within the furnace. The glass joint ends of the quartz tube were outside the furnace. The tube was connected with the nitrogen supply at one side, while the other was connected with a recipient trap filled with solvent. The sample was situated in a porcelain vessel, and the vessel was transferred in the middle of a quartz tube. The heating rate was 100 °C/min. The liquid fraction was collected in HPLC-grade acetone. The solvent was removed after pyrolysis in an inert nitrogen atmosphere. The yield of liquid fraction was calculated according to the mass of pyrolyzed samples.

Physicochemical characterization of biomass and bio-oil

The composition of biomass. The composition of corn stalks samples was analysed in detail to determine the lignin, cellulose, hemicellulose, and extractable material content. The extractives were isolated from the sample using acetone with heating, after which the sample was dried to a constant mass at a temperature of 110 °C. The quantity of extractives was determined from the difference between the initial and dried masses after extraction. Subsequently, the hemicellulose content was determined in the sample without extractives by extraction with a 0.5 mol dm^{-3} solution of sodium hydroxide with heating. The sample was then rinsed with distilled water until the reaction was negative for Na^+ and dried to a constant mass. The lignin content was obtained by extraction with 98 % sulfuric acid on a sample from which extractives had been previously removed. The sample was rinsed with distilled water until a negative reaction for sulphate ions and then dried to a constant mass. The cellulose content was calculated as a difference of up to 100 %.[13]

Determination of pH, moisture and ash content, elemental analysis and calorific value for biomass and bio-oil samples. The pH value of corn biomass and bio-oil samples was measured using the standard ASTM E70 method. The moisture content of biomass samples was determined by drying in an oven according to the ASTM E871 standard. The moisture content in bio-oil samples was determined using the standard procedure outlined in SRPS EN ISO

12937:2011, "Petroleum products- Determination of water- Coulometric Karl Fischer titration method" on an 831 KF Coulometer (Metrohm, Switzerland). The ash content in biomass samples was determined using the thermal analysis following the ASTM E1755 standard, while for bio-oil, the ASTM D482 standard was used. Elemental analysis of biomass and bio-oil samples was conducted on a CHNS Elementar- Vario Macro Cube (Elementar, Germany) for carbon, hydrogen, nitrogen, and sulphur analysis, using the standards SRPS ISO 13878:2005, SRPS ISO 10694:2005, and SRPS ISO 15178:2019. At the same time, the oxygen content was calculated as a difference of 100%. The calorific value of corn biomass and bio-oil samples was determined on an instrument IKA C400 (IKA, Germany), using the standard SRPS CEN/TS 16023:2014.

Density, viscosity and the group composition of the bio-oil. The bio-oil was characterized by the parameters such as density, viscosity, the group composition, FTIR analysis, and the toxic elements content. The density was determined using the ISO 12185 standard. The rheological behaviour of bio-oil samples was investigated using shear measurements in the parallel plate geometry (diameter 25 mm; gap 500 μm) on a Discovery hybrid rheometer HR2 (TA Instruments, USA). The experiments were conducted at 25 and 40 °C using a Peltier plate heating system, and viscosity curves were obtained within a shear rate range from 0.1 to 100 s^{-1}. To determine the group composition of the bio-oil, samples were fractionated into aliphatic, aromatic, and NSO fractions (polar fraction containing nitrogen, sulfur and oxygen compounds). The fractionation process involved the separation of different compounds using different eluents. A 15 mg sample was dissolved in 0.100 cm^3 of acetone and transferred to silica gel. Column chromatography was performed using 2 g of dried silica gel, with the sample transferred to the top of the column. Below this column section, dry Na_2SO_4 is placed to remove moisture from the sample. The Fractions were eluted with the following solvents: aliphatic with 5 cm^3 *n*-hexane; aromatic with 5 cm^3 of a mixture of *n*-hexane/dichloromethane (40/60); and NSO fraction with 5 cm^3 of methanol. The fractions were collected in receiving vessels, and after the solvent evaporation, the vessels weights were measured. The proportions of these fractions were determined gravimetrically after elution.[14]

FTIR analysis of bio-oil. Liquid bio-oil samples (~0.01 cm^3) were placed between two KBr plates, and spectra were obtained using a transmission technique. Infrared spectra over the wavelength range 4000–400 cm^{-1} were recorded with an IRAffinity-1 FTIR spectrophotometer (Shimadzu, Japan). The measurement resolution was 4 cm^{-1}.

ICP-OES analysis of bio-oil. The samples were prepared using a microwave digestion oven CEM Mars 5 (MARS, USA) according to the standard method EPA 3052. For the bio-oil samples, 0.25 g was measured, and then 9 cm^3 of concentrated nitric acid, 3 cm^3 of hydrochloric acid, and 0.5 cm^3 of hydrofluoric acid were added. The samples were placed in a microwave digestion oven, and the heating temperature was set to 180±5 ℃ for 5.5 min. After cooling, the samples were filtered through "blue band" filter paper (pores size < 2 μm) and topped up to a volume of 50 cm^3. Then they were analysed using the ICP-OES technique („Spectroblue TI"-Spectro, Germany) following the standard method EPA 200.7.

GC–MS analysis of bio-oil. GC–MS analysis was performed in order to determine the molecular composition of liquid pyrolysates and to identify the most dominant compounds. The samples were analysed using the GC–MS technique (Varian 450-GC with 220-MS, USA). The separation of compounds was performed on FactorFour capillary column VF-5ms 30 m×0.25 mm with 0.25 μm film thickness (Varian, USA). The injector temperature was 200 °C, and the injection volume was 1 mm^3 in split mode 90 %. The carrier gas was helium at a constant flow rate of 1 cm^3 min^{-1}. The oven program started at 50 °C. Afterward, the temperature was inc-

remented at 3 °C min^{-1} to reach 150 °C, and then immediately at 25 °C min^{-1} until it reached 280 °C, where it was held for 20 min. The parameters for MS analysis were as follows: EI (70 eV) temperature 200 °C, solvent cut time 3 min, scan 45–650 *m*/*z*. The identification was based on comparing a particular compound's mass spectra and retention time with the reference materials using the "Wiley registry of mass spectral data, 8th edition" library.

RESULTS AND DISCUSSION

The results of physicochemical characterization of biomass

The composition of corn stalk samples, pH value, moisture and ash content, elemental analysis, and calorific value are presented in Table I. These analyses provide the key information regarding the chemical composition of corn biomass and its suitability for conversion into biofuels. The moisture content was about 6 % in both samples, which was acceptable for the pyrolysis experiments. Biomass rich in cellulose and hemicellulose is a better source for obtaining bio-oil than lignin-rich biomass.[15] The lignin content was higher in the Kn sample, which indicated that this sample would give a lower yield of liquid fraction than the Kz sample. All values provided in Table I were within the range of literature values,[16,17] except for the sulphur content, which was present in significant amounts in the Kz sample. This can be explained by the specific composition of the soil where the Kz sample was grown, which is probably rich in sulphur compounds.

TABLE I. Results of the composition and physico-chemical characterization of the biomass; P – parameters; S – sample; Ext – extractives; Lig – lignin; Cell – cellulose; HC – hemicellulose; MC – moisture content; AC – ash content; CV – calorific value

S	Ext.	Lig	Cell	HC	pH	MC	AC	Elemental analysis, wt. %					CV
	%	%	%	%		%	%	C	H	N	O	S	MJ kg^{-1}
Kn	6.00	19.43	28.86	45.72	6.26	6.20	4.78	45.68	6.44	0.86	46.64	0.384	17.80
Kz	4.23	13.25	34.29	48.24	6.32	6.25	4.25	41.90	4.15	0.90	34.89	18.16	18.80

TGA results of two types of corn biomass

The thermogravimetric analysis was applied to monitor the thermal behaviour of corn stalk samples, which is essential for understanding the pyrolysis process and characterizing this biomass as a feedstock for biofuel production. The TGA analysis of two types of corn stalks is shown in Fig. 1. Given that corn biomass is a complex mixture mainly consisting of three major components – lignin, cellulose, and hemicellulose, it is expected that the thermogravimetric analysis of corn stalks is more complex than the TGA of individual components. According to the information from Chen et al., each individual component exhibits different thermal stability and thermogravimetric behaviour depending on its chemical structure. Lignin, with the most stable structure compared to hemicellulose and cellulose, rapidly degrades over a wide temperature range from 311.5 to 461.3 °C. Cellulose,

less stable than lignin but more stable than hemicellulose, degrades during the second phase in the 326.8 to 369.7 °C range. As the least stable of the three components, hemicellulose degrades during the second phase in the 223.4 to 332.8 °C range.[18]

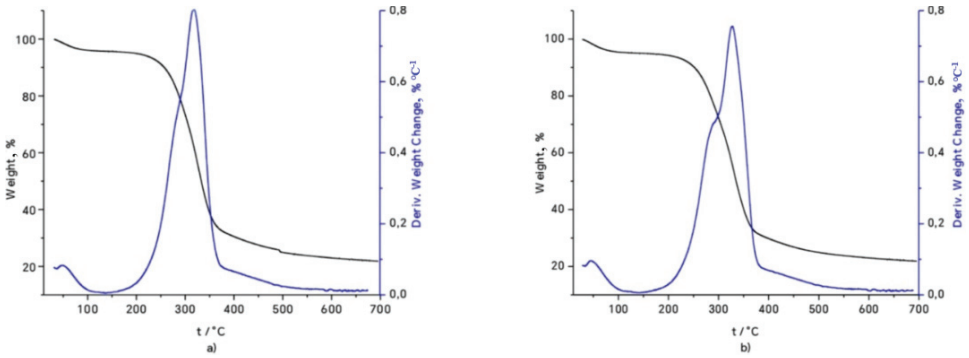

Fig. 1. Thermogravimetric curves for a corn sample: a) Kn and b) Kz.

The obtained thermogravimetric curves of corn stalks contained three main steps (Fig. 1). During the first degradation step, at around 120 °C, there was a minimal weight loss below 5 % in both pre-dried corn stalk samples, corresponding well to a water content of about 6 % (Table I). The second phase of thermal degradation (200–400 °C) involves rapid sample decomposition, resulting in the most substantial weight loss. Finally, the third step represents the slow stage where bio-char is formed (400–600 °C). The second step was more complex in the case of the Kz sample, showing a maximum of 330 °C on the DTG curve and a visible "shoulder" at 268 °C, unlike the Kn sample, where the "shoulder" was much less pronounced. This phenomenon corresponds to the chemical composition, where the "shoulder" appears due to the decomposition of hemicellulose and part of cellulose. The Kz sample contained higher amounts of hemicellulose (48.24 %) and cellulose (34.29 %) in comparison with the Kn sample, where the quantities of hemicellulose (45.72 %) and cellulose (28.86 %) were lower. It can be concluded that the higher content of hemicellulose and cellulose caused the appearance of a "shoulder" on the DTG curve of sample Kz. The maximum degradation rate corresponds to the decomposition of the mixture of cellulose and lignin. Lignin coats cellulose and hemicellulose, protecting these structures, which may influence the thermal degradation behaviour. The total weight loss amounted to 73.2 % for the Kn sample and 78.9 % for the Kz sample, which can be linked to the biomass composition. Since the lignin content is higher in the Kn sample (19.43 %), it was expected that the residue after TGA analysis would be larger, which was confirmed in comparison to the other sample with a lower lignin content (13.25 %). Since the study aimed to obtain the highest possible bio-oil yield, we concluded that a temperature of 400 °C to perform pyrolysis is sufficient to decompose the entire sample.

Pyrolysis of two types of corn biomass

The pyrolysis of corn biomass produces three fractions: liquid, solid and gaseous. This study focused on the liquid fraction, which was isolated and characterized in detail. The values for the amount of pyrolyzed sample are given in Table II, as well as the obtained yield of bio-oil in relation to the pyrolyzed mass of corn stalks. The obtained results were compared with the literature data for bio-oil yield. It can be noted that there is a difference in the yield of bio-oil obtained from these two types of corn stalks, where the sample Kz gave a significantly higher yield of bio-oil (33.5 %) compared to the sample Kn (22.8 %).

TABLE II. The yield of the liquid fraction concerning the mass of the pyrolyzed sample and comparison with literature data

Sample	m^a/ g	Yield of liquid fraction, wt. %	Yield of liquid fraction, wt. %[19]
Kn	19.14	22.8	30–33
Kz	19.61	33.5	

[a]Pyrolyzed biomass

The difference in the bio-oil content obtained by the pyrolysis of these two samples may be attributed to their distinct chemical compositions. The difference in the content of bio-oil obtained by pyrolysis of these two samples can be attributed to their different chemical composition. As mentioned before, higher lignin content leads to lower bio-oil yield, which is the case with the sample Kn.

The results of physicochemical characterization of bio-oil

The results obtained for density, pH, ash and moisture content, elemental analysis, calorific value and viscosity are presented in Table III. The density of the bio-oil is slightly higher than that of crude oil, which may be attributed to the presence of a large number of oxygenated compounds, and according to the literature, it is similar to the data obtained from other authors.[19] The acidity of bio--oil can affect its corrosiveness during application, so it is desirable to modify the liquid fraction.[20] The presence of water in bio-oil increases the oxygen content and potentially leads to corrosion, so it is desirable to minimize the water content.[19] Based on the obtained results, a significant amount of water is present, so it is necessary to reduce these values by prior biomass drying or using dehydration agents for bio-oil. The ash content is crucial for assessing the energy properties of biomass. The lower the ash content in the samples, the more energy-efficient the use of bio-oil.[21] Based on the values in Table III, it can be seen that the ash content values in bio-oil samples are lower compared to the initial biomass and according to literature data for bio-oil,[17] which correlates with the sulphur content, also lower in the bio-oil compared to the initial biomass. It can be concluded that sulphur is removed from the samples during the pyrolysis and annealing processes, most likely in the form of gases, such as sulphur dioxide, for example. The elemental

analysis is vital for determining the essential chemical characteristics of biomass. The elemental analysis shows that the content of all elements, carbon, oxygen, hydrogen, and nitrogen, are within the literature values.[18,21] The difference in carbon content in the initial biomasses is not significant – 45.68 % for Kn and 41.90 % for Kz. However, there is a significant imbalance in the carbon content in the bio-oil, with a higher proportion in the Kn sample (43.93 %) compared to Kz (26.97 %). The oxygen content is also significantly different, with a higher proportion in Kz (60.19 %) compared to Kn (34.14 %). This variable of the elemental composition may be associated with the content of lignin, cellulose and hemicellulose in the samples. In the Kn sample, where lignin is dominant (19.43 %), containing more carbon compared to cellulose and hemicellulose, a higher carbon content was observed in the bio-oil. In contrast, in the Kz sample, where there is a higher proportion of cellulose (34.29 %) and hemicellulose (48.24 %), higher oxygen content was observed in the resulting bio-oil. The calorific value is a parameter used to determine biomass's energy potential and potential for energy production during the pyrolysis process. It can be concluded that bio-oil has a better energy potential compared to the initial biomass,[1] which fits with the literature values for the liquid fraction of pyrolysis products.[19] Viscosity can affect engine performance and injection processes, so determining it is essential. Viscosity was measured at temperatures of 25 and 40 °C. It can be concluded that the obtained values for viscosity also correspond to literature data.[18] Results of the ICP analysis are provided in the table in the supplementary material (Table S-I of the Supplementary material to this paper). Determining the concentration of specific elements such as Si, K and S is important for the engine operation because a higher presence of these elements results in increased ash in the engine, making such bio--oils unsuitable for use as fuels.[21] The concentration of Si for both samples and K for sample Kn was below the detection limit (< 100 mg kg^{-1}), while the concentration of K for sample Kz was 155.94 mg kg^{-1}, and the concentrations of S for the same sample were 154.29 mg kg^{-1} and for Kn 722.38 mg kg^{-1}. Additionally, the presence of toxic elements that can harm human health, such as lead, mercury, and cadmium, was below the detection limit (< 0.25 mg kg^{-1} for Pb, and < 0.15 mg kg^{-1} for Hg and Cd), indicating that using such bio-oil as liquid fuel would not lead to emissions of these elements in the environment.

TABLE III. The results of physico-chemical parameters of bio-oil; S – sample; MC – moisture content; AC – ash content; CV – calorific value

S	pH	*MC*	*AC*	Elemental analysis, wt. %					*CV*	*ρ*	*η* / Pa s	
		%	%	C	H	N	O	S	MJ kg^{-1}	g cm^{-3}	25 °C	40 °C
Kn	2.35	23.06	0.07	43.93	6.40	14.83	34.14	0.70	24.18	1.15	0.014	0.010
Kz	2.43	18.09	0.04	26.97	7.86	4.79	60.19	0.19	22.62	1.08	0.006	0.003

The results of FTIR analysis of bio-oil

The FTIR analysis was performed on the bio-oil samples; the results are presented in Fig. 2. Corn samples were subjected to infrared spectroscopy (IR) to identify and analyse functional groups and structures. A characteristic peak around 3400 cm^{-1} of a hydroxyl group originates from water, alcohols, phenols or their derivatives. A peak at around 1700 cm^{-1} is associated with the axial deformation of the carbonyl group. The peak around 1400 cm^{-1} could be attributed to the deformation of C–H in CH_2 and CH_3 groups. The presence of C–O and deformed C–OH groups is linked to a value of around 1050 cm^{-1}. The phenolic compounds were from lignin. The ketone was formatted from hemicellulose/cellulose.[22] The lower pH value of the bio-oil compared to crude oil, which typically has a pH range between 6 and 8,[23] can be attributed to the presence of carboxylic and hydroxyl groups.

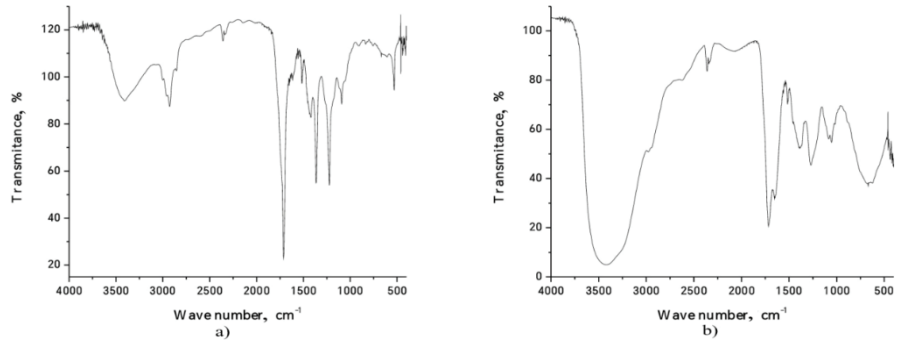

Fig. 2. The FTIR analysis for corn samples of bio-oil: a) Kn and b) Kz.

Results of the compositional analysis of bio-oil

The compositional analysis of the bio-oil can show whether it is suitable or makes sense to separate fractions and utilize them for different purposes. Based on the results presented in Table IV, it is evident that the aliphatic and aromatic fractions are negligible compared to the NSO fraction, which is expected for the bio-oil derived from biomass, considering that the basic structures in biomass are cellulose, hemicellulose, and lignin, which are rich in oxygen.

TABLE IV. The group composition of the bio-oil

Sample	Alifatic fraction, %	Aromatic fraction, %	NSO fraction, %
Kn	2.5	2.5	95.0
Kz	1.1	0.5	98.4

Diesel and gasoline are liquid fuels consisting of linear saturated hydrocarbons, branched saturated hydrocarbons, saturated cyclic alkanes and aromatic

compounds, with a dominant aromatic fraction of up to 50 % and iso-paraffins of up to 35 %.[24] The fractions that make up a significant part of liquid fuels are not present in bio-oil, which suggests that bio-oil in its native form is unsuitable for direct use, considering that it is similar to crude oil. Therefore, it must be processed and modified to be used as a fuel.

GC–MS analysis of bio-oil

The compounds identified in obtained bio-oil using GC–MS analysis include: 3-penten-2-one, 4-methyl-; 2-furancarboxaldehyde; 2-cyclopenten-1-one, 2-methyl-; phenol; 2-cyclopenten-1-one, 2-hydroxy-3-methyl-; 2-cyclopenten-1-one, 2,3--dimethyl-; phenol, 2-methyl-; phenol, 4-methyl-; phenol, 2-methoxy-; phenol, 3-ethyl-; guaiacol, 4-ethyl-; phenol, 2,6-dimethoxy. The remaining compounds are isomers formed either during pyrolysis or afterward. According to the literary data, the identified compounds have also been found in bio-oil from corn, reported by other researchers, along with their isomers which include 2-furancarboxaldehyde, 2-cyclopenten-1-one, 2-methyl-; phenol; 2-cyclopenten-1-one, 2,3-dimethyl-; phenol, 2-methyl-; phenol, 4-methyl-; phenol, 2-methoxy-; 2-cyclopenten-1-one, 3-ethyl-2-hydroxy-; and phenol, 2,6-dimethoxy-.[1,25] The results of the GC–MS analysis complement those of the FTIR analysis, group composition, and the oxygen content in the bio-oil samples. Based on the results of the FTIR analysis, the presence of hydroxyl and carbonyl groups was found, which correlates with the GC-MS analysis confirming the presence of compounds containing these groups, such as various phenols derivates and 2-furancarboxaldehyde, for example.

CONCLUSION

In this study, the composition of bio-oil obtained by pyrolysis of corn stalks was analysed. The ash content in the bio-oil was below 1 %, consistent with the literature data and the sulphur content determined by the elemental analysis. Based on the elemental composition, the carbon and oxygen content were determined, correlating with the composition of the initial biomass. The presence of a significant amount of oxygen, besides elemental analysis, was confirmed through other parameters, including pH, moisture content, density, FTIR analysis, and GC––MS analysis. The functional groups identified by FTIR analysis were further identified as various compounds by GC–MS analysis. Such compound classes contribute to the acidic pH, as observed here. Additionally, the high density indicates the presence of heavier compounds, such as oxygen compounds. The bio-oil exhibits a slightly higher calorific value than the original biomass, suggesting it may be a better energy source. The lower C/H ratio affects the calorific value due to the significant presence of oxygen, so this bio-oil cannot be used as a liquid fuel in its current form. Further research should focus on improving the quality of bio-oil, including increasing the carbon and hydrogen content, reducing the oxygen and water content, as well as the calorific value. Some possibilities include the

addition of other waste materials with high carbon and hydrogen content, such as synthetic polymers, and the use of catalysts in pyrolysis processes, which would undoubtedly improve bio-oil characteristics and enable its more efficient and sustainable use for various purposes. In conclusion, this study highlights the need for further research and the development of biofuels that would result in a more sustainable and environmentally friendly alternative to fossil fuels.

SUPPLEMENTARY MATERIAL

Additional data and information are available electronically at the pages of journal website: https://www.shd-pub.org.rs/index.php/JSCS/article/view/12769, or from the corresponding author on request.

Acknowledgement. This work is supported by the project "Agricultural residues and plastic waste as a sustainable source of alternative fuels and valuable chemicals" (AGRIPLAST), grant No.01DS21008.

ИЗВОД

ПИРОЛИЗА СТАБЉИКА КУКУРУЗА: ПОТЕНЦИЈАЛ КОРИШЋЕЊА БИО-УЉА КАО БИОГОРИВА

ЈЕЛЕНА ИСАИЛОВИЋ[1], ЕМИЛИЈА ВУКИЋЕВИЋ[2], МАЛИША АНТИЋ[1], JAN SCHWARZBAUER[3], ЉУБИША ИГЊАТОВИЋ[4], ГОРДАНА ГАЈИЦА[5] и ВЕСНА АНТИЋ[1]

[1]Пољопривредни факултет, Универзитет у Београду, Немањина 6, Земун, [2]Хемијски факултет, Универзитет у Београду, Студентски трг 12–16, Београд, [3]Institute for Geology and Geochemistry of Petroleum and Coal, RWTH, Lochnerstr. 4-20, Aachen, Germany, [4]Факултет за физичку хемију, Универзитет у Београду, Студентски трг 12–16, Београд и [5]Институт за хемију, технологију и металургију, Национални институт Републике Србије, Његошева 12, Београд

Због све веће потрошње фосилних горива, постоји растућа потражња за обновљивим изворима енергије. Истовремено, акумулира се значајна количина пољопривредног отпада, укључујући остатке кукуруза, чије ефикасно управљање представља изазов. У овом раду, отпадна биомаса, која се састојала од стабљика два типа кукуруза, окарактерисана је и подвргнута процесу пиролизе на 400 °C. Урађена је физичко-хемијска карактеризација добијене течне фракције (био-уља), а вредности су упоређене са литературним подацима за течно биогориво. Топлотна моћ био-уља била је изнад 22 MJ kg^{-1}, што указује на добар потенцијал кукурузног отпада као енергента. Уз одговарајуће даље промене у саставу отпада, додавање материјала са већим садржајем угљеника и водоника, стабљике кукуруза могу представљати значајан извор енергије, са бољом регулацијом одлагања и складиштења пољопривредног отпада.

(Примљено 10. јануара, ревидирано 20. јануара, прихваћено 6. априла 2024)

REFERENCES

1. G. Q. Calixto, D. M. A. Melo, M. A. F. Melo, R. M. Braga, *Braz. J. Chem. Eng.* **39** (2021) 137 (https://doi.org/10.1007/s43153-021-00099-1)
2. FAO. (2021). FAOSTAT database. Retrieved from http://www.fao.org/faostat/en/#data (accessed 25.12.2023)
3. Statistički kalendar Republike Srbije (2022) 218 https://www.stat.gov.rs/sr-Latn/calendar (accessed 25.12.2023)

4. V. Semenčenko, Dušanka Terzić, M. Radosavljević, Slađana Žilić, „Korišćenje agrorezidua kukuruza u proizvodnji biogoriva, bioapsorbenata i hrane za ljude i životinje“ INDUSTRIAL WASTE 2nd International Scientific Conference on Waste Management, Tara, Serbia, 2009. (http://dx.doi.org/10.13140/2.1.4549.3769)
5. M. E. Himmel, S.-Y. Ding, D. K. Johnson, W. S. Adney, M. R. Nimlos, J. W. Brady, T. D. Foust, *Science* **315** (2007) 804 (http://dx.doi.org/10.1126/science.1137016)
6. G. Ungureanu, G. Ignat, C. R. Vintu, C. D. Diaconu, I. G. Sandu, *Rev. Chim.* **68** (2017) 570 (http://dx.doi.org/10.37358/RC.17.3.5503)
7. J. B. Sluiter, R. O. Ruiz, C. J. Scarlata, A. D. Sluiter, D. W. Templeton, *J. Agric. Food Chem.* **58** (2010) 9043 (http://dx.doi.org/10.1021/jf1008023)
8. P. McKendry, *Bioreso. Techn.* **83** (2002) 37)https://doi.org/10.1016/S0960-8524(01)00118-3)
9. D. L. Klass, *Biomass for Renewable Energy, Fuels, and Chemicals*, Elsevier, San Diego, 1998, 1-27 (https://doi.org/10.1016/B978-012410950-6/50003-9)
10. R. D. Perlack, *Biomass as Feedstock for a Bioenergy and Bioproducts Industry: The Technical Feasability of a Billion-Ton Annual Supply*, USDA, Springfield, 2005, 1-38 (https://doi.org/10.2172/885984)
11. C. Corvalan, S. Hales, A. J. McMichael, *Ecosystems and human well-being: health synthesis*, World Health Organization, Geneva, 2005, 27-49 ISBN: 9241563095
12. A. J. Ragauskas, C. K. Williams, B. H. Davison, G. Britovsek, J. Cairney, C. A. Eckert, W. J. Frederick Jr., J. P. Hallett, D. J. Leak, C. L. Liotta, J. R. Mielenz, R. Murphy, R. Templer, T. Tschaplinski, *Science* **311** (2006) 484 (https://doi.org/10.1126/science.1114736)
13. H. Yang, R. Yan, H. Chen, C. Zheng, D. H. Lee, D. T. Liang, *Energy Fuels* **20** (2005) 388 (https://doi.org/10.1021/ef0580117)
14. D. Vitorović, B. Jovančićević. *Osnovi organske geohemije.* Faculty of Chemistry University of Belgrade, Belgrade, 2005, 153 ISBN 978-8672200195
15. T. Qu, W. Guo, L. Shen, J. Xiao, K. Zhao, *Ind. Eng. Chem. Res.* **50** (2011) 10424 https://doi.org/10.1021/ie1025453
16. T. Sun, Z. Li, Z. Zhang, Z. Wang, S. Yang, Y. Yang, X. Wang, S. Liu, Q. Zhang, T. Lei, *Bioresource Technology* **301** (2020) 122739 (https://doi.org/10.1016/j.biortech.2020.122739)
17. L. Wang, W. Yi, A. Zhang, Z. Li, H. Cai, Y. Li, *Front. Energy Res.* **7** (2019) (https://doi.org/10.3389/fenrg.2019.00086)
18. D. Chen, K. Cen, X. Zhuang, Z. Gan, J. Zhou, Y. Zhang, H. Zhang, *Comb. and Flame* **242** (2022) 112142 (https://doi.org/10.1016/j.combustflame.2022.112142)
19. L. Maulinda, H. Husin, N. Arahman, C. M. Rosnelly, E. Andau, W. Lestari, J. Karo-Karo, *IOP Conf. Ser.: Mater. Sci. Eng.* **1098** (2021) 022007 (https://doi.org/10.1088/1757-899X/1098/2/022007)
20. R. Chen, L. Lun, K. Cong, Q. Li, Y. Zhang, *Energy* **183** (2019) 25 (https://doi.org/10.1016/j.energy.2019.06.127)
21. M. Praspaliauskas, N. Pedišius, D. Čepauskienė, M. Valantinavičius, *Biom. Conv. Bioref.* **10** (2019) 937 (https://doi.org/10.1007/s13399-019-00457-7)
22. S. Nizamuddin, H. A. Baloch, N. M. Mubarak, S. Riaz, M. T. H. Siddiqui, P. Takkalkar, M. M. Tunio, S. Mazari, A. W. Bhutto, *Wast. Biom. Valor*. **10** (2018) 1957 (https://doi.org/10.1007/s12649-018-0206-0)
23. J. E. Strassner, *J. of Petrol. Techn.* **20** (1968) 303–312 (https://doi.org/10.2118/1939-PA)

24. R. Marchal, S. Penet, F. Solano-Serena, J. P. Vandecasteele, *Oil and Gas Sci. and Tech.* **58** (2003) 441 (https://doi.org/10.2516/ogst:2003027)
25. H. Wei, Y. L. Liu, D. Y. Chen, *AMM* **737** (2015) 14 (https://doi.org/10.4028/www.scientific.net/AMM.737.14).

Journal of the Serbian Chemical Society
JSCS-info@shd.org.rs • www.shd.org.rs/JSCS
J. Serb. Chem. Soc. *89* (12) S537 (2024)
Supplementary material

SUPPLEMENTARY MATERIAL TO

Pyrolysis of corn stalks: the potential of using bio-oil as a fuel

JELENA ISAILOVIĆ[1]*, EMILIJA VUKIĆEVIĆ[2], MALIŠA ANTIĆ[1], JAN SCHWARZBAUER[3], LJUBIŠA IGNJATOVIĆ[4], GORDANA GAJICA[5] and VESNA ANTIĆ[1]

[1]University of Belgrade – Faculty of Agriculture, Nemanjina 6, 11080 Zemun, Serbia, [2]University of Belgrade – Faculty of Chemistry, Studentski trg 12-16, 11158 Belgrade, Serbia, [3]Institute for Geology and Geochemistry of Petroleum and Coal, RWTH, Lochnerstr. 4-20, Aachen, Germany, [4]University of Belgrade – Faculty of Physical Chemistry, Studentski trg 12-16, 11000 Belgrade, Serbia, and [5]Institute of Chemistry, Technology and Metallurgy, National Institute of the Republic of Serbia, Njegoševa 12, 11000 Belgrade, Serbia.

J. Serb. Chem. Soc. *89* (12) (2024) 1675–1687

TABLE S-I. Results of ICP-OES analysis of metal content in bio-oil samples.

Parameters / The metal content	Method	m Kn / mg kg^{-1}	m Kz / mg kg^{-1}
Si	VM 129	< 100	< 100
K	VM 129	< 100	155.94
S	VM 129	722.38	154.29
Pb	VM 092-1	< 0.25	< 0.25
Hg	VM 092-1	< 0.15	< 0.15
Cd	VM 092-1	< 0.15	< 0.15

* Corresponding author. E-mail: jelena.isailovic@agrif.bg.ac.rs

Journal of the Serbian Chemical Society
JSCS-info@shd.org.rs • www.shd.org.rs/JSCS
J. Serb. Chem. Soc. 89 (12) 1689–1698 (2024)

Contents of Volume 89

NUMBER 1

NUMBER 2

NUMBER 3

NUMBER 6

NUMBER 9

NUMBER 10

Journal of the Serbian Chemical Society
JSCS-info@shd.org.rs • www.shd.org.rs/JSCS
J. Serb. Chem. Soc. *89* (12) 1699–1704 (2024)

Author Index

Subject Index of Vol. **89** and List of Referees in 2024 are given in the electronic form at the Internet address of the Journal of the Serbian Chemical Society: http://www.shd.org.rs/JSCS

End of Volume 89.

Journal of the Serbian Chemical Society
JSCS-info@shd.org.rs • www.shd.org.rs/JSCS
Volume *89* (2024)

Subject index